Impregnation of Solid Dielectric Cable Insulation

EL-1435
Research Project 7854

Final Report, July 1980
Work Completed, November 1979

Prepared by

PHELPS DODGE CABLE AND WIRE COMPANY
Research and Development Center
Foot of Point Street
Yonkers, New York 10702

Principal Investigators
K. D. Kiss
D. Mangaraj
H. C. Doepken, Jr.

Associate Investigators
M. C. Biskeborn
E. Malawer
A. L. McKean
K. Tsuji

Prepared for

Electric Power Research Institute
3412 Hillview Avenue
Palo Alto, California 94304

EPRI Project Manager
F. G. Garcia

Underground Transmission Program
Electrical Systems Division

ORDERING INFORMATION

Requests for copies of this report should be directed to Research Reports Center (RRC), Box 50490, Palo Alto, CA 94303, (415) 965-4081. There is no charge for reports requested by EPRI member utilities and affiliates, contributing nonmembers, U.S. utility associations, U.S. government agencies (federal, state, and local), media, and foreign organizations with which EPRI has an information exchange agreement. On request, RRC will send a catalog of EPRI reports.

NOTICE

This report was prepared by the organization(s) named below as an account of work sponsored by the Electric Power Research Institute, Inc. (EPRI). Neither EPRI, members of EPRI, the organization(s) named below, nor any person acting on their behalf: (a) makes any warranty or representation, express or implied, with respect to the accuracy, completeness, or usefulness of the information contained in this report, or that the use of any information, apparatus, method, or process disclosed in this report may not infringe privately owned rights; or (b) assumes any liabilities with respect to the use of, or for damages resulting from the use of, any information, apparatus, method, or process disclosed in this report.

Prepared by
Phelps Dodge Cable and Wire Company
Yonkers, New York

ABSTRACT

Laboratory scale investigations were conducted to assess the feasibility of improving the dielectric characteristics of crosslinked polyethylene (XLPE) insulated cables rated 138 kV and above. Impregnation of slabs cut from 138 kV cables and of model cables with liquids increased the AC breakdown strength, presumably by filling the microvoids (and possibly in some cases acting as a "voltage stabilizer") and preventing premature failure due to electrical discharge. The degree of improvement depends on the chemical nature of the impregnant. Vinyl toluene, styrene, styrene oxide and vinyl pyrrolidone were found to increase the dielectric strength substantially and in some cases improve the VT curve. With vinyl toluene, the improved strength is approximately 3750 V/mil compared to 2300 V/mil for the control. In situ polymerization with lauryl methacrylate and vinyl toluene monomers and impregnation with polyethylene wax have proven that the solid polymer is as effective as the liquid monomer. Optical and scanning electron microscopic examination supports the concept of void filling. The volume resistivity of semiconducting shields is not materially affected by the impregnation and polymerization, probably because the carbon black inhibits the polymerization. An economic analysis including raw materials' costs and manufacturing costs suggests that the process of impregnation and polymerization costs somewhat less than lead sheathed, dry cured power cables.

EPRI PERSPECTIVE

PROJECT DESCRIPTION

The bulk of underground transmission in the U.S. is based on paper-insulated, high-pressure oil-filled (HPOF) cable systems. Over the years, these systems have established an enviable record of reliability.

However, transmission systems based on cross-linked polyethylene (XLPE) insulated cables offer some potential advantages. Because a pressurized ambient is not needed for XLPE cables, transmission systems can be simpler and would require less routine maintenance. Furthermore, if XLPE cables rated 345 kV and higher are successfully developed in the future, the extremely low dielectric losses of XLPE (approximately 5 percent of those of oil-impregnated paper) would result in substantial decreases in energy losses.

But experience to date with XLPE cables, particularly at distribution voltage levels, indicates they are less reliable than paper-insulated cables. Previous investigations of breakdown mechanisms in XLPE cables (EPRI Final Report TD-138, July 1976) indicated that microvoids occurring in XLPE were one of the factors limiting its performance. It was found that impregnation of these microvoids with various liquids substantially improved the dielectric strength of XLPE. The problem with liquid-impregnated XLPE cables is that in time the liquid will diffuse out of the cable, unless the cable is installed in a liquid-filled enclosure similar to HPOF cables. Such an installation, however, would negate the basic simplicity of XLPE cable systems.

PROJECT OBJECTIVE

The objective of this project was to investigate the feasibility of impregnating the microvoids in XLPE cables with a catalyst-bearing monomer that would subsequently be polymerized into a solid to prevent diffusion out of the cable.

PROJECT RESULTS

The results of this work indicate there are several monomers available that substantially increase the dielectric strength of XLPE both before and after polymerization. Although these results are quite encouraging, two major problems emerged:

1. The permeation rates of monomers in XLPE are considerably greater than the permeation rates of suitable catalysts. Hence, as a catalyst-bearing monomer

permeates the insulation, the catalyst concentration decreases. The proposed solution requires a double-impregnation process: (1) impregnation of the cable with a catalyst dissolved in a suitable "carrier" solvent, (2) vacuum "drying" of the cable to remove the solvent, (3) impregnation with the monomer, (4) heat polymerization, and (5) vacuum "drying" to remove the nonpolymerized fraction of the monomer.

It is most unlikely that the cost of these additional manufacturing steps would be compensated by the attainable improvement in cable performance.

2. The carbon black in the semiconducting shields inhibits polymerization of the monomer within the shields. Although this is beneficial to the shields in that their electrical resistivity is not materially increased, unfortunately this inhibiting effect extends to a thin layer of insulation adjacent to the shield. The insulation immediately adjacent to the conductor shield is subjected to the highest voltage stress and is most in need of any improvements that might be obtained by impregnation with polymerizable monomers.

Although the impregnation/polymerization process looks promising, successful implementation of the process on a commercial scale would require overcoming the two obstacles noted above.

F. G. Garcia, Project Manager
Underground Transmission Program
Electrical Systems Division

CONTENTS

Section			Page
1	INTRODUCTION		1-1
2	THEORETICAL CONSIDERATIONS		2-1
	2.1	REMOVAL OF VOLATILES	2-1
	2.1.1	Vacuum Drying	2-1
	2.1.2	Removal of Excess Impregnant	2-3
	2.2	IMPREGNATION	2-3
	2.2.1	Mechanism of Impregnation	2-3
	2.2.2	Estimation of Time Required for Impregnating the Cable	2-7
	2.3	POLYMERIZATION	2-9
	2.4	AC BREAKDOWN TEST	2-14
	2.4.1	Measurement of Dielectric Strength	2-16
	2.4.2	Lifetime Test	2-16
3	RESULTS AND DISCUSSION, IMPREGNATION AND POLYMERIZATION		3-1
	3.1	CONTROLS	3-1
	3.1.1	Volatile Content	3-1
	3.1.2	AC Breakdown Strength	3-4
	3.1.3	Microscopy	3-10
	3.2	DRYING AND HEAT TREATMENT	3-22
	3.2.1	Vacuum Drying	3-22
	3.2.2	Heat Treatment	3-29
	3.2.3	AC Breakdown Strength	3-29
	3.2.4	Microscopy	3-35
	3.3	IMPREGNATION	3-41
	3.3.1	Wafers	3-41
	3.3.2	Slabs	3-41
	3.3.3	Model Cables	3-55
	3.3.4	Impregnation with Polymerization Catalysts	3-66
	3.3.5	AC Breakdown Strength	3-73
	3.3.6	Microscopy	3-108
	3.4	POLYMERIZATION	3-115
	3.4.1	Polymerization of LMA	3-115
	3.4.2	Polymerization of Vinyl Toluene	3-134

	3.4.3	AC Breakdown Strength	3-138
	3.4.4	Microscopy	3-149
4	EXPERIMENTAL DETAILS		4-1
	4.1	MATERIALS	4-1
	4.1.1	Test Samples	4-1
	4.1.2	Impregnants	4-4
	4.1.3	Catalysts	4-4
	4.1.4	Miscellaneous Materials	4-4
	4.2	EQUIPMENT	4-9
	4.2.1	Reaction Chambers	4-9
	4.2.2	Auxiliary Equipment	4-10
	4.2.3	Miscroscopic Equipment	4-10
	4.2.4	AC Breakdown Test	4-10
	4.3	PROCEDURES	4-13
	4.3.1	Vacuum Drying	4-13
	4.3.2	Impregnation	4-17
	4.3.3	Polymerization	4-17
	4.3.4	Removal of Residual Monomer	4-18
	4.3.5	AC Breakdown Strength Measurement	4-18
	4.3.6	Miscroscopic Examination	4-19
5	SUPPLEMENTARY INVESTIGATION		5-1
	5.1	COMPARISON OF CURING PROCESSES	5-1
	5.1.1	Characterization of Samples by Microscopy and SEM	5-2
	5.1.2	Physico-Chemical Characterization	5-2
	5.1.3	Chemical Analysis	5-21
	5.2	IMPREGNATION AND IN SITU POLYMERIZATION WITH SEMICONDUCTING SHIELDS	5-21
	5.2.1	Experimental	5-25
	5.2.2	Results and Discussion	5-25
	5.3	IMPREGNATION WITH A CARBONIZABLE GAS	5-33
6	ECONOMIC ANALYSIS		6-1
	6.1	PRELIMINARY STUDY	6-1
	6.2	COMPREHENSIVE ANALYSIS OF ADVANCED CABLES	6-10
	6.2.1	Basis of Analysis	6-10
	6.2.2	Comparison of Designs	6-13
	6.2.3	Details of Cost Comparison	6-15
	6.2.4	Cost of Comparable Performance	6-17
7	CONCLUSIONS		7-1
8	REFERENCES		8-1

ILLUSTRATIONS

Figure		Page
2-1	Reaction Steps in Addition Polymerization	2-11
2-2	Reaction Steps in Graft Polymerization	2-13
	WEIBULL PLOTS	
3-1	Control A and J	3-6
3-2	Control B	3-6
3-3	Control D	3-7
3-4	Control C	3-7
3-5	Control H and E	3-8
3-6	Control F and G	3-8
3-7	Test at Constant Stress, Cable E	3-9
3-8	Test at Constant Stress, Cable H	3-9
3-9	Stress-Time Correlation for Controls	3-11
	OPTICAL MICROGRAPHS	
3-10	Cable A, Control	3-12
3-11	Cable B, Control	3-13
3-12	Cable J, Control	3-14
3-13	Model Cable C, Control	3-15
	SCANNING ELECTRON MICROGRAPHS	
3-14	Cable A, Blade Cut Specimen	3-17
3-15	Cable J, Blade Cut Specimen	3-17
3-16	Cable A, Cold Fractured, Control	3-18
3-17	Cable B, Control	3-19
3-18	Cable B, Control	3-19
3-19	Model Cable E, Control	3-20
3-20	Model Cable H, Control	3-20
3-21	Cable A, "Ditch" Surface	3-21
3-22	Cable A, "Ditch" Surface	3-21
3-23	View of AC Breakdown Channel	3-23
3-24	View of AC Breakdown Channel	3-23
3-25	View of AC Breakdown Channel	3-24
3-26	Removal of Volatiles at 70°C, Cable A	3-25
3-27	Removal of Volatiles at 90°C, Cable A	3-26
3-28	Removal of Volatiles at 70°C, Cable B	3-27

Figure		Page
3-29	Vacuum Drop Test	3-28
	WEIBULL PLOTS	
3-30	Vacuum Dried Slabs, Cable A	3-31
3-31	Vacuum Dried Slabs, Cable B	3-31
3-32	Vacuum Dried Slabs, Cable J	3-32
3-33	Vacuum Dried Model Cable E	3-32
3-34	Heat Treated Slabs, 100°C	3-33
3-35	Heat Treated Slabs, 150°C	3-33
3-36	Effect of Temperature on AC Breakdown Strength	3-34
	OPTICAL MICROGRAPHS	
3-37	Cables A and J, Vacuum Dried	3-36
3-38	Cable B, Vacuum Dried	3-37
3-39	Effect of AC BD Step Time (One hour)	3-38
3-40	Effect of AC BD Step Time (168 hours)	3-38
3-41	Effect of Heat Treatment	3-39
	SCANNING ELECTRON MICROGRAPHS	
3-42	Vacuum Dried Specimens	3-40
3-43	Vacuum Dried Specimens	3-40
3-44	Effect of Heat Treatment	3-42
3-45	Effect of Heat Treatment	3-42
3-46	Effect of Heat Treatment	3-43
3-47	Effect of Heat Treatment	3-43
3-48	Impregnation with Acrylic Monomers	3-44
3-49	Effect of Pressure on Level of Impregnation	3-45
3-50	Impregnation of XLPE	3-50
3-51	Impregnation of XLPE	3-51
3-52	Impregnation of XLPE	3-52
3-53	Impregnation of XLPE	3-53
3-54	Comparison of Initial Impregnation Rates	3-57
3-55	Time-Temperature Correlation for Impregnation	3-58
3-56	Impregnation Isotherms for Vinyl Toluene	3-59
3-57	Impregnation Isotherms for Styrene Oxide	3-60
3-58	Impregnation Isotherms for Styrene	3-61
3-59	Impregnation Isotherms for Dodecyl Vinyl Ether	3-62
3-60	Impregnation Isotherms for Vinyl Pyrrolidone	3-63
3-61	Impregnation Isotherms for Lauryl Methacrylate	3-64
3-62	Rate of Catalyst Permeation	3-67
3-63	Effect of Impregnant Composition and Temperature on BPO Migration	3-70
3-64	Effect of Impregnant Composition and Temperature on XLPE Insulation	3-71
3-65	Effect of Impregnant Composition and Temperature on XLPE Insulation - Net Change	3-72

Figure		Page
3-66	Impregnation with MEK Containing 10% BPO	3-74
	WEIBULL PLOTS	
3-67	Impregnation with p-Xylene, Ethyl Alcohol	3-76
3-68	Impregnation with Acetophenone	3-76
3-69	Impregnation with Paraffin Oil	3-77
3-70	Impregnation with PE Wax	3-77
3-71	Impregnation with LMA	3-78
3-72	Effect of Acetophenone on AC Breakdown Strength	3-80
3-73	Effect of Mineral Oil and PE Wax on AC Breakdown Strength	3-81
3-74	Effect of LMA and Polymerized LMA on AC Breakdown Strength	3-82
3-75	Typical AC Breakdown Strength-Impregnation Level Correlation	3-83
3-76	Chemical Structure of Impregnant Candidates	3-84
3-77	Effect of Various Impregnants on AC Breakdown Strength	3-87
	WEIBULL PLOTS	
3-78	Impregnation with Vinyl Toluene	3-89
3-79	Impregnation with Vinyl Toluene	3-89
3-80	Impregnation with DVE	3-90
3-81	Impregnation with DVE	3-90
3-82	Impregnation with Styrene Oxide	3-91
3-83	Impregnation with Styrene Oxide	3-91
3-84	Impregnation with PE Wax	3-92
3-85	Impregnation with PE Wax	3-92
3-86	Impregnation with Naphthalene	3-93
	STRESS TIME CORRELATIONS	
3-87	Effect of Vinyl Toluene	3-96
3-88	Effect of Dodecyl Vinyl Ether	3-97
3-89	Effect of Styrene Oxide	3-98
3-90	Effect of PE Wax	3-99
3-91	Effect of Naphthalene	3-100
3-92	Comparison of Impregnants	3-101
3-93	Comparison of 1 and 24 Hour Step AC BD Results	3-102
	WEIBBULL PLOTS	
3-94	Impregnation with VT	3-103
3-95	Impregnation with VT	3-103
3-96	Impregnation with VT	3-104
3-97.	Effect of Impregnation with Vinyl Toluene-10 Minute Step Test	3-106

Figure		Page
3-98	Effect of Impregnation with Vinyl Toluene-One Hour Step Test	3-107
3-99	Stress-Time Correlation for Model Cables	3-109
	OPTICAL MICROGRAPHS	
3-100	Impregnation with TEG-pX-Ethyl Alcohol	3-111
3-101	Impregnation with Acetophenone	3-112
3-102	Impregnation with LMA	3-112
3-103	Impregnation with Vinyl Toluene	3-113
3-104	Impregnation with PE Wax	3-113
	SCANNING ELECTRON MICROGRAPHS	
3-105	Impregnation with LMA	3-116
3-106	Impregnation with Vinyl Toluene	3-117
3-107	Impregnation with Mineral Oil	3-118
3-108	Impregnation with PE Wax	3-119
3-109	Impregnation with Naphthalene	3-120
3-110	Effect of Post Polymerization Drying Time on Weight Gain	3-130
	WEIBULL PLOTS	
3-111	Effect of Polymerized LMA	3-140
3-112	Effect of Polymerized LMA	3-140
3-113	Effect of Polymerized LMA	3-141
3-114	Effect of Polymerized LMA	3-141
3-115	Slab Weight: AC Breakdown Strength Correlation	3-143
3-116	WEIBULL PLOT, Effect of Polymerized LMA	3-145
3-117	Effect of Polymerized LMA on AC Breakdown Strength	3-146
	WEIBULL PLOTS	
3-118	Effect of Polymerized VT	3-148
3-119	Effect of Polymerized VT	3-148
3-120	Effect of Vinyl Toluene and Polymerized Vinyl Toluene on AC Breakdown Strength	3-150
	OPTICAL MICROGRAPHS	
3-121	Effect of In Situ Polymerized LMA	3-152
3-122	Effect of In Situ Polymerized LMA	3-152
3-123	Effect of In Situ Polymerized LMA	3-153
3-124	Effect of In Situ Polymerized LMA	3-153
3-125	Effect of In Situ Polymerized VT	3-154
	SCANNING ELECTRON MICROGRAPHS	
3-126	Effect of In Situ Polymerized LMA	3-156
3-127	Effect of In Situ Polymerized LMA	3-156

Figure		Page
3-128	Effect of In Situ Polymerized VT	3-157
3-129	Effect of In Situ Polymerized VT	3-157
4-1	Schematic View of 138 kV Cable and Slabs	4-3
4-2	Setup for Vacuum Drying, Impregnation and Polymerization	4-11
4-3	AC BD Test Cell for Slabs	4-12
4-4	AC BD Test Setup for Model Cables	4-14
4-5	Vacuum Drop Test (Rate of pressure buildup)	4-15
4-6	Vacuum Drop Test (Rate of drying)	4-16
	OPTICAL MICROGRAPHS	
5-1	Voids in Steam Cured XLPE at 3/4 Wall	5-4
5-2	Voids in Steam Cured XLPE at Surface	5-4
5-3	Voids in Dry Cured XLPE (DPI at the conductor)	5-5
5-4	Voids in Dry Cured XLPE (DPI middle of wall)	5-5
5-5	Voids in Dry Cured XLPE (DPI at the middle of the wall)	5-6
5-6	Voids in Dry Cured XLPE (DP3 at insulation surface)	5-6
5-7	Voids in Dry Cured XLPE (DP4 at conductor)	5-7
5-8	Voids in Dry Cured XLPE (DP4 at the conductor)	5-7
5-9	Voids in Dry Cured XLPE (DP4 at the insulation surface)	5-8
	SCANNING ELECTRON MICROGRAPHS	
5-10	Dry Cured Insulation with Gel Particle	5-10
5-11	Dry Cured Insulation Shield-Process:DP1	5-10
5-12	Voids in Dry Cured XLPE-Process: DP2, 2200x	5-11
5-13	Voids in Dry Cured XLPE-Process: DP2, 10,300x	5-11
5-14	Gel in Dry Cured Insulation-Process: DP3, 2200x	5-12
5-15	Voids at Conductor Shield-Insulation Interface DP3	5-13
5-16	Voids in Dry Cured Insulation-Process: DP3	5-14
5-17	Conductor Shield-Insulation Interface in Dry Cured Cable	5-15
5-18	Void Details in Insulation Shield-Process: DP4	5-15
5-19	Typical Thermogravimetrical Curve	5-18
5-20	Melting Characteristics by DSC (Near Insulation shield)	5-19
5-21	Melting Characteristics by DSC (Near conductor)	5-20
5-22	Volatiles by Gas Chromatography	5-23
5-23	Rate of Impregnation into Semicon Specimens	5-26
5-24	Volume Resistivity of Impregnated Semiconducting Rods	5-29
5-25	Effect of Aging on Volume Resistivity (PVT in Insulation shield)	5-30

Figure		Page
5-26	Effect of Aging on Volume Resistivity (PVT in semicon rods)	5-31
5-27	Effect of Aging on Volume Resistivity (PE wax in semicon rods)	5-32
	WEIBULL PLOTS	
5-28	15 kV Cable Impregnated with Ethylene Gas-1 Hour Step Test	5-35
5-29	15 kV Cable Impregnated with Ethylene Gas-6 Hour Step Test	5-35
5-30	15 kV Cable Impregnated with Ethylene Gas-24 Hour Step Test	5-36
5-31	15 kV Cable Impregnated with Ethylene Gas-VT Curve	5-37
6-1	Estimated Cost of 138 kV Cables at 800 mil Insulation Thickness	6-7
6-2	Estimated Cost of 138 kV Cables at 500 mil Insulation Thickness	6-8
6-3	Estimated Normalized Cost of 138 kV Cables-Wire Shield Construction	6-9
6-4	Estimated Normalized Cost of 138 kV 500 KCM Cables-Comparison of Standard and Impregnated Cables	6-11
6-5	Comparison of Relative Costs	6-16
6-6	Comparison of Relative Costs	6-19

TABLES

Table		Page
2-1	Literature Data on Diffusivity and Transmission Rate	2-6
2-2	Diffusion Coefficient of Styrene for Polyethylene (Marlex 50)	2-10
2-3	Characteristics of Polymerization	2-10
3-1	Volatile Content of Control Samples	3-3
3-2	AC Breakdown Strength of Controls	3-5
3-3	Effect of Vacuum Drying and Heat Treatment	3-30
3-4	Effect of Inhibitor on Stopping Polymerization	3-47
3-5	Effect of Temperature on Permeation Rate	3-48
3-6	Impregnation and Diffusivity	3-54
3-7	Linear Regression on Time/Weight Gain Correlation	3-65
3-8	Effect of Impregnation on the Weight of Insulation	3-69
3-9	Summary of Results on Liquid Impregnation	3-75
3-10	Summary of Results on Liquid Impregnation	3-86
3-11	Comparison of Impregnants	3-88
3-12	Grid Program Summary	3-95
3-13	Effect of Vinyl Toluene on AC Breakdown Strength, Model Cable E	3-105
3-14	Comparison of Slabs and Model Cable	3-110
3-15	Summary of Optical Micrographs	3-114
3-16	Summary of Scanning Electronmicrographs	3-121
3-17	Effect of Inhibitor Presence on the Degree of Polymerization	3-125
3-18	Effect of Catalyst Concentration	3-127
3-19	Studies on Factors Affecting Polymerization	3-129
3-20	Polymerization of LMA with Different Catalysts	3-132
3-21	In Situ Polymerization of Vinyl Toluene	3-137
3-22	Summary of the Results of Impregnation and In Situ Polymerization	3-139
3-23	Effect of Polyvinyl Toluene on AC Breakdown Strength	3-147
3-24	Summary of Optical Micrographs	3-151
4-1	Comparison of Specimen Configurations for AC BD Test	4-2
4-2	Impregnants	4-5
4-3	Polymerization Catalysts	4-8
5-1	Comparison of Void Distribution by Optical Microscopy	5-3
5-2	Comparison by Scanning Electron Microscopy	5-9
5-3	Thermoanalytical Characterization	5-17
5-4	Analysis of Insulations	5-22

Table		Page
5-5	Comparison of IR Spectra	5-24
5-6	Impregnation and Polymerization of Vinyl Toluene in Semicon Rods	5-28
6-1	Cable Construction I Wire Shield	6-2
6-2	Cable Construction II Lead Sheath	6-3
6-3	Cable Construction III CLX Sheath	6-4
6-4	Construction Details of 138 kV Cable	6-6
6-5	Comparison of Improved Cables	6-14
6-6	Summary of Relative Costs	6-18

SUMMARY

One major imperfection in high voltage cables with solid polymeric insulation is their microporous structure consisting of voids and interfacial gaps around protrusions and contaminants. Earlier investigation by Phelps Dodge Cable and Wire Company has shown that filling up these voids with a liquid mixture improves the dielectric strength and the slope of the volt-time curve. However, most liquids evaporate at service temperature. The primary objective of the present program was to develop a process for healing the voids permanently by impregnating the cable with a suitable monomer and polymerizing the latter in situ, and to investigate the effect of this treatment on the dielectric properties.

This program involved the study and selection of:

- Test specimens and procedures
- Monomers and catalysts
- Process conditions such as pre and post polymerization drying, impregnation and polymerization

Slabs (2.75 x 1.5 x 0.4 in.) cut from actual 138 kV cables and ditched to 13 or 18 mil were used as test specimens. Subsequently, model cables with 15 mil strand shield and 25 mil insulation were used to confirm the results obtained on the slabs. Measurement of AC breakdown strength at various step intervals was used for monitoring the improvement in the dielectric strength of the insulation. Microscopy, both optical and scanning electron type, was used to monitor the filling of voids and gaps.

It was found that the different specimens have different concentrations of volatiles, depending on their thickness, manufacturing and storage history. Since the volatiles influence the dielectric strength, a process was developed to remove the volatiles by high vacuum drying and obtain a standard base line for monitoring the improvement.

Preliminary work with lauryl methacrylate showed that the rate of impregnation is not enhanced by application of external pressure up

to 100 psi but is substantially increased by raising the temperature. Autopolymerization of monomer-catalyst solutions, a drawback of high temperature impregnation, was successfully overcome by using 100 to 200 ppm of hydroquinone, a polymerization inhibitor.

Systematic investigation of impregnation of slabs with liquids showed that the rate of impregnation varies widely, depending on the chemical structure of the liquid. Aromatic hydrocarbons permeate faster, followed by paraffinic liquids with long alkyl chains. Polar liquids and monomers diffuse at a lower rate into the crosslinked polyethylene matrix. The diffusivity also depends on the molecular size, the small ones migrating faster than the large ones.

Of the number of peroxides and azo catalysts tried, benzoyl peroxide (BPO) was found to be the most efficient catalyst for polymerization of both lauryl methacrylate and vinyl toluene monomers. With 2% catalyst and 200 ppm hydroquinone inhibitor, up to 80% of the impregnated monomer got polymerized. Attempts to get higher yields using higher temperatures and longer times for polymerization were not successful, possibly due to slower diffusion of peroxides into the polymer matrix and faster evaporation of the impregnated monomer. This was confirmed in a grid program on migration of BPO in an ethyl benzene (similar to vinyl toluene) solution. Use of γ radiation (0.11 rad/hour) brought about 100% polymerization in less than three hours, which confirmed the above suggestion. However, the dielectric strength of the irradiated insulation decreased, possibly due to the degradation of the polyethylene chain and the escape of degradation products such as hydrogen.

In model cables, the polymerization yield was found to be low due to the inhibiting effect of the carbon black in the semiconducting layer. In 15 kV and 138 kV cables, where the ratio of strand shield to insulation was smaller, the polymerization yield was substantially higher. Later on, a two step process in which the peroxide and the monomer were impregnated separately, gave a higher yield in the model cables.

The breakdown strength of untreated, 18 mil ditched slabs from 138 kV cables was found to be approximately 2000 V/mil. This decreased by about 25 to 30% on the removal of volatiles. Treatment of the slabs at higher temperatures, particularly beyond the melting point, of polyethylene, improved the dielectric strength. Impregnation with liquids or solids invariably increased the dielectric strength; for example, from 2300 to 3750 V/mil for vinyl toluene. The degree of improvement depends both on the level of impregnation as well as on the chemical nature of the impregnant. Among the liquids and solids tried: vinyl toluene and its polymer, styrene, styrene oxide, acetophenone, 2 phenyl ethyl acrylate, dodecyl vinyl ether and vinyl pyrrolidone were found to give the best results. The level of impregnation for the highest improvement also varies with impregnants,

being minimum (0.5%) for acetophenone. It has been concluded from these results that whereas some liquids act as a void filler, others not only fill the void but act as voltage stabilizers. Most of the liquids belonging to the latter group have aromatic nuclei and three to four double bonds in conjugation. The polymers and the solid form of the liquids bring about similar improvement in dielectric strength as their liquid counterparts. Hence, the physical state does not appear to influence the improvement due to impregnation.

The model cable with 15 mil strand shield and 25 mil insulation showed a dielectric strength of approximately 1200 V/mil. Evacuation reduces this to about 1000 V/mil. The uncured model cable had dielectric strength about 700 V/mil. Impregnation of the model cable with vinyl toluene and subsequent polymerization of the latter improves the dielectric strength to about 1400 V/mil, the same extent as vinyl toluene monomer alone.

Optical micrographs of dyed samples revealed the microporous structure of the cable. The void propensity is higher in the middle of the insulation than at the boundaries. The voids are spherical. Impregnation and in situ polymerization reduced void number and size. Impregnation with lauryl methacrylate and polymerization shows irregular shaped dark spots, which are probably polymer particles in the voids.

Scanning electron micrographs reveal spherulite-like structures with dark spots at the center, which appear to be voids. Impregnation and in situ polymerization fill up the voids but do not affect the spherulite-like structures. Heating beyond 115^{o}C also seems to close the voids.

The reciprocal slope of the VT curve tends to improve on impregnation and in situ polymerization with vinyl toluene.

Impregnation and in situ polymerization with semiconducting shields show that for low levels of impregnation, the volume resistivity does not increase beyond the specified range. The carbon black in the semiconducting layer prevents polymerization so that in any process involving impregnation and in situ polymerization, the level of polymer formed in the strand shield will be minimal.

From the results mentioned above, it is concluded that:

1. Substantial improvement in the dielectric strength and an upward trend in the reciprocal slope of the VT curve of XLPE insulation, can be achieved by impregnation and in situ polymerization of monomers.

2. Whereas some impregnants mainly act as void fillers, others act both as a void filler and voltage stabilizer.

3. It is possible to develop a practical process for impregnation and in situ polymerization of 138 kV cables, especially using monomers containing aromatic nuclei and non-polar groups.

4. This process appears to give cable costing about the same as other advanced processes-dry cure with a lead jacket or additives.

Based on the above observations, it is recommended that:

1. The studies on impregnation and in situ polymerization as a tool to heal the microporosity of power cables be continued using 15 kV or 35 kV vinyl toluene impregnated cables. This will minimize the difficulty involved in polymerization and give valuable data relevant to cable performance. The objective here will be to evaluate the improvement more quantitatively, using both short term and long term electrical aging tests and to evaluate other vital electrical properties such as dielectric constant, power factor and water tree resistance.

2. Carry out a similar study with dodecyl vinyl ether and polyethylene oligomers.

3. Select the best monomer and the optimum process conditions.

4. Carry out impregnation and polymerization with a 138 kV cable and subject it to both long term and short term tests.

Section 1

INTRODUCTION

At the present time in the United States, most high voltage transmission cables, 138 kV and above, are oil impregnated paper insulated pipe cables. They have established an enviable record of reliability through decades of supportive research, testing and service. However, the extruded cables in this range offer sound economic and operational advantages such as:

- Greater transmission efficiency due to lower dielectric loss.
- Greater economy due to lower capital and operating cost particularly due to the elimination of pipes, oil and oil pumping facilities.
- Possibility of higher rating for the same conductor size due to better heat transfer.

Their widespread use is hindered due to concern regarding their reliability. This arises from the variation in dielectric behavior of polyethylene and ethylene-propylene copolymer insulated cables both in laboratory testing and in limited field experience. Data (1) from the last 10 to 15 years of service shows that crosslinked polyethylene (XLPE) insulated 5-35 kV cables are superior to thermoplastic polyethylene 5-35 kV cables, yet there are failures with it and the frequency of such failures increases with service life. Hence, it is desirable for XLPE cables, 138 kV and above, that their quality be improved and their service reliability established.

Although the mechanism of breakdown has not been firmly established, it is generally accepted that the breakdown starts from imperfections present in the bulk of the insulation as well as at the shield insulation interfaces. They are:

- Contaminants, metallic and non-metallic, present in the starting materials or introduced during manufacture.
- Protrusions starting from conductor or insulation shields.

- Ambers and gels, due to improper mixing and scorch.

- Voids and interfacial gaps caused by, for example, solubility and subsequent condensation of steam or shrinkage on cooling from curing temperature to room temperature.

With steam curing, voids are large in number (2), of the order of 10^5 per cubic millimeter and their sizes vary from a few tenths of a micrometer to about 50 μm. Their number (3) is smaller near the conductor and outer sheath but appreciably greater in the middle. Interfacial gaps, due to poor wetting, may occur at the interface between the polyethylene and contaminants, protrusions and ambers.

At present, two basic modes of failure are generally recognized:

- Electrical treeing

- Electrochemical or water treeing

The inhomogenities accentuate (4) the applied electrical stress, causing high local stress concentration. In electrical treeing, as the local stress reaches the corona inception level, discharges take place (5). The gases in the voids and interfacial gaps ionize resulting in electron injection and trapping. The latter leads to chain scission, degradation and carbonization of the polymeric insulation, resulting in a rapid tree-like growth and failure.

In contrast to electrical treeing, water trees (6) grow slowly and are due to interaction of the electrical field and water at imperfections. There are many theories (7) regarding the inception and growth of water trees in the solid insulation, although none of them so far explain all the observed phenomena.

As the trees grow and bridge a significant portion of the insulation wall, they reduce the volume resistivity, increase the dielectric loss and lower the breakdown strength. It has been shown (8) that electrical trees may start from water trees. In short, failure of cables is probably initiated by electrical or electrochemical phenomena at voids, protrusions, contaminants or interfacial gaps between protrusions or contaminants and the insulation. Hence, the deactivation, elimination or healing of the voids and interfacial gaps should result in improved insulation quality (9).

In this program we evaluated ways to deactivate, eliminate or otherwise heal voids and interfacial gaps. Our approach has its genesis in the results obtained by Phelps Dodge Cable & Wire Company in its study on the mechanism of breakdown, funded by EPRI and DOE in its

contract #7809-1 (10). During this study it was observed that:

- Impregnation of the cable with gases like sulfur hexafluoride improves the dielectric strength of the cable.
- The degree of improvement increases with increased gas pressure.
- Impregnation of the cable with a liquid, principally triethylene glycol and a small amount of penetrant such as para xylene, significantly improves the dielectric strength and flattens the volt-time curve.

These results pointed to a method to improve the quality of the cable by filling the voids with an impregnant. However, at the 90°C service temperature, most liquid impregnants would migrate out of the insulation in a relatively short period of time. It was therefore proposed that the cable be impregnated with a liquid monomer and the latter polymerized in situ. In this case the voids would be permanently filled. By suitable choice of impregnant and impregnation and in situ polymerization conditions, the quality of the cables could be greatly improved. Since the voids and interfacial gaps are approximately 1 to 1.5% of the total volume of the insulation, the amount of impregnant required is small. In any case once the feasibility of the process is established, the technology could be improved to make this process competitive with other methods of producing quality power cables. Further, this method has the built-in advantage of possibly introducing voltage stabilizing or tree resistant impregnants to the imperfection regions.

Based on the above approach, a three phase work program was planned:

1. Laboratory scale investigation of materials and processes.
2. Development of model cables nominally rated 15 kV.
3. Development of 138 or 230 kV cables.

The goal of the first phase was to select the best polymerizable impregnant which gives the maximum improvement in short term dielectric strength. First we investigated the various process parameters for impregnation, such as the effect of vacuum drying, external pressure and temperature, etc. Then the process conditions for polymerization: Initiator selection and concentration, inhibitor selection and concentration, polymerization time and temperature and the atmosphere in the polymerization chamber, etc. were investigated to develop a method for locking the impregnants in the voids. Then the dielectric

strength of the treated samples was measured at various step times to monitor the improvement in the quality of the cable. Optical and scanning electron microscopy were then performed to examine the level of void filling.

The program was terminated at the end of Phase 1.

Section 2

THEORETICAL CONSIDERATIONS

Several aspects of the proposed work, such as the interaction of solid polymers with liquids, in situ polymerization, grafting and the effect of the modification of polymers on their dielectric properties were studied in the past by a number of researchers. Some general principles derived from their work and available in the pertinent literature were considered in assessing the relative merits of potential approaches, and in formulating the experimental program of this project. These theoretical considerations deal with four basic problem areas:

- Removal of volatiles from the solid polymer matrix (e. g. vacuum drying)
- Impregnation of the insulation with liquid impregnants (e. g. monomers or monomer-catalyst solutions)
- Polymerization of the absorbed monomer in situ and/or its grafting onto the polymer chain
- The effect of modification on the dielectric strength of insulation

2.1 REMOVAL OF VOLATILES

2.1.1 Vacuum Drying

The crosslinked polyethylene insulation contains volatile components consisting of water and of the by-products of the decomposition of Dicumyl peroxide (Dicup): mostly cumyl alcohol (cuminol), acetophenone and α methyl styrene (11). Their concentration in the freshly made cable corresponds to the concentration of Dicup originally present, and decreases with time, due to spontaneous volatilization. This depletion is accelerated by the application of heat and/or vacuum.

The cross section of a slab of insulation is represented by the fol-

lowing schematic diagram,

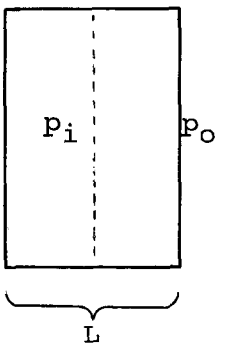

where: L = thickness of the slab
p_i = partial pressure of each volatile inside the slab
p_o = partial pressure of atmosphere surrounding the slab (vacuum level)

The volatiles such as acetophenone, cumyl alcohol and ∝ methyl styrene are present throughout the matrix. The concentration is higher at the center, compared to that at the surface. However, since we aim at complete removal, the concentration in the center and the distance from the center to the surface (L/2) are important. The loss of volatiles under vacuum should follow Fick's law (12) of diffusion and the rate of removal can be given by the following equation:

$$Q = \frac{ASD\ (p_i - p_o)}{L/2} \qquad (2\text{-}1)$$

where: Q = the amount of each volatile lost per unit time.
A = area of cross section.
S = solubility
D = concentration independent diffusion constant for each species at a given temperature.

In the present case, p_o is equal to the vacuum level maintained in the chamber, which depends on the pumping capacity and the leak rate of the system. It is obvious that the higher the $(p_i - p_o)$ value, the greater the rate of removal. The vapor pressures of the volatiles at 70 and 90°C are presented below (13):

VOLATILES	VAPOR PRESSURE (μm) AT: 70°C	90°C
WATER	233,700	525,760
∝ METHYL STYRENE	28,000	64,000
ACETOPHENONE	6,800	18,000
CUMYL ALCOHOL	3,400	12,000

It appears that even for the least volatile material, namely cumyl alcohol, the vapor pressure at 70°C is very high compared to the vacuum level P_o ($\approx$ 20 μm). Hence, a better vacuum may not exert any significant effect on the rate of removal, Q. On the other hand, by increasing the temperature 20°C (from 70 to 90°C), the value of P_i increases almost 3 times and Q increases significantly. These conclusions are confirmed by analytical results presented elsewhere in this Report (Figures 3-26 and 3-27). They show that it takes about 10 days to remove most of the volatiles at 70°C compared to 7 days at 90°C. However, high temperature may have some effect on the morphology of the insulation (14). Hence, vacuum drying at 70 or 80°C is preferable to 90°C.

2.1.2 Removal of Excess Impregnant

The removal of unreacted monomer after incomplete polymerization is a process analogous to the removal of the volatiles prior to impregnation and is subject to similar considerations. It can be enhanced by vacuum and by heat. One potential difference of practical consequence is the low volatility of some of the monomers used, giving a longer time for their complete removal.

2.2 IMPREGNATION

2.2.1 Mechanism of Impregnation

The process of impregnation is opposite to that of evacuation. Depending on the morphology of the insulation and on the physical state of the impregnant, three different mechanisms should be considered:

2.2.1.1 Flow Through Microchannels

There is some evidence to support that some of the voids in XLPE

insulation are connected by microchannels (4). If the channels are considered equivalent to capillaries, the rate of flow will be given by Poiseuille's equation (15):

$$Q = \frac{\pi r^4 (P_o - P_i)}{8 \sum l_i \eta} \qquad (2\text{-}2)$$

where: Q = rate of flow through unit cross section and thickness.
P_o = pressure outside the slab.
P_i = pressure inside the slab (initially approximately the same as the vacuum level in the impregnation chamber).
r = average radius of the capillary channels.
l_i = effective length of the channels.
η = viscosity of the impregnant.

The effective length of the channels (l_i) can be greater than the half of the slab thickness ($L_{\frac{1}{2}}$) because the channels may follow a zig-zag path.

2.2.1.2 Gas Phase Permeation

If the impregnant is relatively volatile, it will vaporize at the temperature of impregnation and will be absorbed by the insulation through the process of vapor permeation (16). The rate of impregnation will then be given by Equation (2-3):

$$Q = \frac{DS\ (P_o - P_i)}{L_{\frac{1}{2}}} \qquad (2\text{-}3)$$

where: Q = rate of flow through unit cross section
D = diffusion coefficient
S = solubility
$L_{\frac{1}{2}}$ = one half of slab thickness (L)
P_o = vapor pressure of impregnant outside the slab
P_i = vapor pressure of impregnant inside the slab

In the presence of moderate external pressures, the rate of permeation may be higher, particularly as the solubility increases with pressure (16). However, for organic vapors Henry's law for solubility of gases in a polymer is not strictly obeyed and the diffusion coefficient is not independent of concentration. Hence, the simple equation does not give the proper rate; however, it illustrates

the key parameters governing the impregnation process. The rate will be highly dependent on temperature, as the latter determines the vapor pressure of the permeant and hence $(P_o - P_i)$.

2.2.1.3 Liquid Phase Permeation

The impregnant, if sufficiently non-volatile, will migrate in the liquid phase. The process of impregnation will take place by solubilization and diffusion of the impregnant through the matrix (17). The rate of flow will be given by Equation (2-4):

$$Q = \frac{D\ (C_o - C_i)}{L_{\frac{1}{2}}} \qquad (2\text{-}4)$$

where: Q = rate of flow through unit cross section and thickness
D = Diffusion coefficient
$L_{\frac{1}{2}}$ = one half of slab thickness (L)
C_o = concentration of the impregnant in the outside surface and controlled by the solubility (S) of the permeant
C_i = the same at the center of the slab

The maximum concentration difference for all practical purposes is equal to the equilibrium concentration of the liquid in the substrate. The effect of external pressure will be minimal because S does not change very much with external pressure; but that of temperature will be great, due to the increase both in D and in S.

Preliminary experiments carried out at various pre-impregnation vacuum levels and external pressures confirm that the pressure differential between outside and inside the voids $(P_o - P_i)$, does not have significant effect on the rate. It would therefore follow that the impregnation is taking place mainly by liquid phase permeation. To make this process effective, one has to increase D, S or C_o, the surface concentration of the impregnant.

Diffusion is an activated process and hence the diffusion coefficient corresponding to zero concentration, D_o, increases substantially with increasing temperature. The D_o values of some alkyl esters (18) and solvents into polymethyl methacrylate are given in Table 2-1. It shows that D_o increases by an order of magnitude for every 10°C rise in temperature.

Solubility of an organic liquid in a polymer also increases with temperature, mainly because of the higher entropy change in mixing. This is especially true for semi-crystalline polymers like polyeth-

Table 2-1

LITERATURE DATA ON DIFFUSIVITY AND TRANSMISSION RATE

Diffusivity of Organic Liquids Through Polymethyl Methacrylate (18)

TEMP.°C	D_o For METHYL ACR.	D_o For ETHYL ACR.	D_o For BUTYL ACR.	TEMP.°C	D_o For METHANOL	D_o For BENZENE
25	1.0×10^{-10}	6.0×10^{-10}	5×10^{-10}	30	0.1×10^{-6}	0.06×10^{-8}
45	10×10^{-8}	6.3×10^{-8}	1.1×10^{-8}	50	1.2×10^{-6}	5.40×10^{-8}
65	10.5×10^{-7}	5.7×10^{-7}	2.0×10^{-7}	60	3.8×10^{-6}	20.0×10^{-8}

ACR = Acrylate $D_o = cm^2/sec.$

Rate of Transmission of Organic Liquids Through LDPE (20)

Rate of Transmission (T) in (g) (mil)/(m^2) (24 hr.)

LIQUID	T @ 0°C	T @ 21.1°C	T @ 54.4°C
N HEXANE	3.88	10.4	186
DECANE	490	3.890	57,000
TETRADECANE	26.6	220	6260
ETHYLACETATE	29.5	256	5,860
N BUTYLACETATE	8.68	13.4	4,170
METHYLALCOHOL	3.88	18.9	448
AMYLALCOHOL	-	3.10	-

ylene, where change in morphology aids this process. An independent study (19) shows that the saturation level of water in polyethylene increases dramatically above 40°C. In Table 2-1 the transmission rates (T) of a number of paraffinic liquids, alkyl esters and alcohols, through polyethylene are presented (20). The rate increases substantially with temperature, especially as 50°C is approached. This is in agreement with the solubility data for water. In the homolog series of paraffinic liquids the T values increase from Hexane (C_6H_{14}) to Decane ($C_{10}H_{22}$) but then decrease for Tetradecane ($C_{14}H_{30}$).

In the case of alkyl esters and alcohols the T values decrease with an increase in molecular size. This is possibly due to a complex interplay of D and S which are affected differently by the chemical structure and molecular size. In conclusion, one can effectively increase the rate of impregnation of liquids through XLPE slabs by:

- Increasing the temperature of impregnation.
- By proper choice of impregnant for which both D and S are high.

2.2.2 Estimation of the Time Required for Impregnating the Cable

Since the ultimate objective is to impregnate a full size cable, it is important to have an approximate estimate of the time required for this process. For cylindrical geometry, Equation 2-4 for the rate of impregnation (Q) is modified as:

$$Q = \frac{2\pi D\ (C_o - C_i)}{\ln\ (b/a)} \qquad (2\text{-}5)$$

where: b = outer radius of insulation
a = inner radius of insulation
C_o = concentration of the impregnant liquid in the outside surface layer of insulation
C_i = the same at the insulation/conductor shield interface

This equation applies to thin layers where the concentration gradient across the thickness is linear. For thick layers the concentration gradient in the initial state is non-linear. Assuming that the equation holds, the rate of impregnation can be calculated if D, C_i, C_o, b and a are known.

Diffusion constants for monomers are not readily available in the

literature. Mangaraj, et al has measured diffusivity of styrene (21) in Marlex polyethylene for various film thicknesses. The results are presented in Table 2-2. It has been observed that diffusivity increases with film thickness, although the crystallinity remains the same, approximately 75%. This may be due to the presence of increasing number of voids in the thicker films. Although the insulation thickness in our case is around 2 cm (0.8 inch) and the insulation is crosslinked polyethylene instead of Marlex 50, in the absence of more suitable data, the diffusity for 95 mil film may be used for this calculation. The concentration C_o on the outer surface may be assumed to be 15% at room temperature, and the concentration on the inner surface C_i may be assumed to be zero. The outer and inner radii for a 138 kV cable is approximately 3.5 and 1.5 cm respectively. Using the above data, the rate of flow across a unit section:

$$Q = \frac{2 \times 3.141 \times 2.98 \times 10^{-8} \text{ cm}^2/\text{sec.} \ (15-0)\%}{2.303 \log \ (3.5/1.5)} = 0.5 \times 10^{-5} \%/\text{sec}$$

In order to impregnate the cable with 7.5% styrene, i. e., up to half saturation level, approximately 17.4 days are required. An alternate solution using Equation 2-4 (22) is:

$$\frac{t_{\frac{1}{2}}}{L^2} = \frac{0.04919}{D} \qquad (2\text{-}6)$$

where: L = insulation thickness
$t_{\frac{1}{2}}$ = the time required for half-saturating the slabs

If the diffusion takes place from one side, L = 2 cm and $t_{\frac{1}{2}}$ equals 76.4 days. On the other hand if the diffusion proceeds from both sides, the time required is approximately 19.1 days. Since the void volume is around 1 to 2%, time required for impregnation of a monomer similar to styrene to that level should be much smaller than the 17.4-19.1 days calculated.

The above discussion therefore supports the conclusions:

- Time required for impregnation is not impractical.
- Rate of impregnation can be increased by:
  --increasing temperature
  --proper choice of the impregnant

2.3 POLYMERIZATION

Monomers, by repetitive chemical reaction, form large molecules or polymers. This process is known as polymerization. There are two main types of polymerization, namely stepgrowth and chain addition (23). The stepgrowth polymerization or condensation polymerization, in the majority of cases, involves condensation of two functional groups such as -OH, $-NH_2$, -COOH, etc., eliminating a small molecule such as water, HCl, etc. Chain polymerization involves repetitive addition of unsaturated molecules initiated either by free radicals, anions or cations generated by a catalyst or by radiation. The important differences between the two processes are given in Table 2-3.

Free radical initiated chain polymerization is preferred for the present work, because it does not involve:

- Catalysts having ionic by-products resulting in inorganic contamination.
- Formation of small molecules like water, HCl, etc., removal of which may result in voids and in undesirable electrical properties.
- High temperature.

Hence throughout the work, only addition polymerization has been used. A scheme of reactions, constituting addition polymerization is given in Figure 2-1.

Catalysts such as organic peroxides (R-O-OH) decompose thermally, giving free radicals (species containing free electrons) such as $R^{\bullet}$ and $RO^{\bullet}$. A free radical combines with an unsaturated monomer ($CH_2 = CHX$) to produce a chain radical ($R-CH_2-\dot{C}HX$). The net change in the process is the shift of the position of the electron from the carbon atom in the free radical to the carbon atom of the monomer to form a primary chain radical. The latter then repeats this process and add a large number of monomer units to give a polymer radical $RO-(CH_2-CHX)_n - CH_2 - \dot{C}HX$. This step is called propagation.

The polymeric radicals, at some stage of their growth, undergo termination either by coupling, disproportionation or activity transfer, lose their free electron and become a saturated molecule known as the polymer. In the schematic representation, Figure 2-1, only coupling is shown to illustrate the termination. In disproportionation one radical takes a hydrogen atom from the other and the latter is left with a double bond. In transfer process, the radical abstracts a hydrogen or an active group from the solvent or foreign material

Table 2-2

DIFFUSION COEFFICIENT OF STYRENE FOR POLYETHYLENE (MARLEX 50)

Film Thickness, mil	D x 10^8 cm^2/sec. at 25°C
1	1.20
10	1.85
30	2.09
95	2.98

Table 2-3

CHARACTERISTICS OF POLYMERIZATION

	Stepgrowth	Addition
1.	Monomers are di or multifunctional.	Monomers are unsaturated compounds.
2.	Chain growth slow, takes place in steps.	Chain growth rapid.
3.	Eliminates small molecules or moieties in majority of cases.	No elimination, simple addition.
4.	Molecular formula of the polymer is not integral multiple of the monomer.	Molecular formula of the polymer is integral multiple of the monomer.
5.	Catalysts are ionic such as acids and bases.	Catalysts are free radical precursors, ion radical or organometallic complexes.
6.	Requires high temperature.	Usually takes place at moderate temperature.

1. CATALYST DECOMPOSITION

$$ROOR \xrightarrow{\text{Heat}} 2RO\bullet \longrightarrow 2R\bullet + O_2$$

Peroxide Catalyst — Oxyradical — Alkyl Radical

2. MONOMER RADICAL FORMATION

$$RO\bullet + CH_2 = CHX \xrightarrow{\text{Initiation}} ROCH_2\text{-}\dot{C}HX$$

Oxy Radical + Monomer — Monomer Radical

3. CHAIN GROWTH

$$ROCH_2\dot{C}HX + n(CH_2{=}CHX) \xrightarrow{\text{Propagation}} RO(CH_2CHX)_n\text{-}CH_2\text{-}\dot{C}HX$$

Monomer Radical + Monomer — Chain Radical

4. CHAIN GROWTH STOP

$$2RO(CH_2\text{-}CHX)_n\text{-}CH_2\text{-}\dot{C}HX \xrightarrow{\text{Termination}} RO(CH_2\text{-}CHX)_{2n+2}OR$$

Chain Radical — (Coupling) — Polymer

RESULT: $\sim(CH_2\text{-}CHX)\sim_m$

Homopolymer

(Repeating Unit)

R = Alkyl or Aryl group such as $-CH_3$, $-C_2H_5$, $-C_6H_5$, etc.
ROOR = Peroxide such as Dicup
X = Functional group such as -OH, -Cl, -COOH, $-COOCH_3$, $-OCOCH_3$, etc.
m = Integer
n = Integer

Figure 2-1 REACTION STEPS IN ADDITION POLYMERIZATION

present in the system, becomes saturated but generates a new radical.

In addition to free radical precursors such as peroxides and azonitriles, active cations (e.g. S_n^{4+}), anions (e. g. butyllithium), organometallic complexes such as trialkyl aluminum with titanium chloride, and active surfaces of chromic and molybdenic oxides initiate polymerization. Radiations such as X-ray, UV light, γ ray, electron beam and active electrodes can initiate chain polymerization.

A special case of polymerization is grafting or graft polymerization. The different steps of this reaction are presented in Figure 2-2. In this case the reaction takes place between an already formed polymer and monomers. An active free radical, anion or cation abstracts a hydrogen atom from the polymer forming a polymeric radical, which carries out the propagation steps like a primary radical in the earlier scheme. The termination takes place by coupling, disproportionation or transfer as mentioned above. The polymer so formed differs from a simple homo or copolymer because in this case long sequences of monomer or monomers grow like brances out of a polymer chain, used as the starting material, and are intimately bound to them. In situ polymerization, on the other hand, refers to the polymerization of the impregnated monomer in place and does not involve bonding between the newly formed polymer and the polymeric matrix. This follows a reaction scheme, same as given in Fig. 2-1.

At the steady state, the rate of generating radicals is equal to the rate of consumption of the same. If the activity of radicals is assumed to be independent of the size (24), and if all termination process is biradical, then the rate (25) is given as:

$$R_p = \frac{K_p}{K_t^{\frac{1}{2}}} \; Kd^{\frac{1}{2}} \; f \; [M] \; [I]^{\frac{1}{2}} \qquad (2\text{-}8)$$

where:
- R_p = rate of polymerization.
- K_p, K_t, Kd = rate constants for propagation, termination and catalyst decomposition processes, respectively.
- f = efficiency factor, showing the fraction of the free radicals generated that actually take part in the initiation process.
- $[M]$, $[I]$ = concentrations of the monomer and catalyst, respectively.

This equation is valid for graft polymerization as well as for bulk

STEPS

1. CATALYST DECOMPOSITION

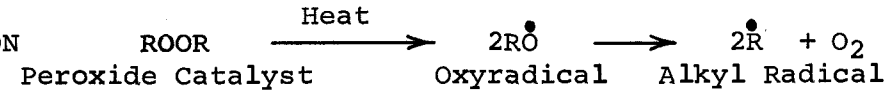

2. HYDROGEN ABSTRACTION FROM PE

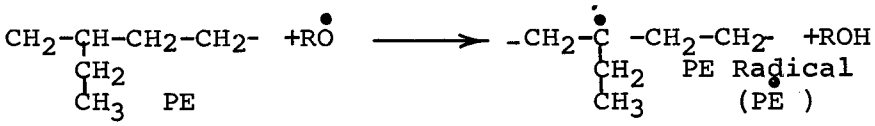

3. INITIATION

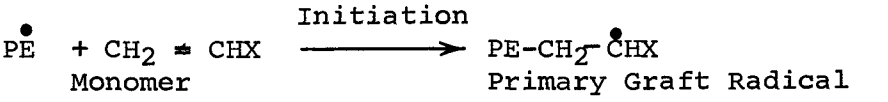

4. GRAFT CHAIN GROWTH

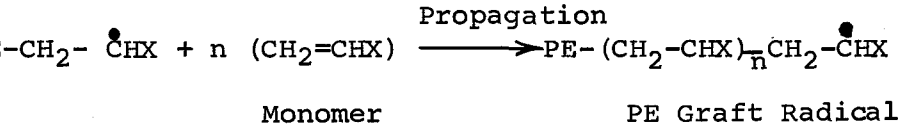

5. CHAIN GROWTH STOP

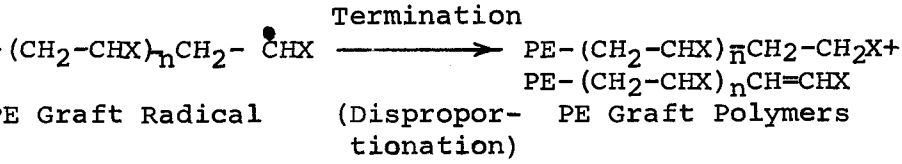

RESULT:

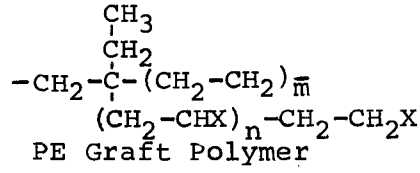

ROOR = Peroxide such as Dicup
R = Alkyl or Aryl group such as $-CH_3$, $-C_2H_5$, C_6H_5, etc.
PE = Polyethylene
X = Functional group such as -Cl, -COOH, $-COOCH_3$, $-OCOCH_3$, $-OCH_3$, etc.
m = Integer
n = Integer

Figure 2-2 REACTION STEPS IN GRAFT POLYMERIZATION

or solution polymerization, since the activity of the radical is independent of the size and medium. In radiation-induced polymerization, the rate of initiation depends on the rate of generation of free radicals. The latter depends on the intensity of radiation and on a "g" factor which gives the number of moles of radicals generated for each unit of radiation.

In the present case the monomers containing dissolved catalysts were absorbed in a crosslinked polyethylene matrix and were subsequently polymerized by heating. The rate of initiation depends on the concentration of the initiator in the matrix which may not necessarily be the same as in the bulk of the solution due to the different rates of migration of the monomer and the initiator. The rate of propagation depends on the concentration of the monomer in the matrix. As the matrix is microporous, the concentration of the monomer in the voids or pores is the same as in the bulk, whereas that in the matrix depends on the level of impregnation in the matrix. The rate of polymerization in the voids therefore could be much higher than the rate of polymerization in the matrix. In the ideal case, as the polymerization takes place in the voids, more monomer will migrate into the void and become polymerized. Hence, the extent of polymerization in the matrix will be small. On the other hand, if the monomer is a good solvent for the matrix, the rates of polymerization in the matrix and in the voids can be comparable. Hence, polymerization takes place throughout the insulation instead of in the voids only.

In the present case the cable or the slabs are immersed in a dilute solution of catalyst in the monomer. In the event the rate of permeation of the catalyst is slower than the monomer, the catalyst concentration in the matrix (with respect to monomer) is smaller, resulting in a slow rate of polymerization.

2.4 AC BREAKDOWN TEST

Among the various methods available for testing improvements in cable quality, the measurement of dielectric strength is highly relevant and widely used. Further, it is known that filling the voids in a cable increases the dielectric strength (5). Hence, any improvement due to filling of the voids is expected to result in an increase in dielectric strength.

It is well known that if the dielectric is free from impurities and imperfections, then electrical failure takes place at very high voltages probably in the form of electron avalanche. The electrical stress gradient (V/mil) in such failure is known as intrinsic dielectric strength. However, all real-life samples have impurities and interfaces. Hence, the measured dielectric strength is far below

the intrinsic strength. There are at least four modes of failure under these conditions (26), namely:

1. Electromechanical breakdown.

2. Breakdown due to electrical discharge.

3. Thermal and chemical failure.

4. Surface breakdown.

1. Electromechanical breakdown: When voltage is applied, the dielectric gets compressed due to the electrostatic field. Compression decreases the thickness, leading to greater field and in consequence, failure takes place due to mechanical collapse. This usually occurs at very high electrical stresses comparable to intrinsic strength.

2. Breakdown due to discharge: This occurs far below the intrinsic strength. The real-life dielectrics often contain voids and interfaces in the matrix. When voltage is applied across the dielectric, discharge occurs in the voids and at the interfaces as soon as the electrical stress across the void reaches a certain minimum value. If voltage V is applied to the insulation, the voltage across the void, V_v:

$$V_v = \frac{VC_s}{C_v + C_s} \qquad (2\text{-}8)$$

where: C_v = the capacitance of the void.
C_s = that of the solid dielectric in line with it.

When V_v reaches V_i, the voltage for inception of corona, discharge takes place and the voltage collapses and then rises again. If the voltage is sufficiently high, discharges take place in every cycle. The walls of the void are eroded due to bombardment by charged particles, the void changes shape, the field is intensified and eventually failure takes place, accompanied by carbonization. This phenomenon is usually known as electrical treeing.

3. Thermal and chemical failure: When alternating electrical stress is applied, heat is generated within the dielectric. Since the heat transfer is poor in solid dielectrics, the temperature rises. In the

course of time, the temperature may rise above the melting or softening point causing electrical failure. On the other hand, chemical reactions such as oxidation may take place at these higher temperatures resulting in enhanced dielectric loss, enhanced heating and dielectric failure.

4. Surface breakdown: This may occur via tracking or flashover. In the latter case the solid dielectric is immersed in a liquid or gas and then breakdown takes place in the liquid or gas phase, and not in the solid phase. Tracking, however, occurs due to discharges on the surface forming a conductive path.

Electrical failure due to discharges in the voids is the main focus in this program. Hence, the breakdown strength measurement in this work relates to the second type of failure mentioned above.

2.4.1 Measurement of Dielectric Strength

Since electrical failure due to voids in the matrix is a random phenomenon, a single measurement does not depict the true breakdown strength of the material. Hence, a number of breakdown tests have to be performed and a statistical average taken. The Weibull statistics used for this, have been described by McKean (27). In actual practice, ten samples of the insulation are subjected to electrical stress, which increases at regular intervals. This is continued until failure takes place. The voltage and time for each failure are noted and the multiple step test result is converted to the equivalent single step value (27). The single step results are then ascribed Weibull probability values of 9, 18, 27...91% in increasing order. A plot is made with dielectric strength as X axis and probability as Y axis in a Weibull chart. The value corresponding to 50% probability gives the mean dielectric strength in Volts/mil.

2.4.2 Lifetime Test

The conversion of a multiple step test to a single step is based on the established stress-time correlation:

$$V_o^n t = A \qquad (2\text{-}9)$$

where: V_o = the applied stress.
t = the time to failure.
n = a life exponent, characterizing the material and its processing.

A = constant

This empirical correlation provides a method for predicting life at low voltage by carrying out experiments at high voltages. In fact, if experiments are carried out in which t, the step time is raised from minutes to weeks, then log V can be plotted against log t. The linear correlation provides negative slopes from which n can be calculated. The higher n is, the longer the cable withstands service stress, usually much smaller than test stress. Thus, measurement of dielectric strength and 'n' is a measure of the improvement that any treatment brings upon the cable. Detailed discussion on this subject has been given by McKean, et al (28).

Section 3

RESULTS AND DISCUSSION, IMPREGNATION AND POLYMERIZATION

A major part of the work consisted of impregnating crosslinked polyethylene insulation (slabs cut from 138 kV cables and model cables) with monomers, followed by in situ polymerization of the impregnant. The effect of treatment on the insulation was monitored by measuring weight gain and dielectric strength, and by observing the effect on voids by optical and scanning electron microscopy. These findings were compared with similar data on controls. The results of this work are presented and discussed under the headings:

- Controls
- Vacuum drying
- Impregnation
- Polymerization

3.1 CONTROLS

Both slabs from cables A, B and J and model cables C to H were used as controls to monitor the effect of the treatments listed above. These cables are specified in detail on pages 4-1 and 4-4. They were carefully examined with respect to volatile content, AC breakdown strength and morphology.

3.1.1 Volatile Content

The volatiles in the XLPE insulation are acetophenone, cumyl alcohol, α methyl styrene and a small amount of water. They are produced by the decomposition of dicumyl peroxide and crosslinking of polyethylene chain, as shown in the scheme below:

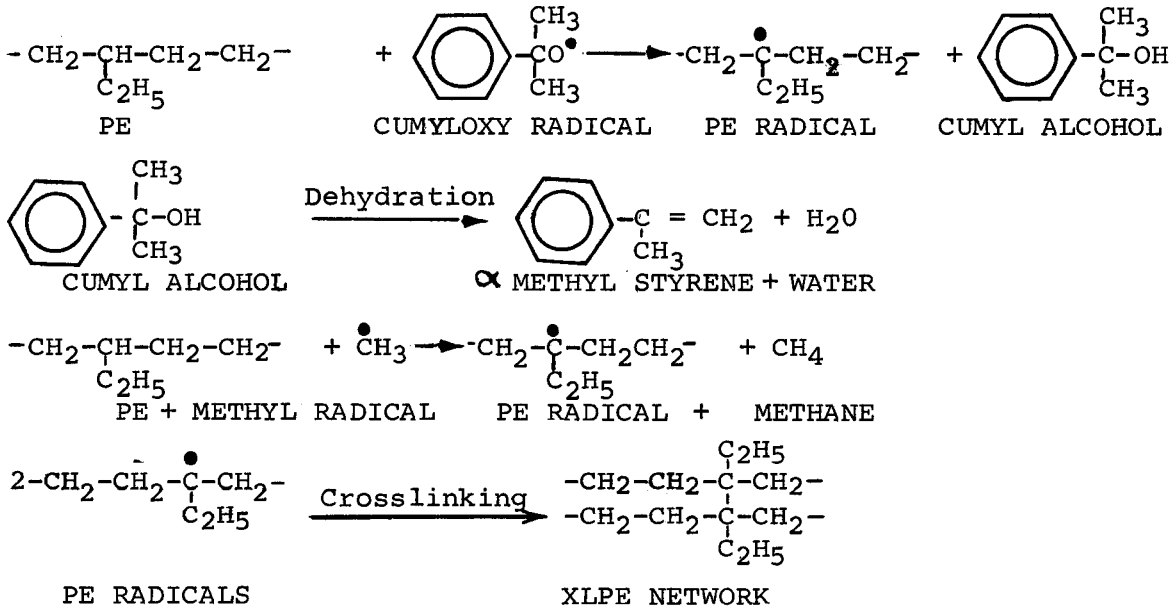

Methane usually escapes within a short time, due to its high permeability. The other by-products stay in the insulation for quite some time and their concentration depends on the age of the cable as well as on the service or storage history. The volatile contents of different cables are compared in Table 3-1. The analysis of volatiles in cable A agree with data reported by Wagner, et al (11). The concentration of volatiles in cable B is somewhat lower than in cable A. This may be attributed to the fact that the insulation in cable B was manufactured with a compound of lower peroxide content. In cable J the low volatile level is attributed to the age of specimens.

The levels of volatiles are significantly lower in the model cables than those in the 138 kV cables probably because the commercial crosslinkable polyethylene compound was supplied with significantly lower dicumyl peroxide (Dicup). Furthermore, part of the volatiles escaped through the thin walls of the model cables before they were analyzed. The rate of escape from the 138 kV cables is much lower due to their much greater thickness (800 mil compared to 25 mil). The rate of permeation is inversely proportional to the thickness, thus making the escape rate at least 30 times lower for the 138 kV cables. In the case of the uncured specimen (cable D), the peroxide decomposed while being injected into the gas chromatograph and hence its decomposition products were caught by the column. Further, it may be noted that the amount of volatiles in the separately cured cable, cable E, is half as much as that cured by continuous vulcanizing process, cable C. This may be because a certain amount of peroxide has decomposed during the extrusion process and part of the volatiles escaped before the beginning of the vulcanization process. Generally the concentration of cumyl alcohol is approximately

Table 3-1

VOLATILE CONTENT OF CONTROL SAMPLES

* Sample	Configuration	Gel Fraction, %	Volatiles as weight % of insulation			
			Acetophenone	Cumyl Alcohol	α Methyl Styrene	Total
Cable A	Slab	> 75	0.283	1.170	0.0290	1.482
Cable B	"	> 75	0.325	0.910	0.0450	1.280
Cable J	"	> 75	0.076	0.374	0.007	0.457
Cable C	Model Cable	80.1	0.025	0.043	0.0004	0.068
Cable E	"	77.5	0.014	0.023	0.0006	0.038
Cable D	"	0	0.355	0.315	0.0005	0.671
Cable F	"	69.0	0.073	0.020	0.002	0.095

* Cables A to J are specified in detail on pages 4-1 and 4-4.

three to four times higher than acetophenone, which suggests that the cumyloxy radicals are better hydrogen abstractors than the methyl radicals. Alternatively, these radicals may have greater reactivity for hydrogen abstraction than for disproportionation.

3.1.2 AC Breakdown Strength

3.1.2.1 AC Step-Up Tests. The breakdown strength of untreated slabs from cables A, B and J was measured, following the procedure described in Section 4.4. The breakdown voltages are plotted against Weibull probability in Figures 3-1 and 3-2. The V_{10}, V_{50} and V_{90} values, i. e., the breakdown strength corresponding to 10, 50 and 90% probabilities respectively are presented in Table 3-2.

The 1 hour step breakdown strength values (V_{50}) for cables A, B and J at 18 mil effective thickness are all about 2000 V/mil whereas cable B at 13 mil thickness is 2300 V/mil. This is in agreement with the well-known fact that the measured dielectric strength usually increases with decreasing thickness.

The breakdown strength of model cables (C to H) was obtained by using the procedure described in Section 4.4. The Weibull plots for untreated model cables are given in Figures 3-3 to 3-6 for the 10 minute and 1 hour step-up tests, in Figures 3-7 and 3-8 for tests at constant stress. The V_{50} values are listed in Table 3-2. The average 1 hour breakdown strength of the continuously cured model cables, approximately 1100 to 1200 V/mil, is somewhat lower than the 2000 V/mil for slabs. This is probably due to the heavier walls, larger volume under stress and the non-uniform electric field of the model cables.

The dielectric strength of uncured model cable (cable D, Figure 3-3) is about one half of that for the cured samples. The flash-cured cables (F and G) have lower dielectric strength than the continuously cured (C) and the separately cured (E) cables.

The gel content of these cables shows a progression from 0% for the uncured cable D to 80.1% for cable C, which approximately correlates with the breakdown strength.

3.1.2.2 Stress Time Correlation. During the service life of cables, they undergo aging due to electrical stress. Hence, the strength measured at longer step times is a better measure of the cable quality than the strength measured at short step-up times. In fact, if the strength of the insulation is measured at different step-up times and the V_{50} values are plotted against step time on logarithmic scales (known as VT curves) a linear correlation is expected.

Table 3-2

AC BREAKDOWN STRENGTH OF CONTROLS

Expt. #	Cable (1)	Thickness, mils	Steptime Hr.	ACBD Strength, V/mil		
				V_{10}	V_{50}	V_{90}
SLABS						
2	A. (Steam Cured, 1975)	18	1	1570	1980	2400
5	"	18	24	980	1260	1450
14	B. (Steam Cured, 1977)	18	1	1530	2000	2450
15	"	13	1	1900	2300	2600
17	"	13	24	1150	1460	1700
19	"	13	168	1180	1400	1550
12	J. (Dry Cured)	18	1	1580	2000	2500
MODEL CABLES						
143	D. (Uncured)	25	1	460	672	856
176	C.	25	0.16	938	1337	1672
104	C.	25	1.0	557	1084	1657
158	E.	25	0.16	1464	1631	1748
142	E.	25	1.0	819	1218	1570
180	E.	25	145*	----	720*	----
185	E.	25	368*	----	640*	----
145	F. (Flash Cured)	25	1	820	960	1100
183	H. (No Semicon)	27	1	585	861	1103
181	"	27	65*	----	667*	----
184	"	27	163*	----	592*	----
190	G. (Flash Cured)	20	1	704	840	940

* Test at constant stress

(1) Cables A to J are specified in detail on pages 4-1 and 4-4.

WEIBULL PLOTS

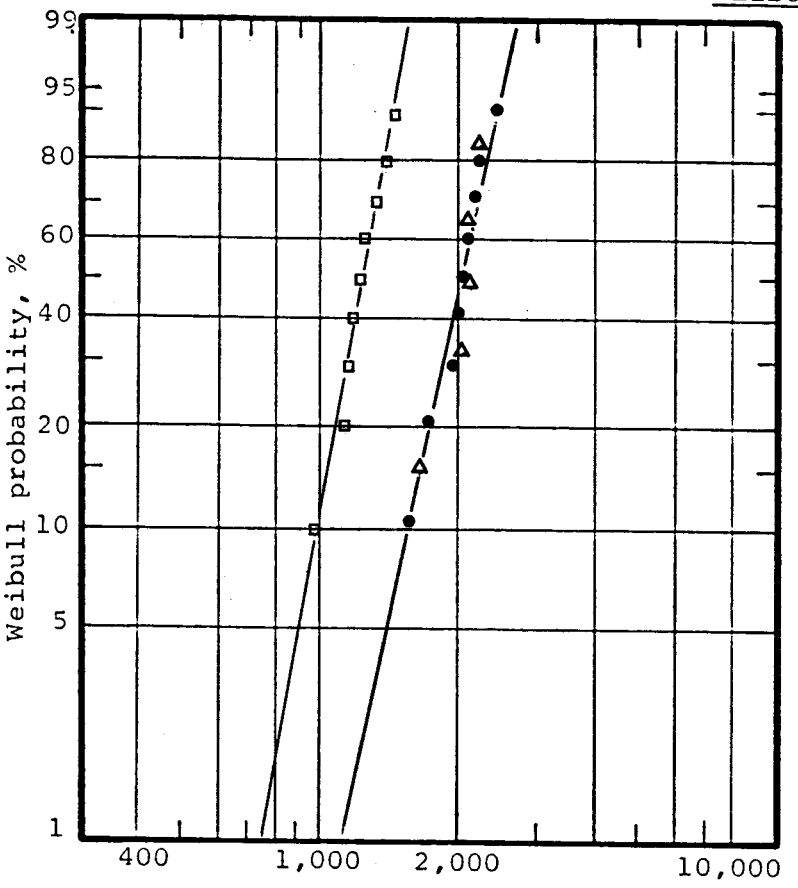

Figure 3-1. Control. Sample: 18 mil slab.
(●) Cable A, 1 hour step test.
(△) Cable J, 1 hour step test.
(▫) Cable A, 24 hour step test.
Experiment Nos. 2, 12 and 5, respectively.

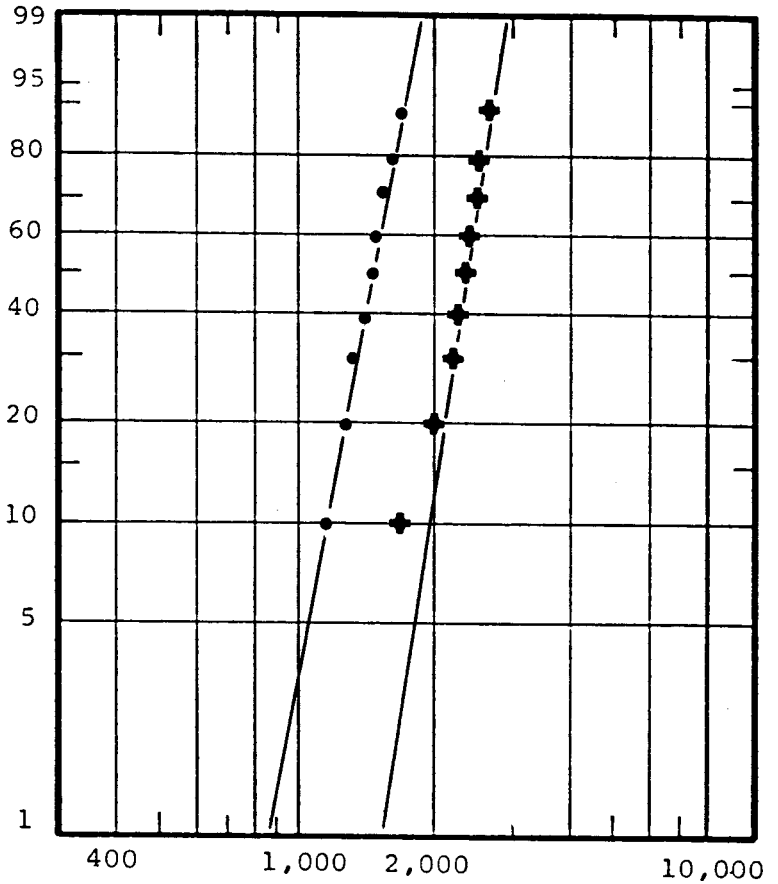

Figure 3-2. Control. Sample: 13 mil slab.
(●) Cable B, 24 hour step test.
(✚) Cable B, 1 hour step test.
Experiment Nos. 17 and 15, respectively.

WEIBULL PLOTS

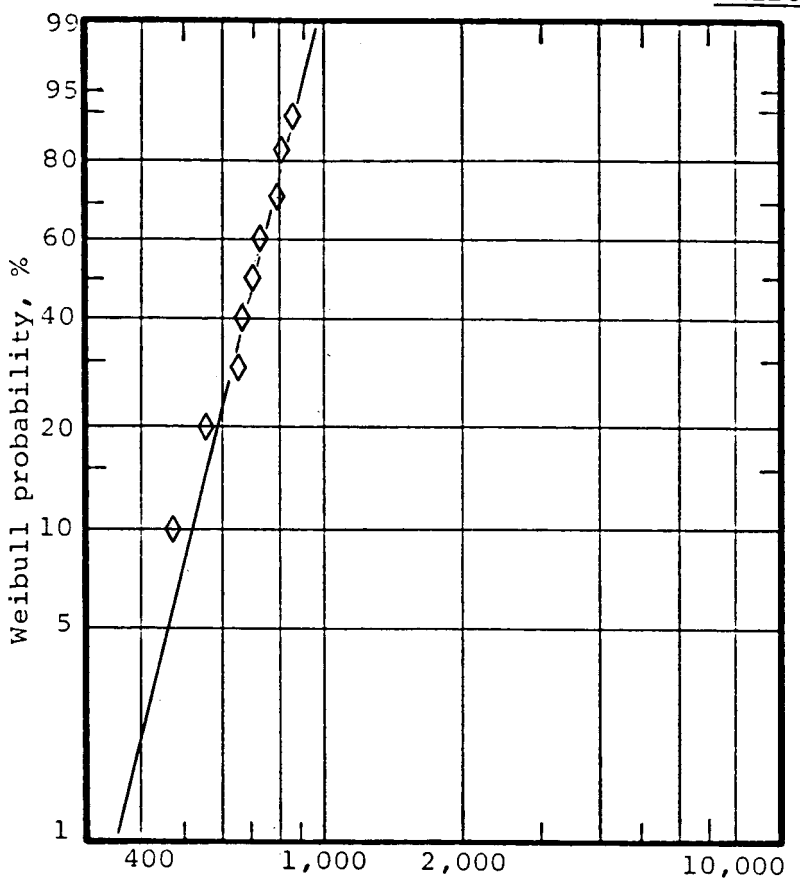

Figure 3-3. Control. Model Cable.
(◊) Cable D, not cured, 1 hour step test.
Experiment No. 143.

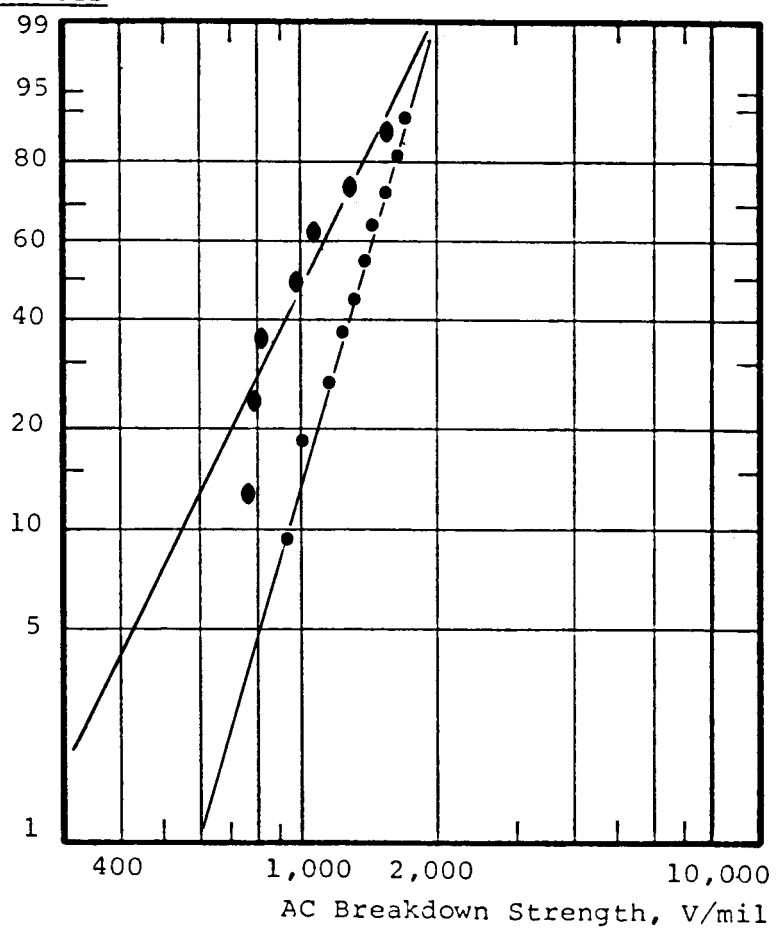

Figure 3-4. Control. Model Cable.
(●) Cable C, 1 hour step test.
(•) Cable C, 10 minute step test.
Experiment Nos. 104 and 176, respectively.

WEIBULL PLOTS

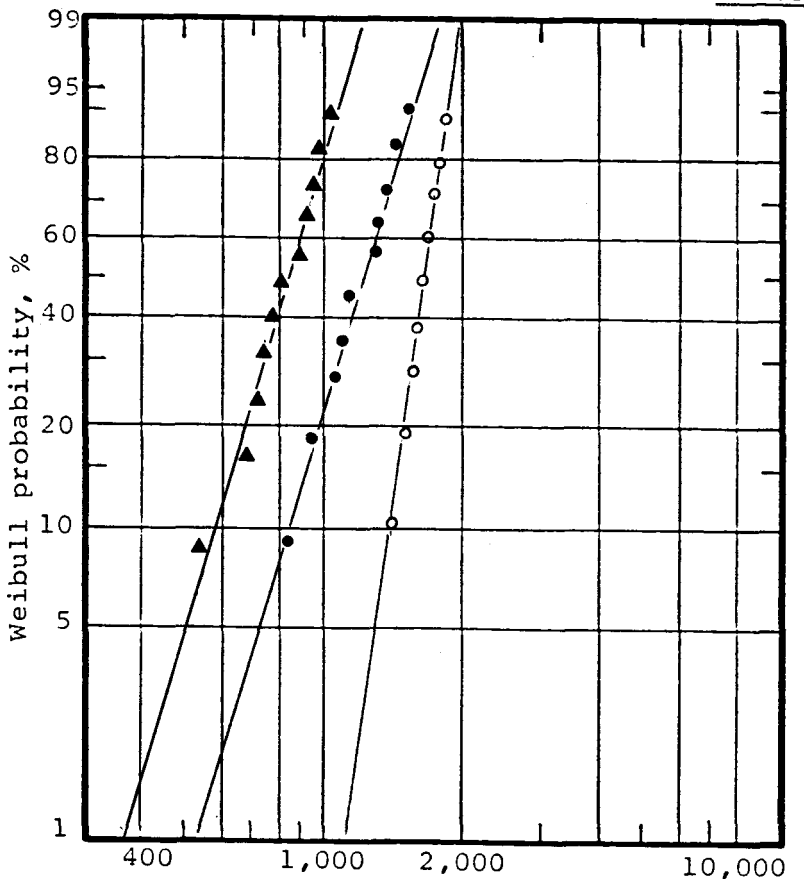

Figure 3-5. Control. Model Cable.
(▲) Cable H, 1 hour step test.
(●) Cable E, 1 hour step test.
(o) Cable E, 10 minute step test.
Experiment Nos. 183, 142 and 158 respectively.

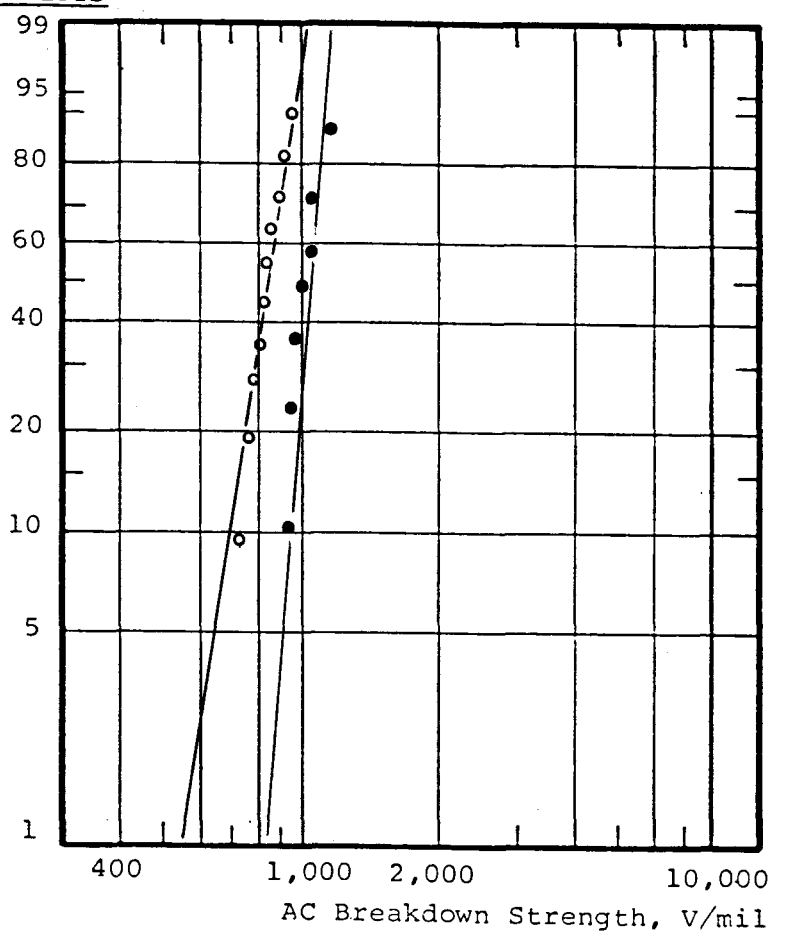

Figure 3-6. Control. Model Cable.
(o) Cable G, flash cured, 1 hour step test.
(●) Cable F, flash cured, 1 hour step test.
Experiment Nos. 190 and 145, respectively.

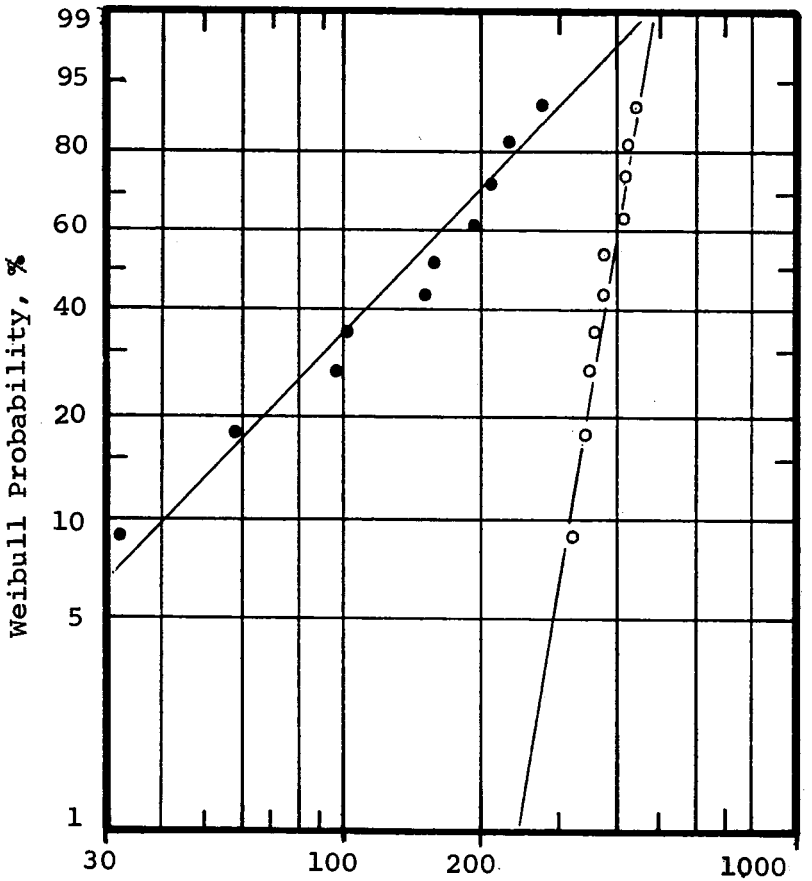

Figure 3-7. Test at Constant Stress.
(•) Cable E at 720 V/mil stress.
(o) Cable E at 640 V/mil stress.
Experiment Nos. 180 and 185, respectively.

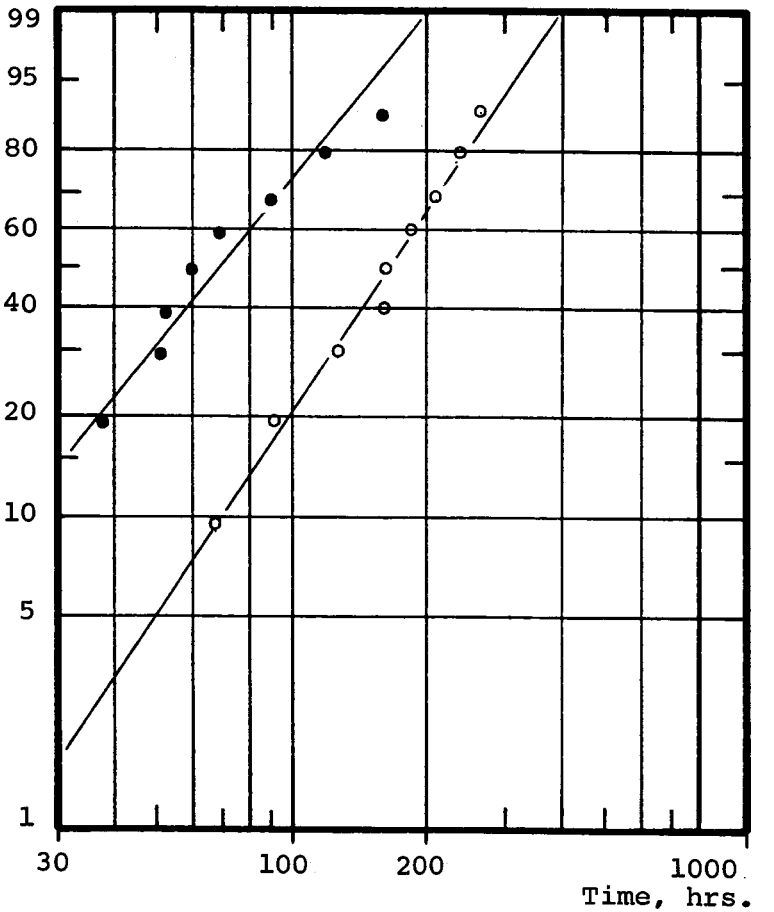

Figure 3-8. Test at Constant Stress.
(•) Cable H at 667 V/mil stress.
(o) Cable H at 592 V/mil stress.
Experiment Nos. 181 and 184, respectively.

The slope of the VT curve is a comparative measure of service life of the cable.

For cables A and B, the tests were carried out at one and twenty-four hour steps. The Weibull plots for 24 hour steps are presented in Figures 3-1 and 3-2. The VT curve is given in Figure 3-9. For cable B, the strength has also been measured at 1 week step-up times and the results are included in Table 3-2 and Figure 3-9. The proximity of individual data points to the regression lines, and the similarity of the slopes are a good indication that the mechanism of breakdown was similar at various step-up times. This in turn justifies the use of the Weibull probability scale.

In the case of model cables the step times have been varied from 10 minutes to 1 hour. This has been supplemented by carrying out AC BD tests at constant stress (15 to 18 kV) and recording the time of failure. The data was treated in the same way, except that the time has been used as the dependent variable instead of stress. Typical Weibull plots are presented in Figure 3-7. Similar experiments have also been carried out with cable H and the results presented in Figure 3-8.

3.1.3 Microscopy

3.1.3.1 Optical Microscopy. Optical micrographs of dyed samples cut from the slabs of cable A, B and J are presented in Figures 3-10 to 3-12 and the data summarized in Table 3-15. It is evident that both cable A and B have a large number of voids. They appear spherical in shape and their size varies from 1 μm to 25 μm. The optical micrograph of cable J shows a much lower number of voids and the largest is about one third the size of the largest voids in steam cured cables. This is due to the fact that in steam cured cables, approximately 0.5% steam dissolves in polyethylene at the curing temperature. As the temperature goes down, the solubility decreases and the steam is rejected from the matrix. This steam forms clusters of water and stays inside the cable. With time, the bulk of this water migrates out, leaving empty voids inside the cable. In the dry cure process (cable J) the heat is conducted by a gas instead of steam and less of the gas dissolves in the insulation during curing. Further, as the gas escapes much faster than water, it does not coalesce in aggregates and does not form a liquid phase upon cooling. Hence, smaller and fewer voids are formed.

Optical micrographs of model cable C are presented in Figure 3-13. They show some similarity to those for slabs from steam cured 138 kV cable. This suggests that the thickness of the insulation does not alter the void size or void propensity drastically, and confirms the suggestion that the change in the solubility of water in polyethylene

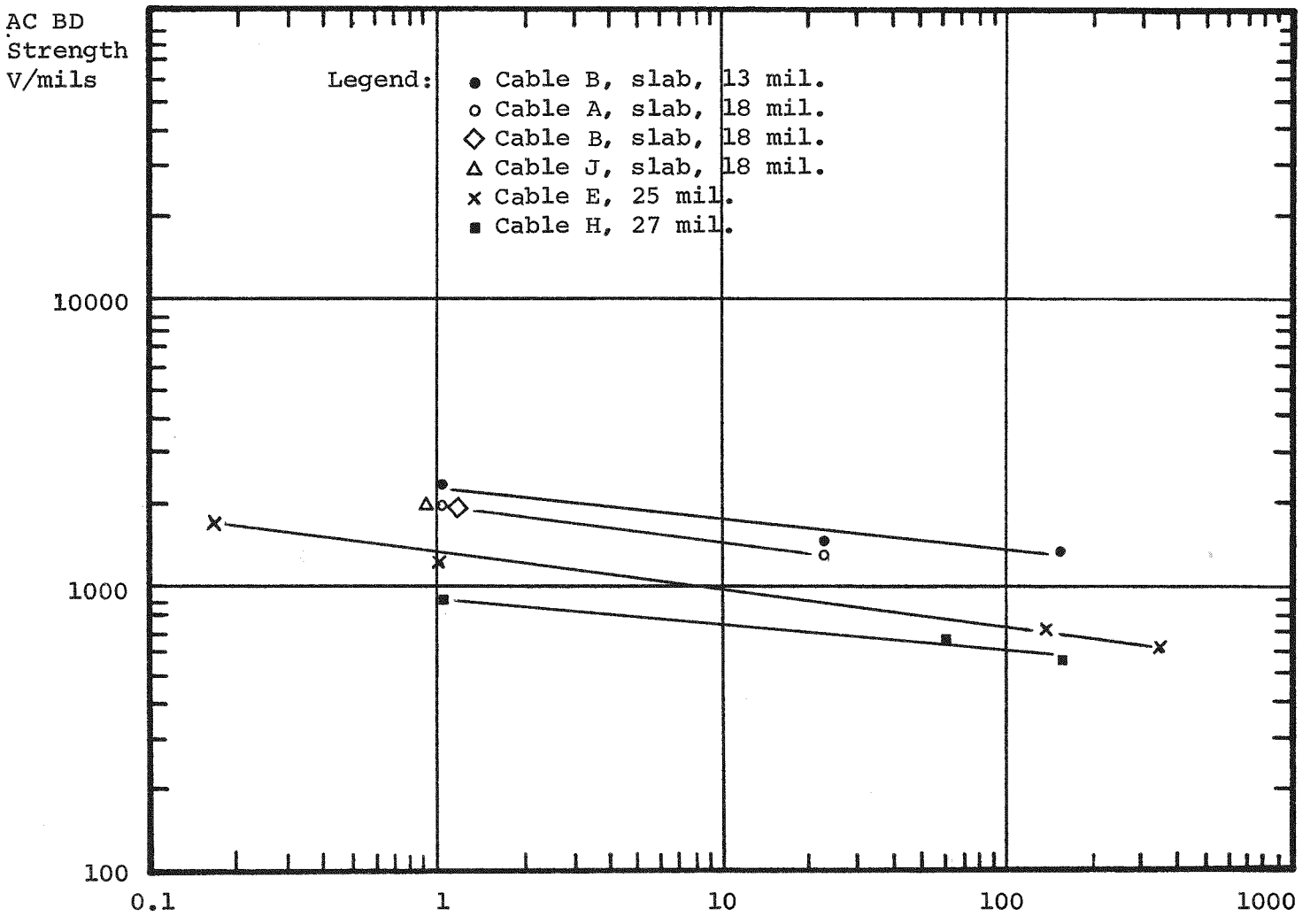

Figure 3-9. Stress-Time Correlation for Controls.

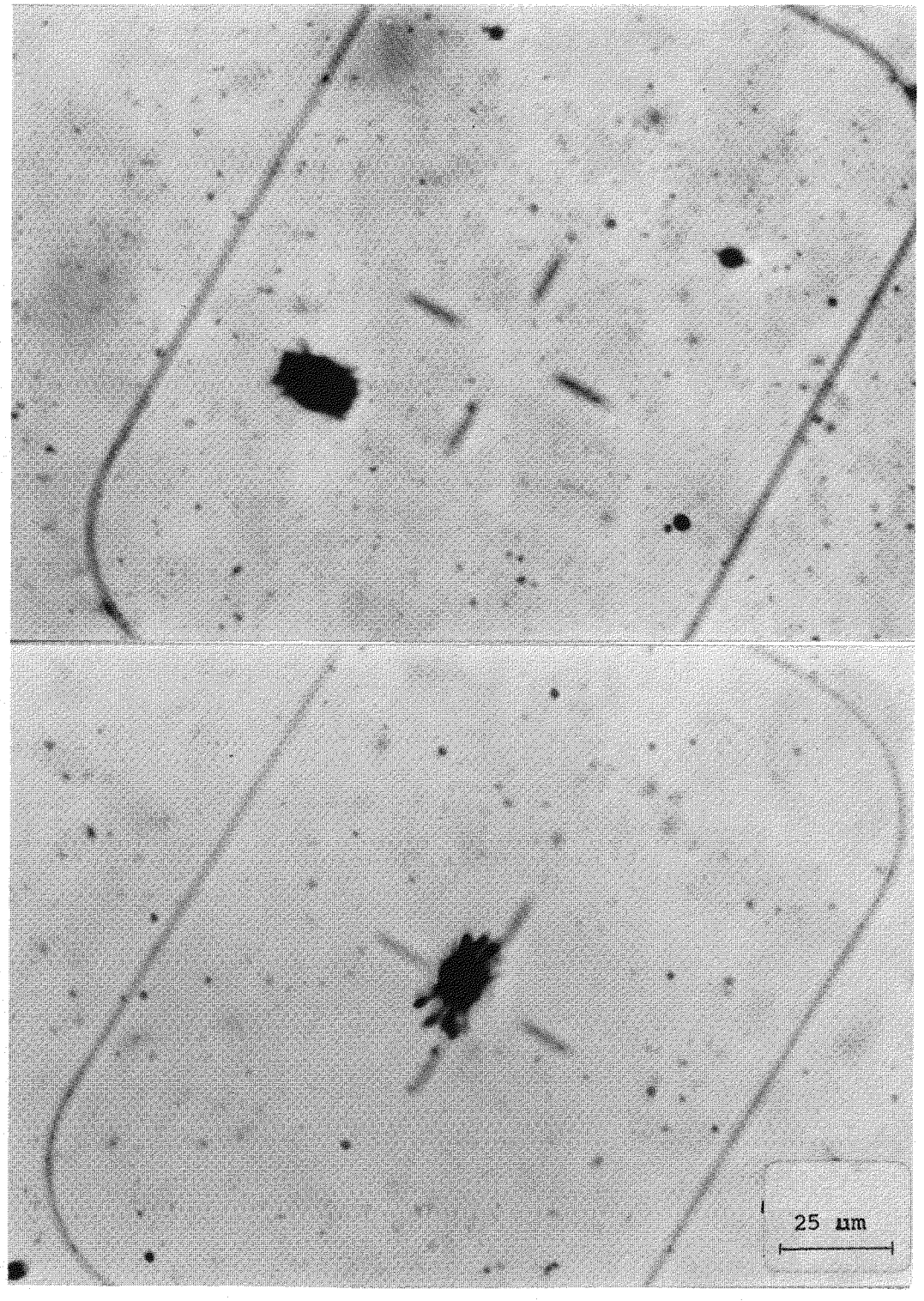

Figure 3-10. Cable A, Control.

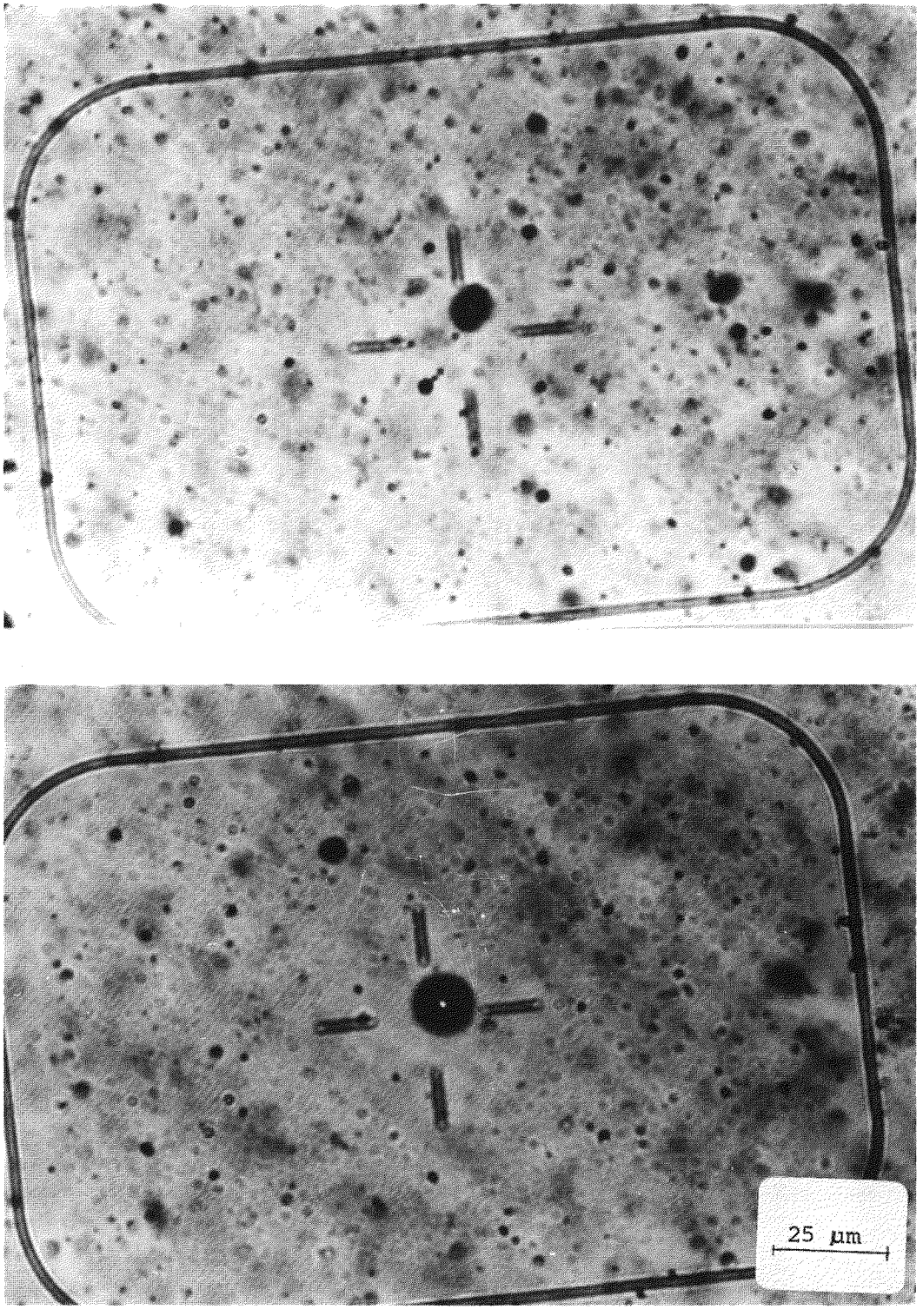

Figure 3-11. Cable B, Control.

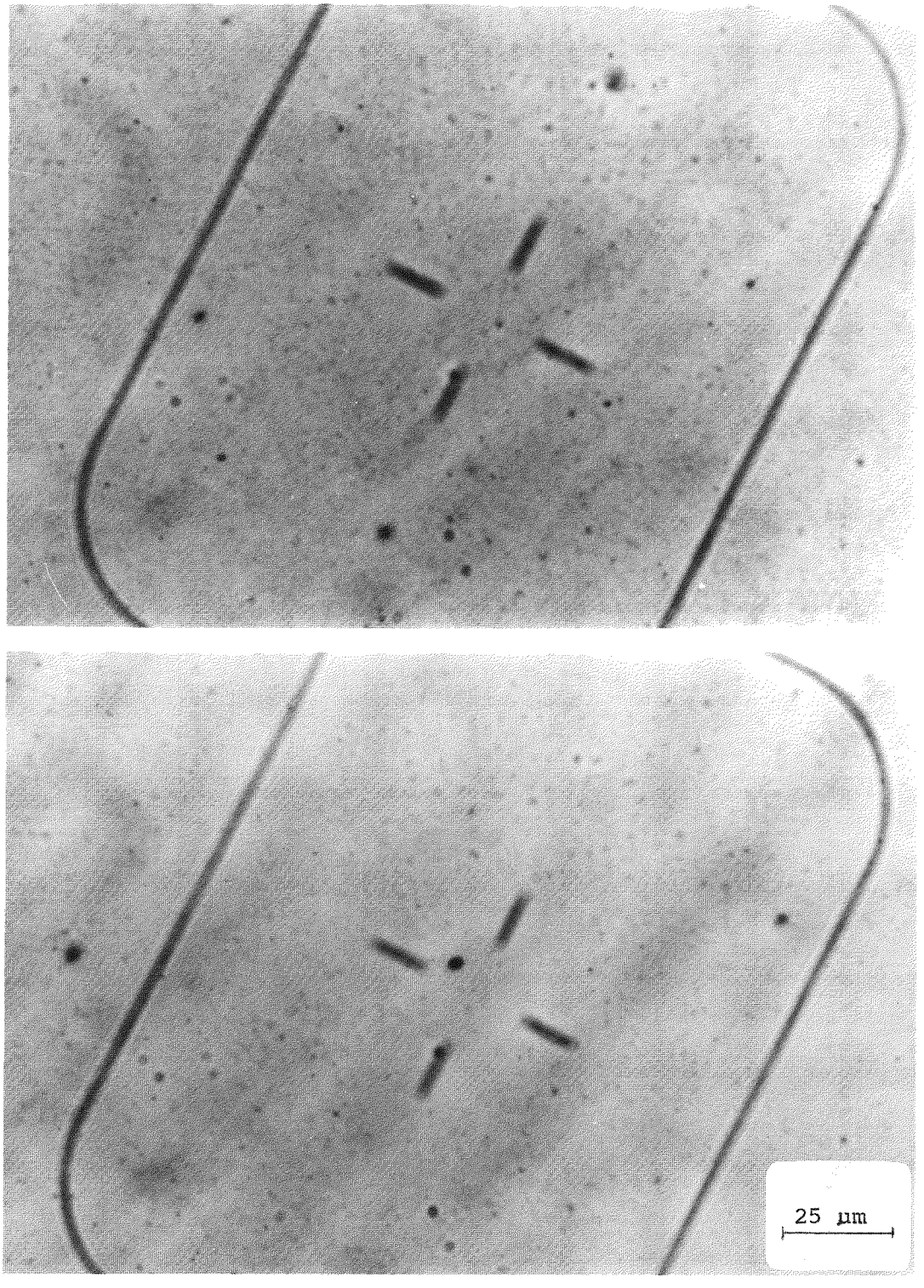

Figure 3-12. Cable J, Control.

OPTICAL MICROGRAPHS

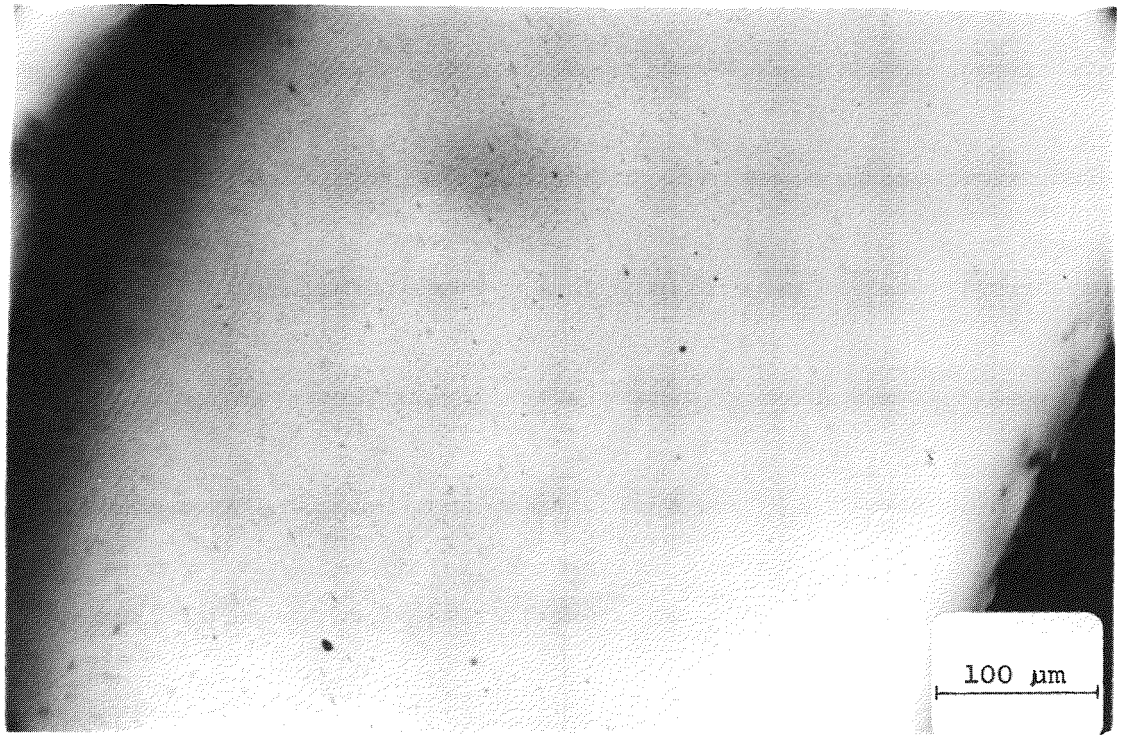

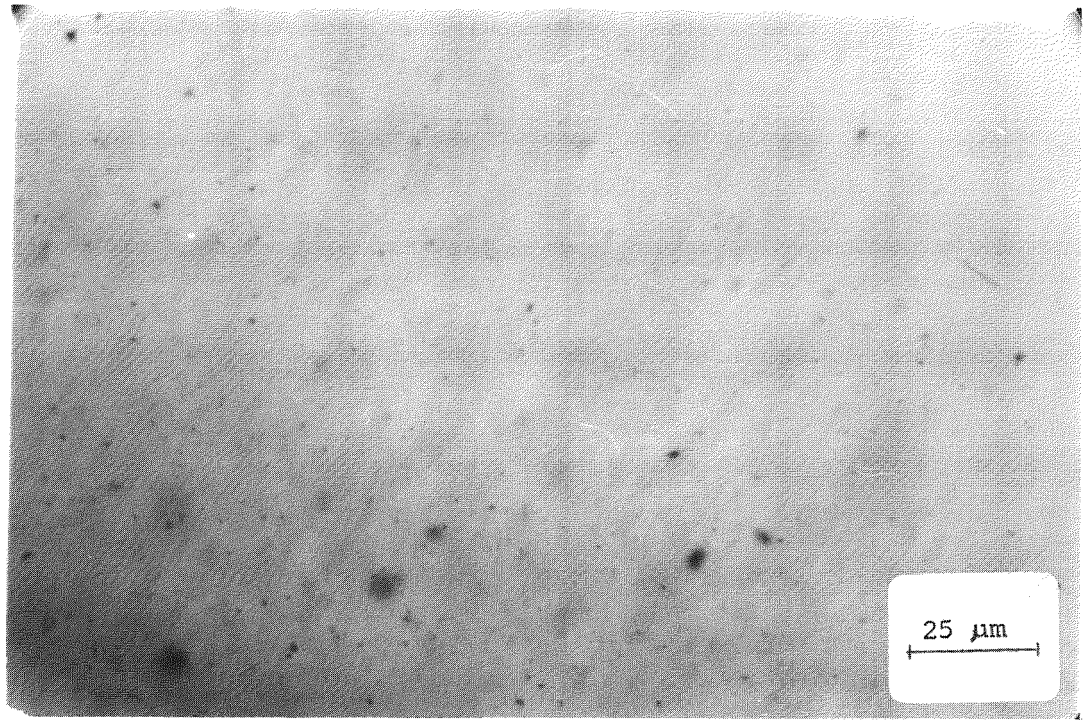

Figure 3-13. Model Cable C, Control.

is mostly responsible for void formation in steam cured cables. There are fewer and smaller voids in the model cable than in the steam cured, full size cables. Especially noticeable is the decrease in the number of larger voids over 10 μm in diameter.

3.1.3.2 Scanning Electron Microscopy. Most of the work was done on cold fractured samples, except cables A and J where sliced specimens were also investigated. The sliced specimens for cable A, Figure 3-14, show roundish, but not perfectly round voids with a pointed end. Long, narrow cracks emanate from this end leading to the speculation that a partially interconnected network of voids and microchannels may exist. The micrographs for cable J, Figure 3-15, show irregular-shaped voids supporting the findings of the optical microscopy, that some voids are present even in dry cured cables.

Scanning electron micrographs of cold fractured samples of cables A, B and J are presented in Figures 3-16 to 3-18. cable A and B exhibit similar morphology, characterized by a large propensity of voids. The voids are located in the spherulite-like structures, usually near their centers. The common boundaries of the spherulite-like structures appear fibrous.

There are doubts regarding the exact nature of the spherulite-like features (29). Wagner (30) has suggested that they are formed where fracture fronts meet. Wagner feels that the dark spots at the center represent weak regions in the XLPE matrix where the fractures start. Hence, the propensity of these dark spots and spherulite-like structures and their size and shape are important morphological characteristics of the insulation.

No spherulite-like structures were found in cable J. The voids appear to be smaller and fewer. An unusual feature is the appearance of groups of voids, small irregular voids in close proximity as shown in Figure 3-18. No attempt was made to establish the effect of these groups of voids on dielectric properties.

The scanning micrographs of model cables are presented in Figures 3-19 and 3-20. They are very similar to the micrographs of 138 kV cable.

Scanning electron micrographs of the ditched surface are presented in Figures 3-21 and 3-22. They show crevices of the order of magnitude (20 μm), quite close to the size of the voids. It is expected that the silver paint used on the surface penetrates into these crevices and forms protrusions on the actual surface. Should the paint not penetrate into the crevices, voids of the same dimension may be formed at the ditched surface. Thus, the test results could be highly dependent on the smoothness of the ditched surface.

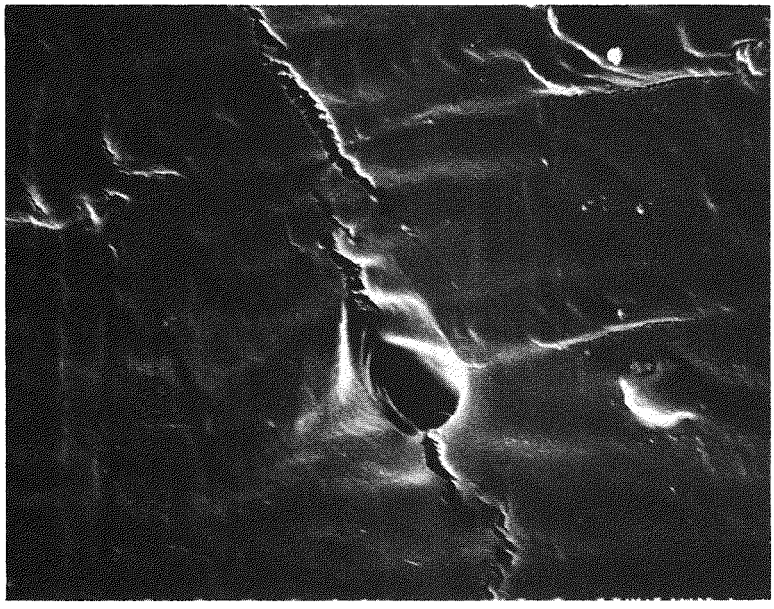

Figure 3-14. Cable A, Blade Cut Specimen.

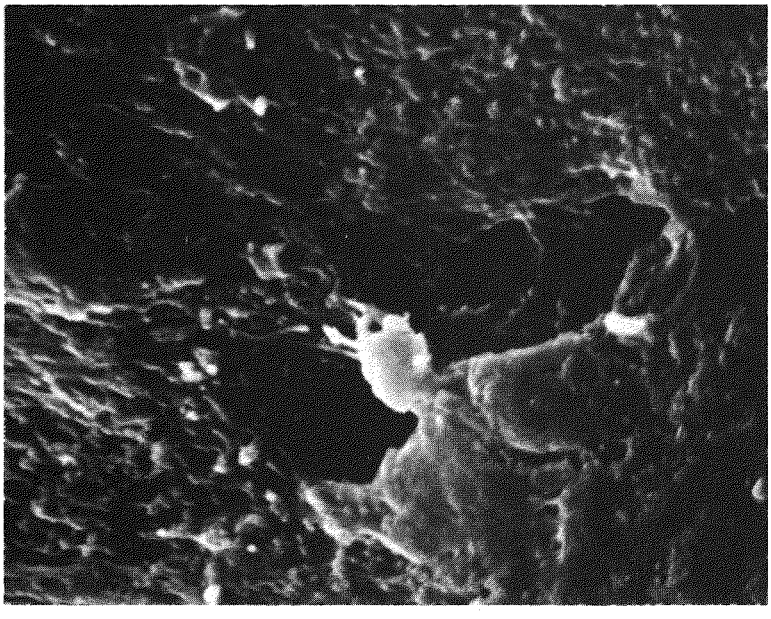

Figure 3-15. Cable J, Blade Cut Specimen.

SCANNING ELECTRON MICROGRAPHS

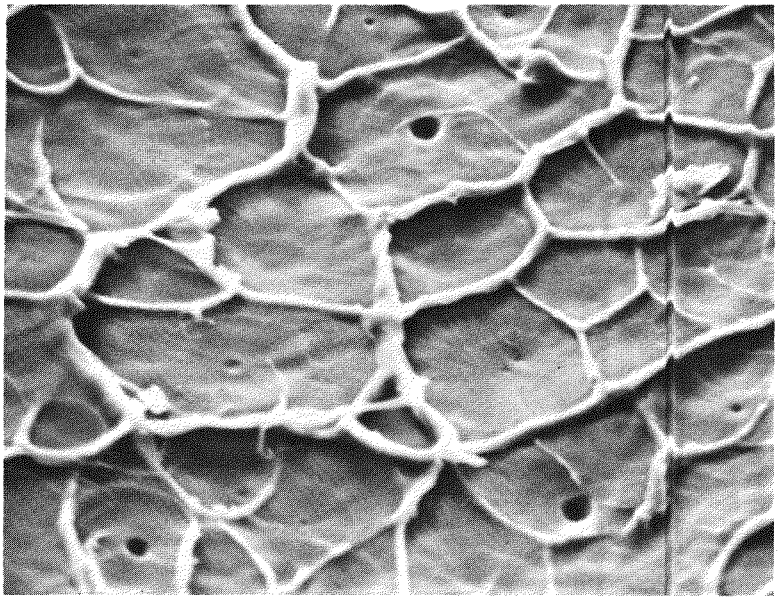

10 μm

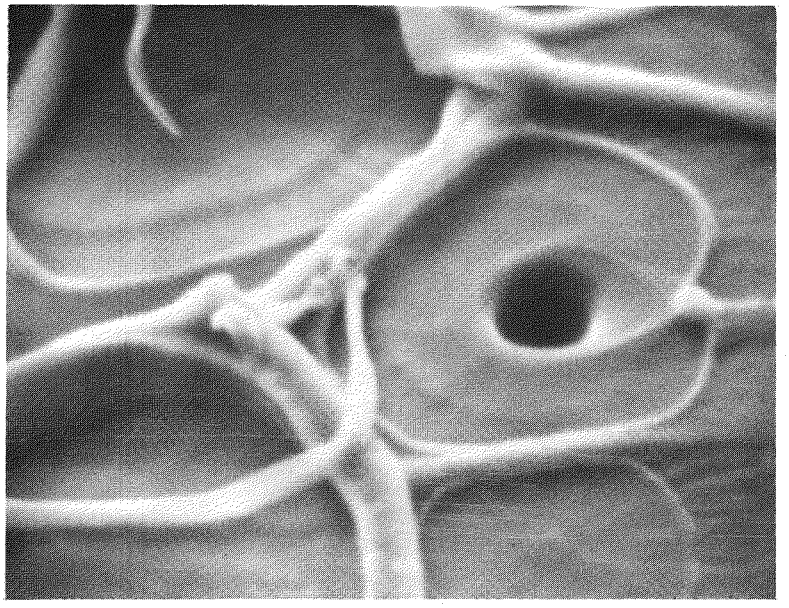

5 μm

Figure 3-16. Cable A, Cold Fractured Specimens. Controls.

SCANNING ELECTRON MICROGRAPHS

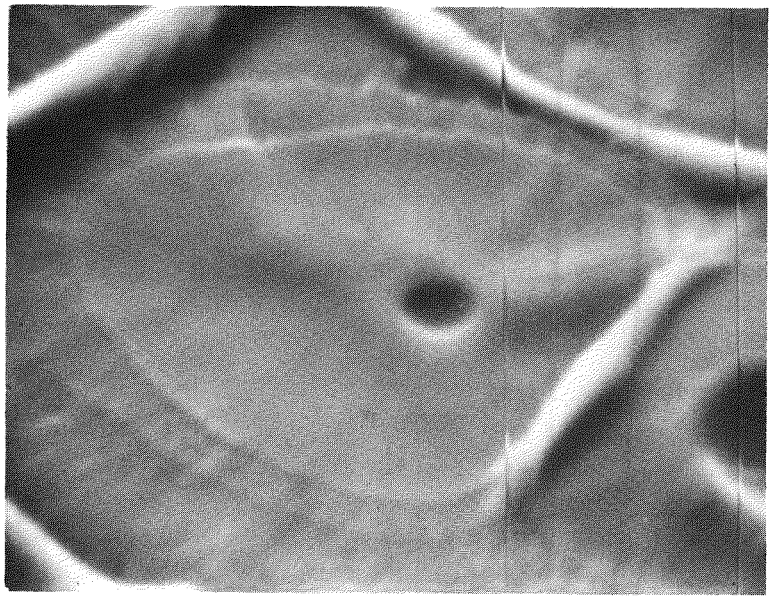

5 μm

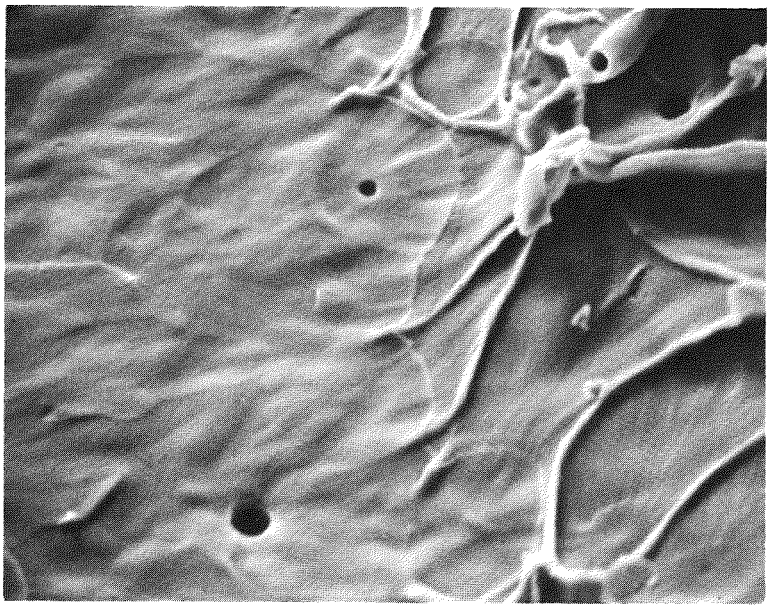

10 μm

Figures 3-17 and -18. Cable B, Cold Fractured Specimens. Controls.

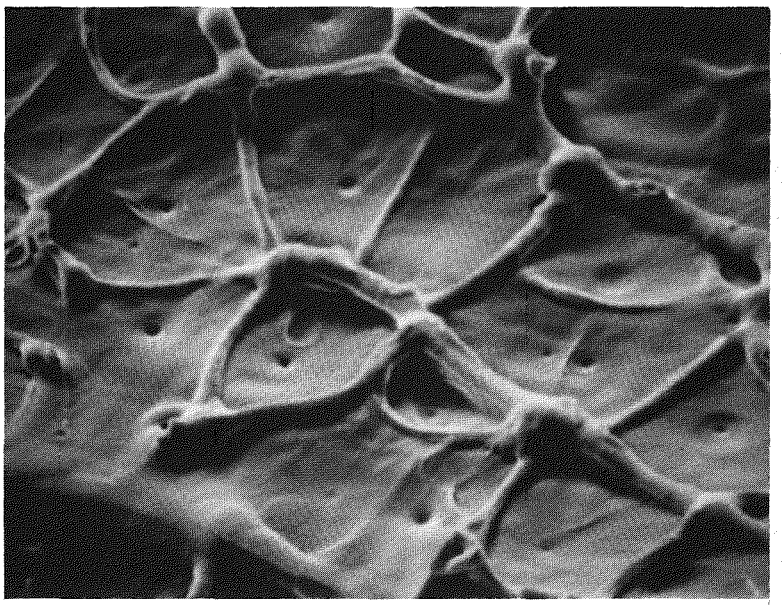

Figure 3-19. Model Cable E, Control.

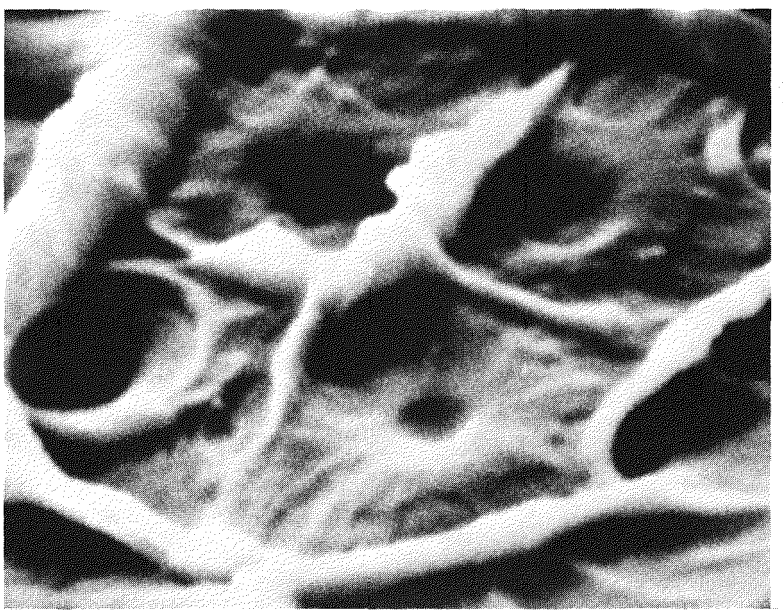

Figure 3-20. Model Cable H, Control.

SCANNING ELECTRON MICROGRAPHS

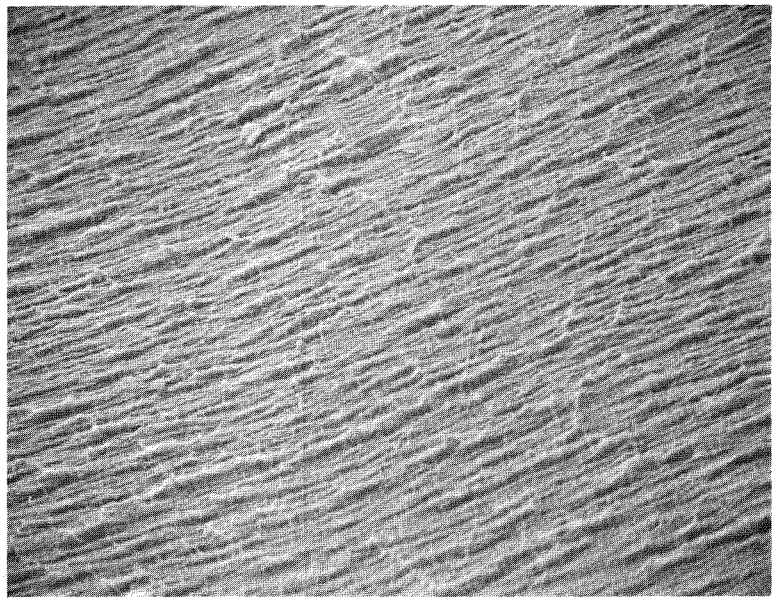

100 µm

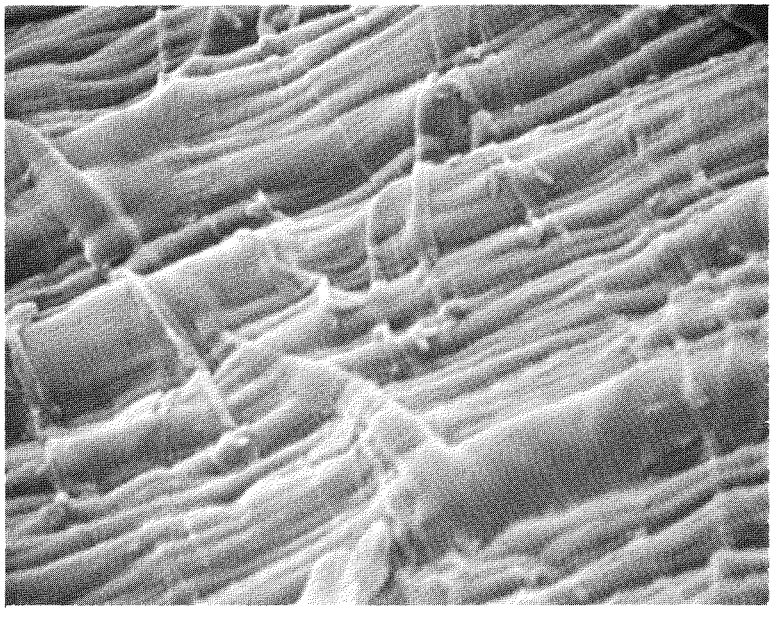

10 µm

Figures 3-21 and -22. Cable A, "Ditch" Surface.

Figures 3-23 to 3-25 show the surface of the breakdown channel in slabs at various magnifications.

3.2 DRYING AND HEAT TREATMENT

The service temperature of transmission cables could be as high as 90°C and the emergency temperature may reach 130°C. At such temperatures, the vapor pressures of volatiles like acetophenone and cumyl alcohol are appreciably high and they migrate out of the insulation. Since these volatiles have a voltage stabilizing effect, their removal may lead to a decrease in dielectric strength and in service life. In a number of experiments, vacuum dried specimens were used to assure a uniform basis for comparability. This necessitated the use of vacuum dried controls, and the assessment of the effect of vacuum drying. Combinations of various vacuum levels and temperatures were covered, and the temperature effect was also assessed in the absence of vacuum.

3.2.1 Vacuum Drying

The drying in the initial experiment was carried out in vacuum ovens operating at approximately 1200 to 1500 μm vacuum. The volatile loss was monitored from time to time by weight measurements and by gas chromatographic analysis. The results for cable A are presented in Figures 3-26 and 3-27 at 70°C and 90°C respectively. Similar data for cable B is presented in Figure 3-28. The rate of loss is asymptotic with time indicating that the process follows Fick's law for diffusion. Cumyl alcohol, having higher concentration, permeates out faster than acetophenone whose concentration is almost one third of the former. The low concentration of α methyl styrene is indicated on the extended right hand scale of Figures. As expected, the rate of loss for all components is higher at 90°C compared to 70°C due to their higher vapor pressures. The total weight loss of the samples plotted in the same Figures shows that weights become constant for cable A in about a week at 90°C and in ten to eleven days at 70°C.

In subsequent experiments the slabs and model cables were dried in steel and glass chambers capable of attaining vacuum levels up to 20 μm. The removal of volatiles was monitored by pressure drop as described in Section 4. The completion of drying was also checked by weight measurements as described above.

A typical pressure drop curve for drying 10 slabs, presented in Figure 3-29 shows complete removal of volatiles in four days at 80°C and at 30 μm absolute pressure. The effect of vacuum drying on the various samples is summarized in Table 3-3.

SCANNING ELECTRON MICROGRAPHS

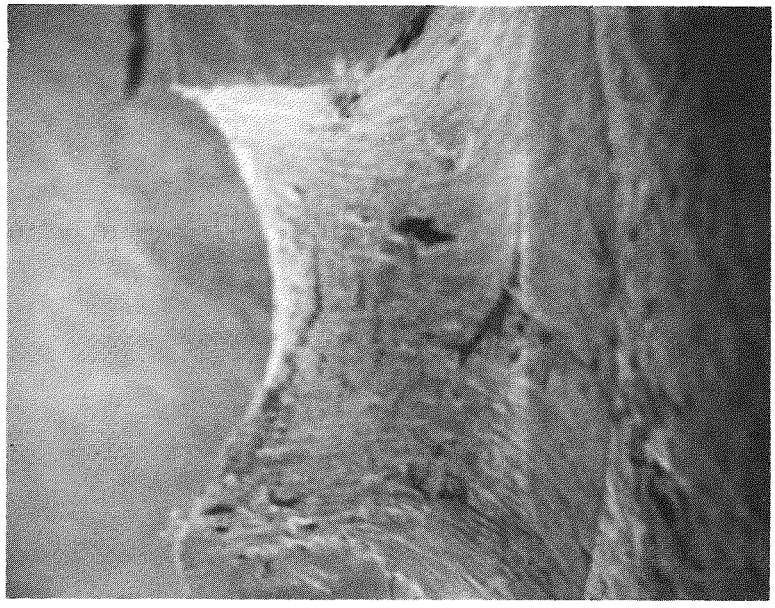

100 μm

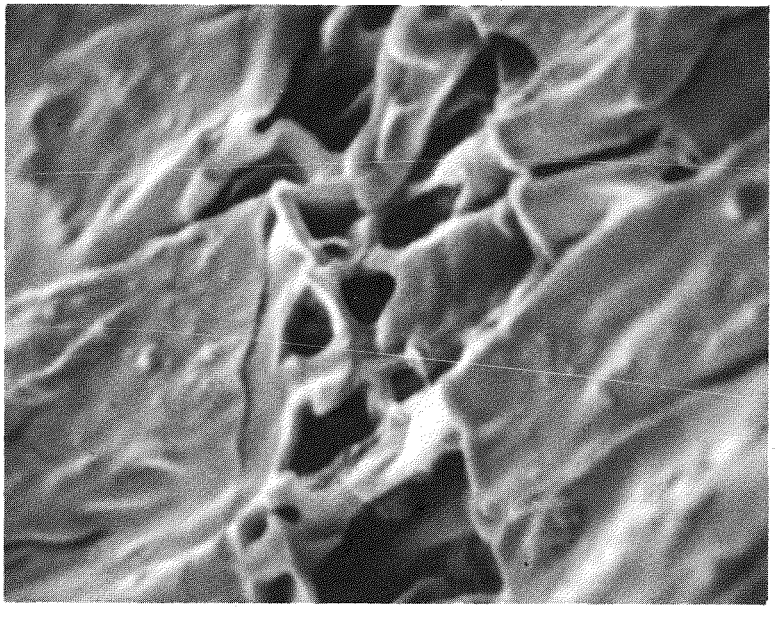

5 μm

Figures 3-23 and -24. View of AC Breakdown Channel. Cable A.

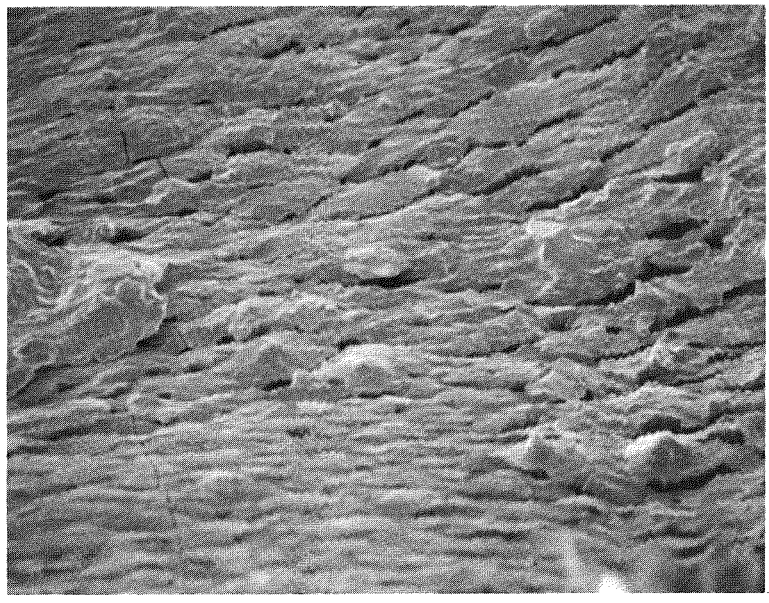

25 μm

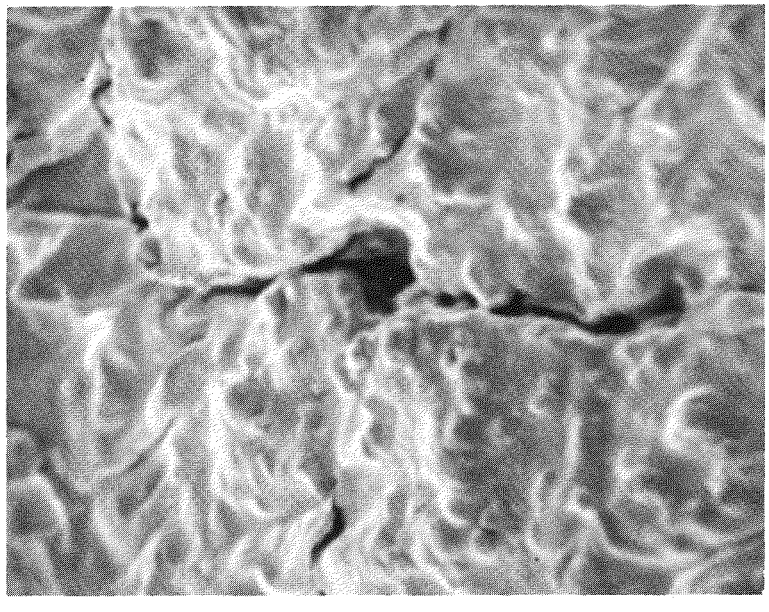

5 μm

Figure 3-25. View of AC Breakdown Channel. Cable A.

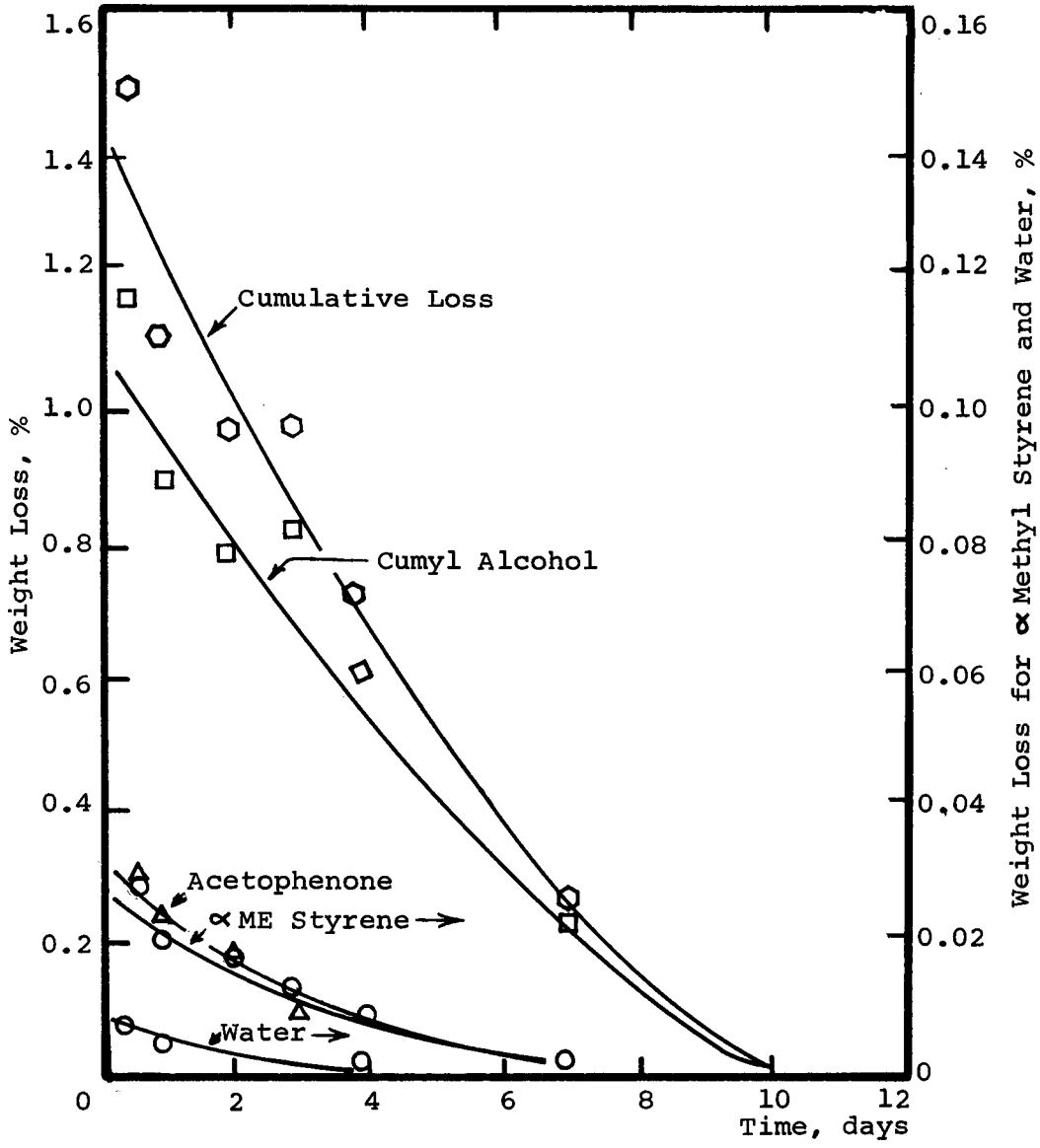

Figure 3-26. Removal of Volatiles at 70°C and 1500μm Pressure. Sample: Cable A slabs.

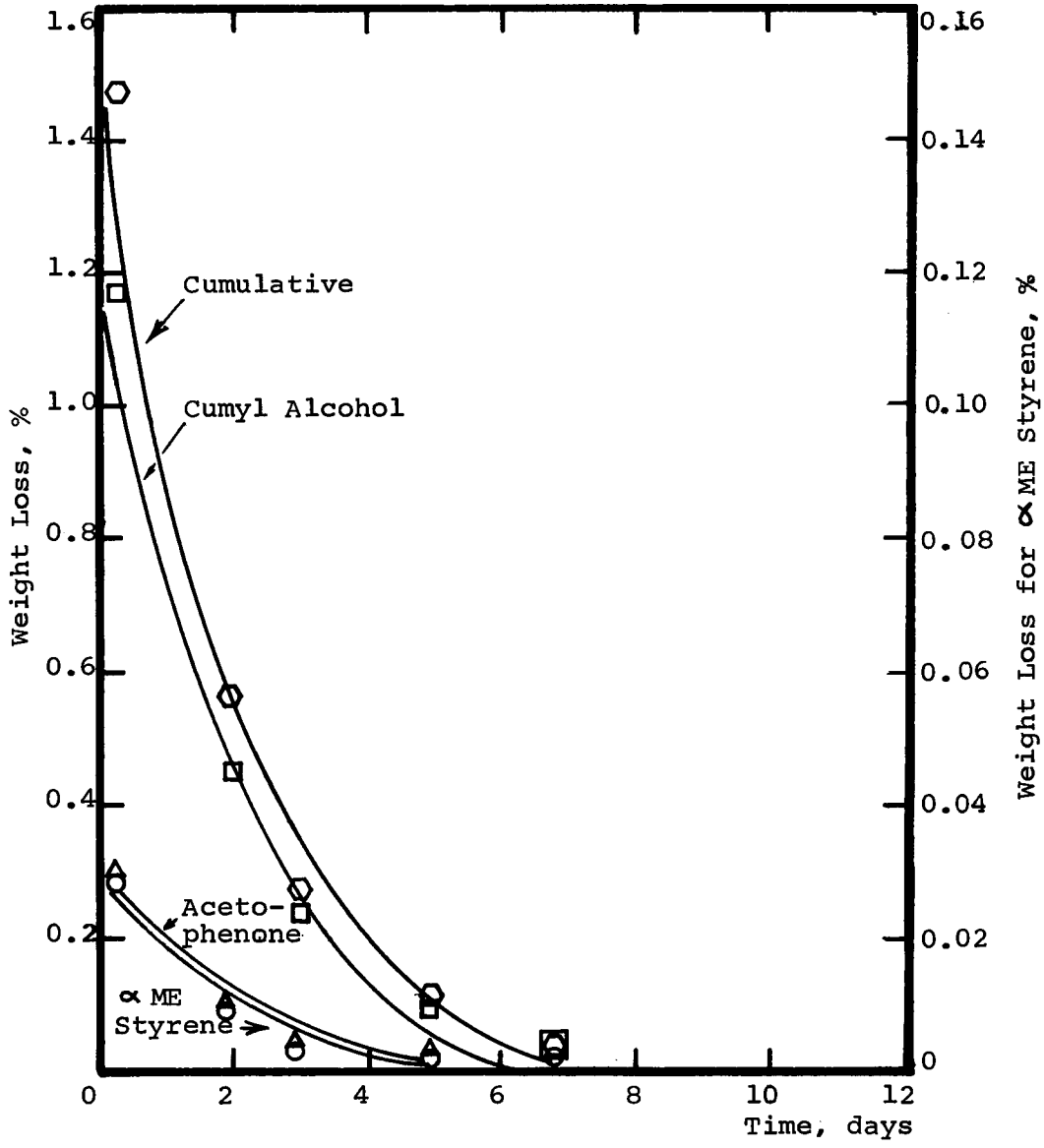

Figure 3-27. Removal of Volatiles at 90°C and 1500 μm Pressure. Sample: Cable A slabs.

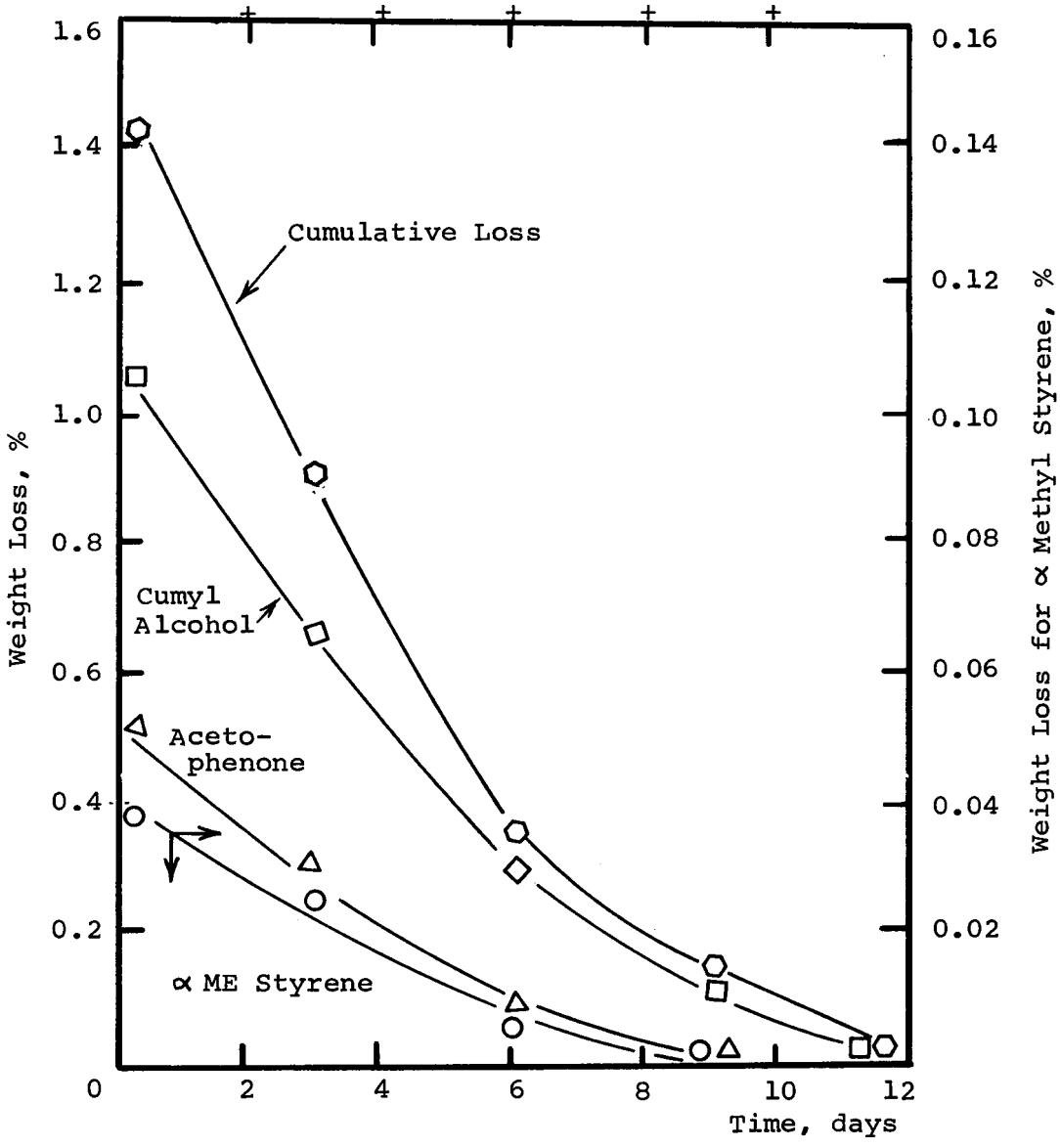

Figure 3-28. Removal of Volatiles at 70°C and 1500 μm Pressure.

Sample: Cable B slabs.

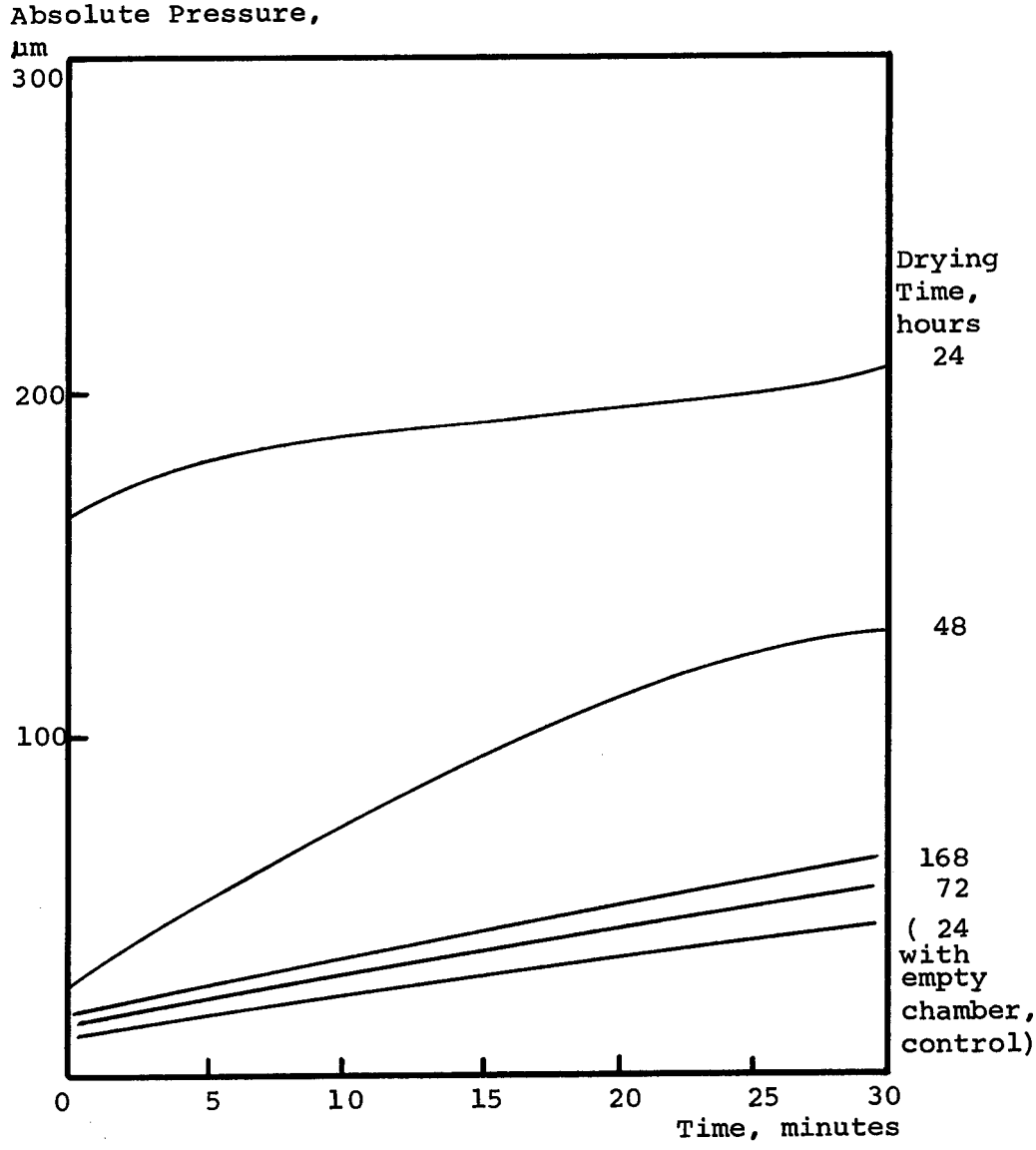

Figure 3-29. Vacuum Drop Test. Temperature 80°C.

3.2.2 Heat Treatment

In the process of drying, impregnation, polymerization and removal of excess impregnant, the samples were subjected to various levels of heating. The effect of heat (temperature) on the dielectric strength of the cable and on the morphology of the insulation was assessed by itself, i. e., without the simultaneous application of vacuum.

To understand this effect, slab samples in sets of ten were heated to different temperatures ranging from 50 to 150°C either in the oven or in a drying chamber. Model cable samples in 30 ft. lengths were exposed to heat in glass chambers. The results are compared to those of vacuum drying in Table 3-3.

3.2.3 AC Breakdown Strength

The breakdown strength of vacuum dried slabs (A, B and J) and cables (C, E and H) was measured in 1 hour step-up tests. In some cases 24 hour step-up tests were also performed. Typical Weibull plots are presented in Figures 3-30 to 3-32 for slabs and in Figure 3-33 for cables. The V_{50} values are listed in Table 3-3 along with normalized weights and time, temperature and vacuum level used in drying. For cable A, the oven drying lowers the dielectric strength by about 20% and the more thorough drying in the high vacuum chamber by about 30% (Experiment Numbers 2, 4 and 16 in Table 3-3). This shows that the dielectric strength may be related to the extent of removal of the volatiles. On the other hand, in the case of cable B, the drying did not show a decrease in dielectric strength as observed with cable A (Experiment Numbers 49 and 51). Similarly, no significant change was observed in the dielectric strength of cable J when subjected to vacuum drying at 80°C. Because of these apparently contradictory results, two carefully controlled experiments were carried out to assess the effect of vacuum drying still further. In this experiment, 20 samples, 10 each of cables A and B were subjected to identical vacuum and heat cycles. Five of each cable were treated together in two different chambers. The cable A samples (Experiment Numbers 68 and 73) had slightly less weight loss than those from cable B. This could be attributed to higher volatile content of the newly-made cable. However, the dielectric strength of all 20 samples was about the same, averaging 1820=(1950 + 1750 + 1800 + 1780)/4 and about 9% less than the average of the controls 1990=(1980 + 2000)/2. The AC breakdown strength of slabs heated to various temperatures but not subjected to vacuum was measured at 1 hour and 24 hour step-up times. The Weibull plots are presented in Figures 3-34 and 3-35. V_{50} values are listed in Table 3-3 and plotted against the temperature of treatment in Figure 3-36. No significant change is apparent in the dielectric strength in the 1 hour step test between 25 and 100°C, but it increased at 150°C. In the

Table 3-3

EFFECT OF VACUUM DRYING AND HEAT TREATMENT

Expt. #	Sample	Treatment				Samples			AC BD Test	
		Equipment	Temp. °C	Time h	Vacuum µm	No.	mil	Normal Weight	Step Time, h	V_{50} V/mil
VACUUM DRYING										
2	Cable A *	-	-	-	-	10	18	100	1	1980
4	"	Oven	80	60	1500	10	18	99.4	1	1610
16	"	Chamber	80	168	15	10	18	98.9	1	1530
48	"	"	80	216	15	10	18	98.6	24	1325
50	Cable J	"	-	-	-	5	18	100	1	2000
50	"	"	80	192	25	5	18	98.4	1	1900
49	Cable B	-	-	-	-	10	18	100	1	2000
51	"	Oven	70	240	1200	10	18	98.9	1	1970
51	"	Oven +	70	240+	1200	10	18	98.7	1	2100
		Chamber	70	120	30					
69B	"	Oven	70	408	1500	10	13	98.8	24	1620
142	Cable E	-	-	-	-	10	25	100	1	1218
144	"	Chamber	70	360	100	10	25	99.5	1	945
73A	Cable A	"	70	216	30	5	18	98.8	1	1950
68A	Cable A	"	70	168	25	5	18	98.9	1	1750
73B	Cable B	"	70	216	30	5	18	98.6	1	1800
68B	"	"	70	168	25	5	18	98.5	1	1780
HEAT TREATMENT										
70	Cable B	Chamber	25	67	-	10	13	100	1	2300
71	"	"	25	67	-	10	13	100	24	1460
80	"	"	50	67	-	10	13	99.8	1	2275
81	"	"	50	67	-	10	13	99.8	24	1750
76B	"	"	100	67	-	10	13	99.3	1	2150
76A	"	"	100	67	-	10	13	99.6	24	1890
93B	"	Oven	150	67	-	10	13	99.2	1	2700
93A	"	"	150	67	-	10	13	99.2	24	2180
171	Cable E	"	150	120	-	10	25	99.4	1	1170

* Cables A to J are specified in detail on pages 4-1 and 4-4.

WEIBULL PLOTS

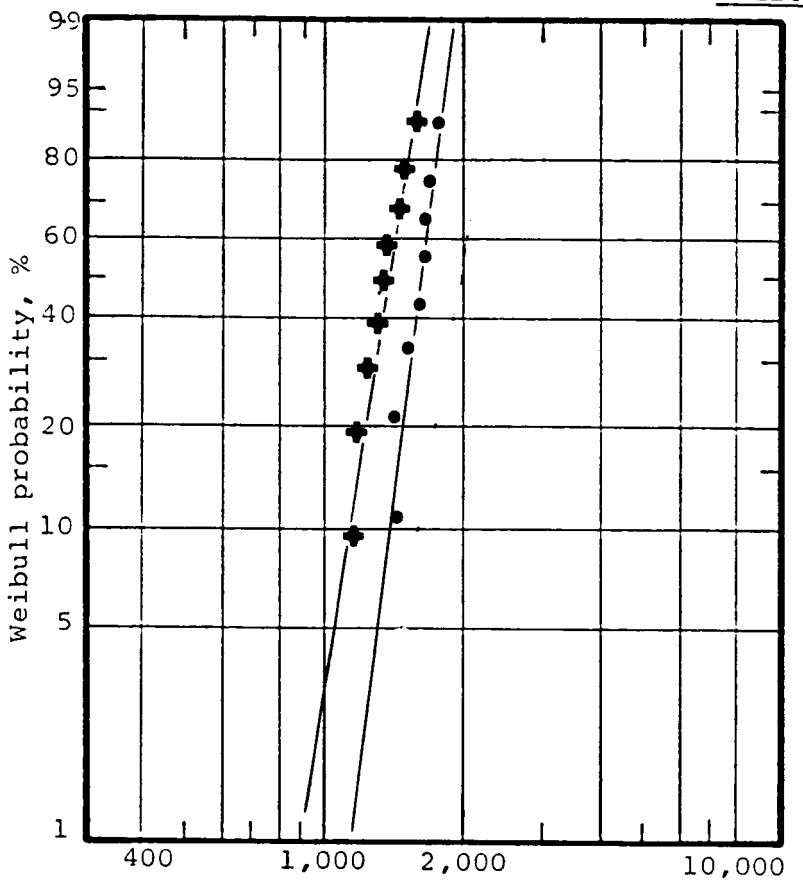

Figure 3-30. Vacuum Dried 18 mil Slabs.
(✚) Cable A, 24 hour step test.
(●) Cable A, 1 hour step test.
Experiment Nos. 48 and 16, respectively.

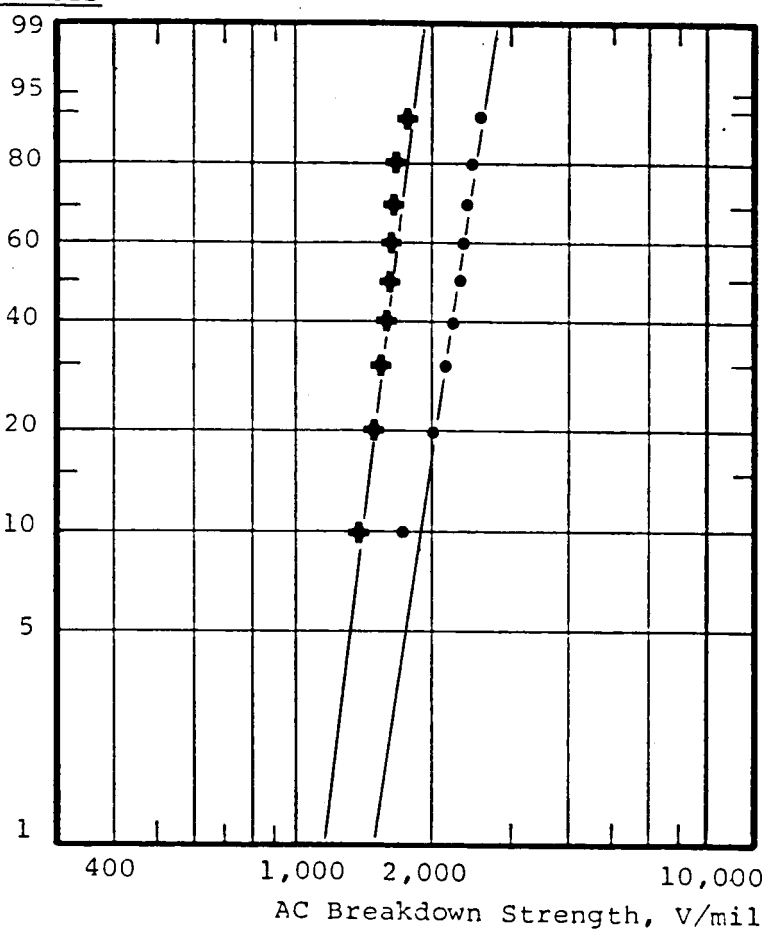

Figure 3-31. Vacuum Dried 13 mil Slabs.
(✚) Cable B, 24 hour step test.
(●) Cable B, 1 hour step test.
Experiment Nos. 69B and 15, respectively.

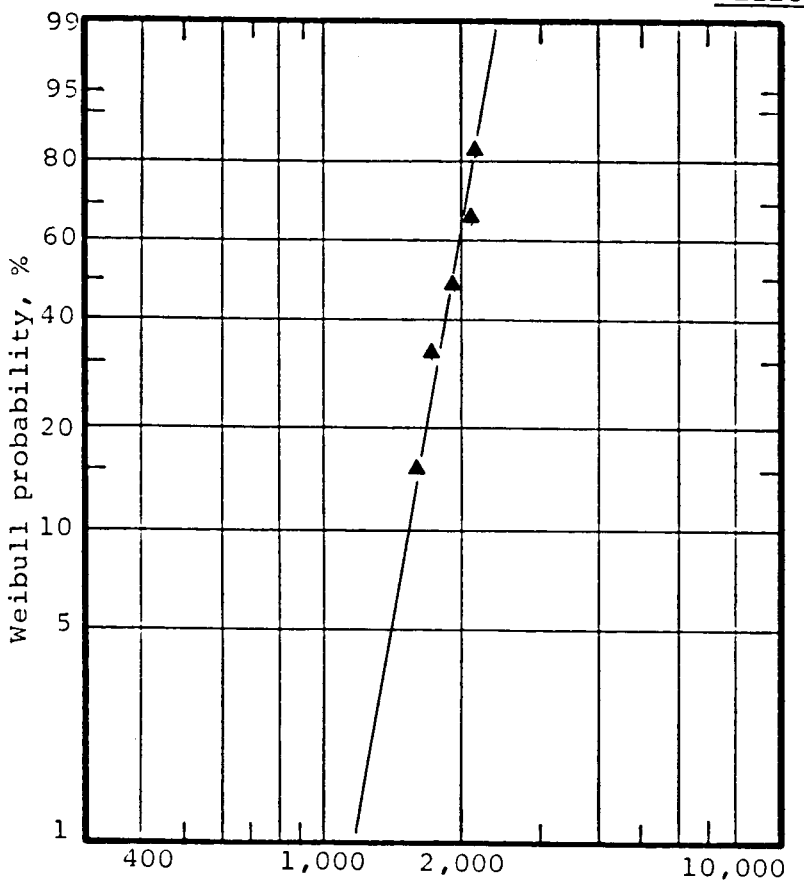

Figure 3-32. Vacuum Dried 18 mil Slabs.
(▲) Cable J, dry cured, 1 hour step test.
Experiment No. 50.

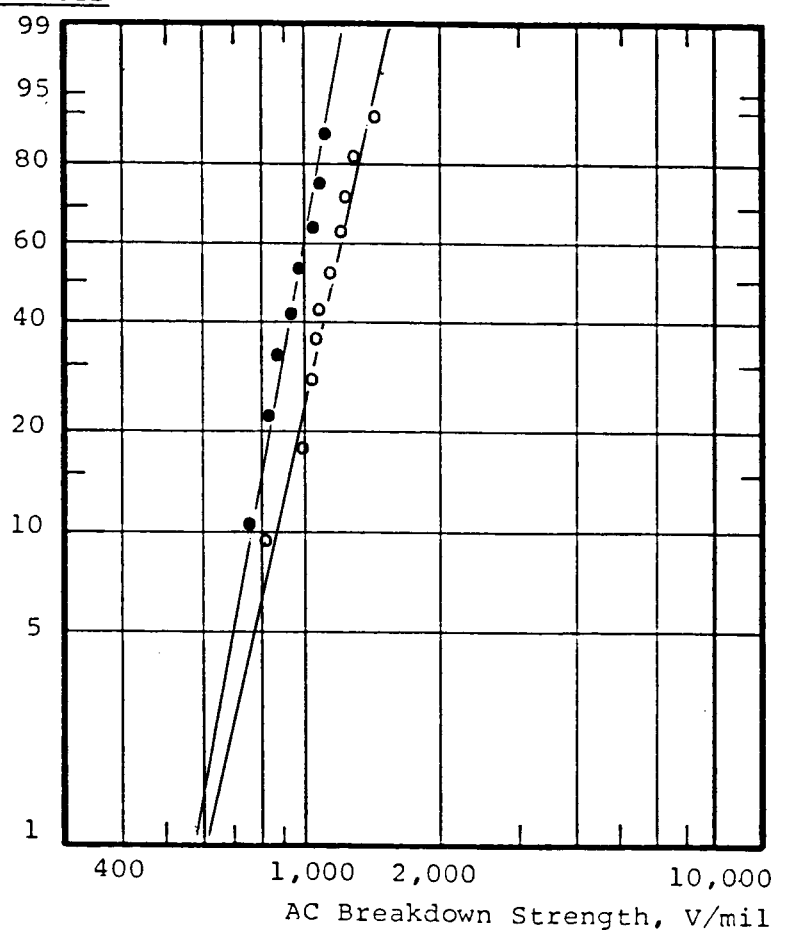

Figure 3-33. Vacuum Dried Model Cables.
(●) Cable E, 1 hour step test, Exp. No. 144.
(o) Same, Exp. No. 173.

WEIBULL PLOTS

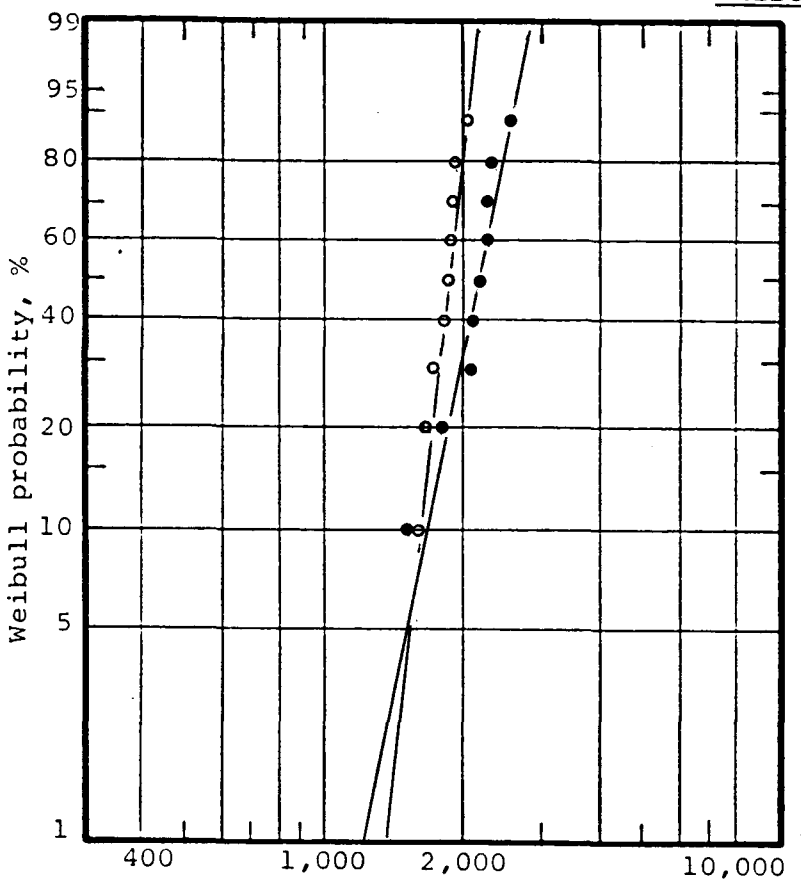

Figure 3-34. Heat Treated Slabs.
(o) Cable B, 13 mil, 67 hours @ 100°C, 24 hour test. Experiment No. 76A.
(•) Cable B, 13 mil, 67 hours @ 100°C, 1 hour test. Experiment No. 76B.

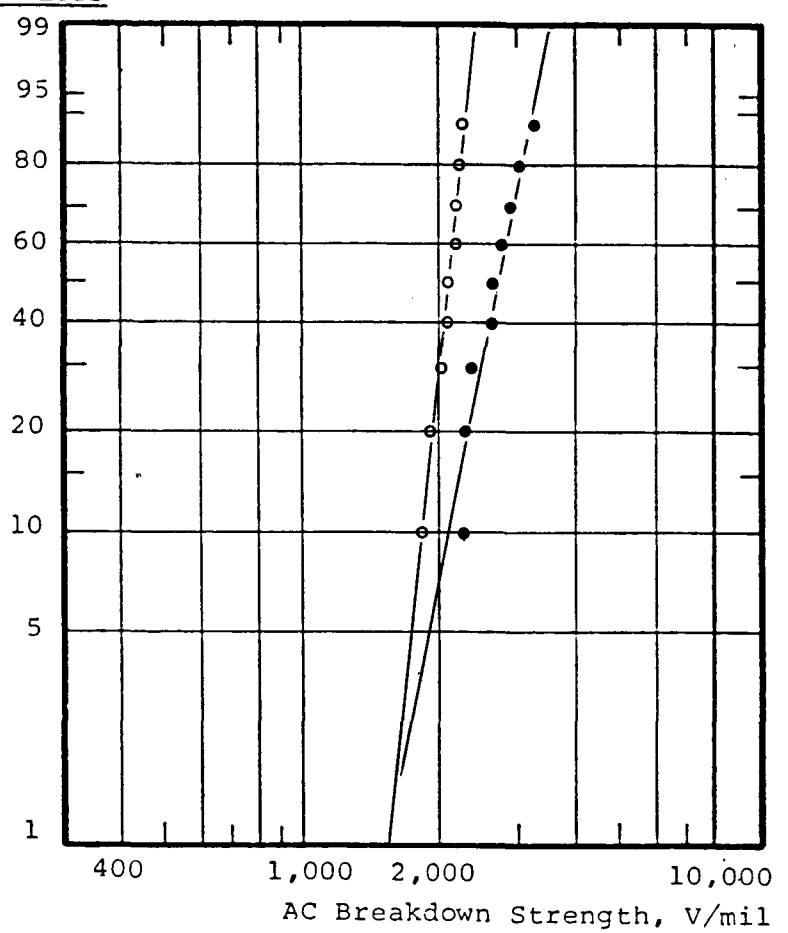

Figure 3-35. Heat Treated Slabs.
(o) Cable B, 13 mil, 67 hours @ 150°C, 24 hour test. Experiment No. 93A.
(•) Cable B, 13 mil, 67 hours @ 150°C, 1 hour test. Experiment No. 93B.

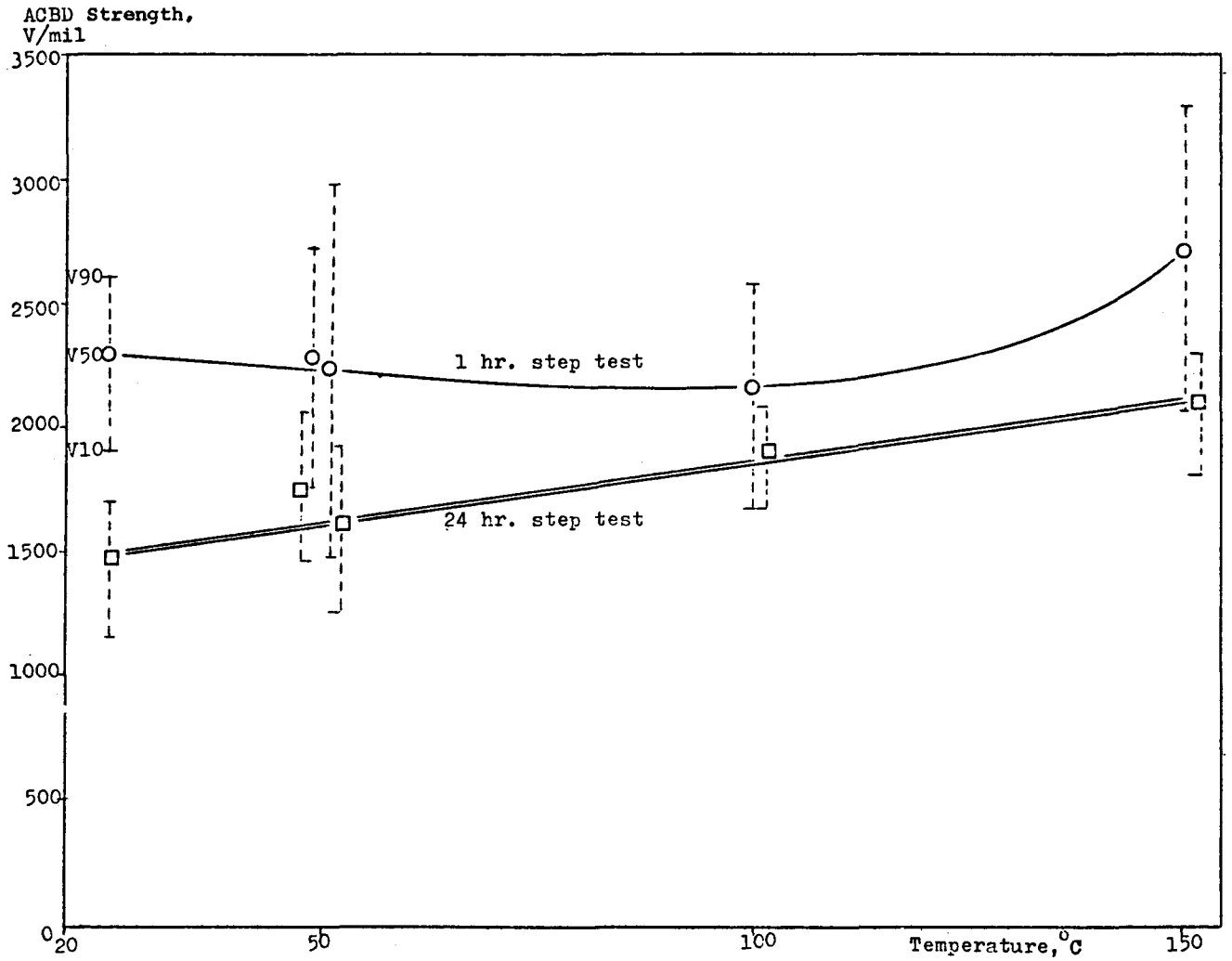

Figure 3-36. Effect of Temperature on AC Breakdown Strength.

Sample: Cable B slabs, 13 mil. Heat treatment for 67 hours.

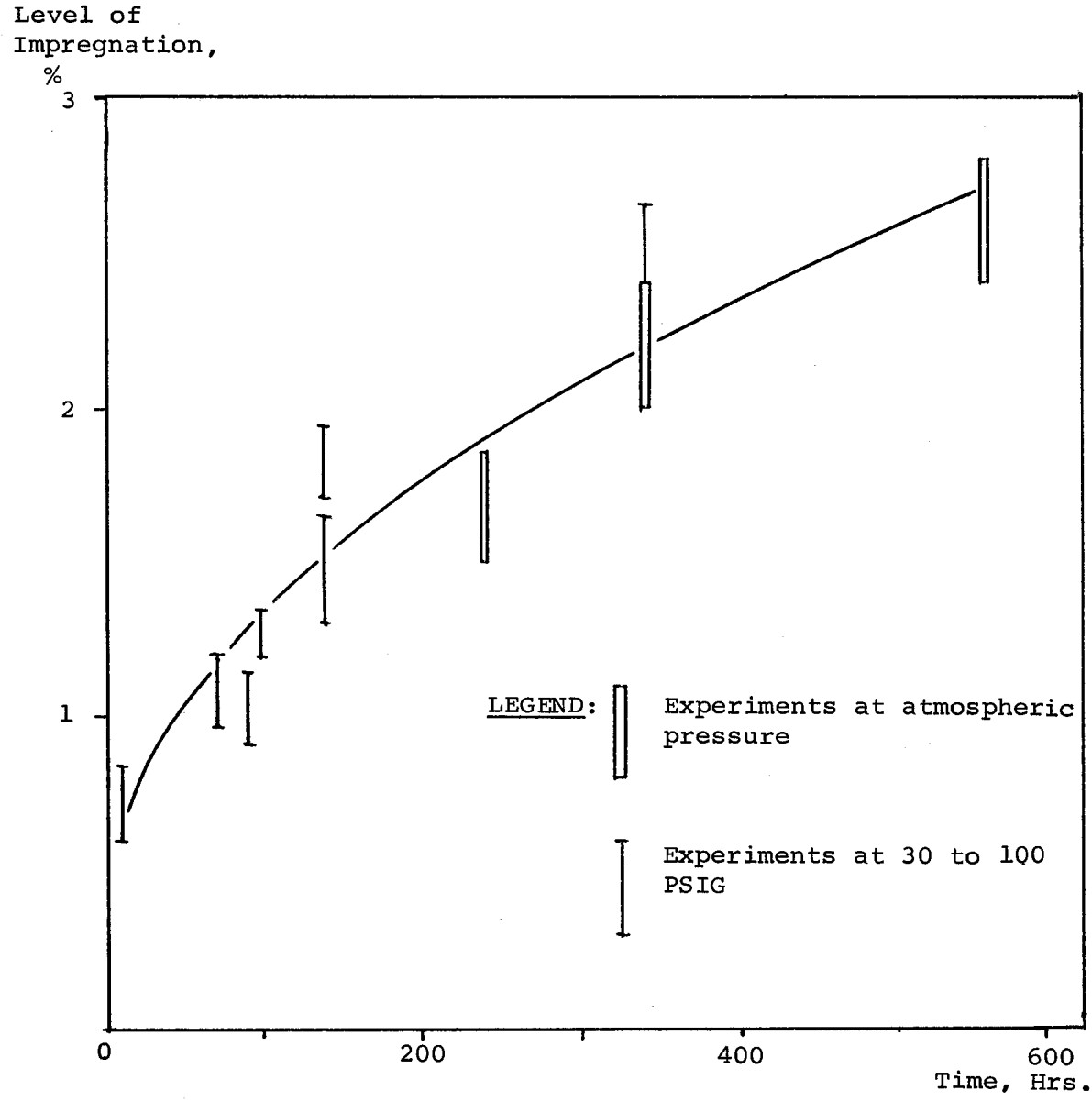

Figure 3-49. Effect of Pressure on Level of Impregnation.

the rate of impregnation is independent of applied pressures up to 100 psi.

3.3.2.2 Effect of Temperature. The lauryl methacrylate (LMA) and benzoyl peroxide (BPO) mixtures were found to have limited shelf life. Hydroquinone (HQ) was used as an inhibitor to prevent premature polymerization. Table 3-4 summarizes some preliminary experiments which show that at 40°C and in the presence of XLPE insulation, 27 days of shelf life is achieved at 2% BPO and 100 ppm, HQ concentrations.

Subsequently, impregnation was carried out on half size slabs at 25 and 40°C with LMA solutions containing different levels of peroxide and inhibitor. The average weight gains have shown that the rate of impregnation more than doubles for a 15° increase in temperature.

Later, a systematic study of LMA impregnation was carried out in the absence of BPO and HQ at 30, 50 and 70°C. The impregnation was carried out to equilibrium values, from which the time ($t_{\frac{1}{2}}$) for half saturation (for weight gain to attain half the equilibrium value) was calculated. The values for diffusivity, Do were calculated using the equation:

$$Do = \frac{0.04919\ L^2}{4\ t_{\frac{1}{2}}} \qquad (3\text{-}1)$$

where: L = the thickness of the slabs.

The results are presented in Table 3-5. The initial rate of permeation was calculated from the initial slopes of weight gain versus time curves and included in the same table. The results show that both rate of permeation and diffusivity increase substantially with temperature and the increase is more than two fold for every 20°C rise of temperature.

3.3.2.3 Effect of Molecular Structure. As discussed earlier, the diffusivity and solubility of the liquids in a polymer matrix are largely dependent on molecular structure and temperature. It was therefore decided to study the rate of permeation of liquids of different chemical structure, especially the ones designed around the molecular structure of acetophenone.

The experiments were performed using 4 x 3.5 x 1 cm slabs cut from cable A. The samples were dried in the same way as our test specimens, weighed and then immersed in the impregnant in a closed bottle. The bottle was held in a constant temperature water bath maintained at either 30, 50 or 70°C.

Table 3-4

EFFECT OF INHIBITOR ON STOPPING AUTOPOLYMERIZATION

MONOMER - LAURYL METHACRYLATE
CATALYST - BENZOYL PEROXIDE
INHIBITOR - HYDROQUINONE
DURATION OF TEST - 27 DAYS

Expt #	Catalyst Conc.	Inhibitor Conc.	In Liquid State After
1	1 PERCENT	00 PPM	4 days
2	1	50	18
3	1	65	24
4	1	80	24
5	1	100	27
6	1	200	27
7	1	500	27
8	1.5	65	20
9	1.5	80	20
10	2	00	3
11	2	50	4
12	2	65	14
13	2	80	15
14	2	100	27
15	2	200	27
16	2	500	27

Table 3-5

EFFECT OF TEMPERATURE ON PERMEATION RATE

TEMPERATURE °C	MONOMER - LMA	MATRIX - XLPE SLAB	
	Time for Half Saturation (Hr.)	Diffusivity $cm^2/sec.$	Rate of Permeation
30	65.6	3.8×10^{-8}	1.37×10^{-4}
50	121	0.84×10^{-7}	3.05×10^{-4}
70	269	1.5×10^{-7}	5.64×10^{-4}

The measured weight gains have been plotted against time in Figures 3-50 to 3-53. The curves for all cases are asymptotic. The time ($t_{\frac{1}{2}}$) i. e., the time required to imbibe half the amount of liquid necessary for saturating the sample, was estimated and the values of diffusivity (D_o) calculated from Equation 3-1. The D_o values, along with the time required for the weight gain to reach 3% level, are recorded in Table 3-6. It must be noted that the accuracy of this data is limited. However, within that limitation, the diffusivity appears to increase as the molecular size decreases. Thus, LMA has smaller D_o values compared to isobutyl methacrylate, the latter in turn being smaller than the D_o value for 2-phenyl ethyl methacrylate. The solubility is reflected in the maximum amount of impregnation (equilibrium impregnation column in Table 3-6). It appears that aromatic nuclei or long alkyl chains increase the solubility while polar groups decrease it. This is in agreement with the results on wafer impregnation reported earlier.

3.3.2.4 Time Required for Impregnating 500 Mil and 800 Mil Thick Insulations. The method of estimating the time required for impregnating 800 mil thick insulation has been outlined in Section 2. Assuming D_o values for styrene as $2.98 \times 10^{-8} cm^2/sec.$ and the maximum permeation level as 15%, it has been shown that it would take appoximately 17 to 19 days to half saturate a 138 kV cable with styrene. The present experiment found the D_o value for styrene (3.85×10^{-8} $cm^2/sec.$) is somewhat larger than $2.98 \times 10^{-8} cm^2/sec.$ taken from the literature. The latter was for Marlex 50, a thermoplastic polyethylene having approximately 75% crystallinity. In the present case, it is crosslinked polyethylene having about 40% crystallinity. Although a decrease in crystallinity would favor permeation, the formation of crosslinks would hinder it. The net result shows the cancellation of the effect of crosslinking by a decrease in crystallinity. Using 3.85×10^{-8} for D_o and a 19.5% maximum impregnation level (see Table 3-6), the time required can be estimated as follows:

$$Q = \frac{2\pi D_o (C_2 - C_1)}{2.303 \log (r_2/r_1)} \qquad (2\text{-}5)$$

and:

$$t_{\frac{1}{2}} = \frac{\frac{1}{2} \times 19.5}{Q} \qquad (3\text{-}2)$$

where:
- Q = the rate of permeation.
- D_o = diffusivity
- C_2, C_1 = concentration of impregnant at the outer and inner surfaces of the cylindrical insulation.
- r_2, r_1 = outer and inner radii.

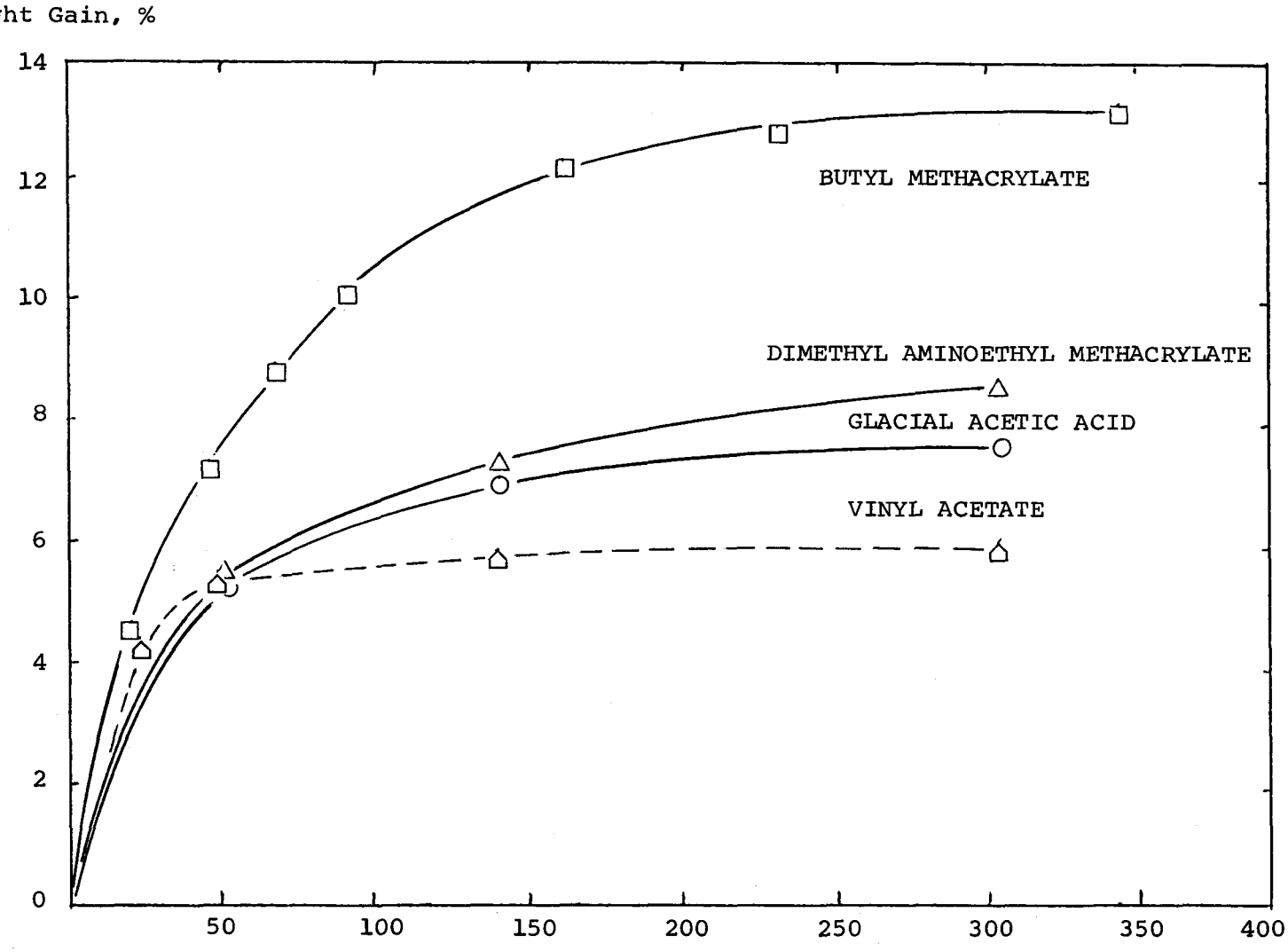

Figure 3-50. Impregnation of XLPE.

Sample: Cable A slabs, 400 mil. Temperature 50°C.

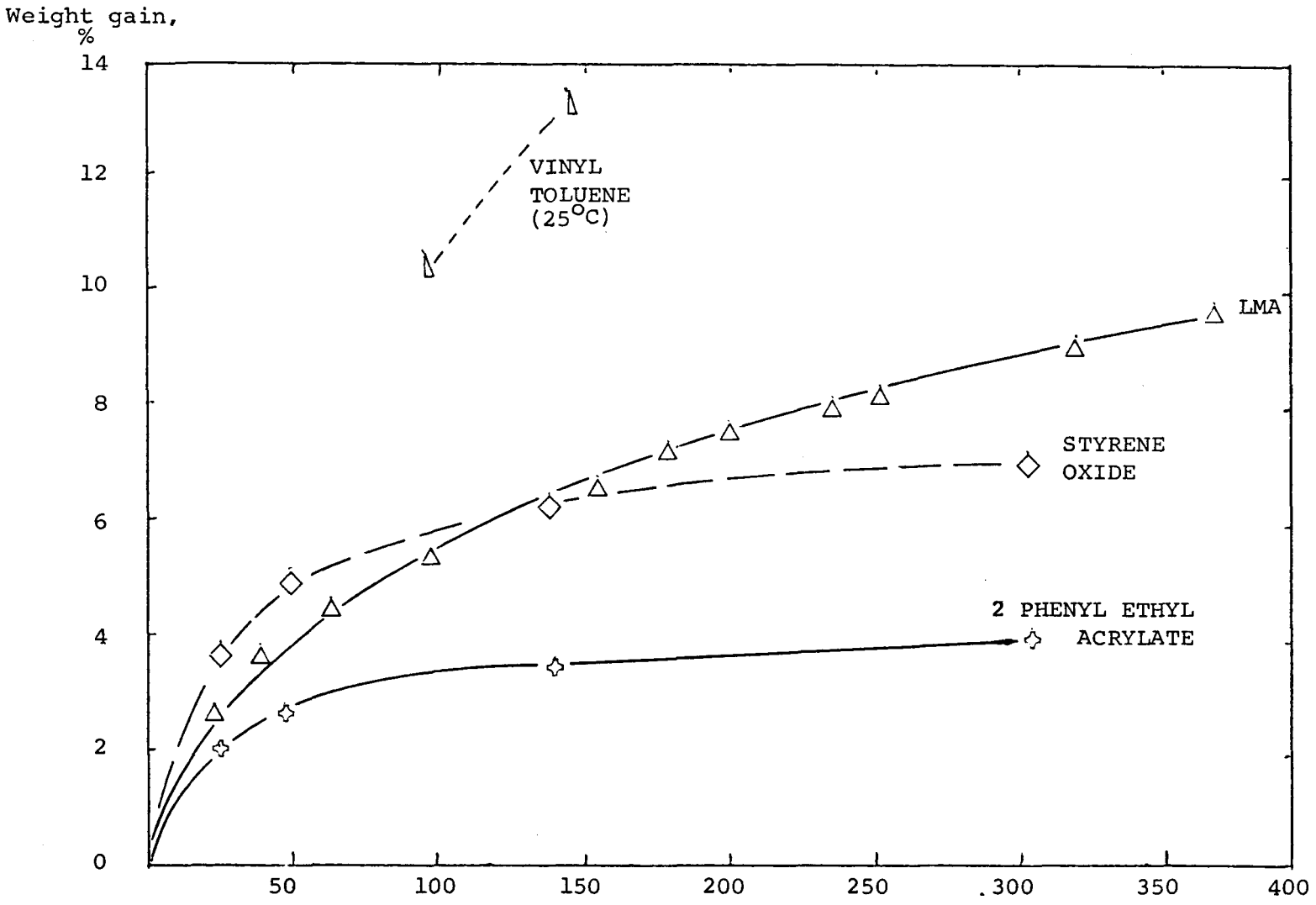

Figure 3-51. Impregnation of XLPE.

Samples: Cable A slabs, 400 mil. Temperature 50°C.

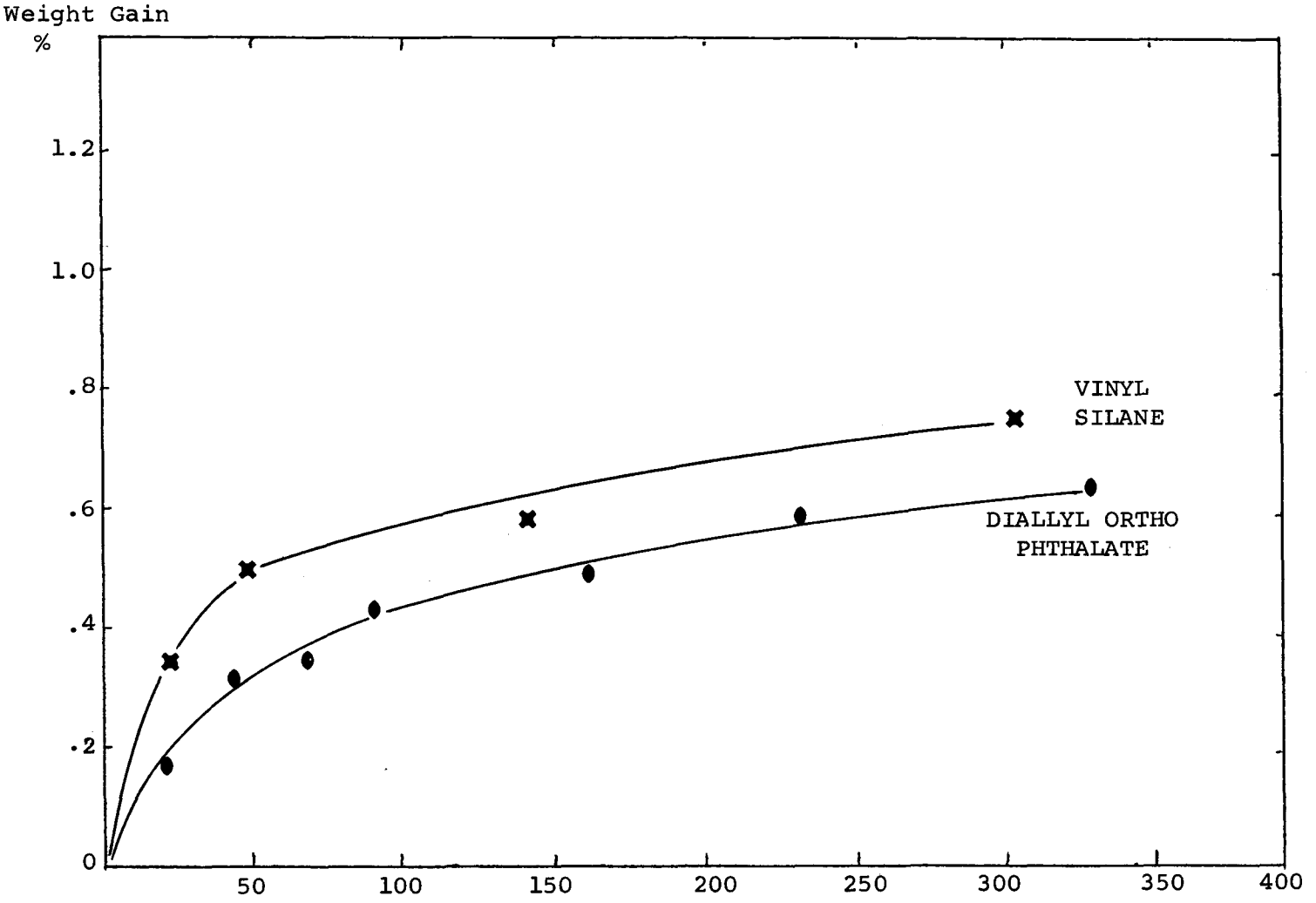

Figure 3-52. Impregnation of XLPE. TIME - HRS.

Sample: Cable A slabs, 400 mil. Temperature 50°C.

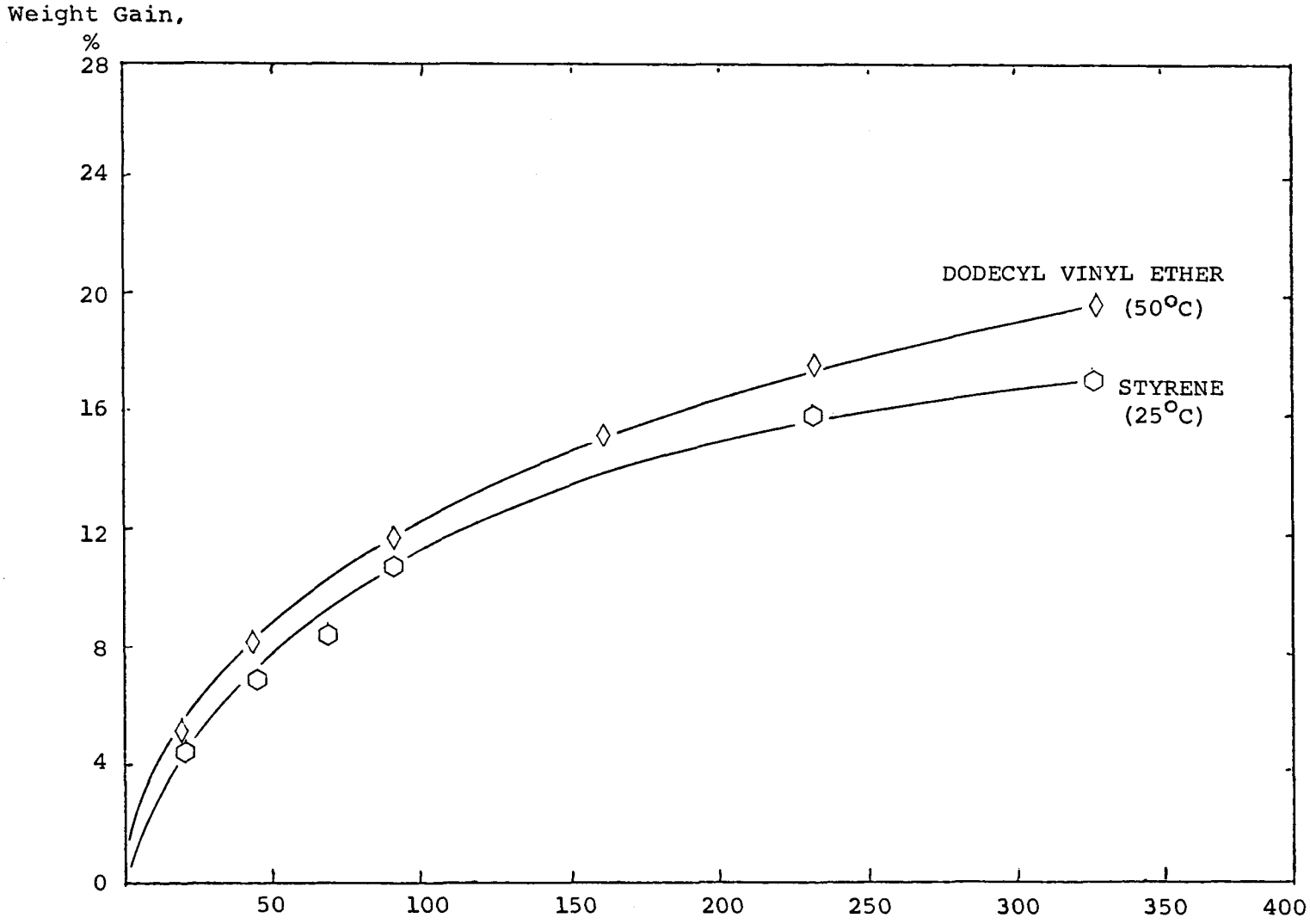

Figure 3-53. Impregnation of XLPE.

Sample: Cable A slabs, 400 mil.

Table 3-6

IMPREGNATION AND DIFFUSIVITY

	IMPREGNANT	TIME FOR 3% IMPREGNATION, HRS.	EQUILIBRIUM IMPREGNATION, %	TIME FOR HALF SATUR'N HRS.	D_o DIFFUSIVITY 10^{-8} $cm^2/sec.$
1	LAURYL MA*	34	11.0	82	3.56
2	DODECYL VINYL ETHER	6	22.0	74	3.95
3	ISOBUTYL MA*	14	14.0	44	6.64
4	DIMETHYL AMINO ETHYL MA*	13	9.0	30	9.74
5	GLACIAL METHACRYLIC ACID	13	8.0	24	12.14
6	2 PHENYL ETHYL ACRYLATE	66	4.0	32	9.13
7	STYRENE (1)	12	19.5	76	3.85
8	VINYL TOLUENE (2)	12.0	19.0	58	5.04
9	STYRENE OXIDE	18	8	30	9.74
10	VINYL ACETATE	16	6.0	16	18.26
11	VINYL SILANE	-	0.85	36	8.12
12	DIALLYL ORTHOPHTHALATE	-	0.70	60	4.87

*MA = METHACRYLATE

(1) ROOM TEMPERATURE
(2) ROOM TEMPERATURE - DATA FROM TWO POINTS.
Temperature: 50°C.

Substituting 3.85 x $10^{-8}cm^2/sec.$ for D_o, 19.5 for C_2, 0 for C_1, and 3.5 and 1.5 cm for r_2 and r_1, it would require 20.3 days to achieve half saturation (9.75%) of the cable with styrene. However, two to three percent impregnation is adequate for filling up the voids. In that case one would need about 115 hours of impregnation, which is well within practical limits.

The time required for 3% impregnation of 370 mil thick slabs has been taken from Figures 3-50 to 3-53 for a number of liquids and is also presented in Table 3-6. As a check, we calculated the 3% impregnation time using the estimated value of D_o and the equation:

$$\frac{C_t}{C_\infty} = 4 \left[\frac{D_o\, t}{L^2}\right]^{\frac{1}{2}} \qquad (3\text{-}3)$$

where: C_t = 3%
C_∞ = the maximum possible permeation level
D_o = diffusivity
L = thickness
t = time required

In the case of styrene it turns out to be 9.1 hours compared to 14 hours determined experimentally.

For lauryl methacrylate D_o = 3.56 x $10^{-8}cm^2/sec.$ and M_∞ = 11.0%. The rate of permeation, Q, is 1.05 x 10^{-2} percent per hour. The time estimated for 3% impregnation of the 370 mil slabs, exposed on both sides, is 31 hours, compared to 34 hours determined experimentally. This shows that the D_o values are fairly accurate.

In a separate experiment a piece of full size cable with the outer shield and strand shield removed (8 cm outer diameter, 3.2 cm inner diameter) was impregnated with vinyl toluene. Calculation using 5.04 x $10^{-8}cm^2/sec.$ as D_o and 19% as C_2, gives the rate of permeation as 0.0241% per hour. In other words, it would require 208 hours for 5% impregnation, compared to the experimental value of 150 hours. The computed and experimental values are thus in fair agreement.

3.3.3 Model Cable

The rate of impregnation of model cables could be different from the rate on slabs because of:

- Difference in morphology of the model cables versus slabs.

- Geometry - cylindrical geometry versus flat slabs.
- Thickness

Hence, instead of calculating the rate of permeation from the D_o values obtained in the slabs, new experiments were carried out with cable H. Impregnation was carried out at 3 different temperatures-15, 30 and 50°C using six candidate monomers. The results are summarized in Figures 3-54 and 3-55. The weight gain results are plotted against time on logarithmic scales in Figures 3-56 to 3-61. It was once again found that hydrocarbon-type monomers, having aromatic nuclei and non-polar moieties, impregnate very fast, followed by monomers with long chain alkyl groups such as dodecyl vinyl ether. The monomers having polar groups, such as esters and ketones, diffuse very slowly.

The individual data points for each monomer at each temperature were subjected to analysis assuming linear correlation on logarithmic scales. The results are presented in Table 3-7. The high values for the correlation coefficient, r, justify the treatment. The effect of temperature was assessed by plotting computed values and weight gain values on logarithmic scale for different time intervals against reciprocal absolute temperature. These Arrhenius-type plots are expected to show linear correlation. Some of the experimental data in Figures 3-54 and 3-55 show non-linearity. Deviation from linearity is attributed to the limitations of this approach.

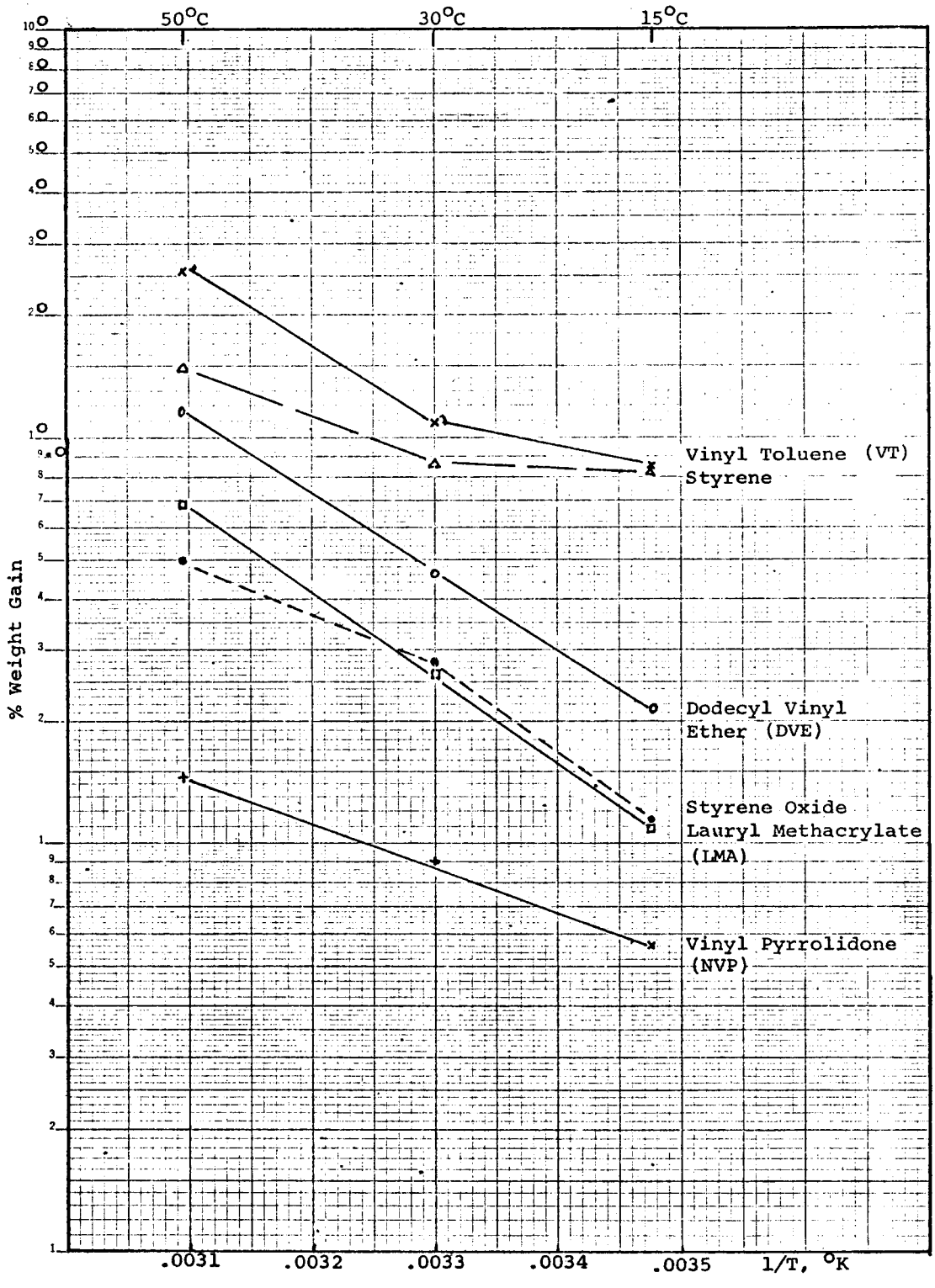

Figure 3-54. Comparison of Initial Impregnation Rates

Sample: Cable B, 13 mil slabs.

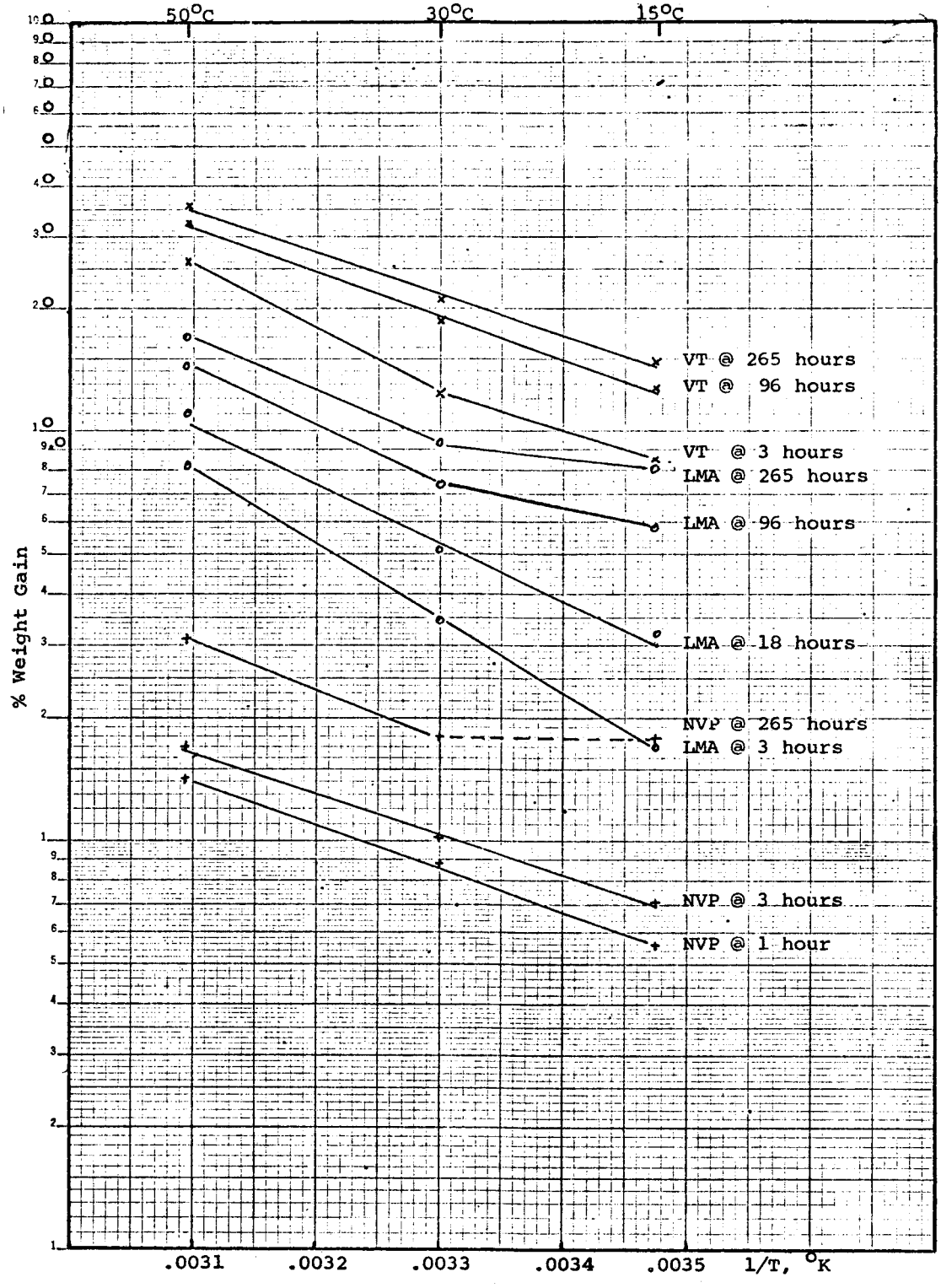

Figure 3-55. Time Temperature Correlation for Impregnation.

Sample: Cable B slabs, 13 mil.

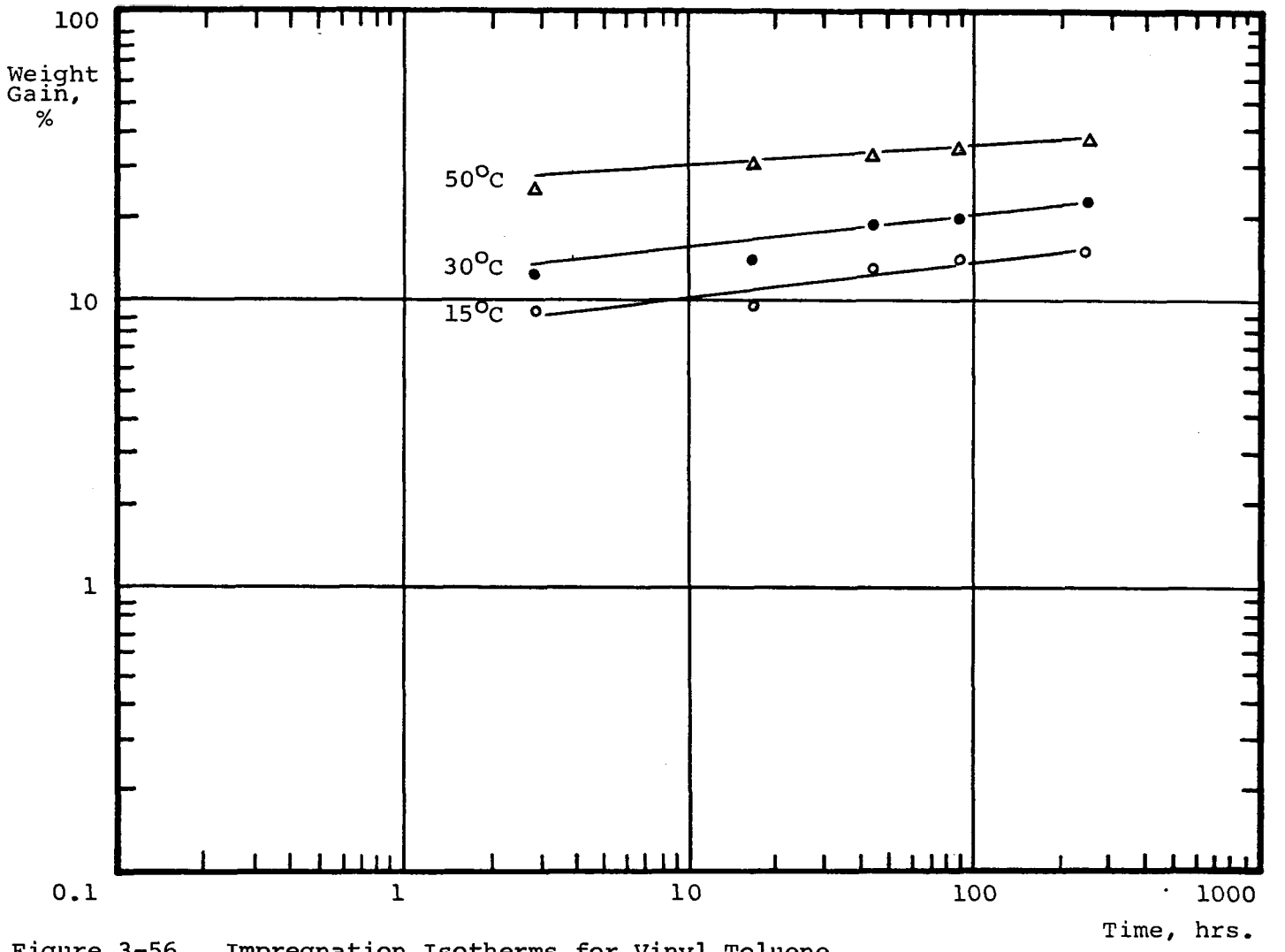

Figure 3-56. Impregnation Isotherms for Vinyl Toluene.

Sample: Cable H, 27 mil insulation.

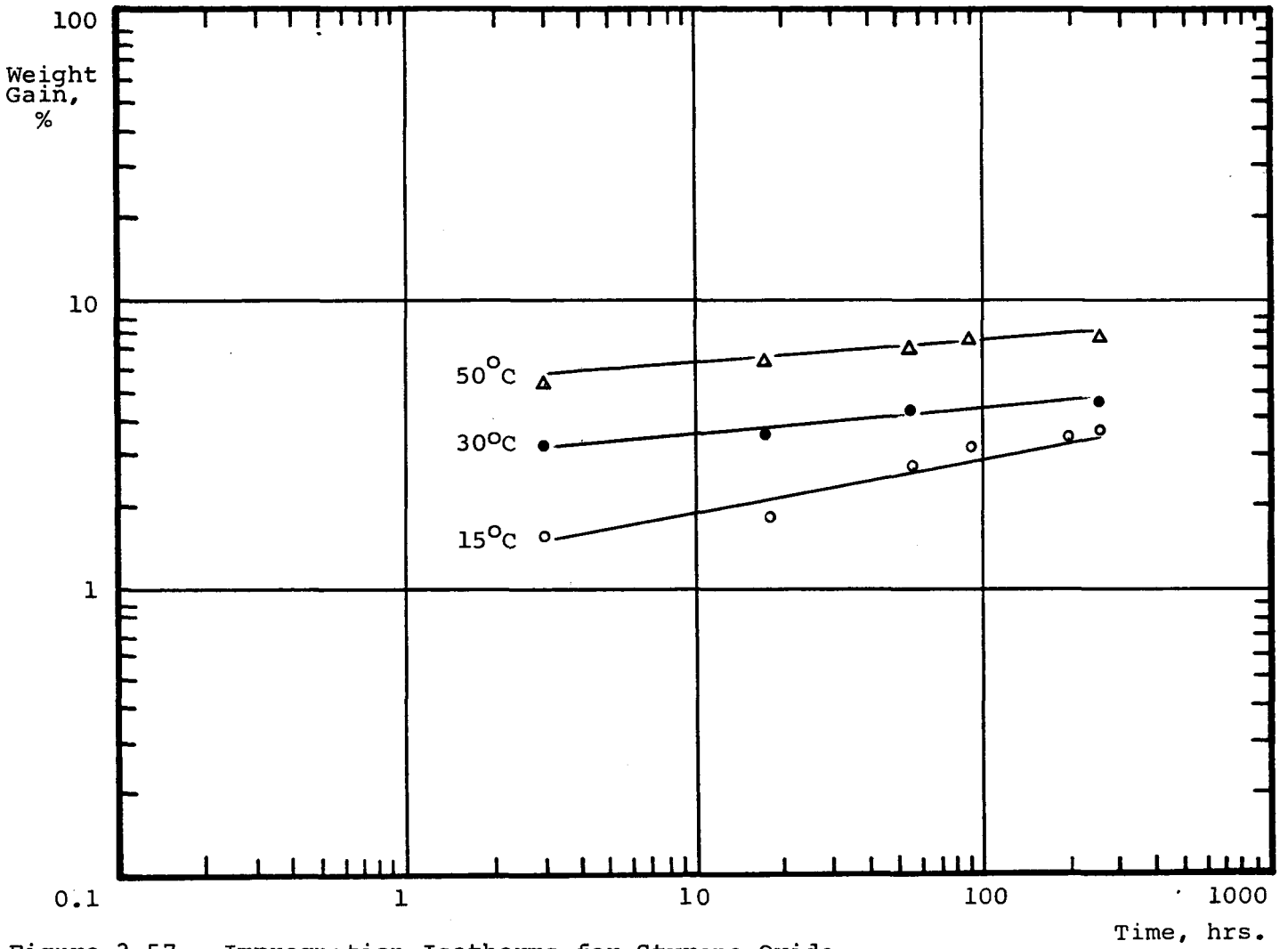

Figure 3-57. Impregnation Isotherms for Styrene Oxide.

Sample: Cable H, 27 mil insulation.

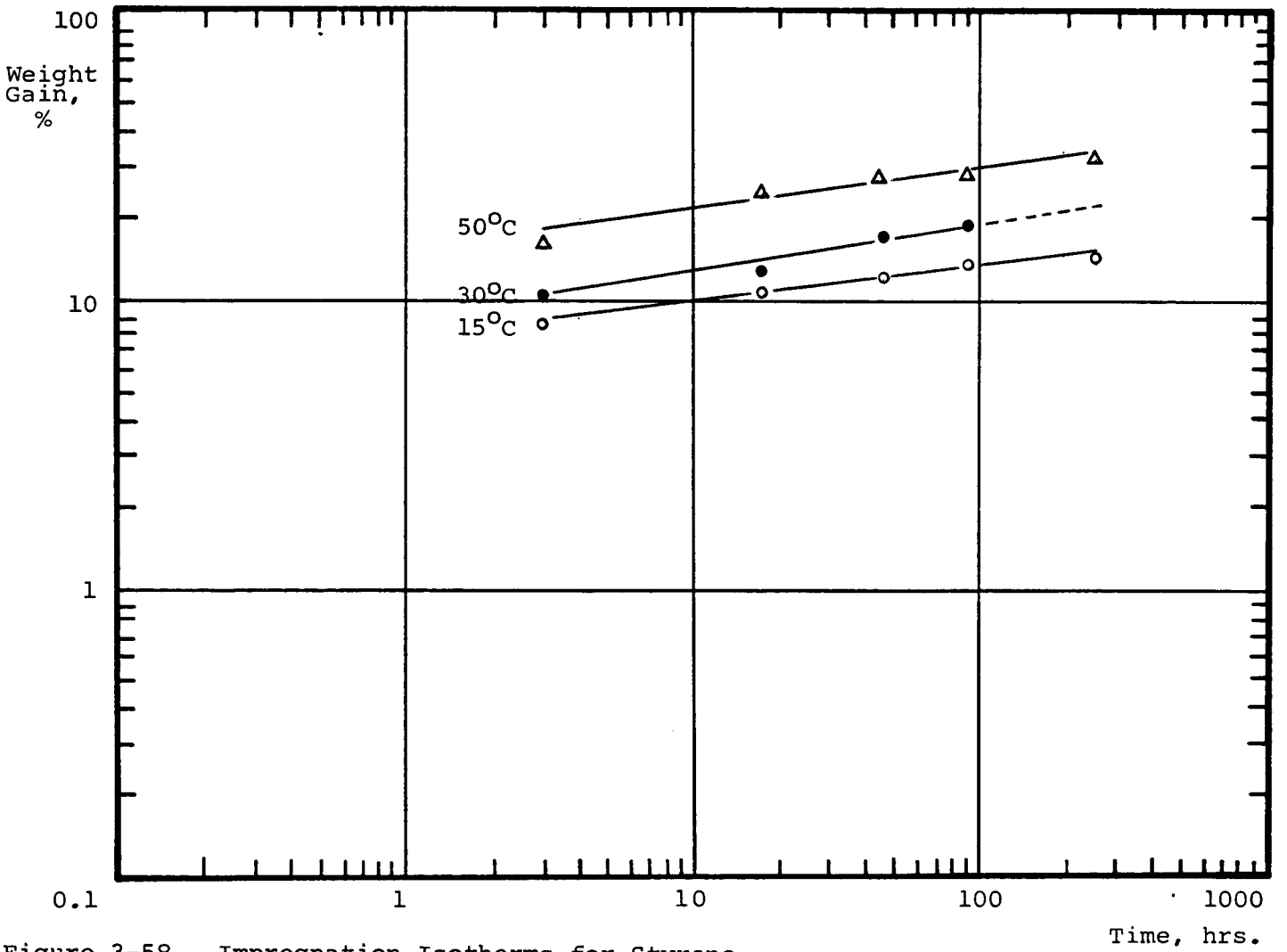

Figure 3-58. Impregnation Isotherms for Styrene.

Sample: Cable H, 27 mil insulation.

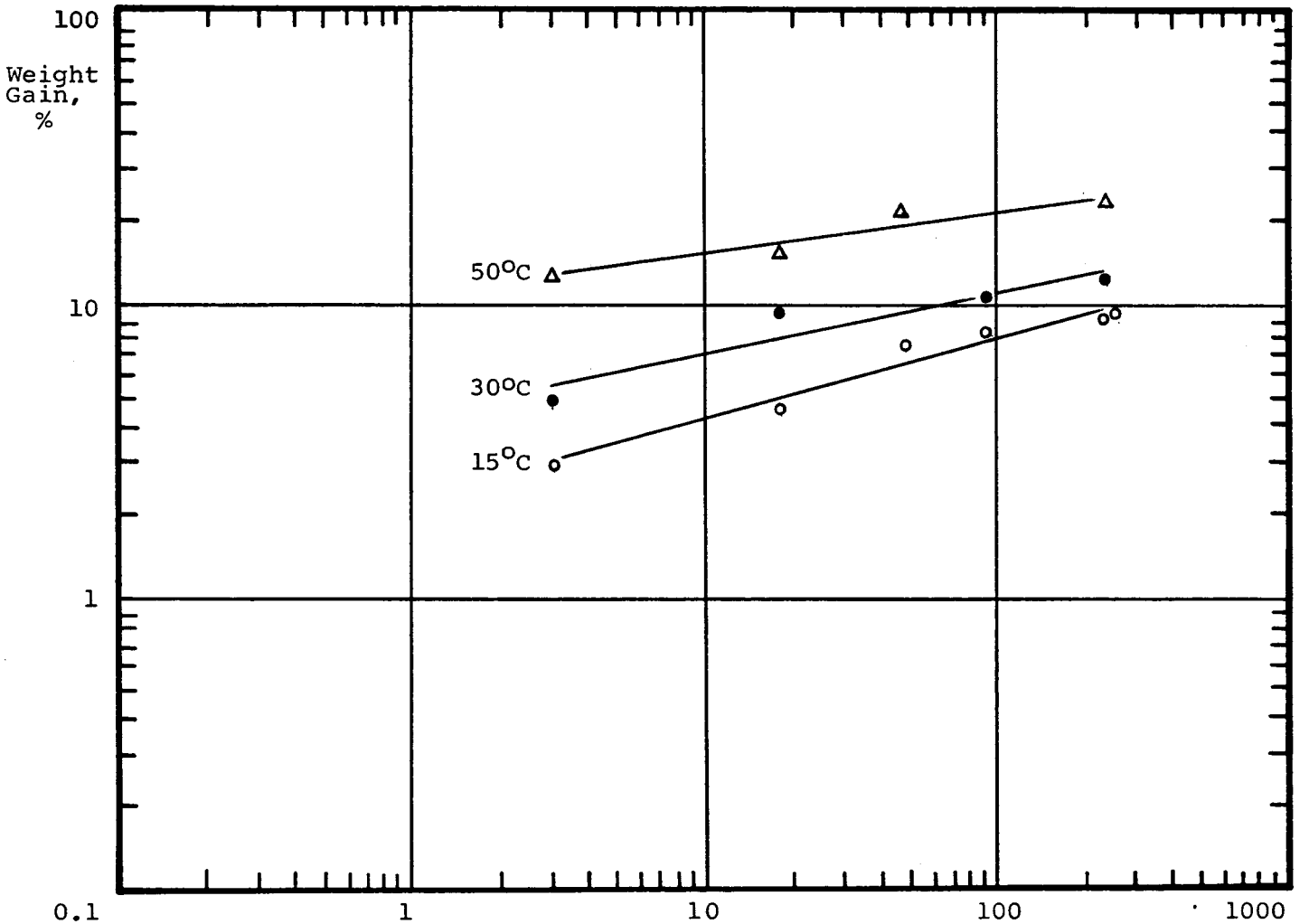

Figure 3-59. Impregnation Isotherms for Dodecyl Vinyl Ether.

Sample: Cable H, 27 mil insulation.

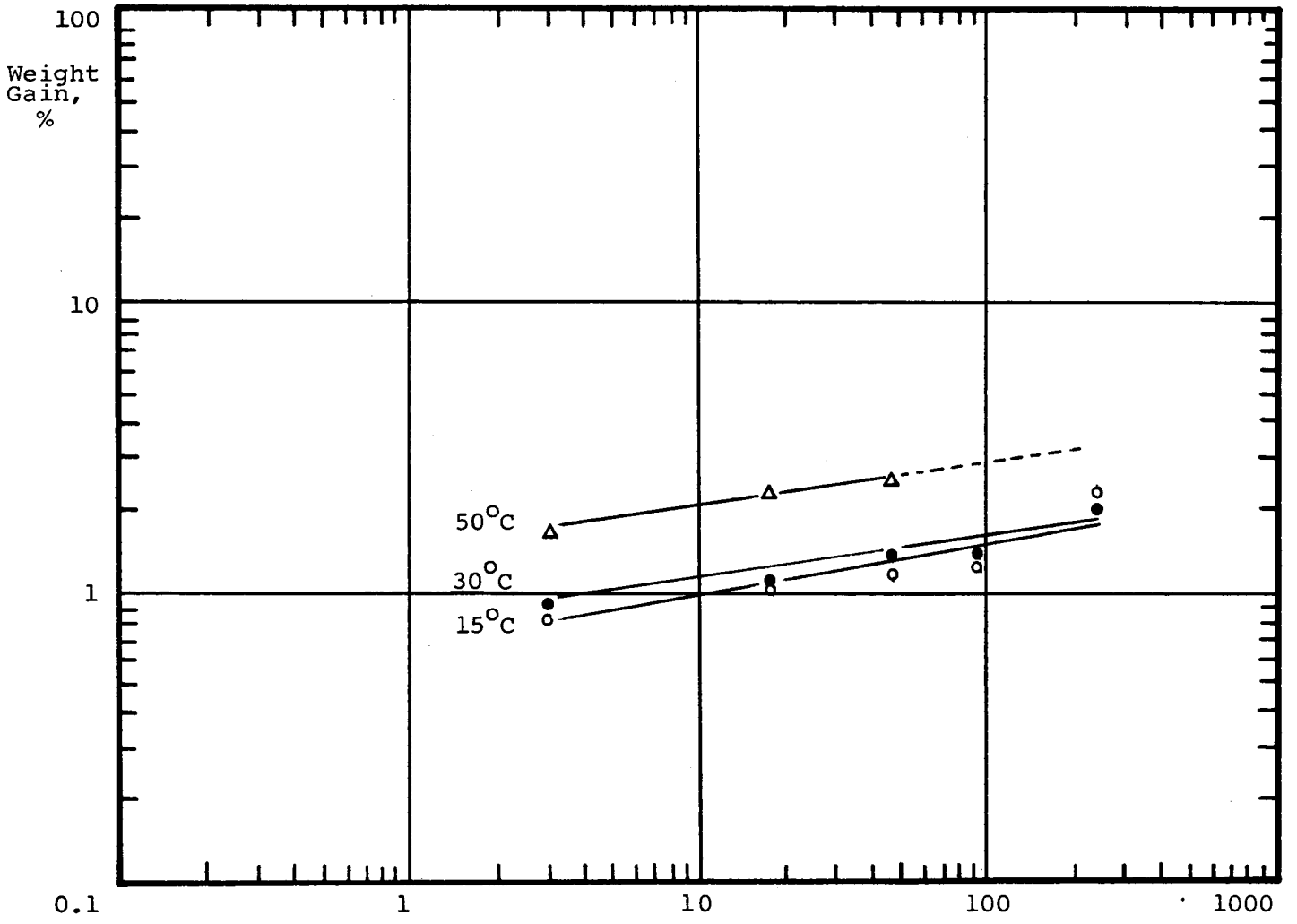

Figure 3-60. Impregnation Isotherms for Vinyl Pyrrolidone.

Sample: Cable H, 27 mil insulation.

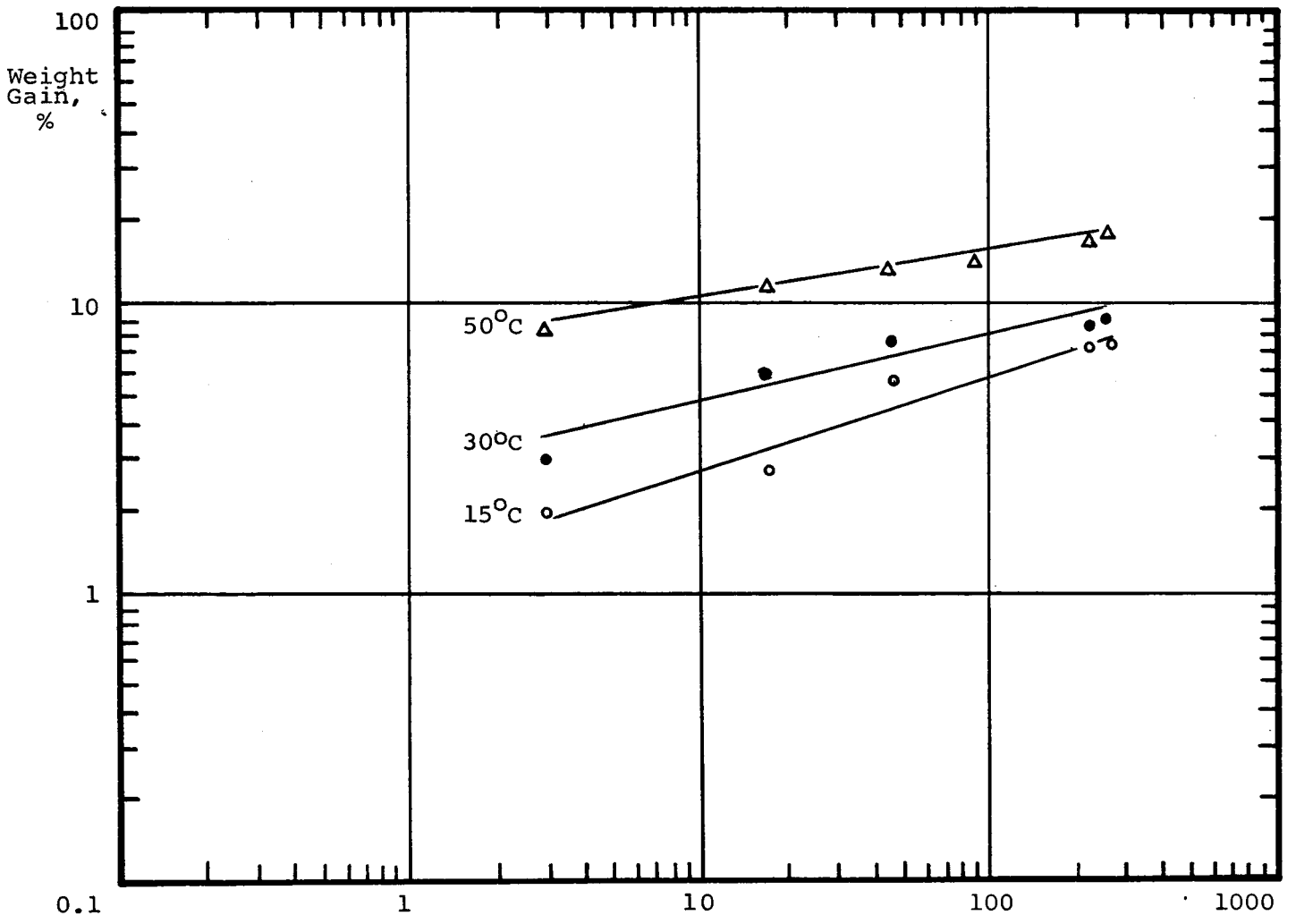

Figure 3-61. Impregnation Isotherms for Lauryl Methacrylate.

Sample: Cable H, 27 mil insulation.

Table 3-7

LINEAR REGRESSION ON TIME/WEIGHT GAIN CORRELATION

Impregnant	Temp. °C	Computed % Weight Gain at Impregnation Times (in hrs.) Indicated						Linear Regression			
		3	18	48	96	240	265	Correl. Coeff., r	Slope	Intercept Log Nat%	Intercept %
Vinyl Toluene	15	8.5	10.5	11.8	12.8	14.2	14.4	0.9233	0.1171	2.0144	7.50
	30	12.3	15.3	17.2	18.6	20.8	21.1	0.9449	0.1201	2.3774	10.78
	50	26.0	29.5	31.6	33.2	35.4	35.6	0.9979	0.0703	3.1815	24.08
Styrene Oxide	15	1.4	2.0	2.5	2.9	3.4	3.5	0.9609	0.2059	0.1167	1.12
	30	3.1	3.6	3.9	4.2	4.5	4.6	0.9549	0.0892	1.0237	2.78
	50	5.4	6.2	6.7	7.1	7.6	7.7	0.9674	0.0802	1.5919	4.91
Styrene	15	8.5	10.4	11.6	12.6	14.0	14.2	0.9736	0.1144	2.0117	7.48
	30	10.3	13.8	16.2	18.2	(21.1)	(21.5)	0.9778	0.1639	2.1521	8.60
	50	17.2	22.3	26.7	28.3	(32.3)	32.8	0.9571	0.1435	2.6893	14.72
Dodecyl Vinyl Ether	15	3.0	5.1	6.8	8.4	11.0	11.3	0.9536	0.2964	0.7697	2.16
	30	5.7	8.3	10.2	11.7	14.2	14.5	0.9085	0.2059	1.5219	4.58
	50	13.5	17.3	19.7	21.7	24.6	24.9	0.9449	0.1370	2.4522	11.61
Vinyl Pyrollidone	15	0.71	1.04	1.3	1.5	1.8	(1.8)	0.8709	0.2145	-0.5822	0.56
	30	1.02	1.27	1.4	1.6	1.8	(1.8)	0.8876	0.1224	-0.1136	0.89
	50	1.7	2.1	2.4	(2.7)	(3.0)	(3.1)	0.9912	0.1383	0.3593	1.43
Lauryl Methacrylate	15	1.7	3.2	4.5	(5.8)	8.0	8.3	0.9704	0.3532	0.1463	1.16
	30	3.4	5.1	6.3	(7.4)	9.1	9.3	0.9451	0.2253	0.9692	2.64
	50	8.3	11.0	12.9	14.4	16.7	17.0	0.9931	0.1601	1.9392	6.95

3.3.4 Impregnation with Polymerization Catalysts

3.3.4.1 Catalysts Liquid at Impregnation Temperature. For sucessful in situ polymerization it is necessary that both monomer and catalyst be present in sufficient quantities. It is, therefore, important to determine the rate of permeation of catalyst into the crosslinked polyethylene matrix. Some of the catalysts found effective in polymerization, are solid at the temperatures foreseen in practical application. Hence, liquid catalysts having structures similar to the solid ones were chosen for the preliminary experiments. These experiments were carried out with half size slabs from cable A. The results presented in Figure 3-62 on logarithmic scales show linear correlation similar to that established with monomers. However, the levels of weight gain with time for these catalysts are one to two orders of magnitude lower than that of vinyl toluene. Azo catalysts diffuse at a slower rate than the peroxides. Among the peroxides cumene hydroperoxide has the highest rate of impregnation. This series of experiments indicated that the direct impregnation with catalysts is not practical due to their low migration rates, and that alternate methods should be considered.

3.3.4.2 Catalysts Dissolved in Monomer. One potential approach is to dissolve the catalyst in the monomer and to impregnate the insulation with this solution. Initial experiments with BPO catalyst dissolved in either LMA or in vinyl toluene monomers have demonstrated that the solution impregnates the matrix at approximately the same rate as the pure monomers. However, subsequent in situ polymerizations, described in detail in Section 3-4 resulted in lower than anticipated polymer yields. This indicated that the dissolved catalyst may migrate substantially slower than the monomer. Direct analysis of the catalyst in the insulation is difficult due to its low concentration. As an example, the impregnation of insulation with 3% monomer containing 2% dissolved catalyst would result in 0.06% catalyst concentration in the insulation assuming identical permeation rates for monomer and catalyst. Conventional analytical methods are not suitable for the quantitative determination of the catalyst under these conditions.

A number of approaches were considered to increase the catalyst level in the insulation:

- Longer impregnation time.
- Higher temperature.
- Higher catalyst concentration.

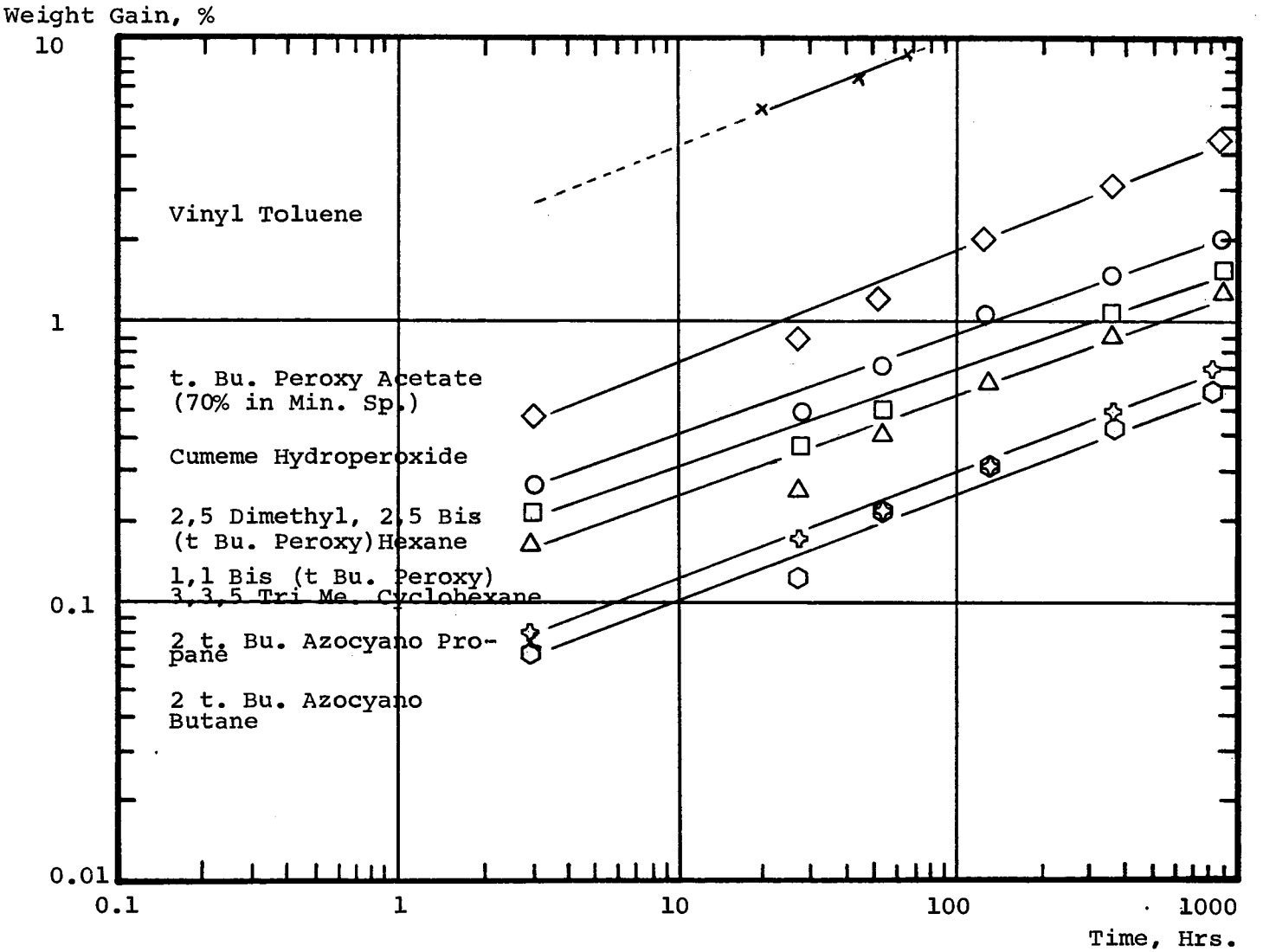

Figure 3-62. Rate of Catalyst Permeation.

Sample: Cable A, slabs, 400 mil. Temperature: 30°C.

These factors are not independent from each other and result in a number of effects in addition to the desired increase in catalyst migration. Longer impregnation times increase the cost of treatment and may result in excessive monomer concentration in the matrix. Higher temperature would increase the rate of monomer migration, possibly even more than the catalysts. An undesirable side effect of higher temperature is the increased solubility of insulation in the monomer. Both higher temperature and higher catalyst concentration in the monomer shorten the shelf life of the solution and cause premature polymerization. This could be controlled by using polymerization inhibitors, but the selection of a suitable inhibitor and the optimization of its concentration would complicate the system. The possible interactions were studied systematically in a grid program with the following variables:

- Catalyst concentration at 0, 2, 5 and 8%.
- Temperature at 30, 50 and 70°C.
- Impregnation time from 0 to 30 hours.

Vacuum dried model cable H was used as specimen, BPO as catalyst and vinyl toluene as monomer. The latter was subsequently replaced by ethylbenzene (its non-polymerizable analogue) to avoid complications with partial polymerization at high catalyst levels, after experiments confirmed that their solubility and impregnation characteristics are not significantly different. Weight gain of the insulation was monitored and compared to the weight of residue of the evaporated solution remaining at the end of each experiment. Regression analysis minimized the experimental variations. The weights of BPO migrated into the matrix, and the weight of insulation dissolved in the solvent were determined. The results are presented in Table 3-8 and Figure 3-63 to 3-65. The data shows that throughout the investigated range the solvent migrates much faster than the catalyst. Neither increased temperature nor increased concentration shows promise to accelerate the catalyst migration to practically acceptable levels. On the other hand the loss of insulation, due to its solubility in ethylbenzene indicates potential problems.

3.3.4.3 Two-Step Impregnation Process. The results of the previous experiments established that benzoyl peroxide is diffusing at a much lower rate than the monomer. Hence, it was proposed to carry out the impregnation in two steps; i. e.:

1. Impregnation with a concentrated catalyst solution, using a solvent which is non-polymerizable followed by the removal of the volatile solvent by vacuum drying.

Table 3-8

Effect of Impregnation on Weight of Insulation

BPO %	Temp. °C	Time Hrs.	% Weight change due to: BPO	XLPE dissolved	Net change
2	25	3	0.10	- 0.01	+ 0.09
		30	0.14	- 0.13	+ 0.01
	50	3	0.22	- 0.07	+ 0.15
		30	0.27	- 0.71	- 0.44
	70	3	0.90	- 3.10	- 2.20
		30	1.82	- 7.60	- 5.78
5	25	3	0.27	- 0.01	+ 0.26
		30	0.38	- 0.13	+ 0.25
	50	3	0.52	- 0.07	+ 0.45
		30	0.76	- 0.71	+ 0.05
	70	3	2.80	- 3.10	- 0.30
		30	3.85	- 7.60	- 3.75
8	25	3	0.43	- 0.01	+ 0.42
		30	0.78	- 0.13	+ 0.65
	50	3	0.82	- 0.07	+ 0.75
		30	1.12	- 0.71	+ 0.41
	70	3	3.50	- 3.10	+ 0.40
		30	5.10	- 7.60	- 2.50

Sample: Model Cable H.
Solvent: Ethylbenzene

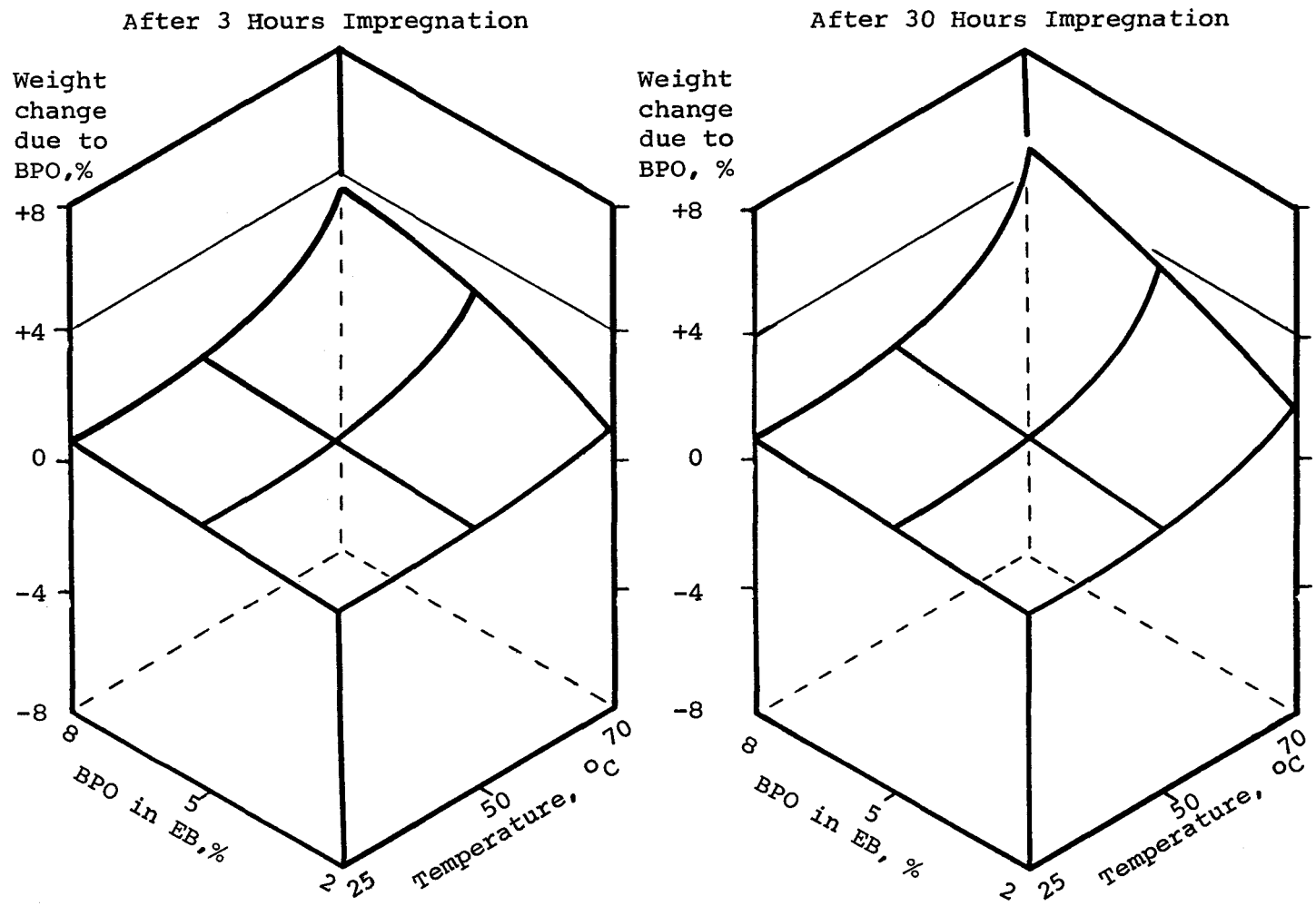

Figure 3-63. Effect of Impregnant Composition and Temperature on BPO Migration into XLPE. Sample: Model Cable H.

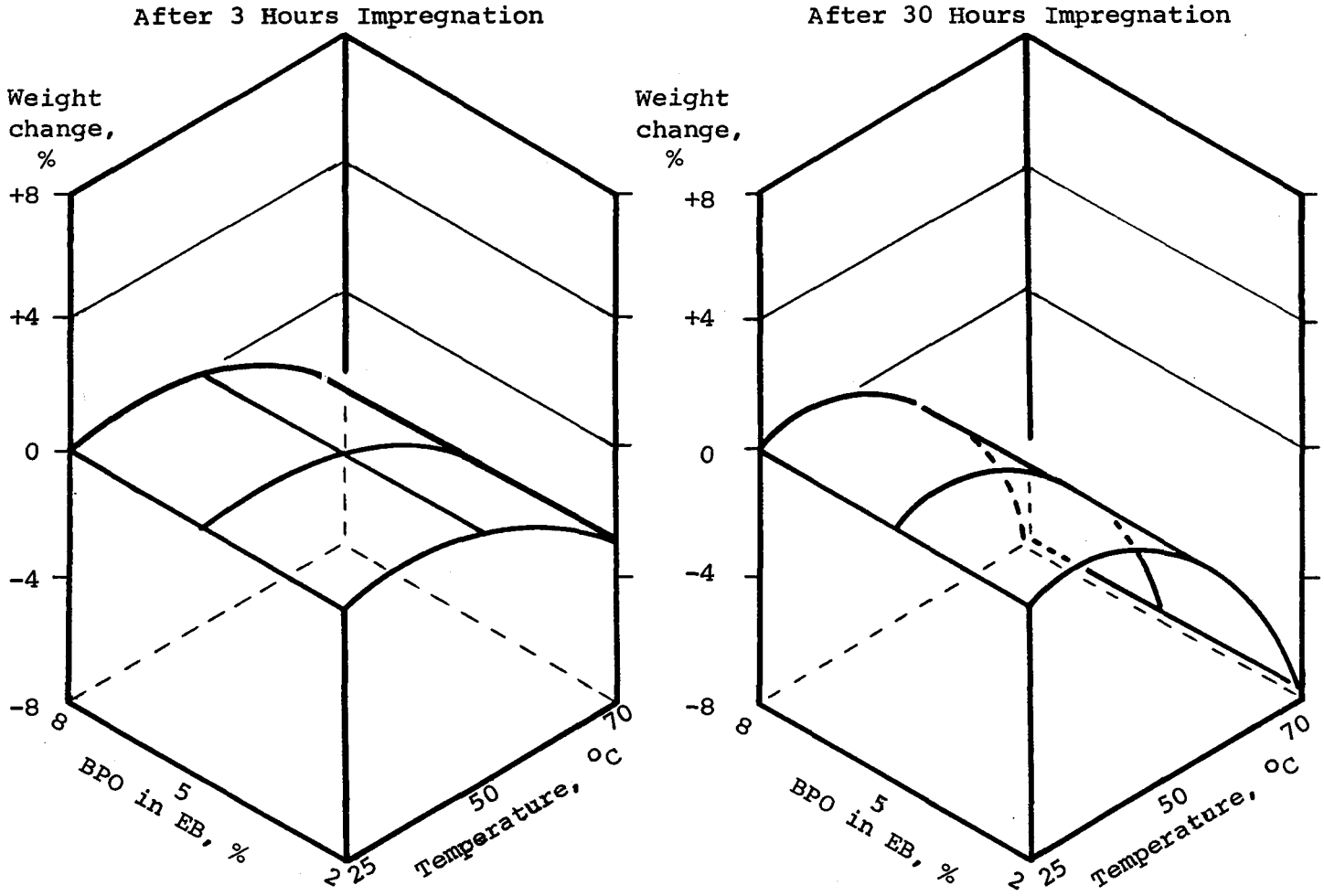

Figure 3-64. Effect of Impregnant Composition and Temperature on XLPE Insulation. Weight loss due to PE dissolved in EB. Sample: Model Cable H.

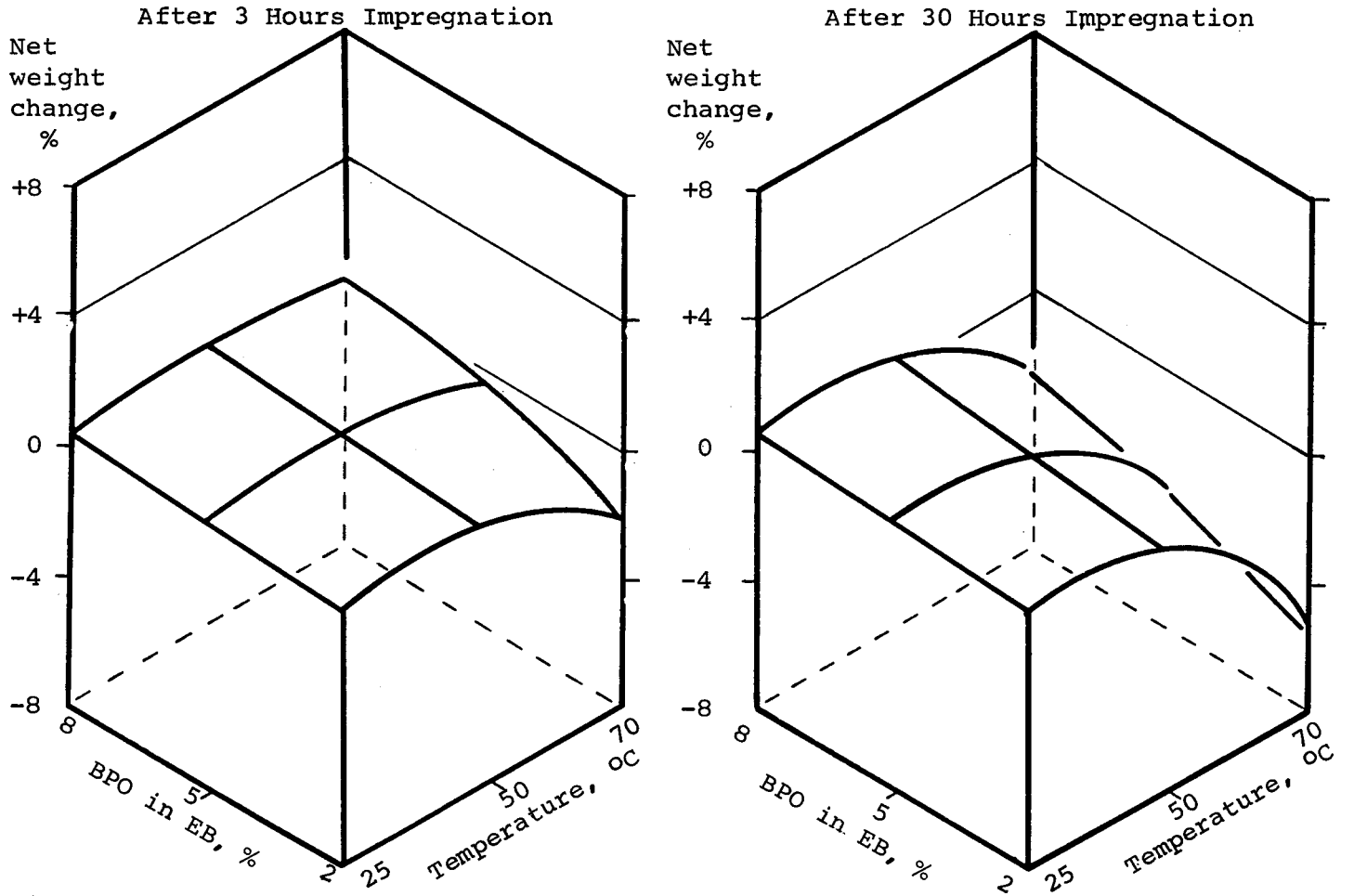

Figure 3-65. Effect of Impregnant Composition and Temperature on XLPE Insulation. Net change combines gain due to BPO and loss due to solubility, Figures 3-63 and -64 respectively. Sample: Model Cable H.

2. Impregnation with a monomer. A small concentration of peroxide may be maintained to stop any backmigration.

To reduce the time and temperature of vacuum drying, the solvent had to be highly volatile. To allow adequate level of peroxide migration, the liquid had to be a good solvent for peroxide. After preliminary screening of a number of candidates, methyl ethyl ketone (MEK) (31) was found to be most suitable. The rate of impregnation of the MEK solution and the amount of peroxide migrated are presented in Figure 3-66. It appears that at 10% concentration of peroxide, the rate of impregnation of peroxide is about half as much as that for the solvent. It must be noted that methyl ethyl ketone is not a good solvent for polyethylene. Hence, the rate of permeation of MEK into polyethylene is small for the reasons discussed in Section 2. The ratio between the rates of migration of peroxide and the carrier solvent is therefore more favorable than the ratio for benzoyl peroxide in ethyl benzene or in vinyl toluene.

Several experiments were carried out to demonstrate the practicality of this process. Since they were carried out through polymerization and most of them subjected to AC breakdown tests, they are discussed in detail in Section 3.4.

3.3.5 AC Breakdown Strength

The effect of liquid impregnation on the AC breakdown strength of the insulation was investigated in three groups of experiments with slabs and the most promising candidate was used in a fourth group with model cables.

A few of the impregnants were subsequently polymerized in situ and are discussed in detail in Section 3.4.

3.3.5.1 Preliminary Investigation on Slabs. Initial experiments on impregnation of liquids were carried out on slabs cut from cable A, ditched to 18 mil and thoroughly dried in high vacuum. A mixture of p-xylene, ethyl alcohol and triethylene glycol at the ratio of 80: 15:5 was used to establish comparability with earlier work on full size cables (10). Acetophenone, lauryl methacrylate (LMA) and a moderately viscous paraffin oil were chosen as prototypes of impregnants of high, medium and zero polarity respectively. The objective was to assess the effect of liquid impregnants on dielectric strength. The conditions for vacuum drying and impregnation, and the V_{50} values in the 1 hour step tests are listed in Table 3-9. The Weibull plots are presented in Figures 3-67 to 3-71. All of them are linear confirming the applicability of Weibull statistics to testing ditched

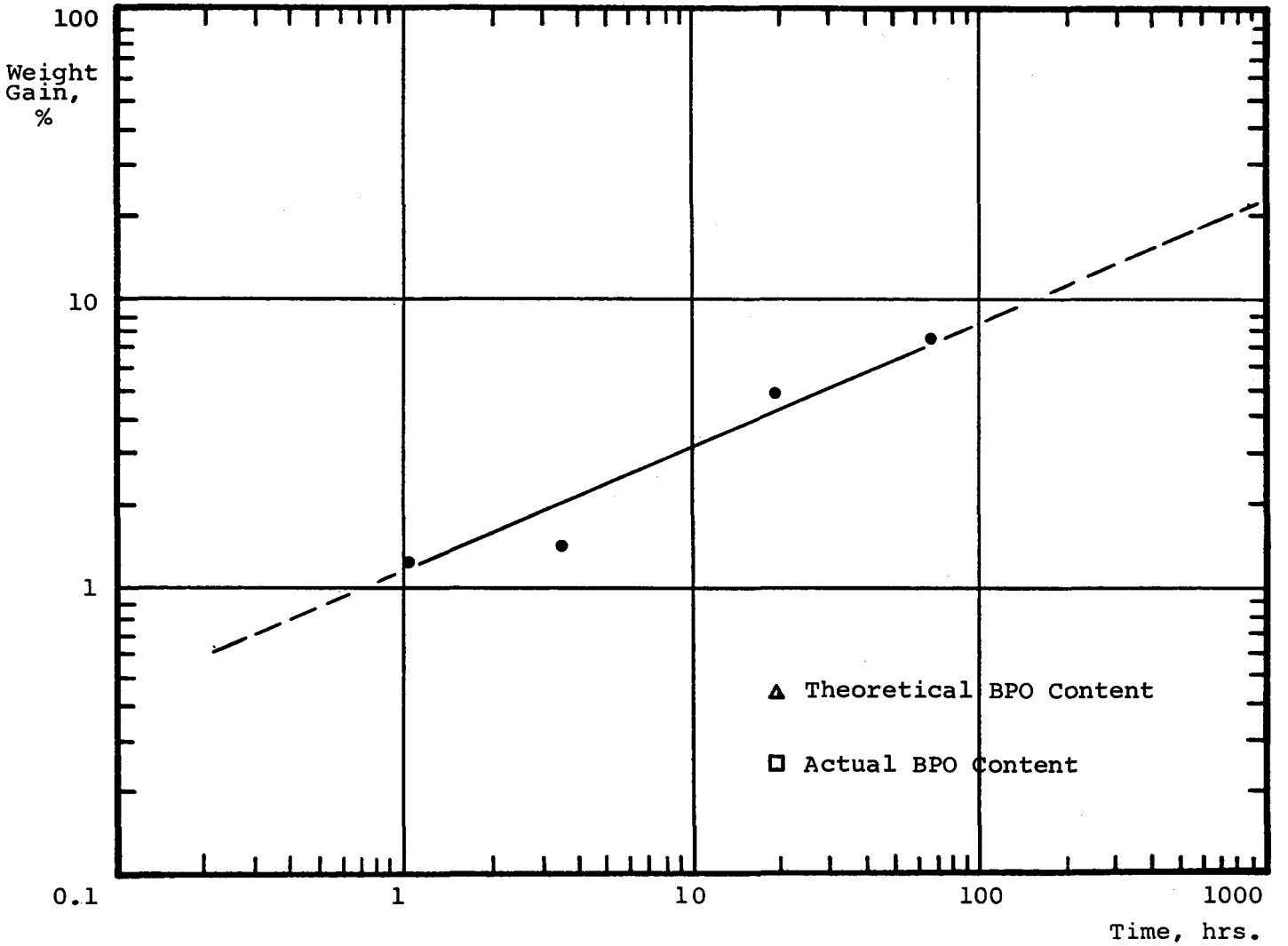

Figure 3-66. Impregnation with Methyl Ethyl Ketone Containing 10% BPO.

Sample: Cable E, 25 mil insulation.

Table 3-9

SUMMARY OF THE RESULTS ON LIQUID IMPREGNATION

(All Weights are based on Original = 100)
Sample: Cable A slabs, 18 mil.

EXPT. NO.	DRYING			IMPREGNATION			IMPREGNATING MATERIALS	WEIGHT AFTER:		AC BREAKDOWN
	Hrs.,	°C	μm	Hrs.	PSI	°C		Drying	Impreg.	V/mil V_{50}
2A	168	80	5	168	50	20	TEG/p-Xylene Ethanol	-	-	2190
5	168	80	5	168	50	20	TEG/pX/Et	-	-	2300
11A	168	80	5	168	50	20	Acetophenone	-	99.14	2700
14	168	80	5	168	50	20	LMA	-	99.88	1800
15	235	80	5	168	50	20	Paraffin Oil	-	99.26	1700
24	192	80	25	168	50	25	Acetophenone	99.20	100.09	2700
25	168	80	5	168	-	50	LMA	-	106.8	2260
25A	168	80	5	168	-	50	Paraffin Oil	99.24	103.1	2330
33	192	80	25	288	-	40	Acetophenone	99.1	101.7	2500
42	168	80	25	96	-	100	PE Wax	99.26	112.6	2200

WEIBULL PLOTS

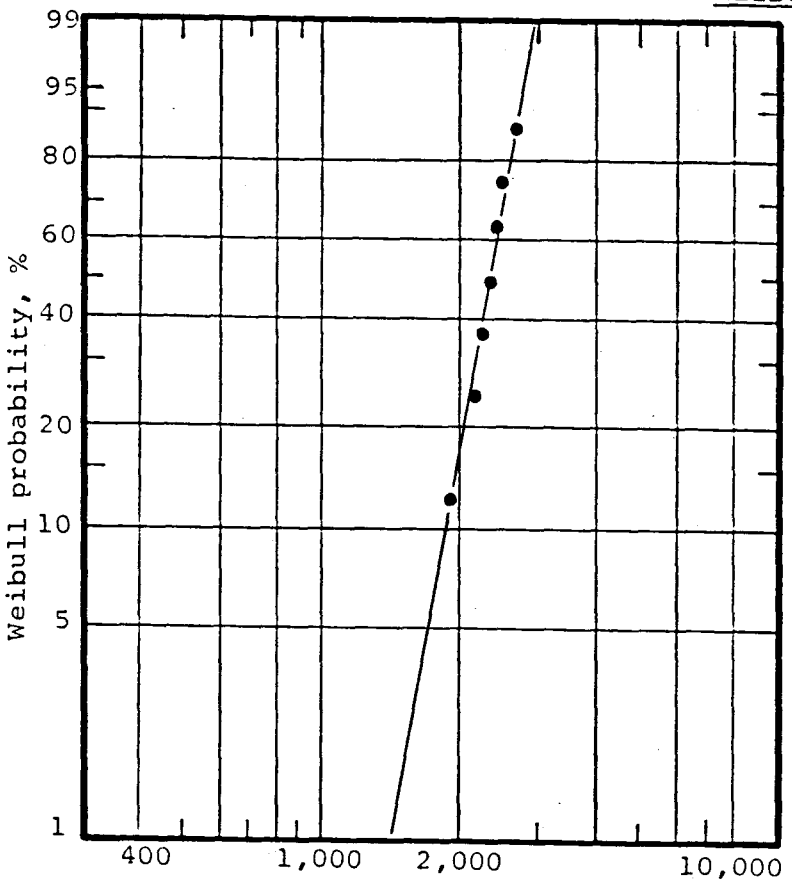

Figure 3-67. Impregnation with p-Xylene, Ethyl Alcohol and Triethylene Glycol Mixture. Experiment No. 5. Cable A, 18 mil slab, 1 hour step test.

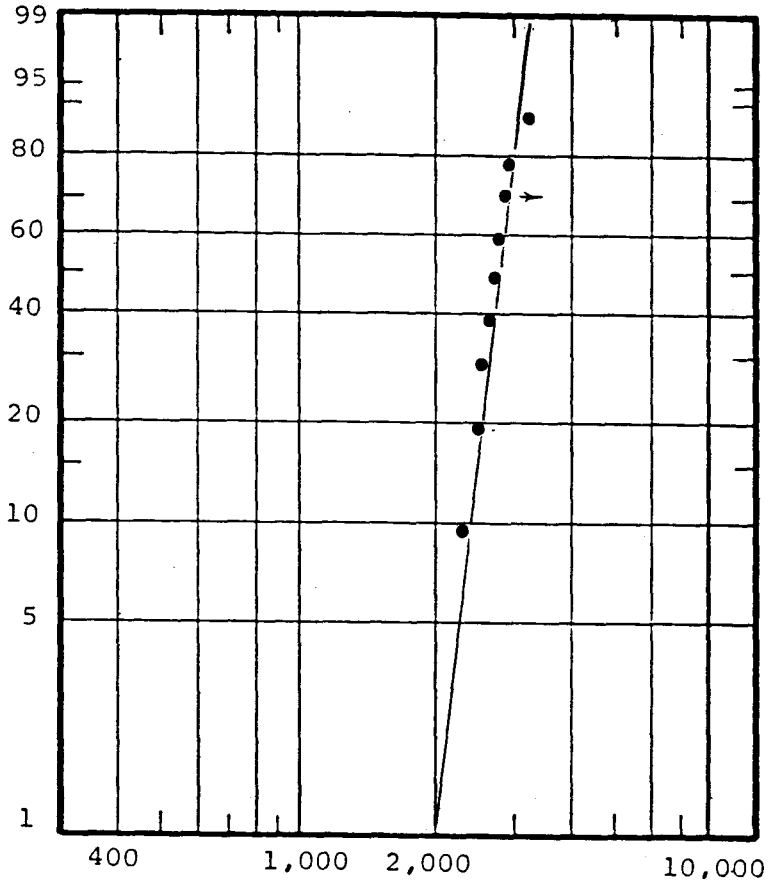

Figure 3-68. Impregnation with Acetophenone. Cable A, 18 mil slab, 1 hour step test. Experiment No. 24.

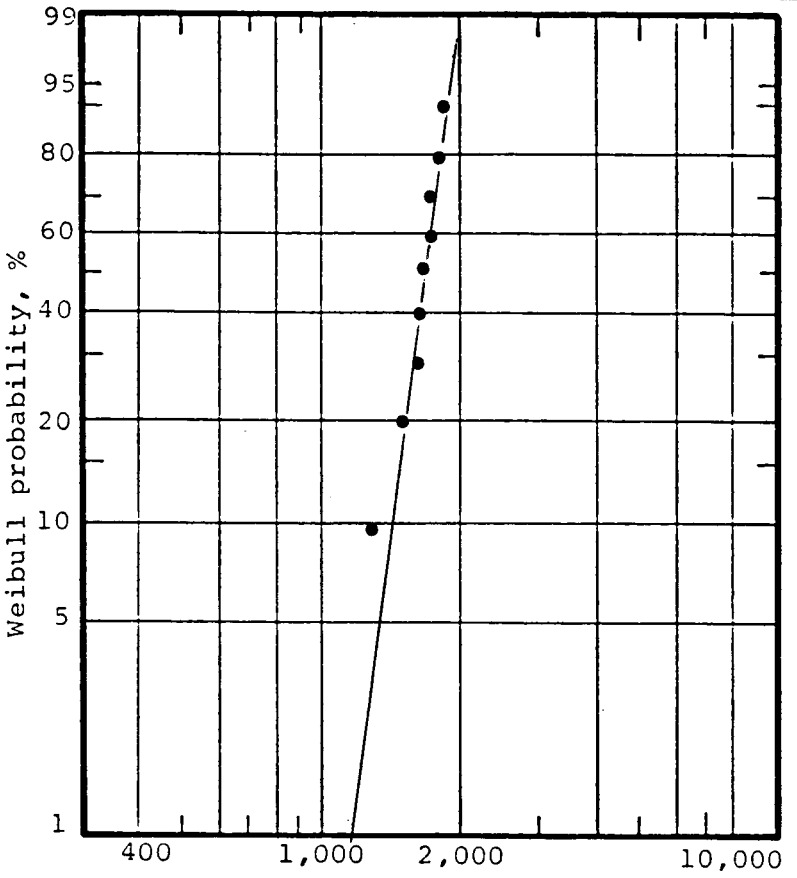

Figure 3-69. Impregnation with Paraffin Oil. Cable A, 18 mil slab, 1 hour step test. Experiment No. 15.

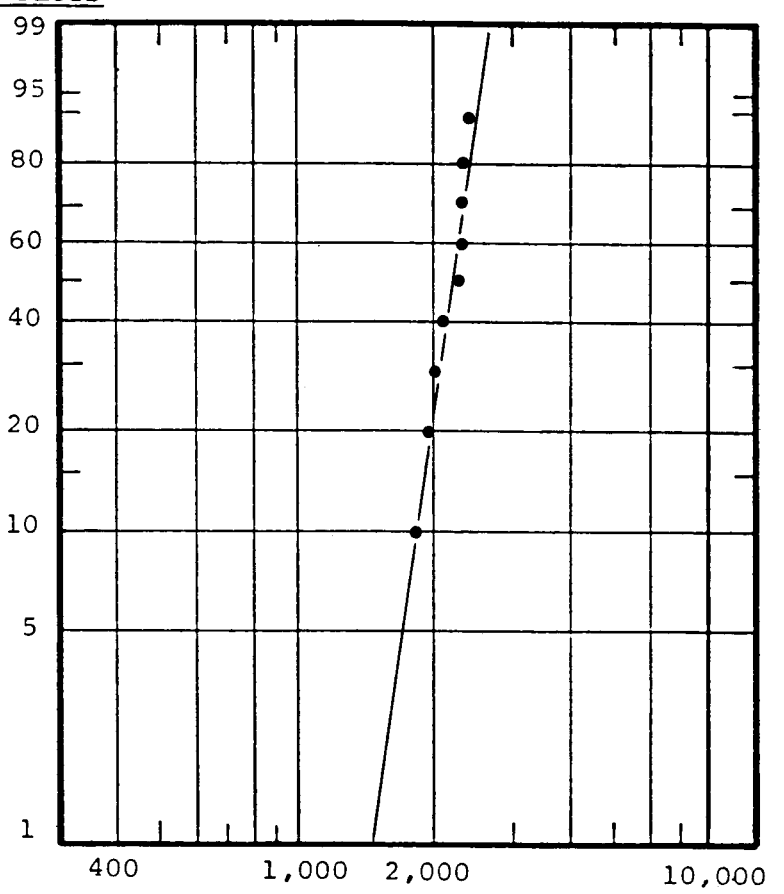

Figure 3-70. Impregnation with PE Wax. Cable A, 18 mil slab, 1 hour step test. Experiment No. 42.

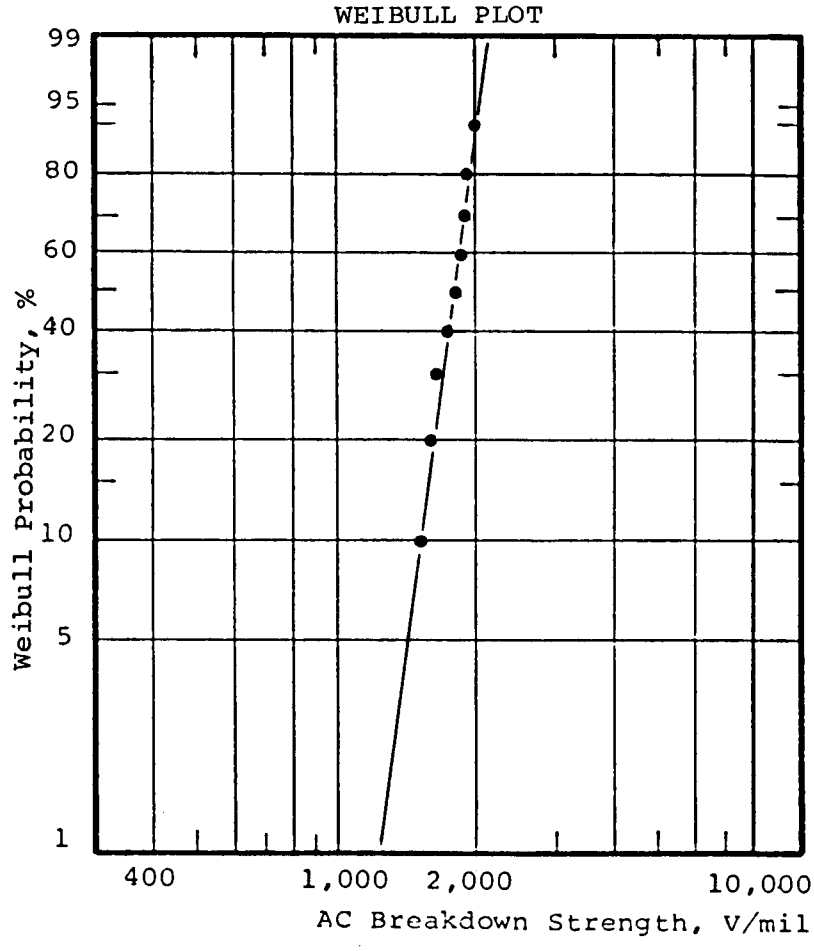

Figure 3-71. Impregnation with LMA.
Cable A, slab @ 18 mil, 1 hour step test.
Experiment No. 14.

slabs at high stresses. The V_{50} values for acetophenone, paraffin oil and PE wax and for lauryl methacrylate monomer and polymer have been plotted against levels of impregnation in Figures 3-72 to 3-74 respectively. It is clearly evident that:

- Impregnation increases the AC breakdown strength.
- The improvement in dielectric strength increases with the increase in the level of the impregnant, reaches maximum and then either decreases slowly or levels off, Figure 3-75.
- The level at which the maximum is seen is different for different impregnants, about 0.5% for acetophenone, 2% for lauryl methacrylate and 1.5% for paraffin oil or PE wax.
- The degree of improvement is probably independent of the physical state of the impregnants. Thus, the results for polylauryl methacrylate and polyethylene wax fit into the curves of their liquid counterparts.

3.3.5.2 Screening of Impregnants. The preliminary experiments showed that the nature of the impregnant is possibly the dominating factor in improving dielectric strength and dramatic improvements can be obtained by using small amounts of acetophenone. Hence, a screening program was undertaken in which liquids similar to acetophenone were used. Acetophenone has three distinct structural moieties namely a phenyl ring, a methyl group and a carbonyl group. Further, the three C=C double bonds in the ring and the -C=O double bond are in conjugation. One or more of these groups might be responsible for the voltage stabilizing effect of acetophenone. Based on this consideration, twelve liquids were selected having one or more of these groups. The chemical structures of these liquids are presented in Figure 3-76 along with that of acetophenone. Preliminary studies were done using small slabs to study the rate of impregnation at different temperatures. This helped the selection of the right temperature and time for impregnation.

In the systematic study of impregnants, slabs from cable B were "ditched" to 18 mil thickness and dried at 70°C in a vacuum oven at moderate vacuum (about 1200μm) instead of drying them in high vacuum chambers. A quick experiment showed that it takes about 12 days at 70°C at 1200μm vacuum to remove 1.2 to 1.3% volatiles, and at that time almost all of the acetophenone is removed. Some impregnants like vinyl toluene, increased the AC breakdown strength beyond the range of available equipment and necessitated the lowering of specimen thickness to 13 mil.

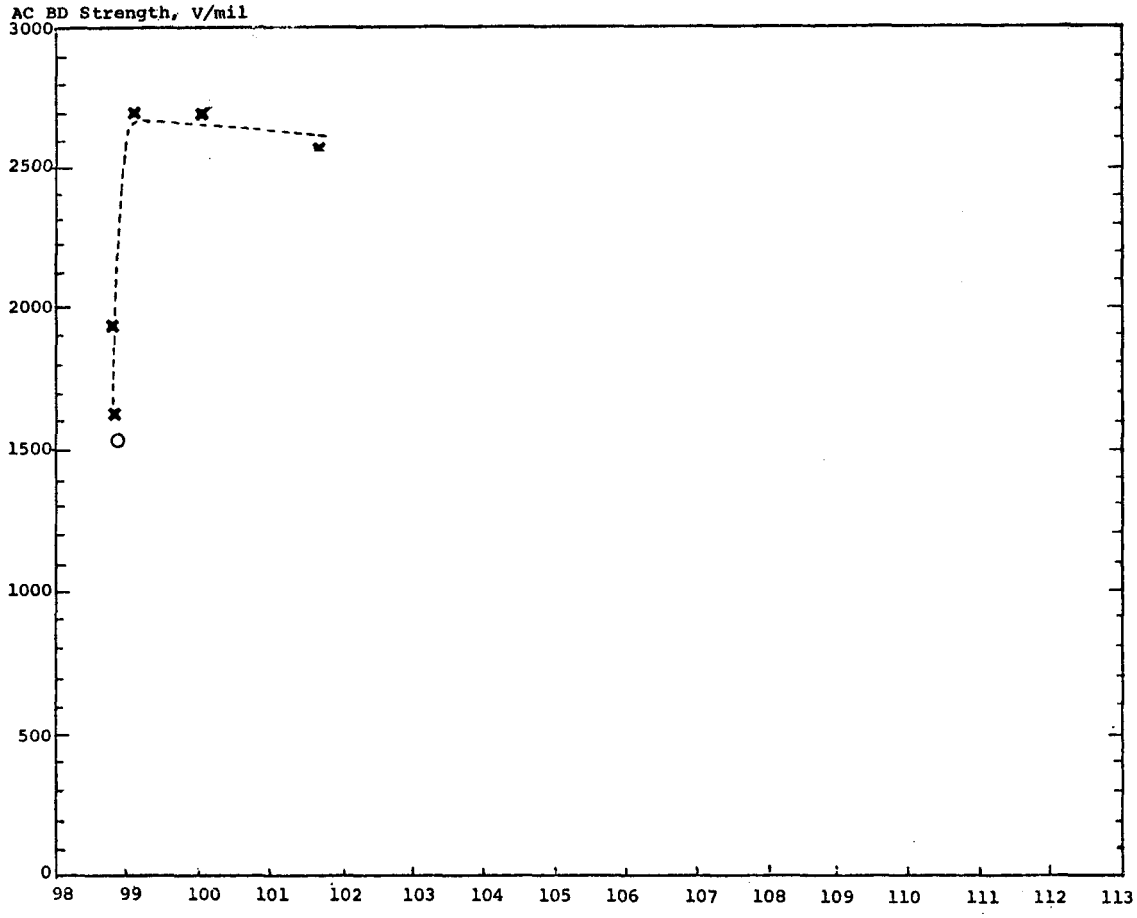

Figure 3-72. Effect of Acetophenone on AC Breakdown Strength.

Sample: Cable A slabs, 18 mil. One hour step test.

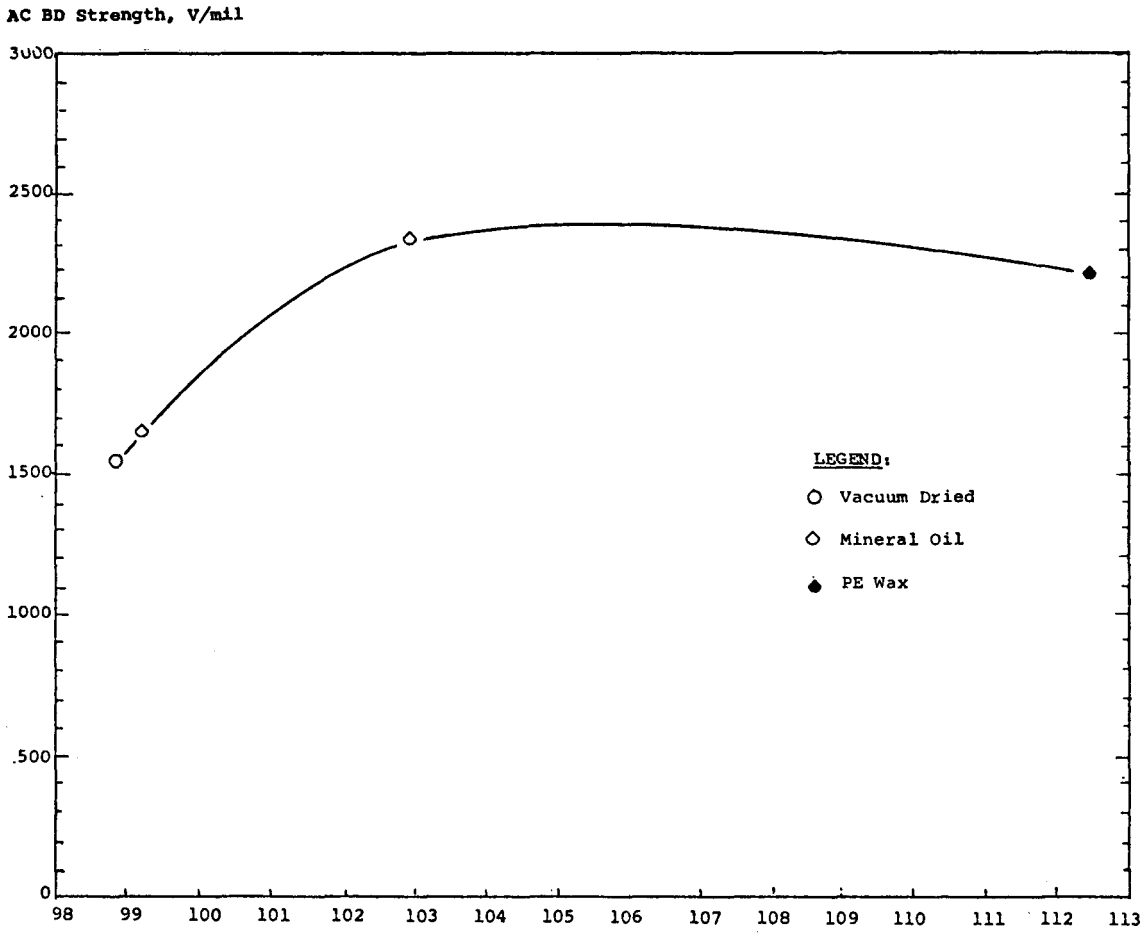

Figure 3-73. Effect of Mineral Oil and PE Wax on AC Breakdown Strength. Normal Weight
Sample: Cable A slabs, 18 mil. One hour step test.

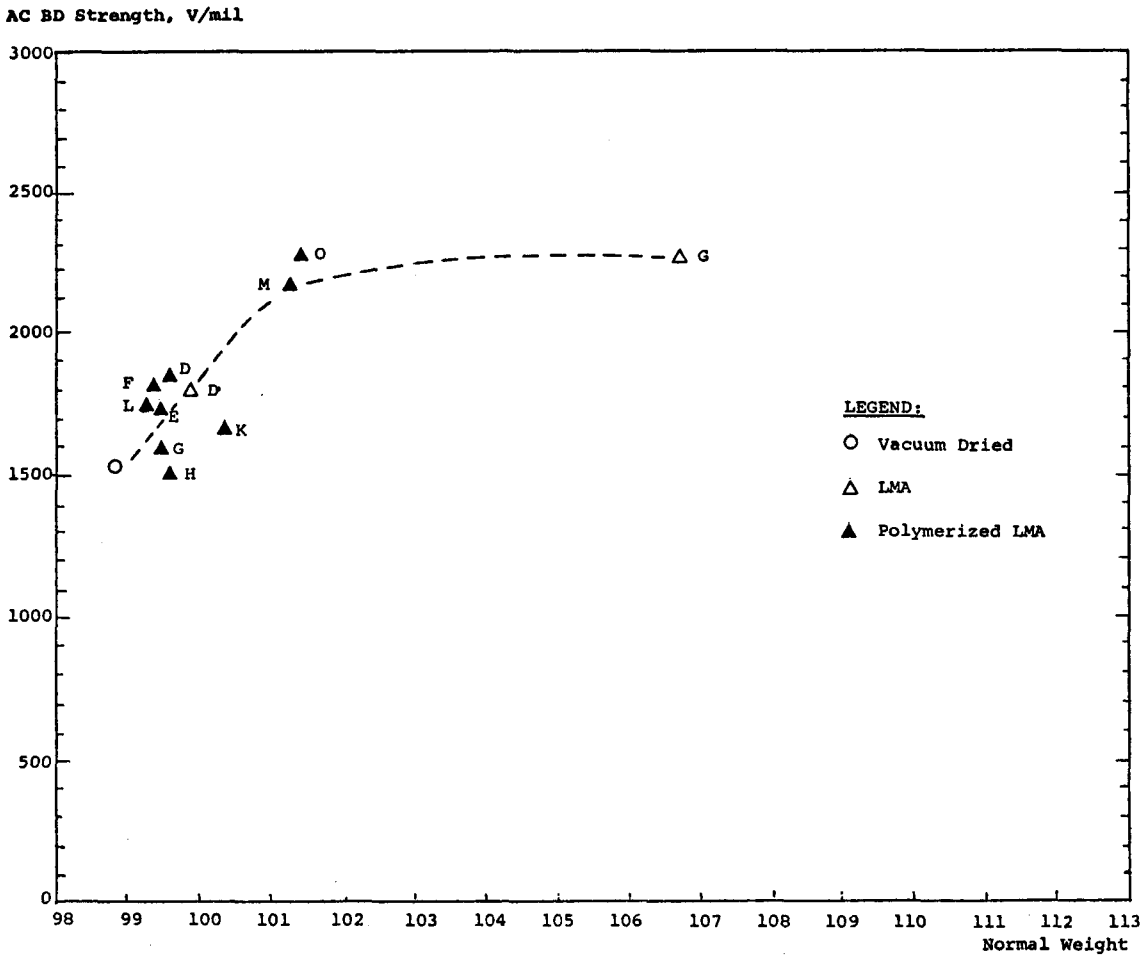

Figure 3-74. Effect of LMA and Polymerized LMA on AC Breakdown Strength. Sample: Cable A slabs, 18 mil. One hour step test.

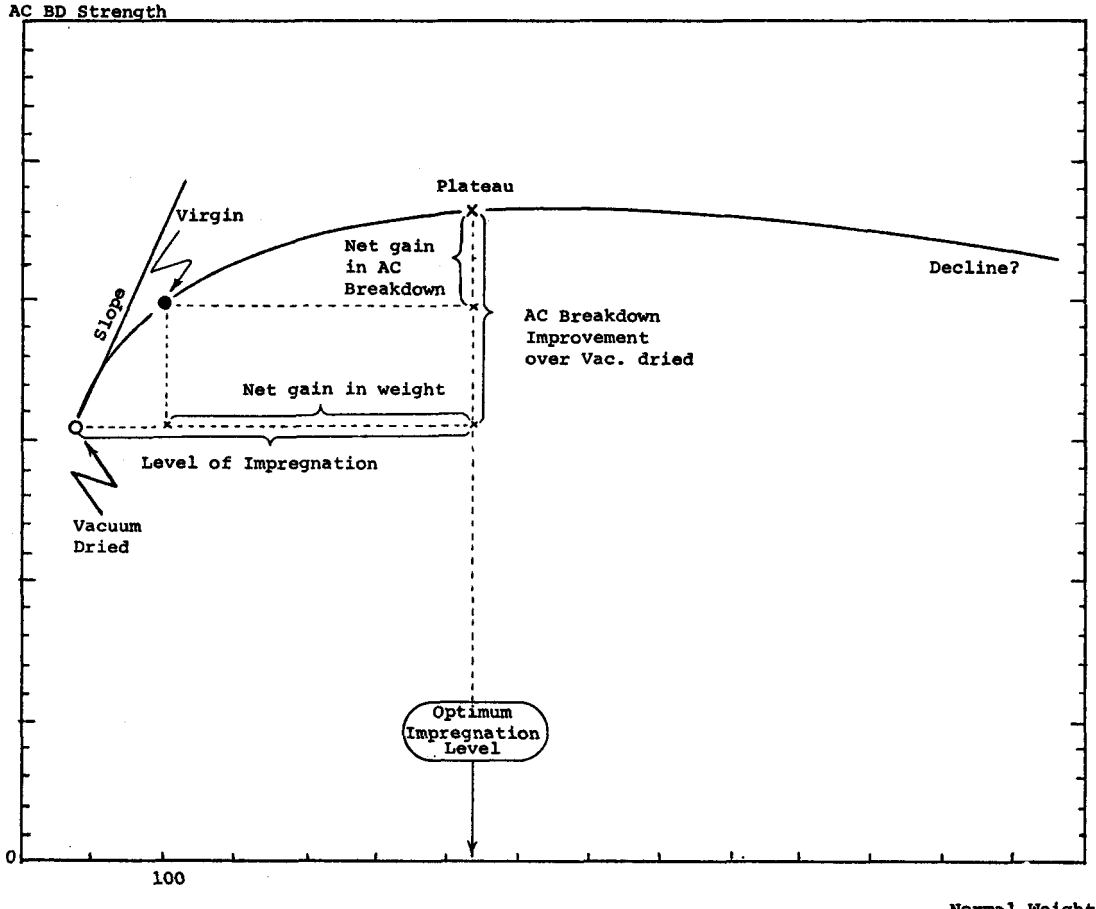

Figure 3-75. Typical AC Breakdown Strength - Impregnation Level Correlation. Cable A slabs, 18 mil. One hour step test.

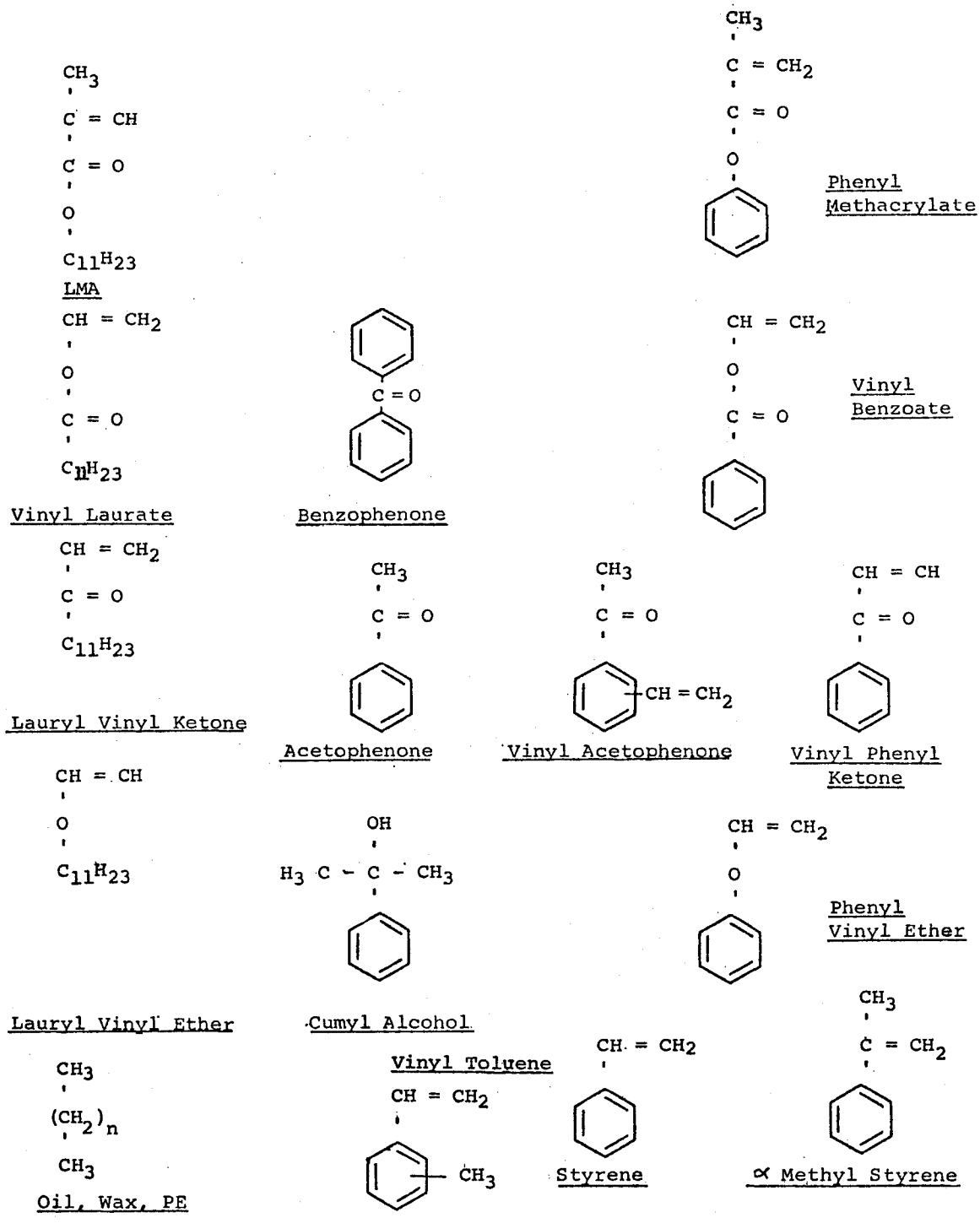

Figure 3-76. Chemical Structure of Impregnant Candidates.

The "ditched" samples, after drying, were introduced into a 1000 cc glass resin kettle containing the impregnating liquid, sealed and evacuated, and maintained at a constant appropriate temperature in a water bath to give 2 to 3% impregnation. After the necessary time interval they were weighed and subjected to the breakdown test.

The results of AC breakdown tests for different liquids are given in Table 3-10 and graphically presented in Figure 3-77. Six liquids, namely vinyl toluene, styrene, styrene oxide, dodecyl vinyl ether, vinyl pyrollidone and 2 ethyl phenyl acrylate showed the highest degree of voltage stabilizing effect.

It would appear that four out of the six liquids mentioned above contain an aromatic nucleus while another (vinyl pyrollidone) contains a heterocyclic ring. Three of them do not contain carbonyl groups and all of them contain a side group of two or more C atoms. The carbonyl effect in vinyl pyrollidone is very weak due to the adjacent - NH - group. On the other hand, materials like benzophenone and ethyl benzene which have close similarity to vinyl toluene do not have comparable stabilizing effect. Materials containing only alkyl and carbonyl groups such as octanone and vinyl acetate are poor voltage stabilizers. The physical (32) and electrical properties (33) of the liquids are listed in Table 3-11. Apparently there is no correlation between the dielectric constant and voltage stabilizing effects. Benzophenone having a dielectric constant of 11.4 as compared to 17.6 for acetophenone, does not have comparable voltage stabilizing effects. The presence of aromatic rings and a system of conjugated double bonds appear to be useful in raising the breakdown voltage of the insulation.

3.3.5.3 Grid Program on Slabs. Three of the six monomers, along with two impregnants that are solid at room temperature found effective in the screening program, were further scrutinized by carrying out AC BD tests at 1 hour and 24 hour steps. In Section 3.1 it was observed that exposure of the samples to higher temperature during vacuum drying or impregnation might increase the AC breakdown strength. Hence, each impregnated set is assessed in comparison with controls of the same heat history. Forty slabs from cable B, ditched to 13 mil, were given identical treatment in cleaning and drying. Twenty of them were impregnated with one of the five impregnants at an appropriate temperature and time to reach 2 to 3% weight gain. Both the control as well as the impregnated samples were held at that temperature in nitrogen atmosphere for a total of 67 hours including the time of impregnation. Subsequently, sets of 10 of the impregnated and of the control samples were used for 1 hour step-up tests in the same set-up whereas the rest of the twenty were used for the 24 hour step up. The Weibull plots for each of these impregnants, presented in Figures 3-78 to 3-86, show good lin-

Table 3-10

SUMMARY OF THE RESULTS ON LIQUID IMPREGNATION

(All Weights are based on Original = 100)

TEST NO.	DRYING Hrs., °C	DRYING µm	IMPREGNATION Hrs.	IMPREGNATION PSI	IMPREGNATION °C	IMPREGNATING MATERIALS	WEIGHT AFTER: Drying	WEIGHT AFTER: Impreg.	AC BREAKDOWN V/mil
51B	192 70	1200	144	-	25	Vinyl Toluene	98.6	110.6	>2600 (1)
	120 70	30							
54C	240 70	1200	216	-	50	Anisole	98.75	113.8	2350
54B	240 70	1200	216	-	50	Octanone	98.74	106.2	1900
54A	240 70	1200	168	-	70	Cumyl Alcohol	98.83	103.0	2250
56C	238 70	1200	288	-	70	DiAllyl Phthalate	98.68	100.25	2380
56B	238 70	1200	48	-	50	Dodecyl Vinyl Ether	98.69	106.9	2450
56A	238 70	1200	24	-	25	Styrene	98.8	104.8	>2850 (1)
58	274 70	1200	100	-	70	Vinyl Pyrrolidone	98.89	101.1	2575
59B	224 70	1200	123	-	70	Benzophenone (2)	98.71	104.26	2410
59A	224 70	1200	29	-	25	Vinyl Toluene (2)	98.69	105.0	2530
61C	240 70	1200	120	-	50	Styrene Oxide (2)	99.14	105.3	2600
61B	240 70	1200	120	-	50	2 Phenyl Ethyl Acrylate (2)	99.05	105.8	2820
61A	240 70	1200	168	-	50	Vinyl Acetate (2)	99.15	104.6	2100
65C	264 70	1200	29	-	25	Ethyl Benzene (2)	98.9	108.6	2550
65B	282 70	1200	24	-	50	Styrene Oxide (2)	98.75	102.6	3350
65A	282 70	1200	7		25	Vinyl Toluene (2)	98.75	101.6	3750

Sample: Cable B slabs.

(1) Flashover
(2) 13 mil (all others 18 mil)

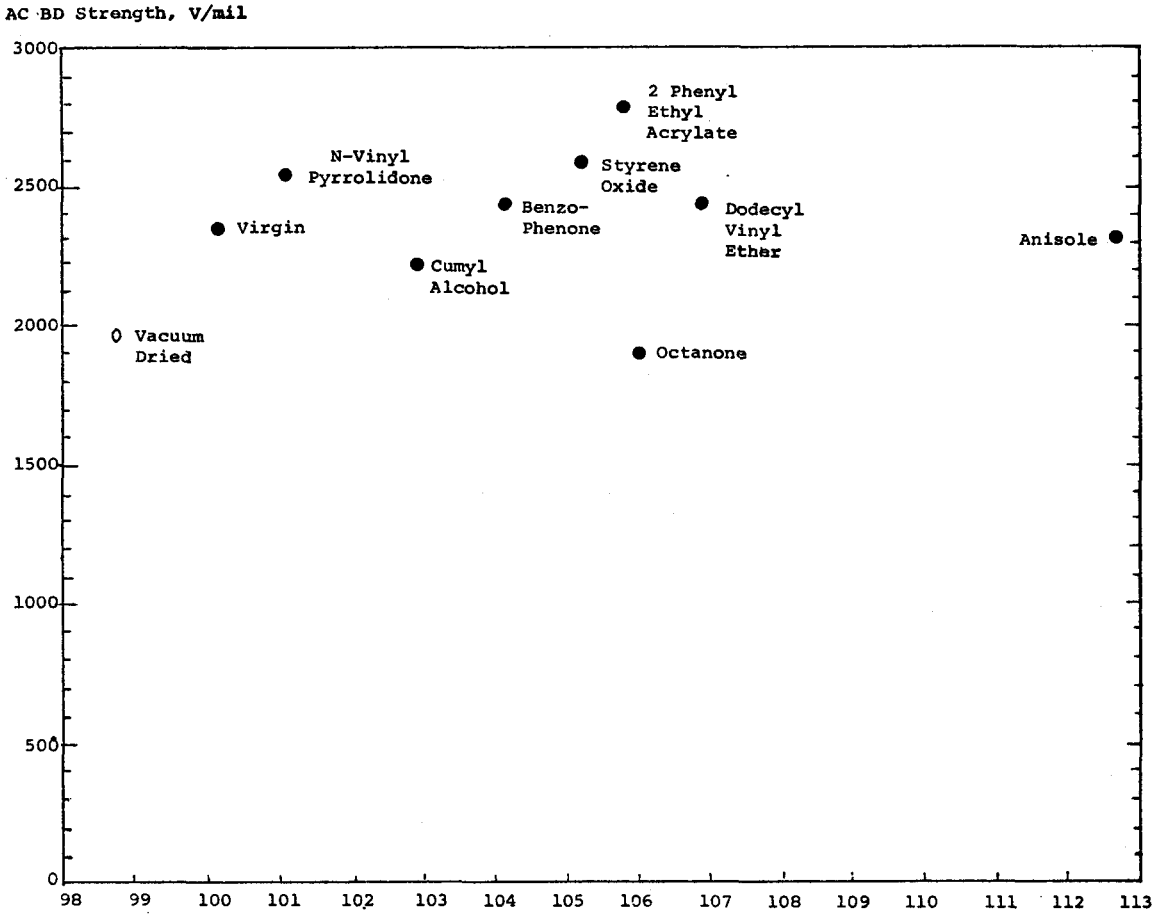

Figure 3-77. Effect of Various Impregnants.
Sample: Cable B slabs, 13 mil. 1 hour step test.

Table 3-11

COMPARISON OF IMPREGNANTS

		Polymerizable	Similar To Acetophenone: Phenyl	Similar To Acetophenone: C = O	Similar To Acetophenone: Alkyl	MP. °C/BP°C	Density	Refrac. Index	Surf. Tension	Appearance	Inhibitor (ppm)	Mol.wt.	Vapor Press.	Dielec. Cons.	Dipole Moment	Polymeriz. kp/kt	Concen.Wt..%	A.C. B.D. V/mil.
1	TEG/pX/ETOH	-	-	-	-	138	0.8611	1.4958	28.9	Clear		106						2300
2	Acetophenone	-	+	+	+	20 bp202	1.026	1.5342	40	Clear	-	120		17.39	3.02		0.3	2700
																-	.89	2700
																-	2.6	2500
3	LMA	+	-	+	+	-8 MP ≈300	0.8680	1.4410		Clear	100 ppm	262	4			1.34	1 8	1800 2260
4	Paraffin Oil	-	-	-	+										0	-	0.5	1700
																-	3.86	2330
5	PE Wax	-	-	-	+	90	0.88				-			2.38	0	-	13.3	2200
6	Vinyl Toluene	+	-	-	+	170	0.9165	1.5437		Clear	12T	118	-			≈4	12	>2600
																	6.31	2530
7	Styrene	+	+	-	-	145	0.9090	1.5482	37.5	Clear	12T	104	5	2.43	0	≈3	6 -	>2850
8	Vinyl Pyrrolidone	+	(1)	(1)	-	95	1.04	1.5120		Pink		111					2.21	2575
9	Aniscle	-	+	-	_	155	0.9954	1.5179	25.8	Clear		108			1.38	-	15.05	2350
10	Octanone	-	-	+	_	173	0.8180	1.4161		Clear		128				-	7.41	1900
11	Cumyl Alcohol	-	+	-	+	229	1.0224	1.5314		Clear		136		≈ 13		-	4.17	2250
12	Di Allyl Phthalate	++	+	+	+												1.55	2380
13	Dodecyl Vinyl Ether	+	-	+	+	≈130	0.817	1.4396		Clear		212	-				8.21	2450
14	Benzophenone	-	++	+	-	mp 49	1.0976	--		Clear	-	182		11.4			5.55	2410
15	Ethyl Benzene	-	+	-	-	bp306 136	0.8670	1.4983	29.2	Clear		106		2.41		-	9.7	2550
16	Vinyl Acetate	+	-	-	+	72.5	0.9338	1.3953		Clear		86	89			17.2	5.45	2100
17	Styrene Oxide	+	+	-	-	-	-	-	-	-	-	119		-	-	-	6.18	2600
18	2 Phenyl ethyl Acrylate	+	+	+	+	-	-	-	-	-	-	174	-	-	-	-	6.74	2820
19	Napthalene	-	++	-	-	80.2		1.5877	28.2	Clear		128		2.54		-		
20	Vinyl ethyl Ketone	+	-	+	+	mp 102		1.4192	at 127C	Clear		84						

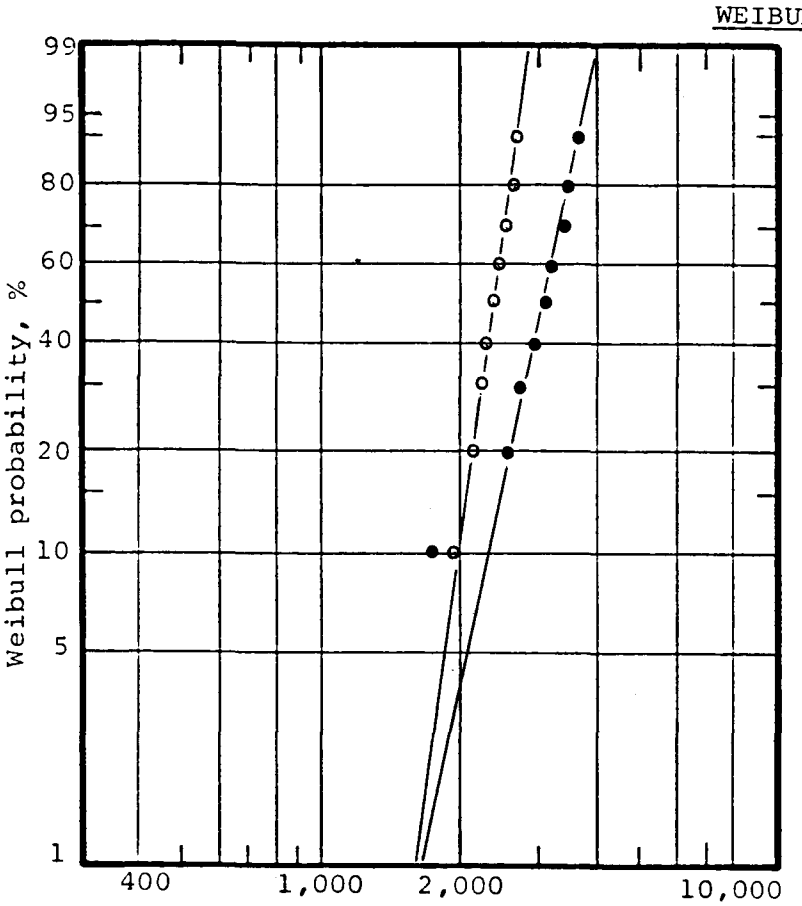

Figure 3-78. Impregnation with VT.
Cable B, 13 mil slabs, 1 hour step test.
(o) Control, (•) Impregnated.
Experiment No.'s 70 and 91B respectively.

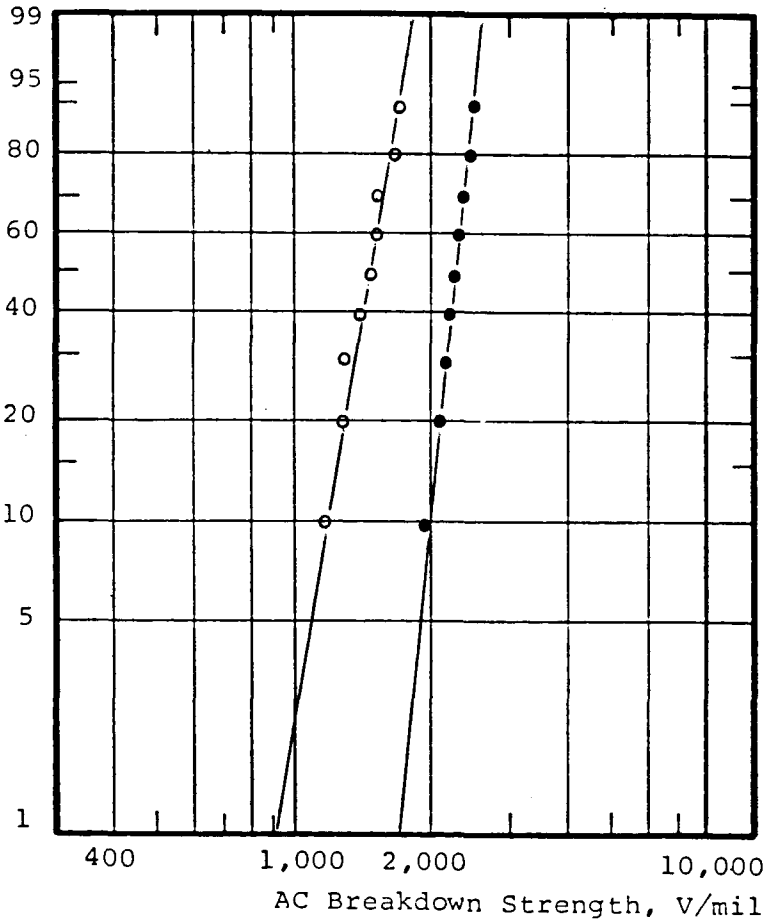

Figure 3-79. Impregnation with VT.
Cable B, 13 mil slabs, 24 hour step test.
(o) Control, (•) Impregnated.
Experiment No.'s 71 and 91A respectively.

WEIBULL PLOTS

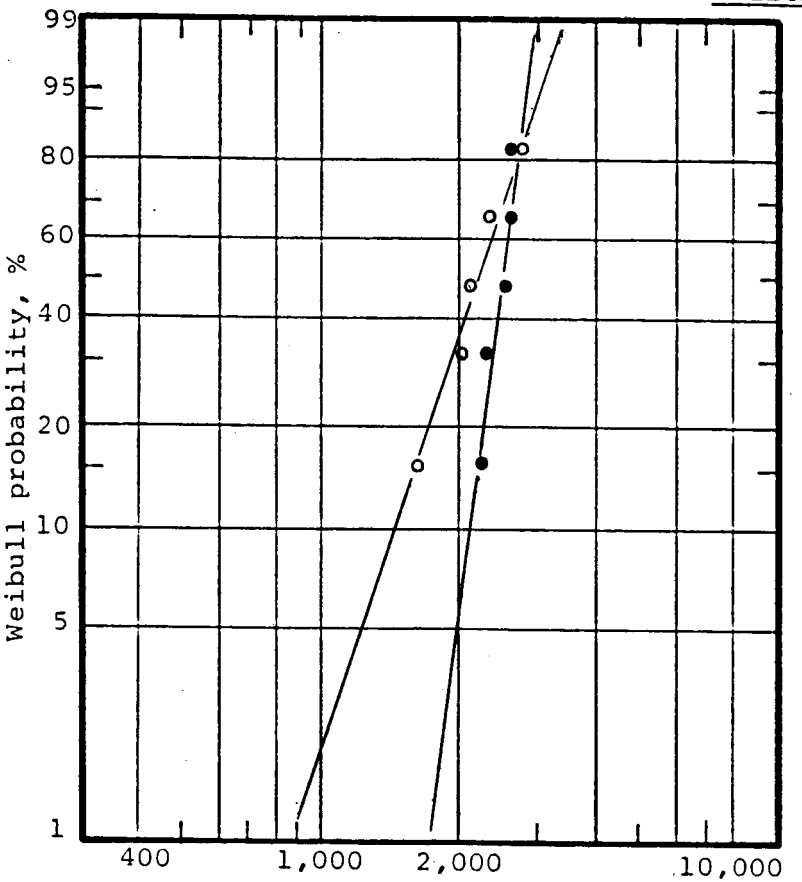

Figure 3-80. Impregnation with DVE.
Cable B, 13 mil slabs, 1 hour step test.
(o) Control, (•) Impregnated
Experiment Nos. 79D and 79B, respectively.

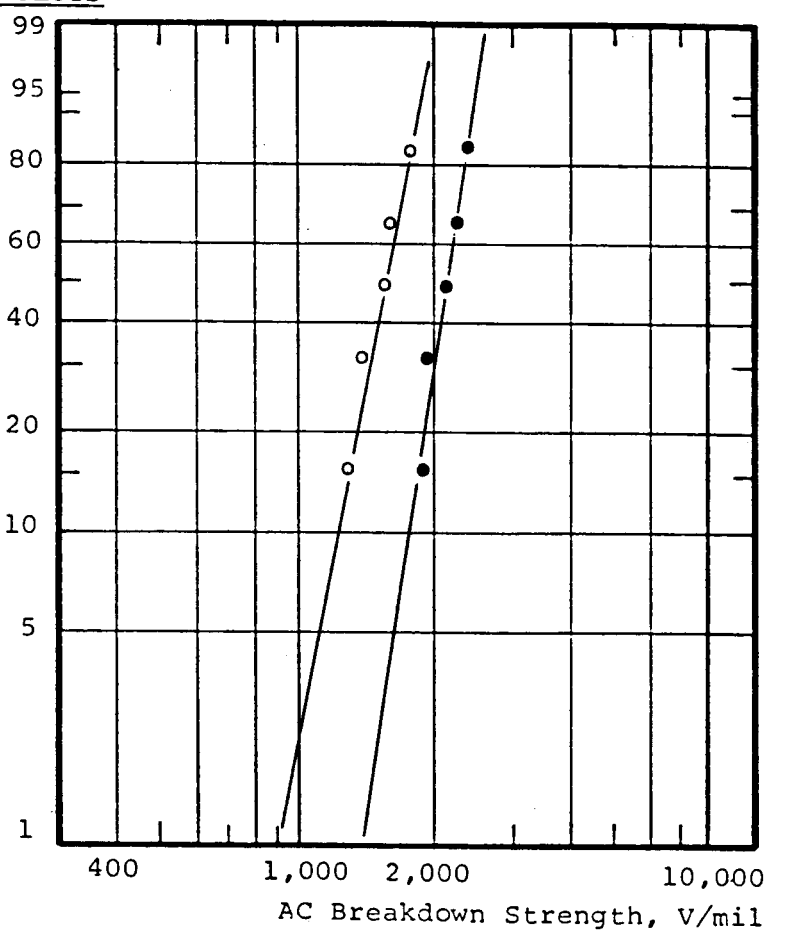

Figure 3-81. Impregnation with DVE.
Cable B, 13 mil slabs, 24 hour step test.
(o) Control, (•) Impregnated
Experiment Nos. 79C and 79A, respectively.

WEIBULL PLOTS

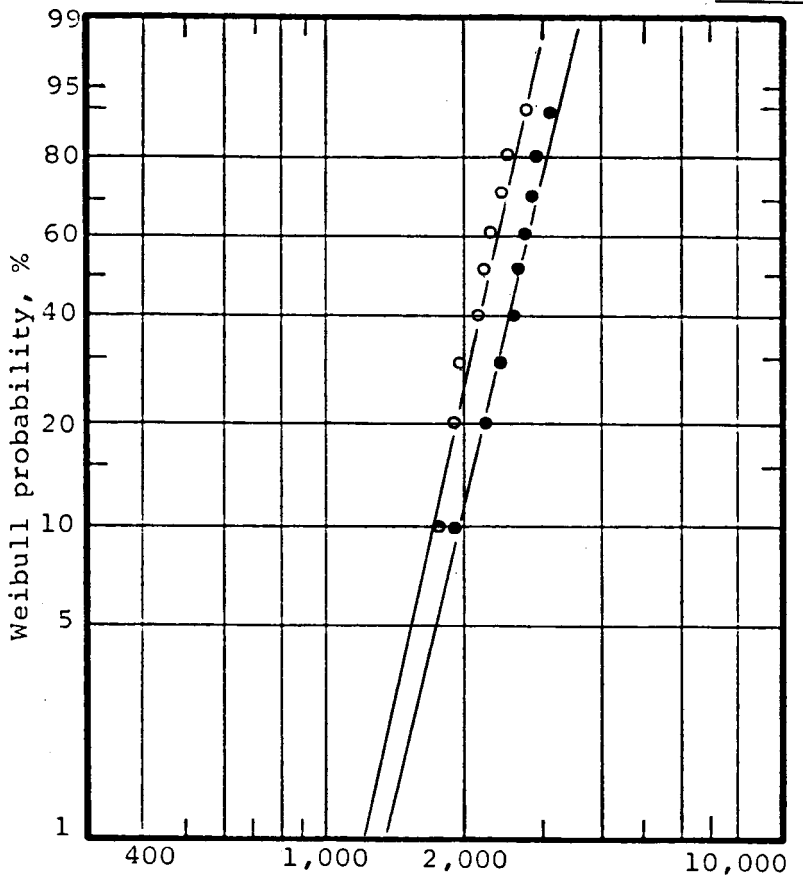

Figure 3-82. Impregnation with Styrene Oxide. Cable B, 13 mil slabs, 1 hour step test. (o) Control, (•) Impregnated Experiment Numbers 80A and 80C, respectively.

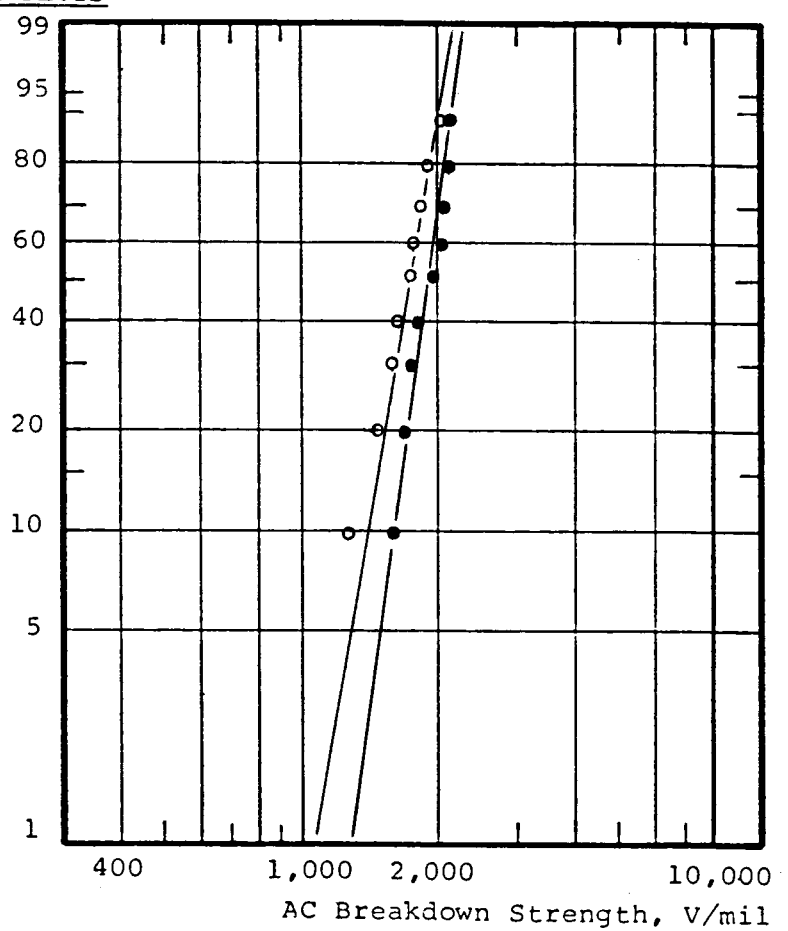

Figure 3-83. Impregnation with Styrene Oxide. Cable B, 13 mil slabs, 24 hour step test. (o) Control, (•) Impregnated Experiment Numbers 81B and 80B, respectively.

WEIBULL PLOTS

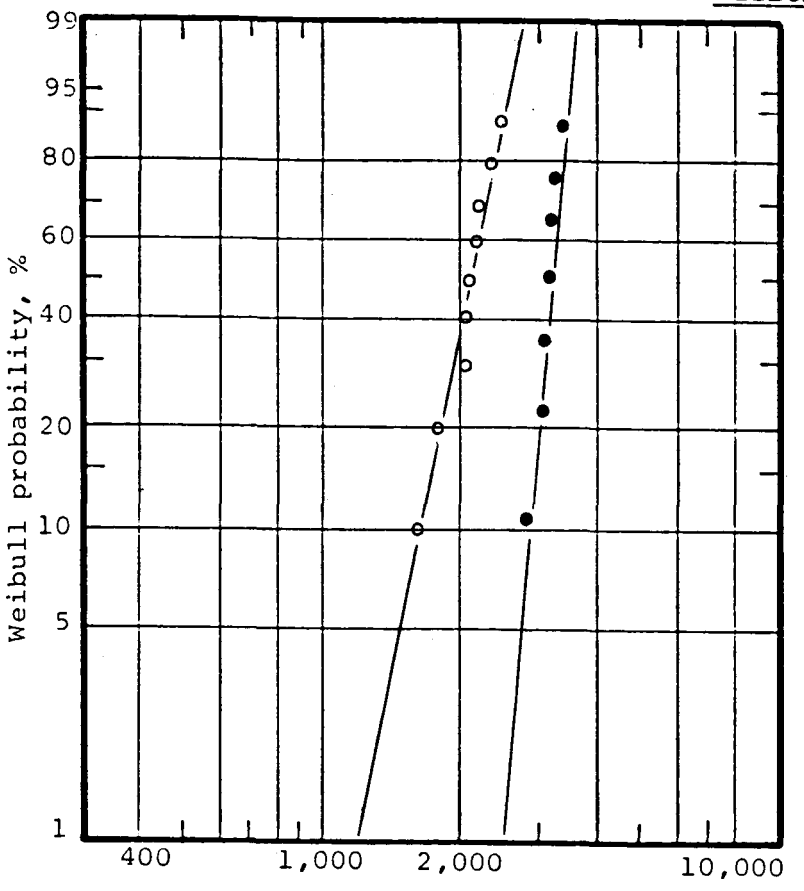

Figure 3-84. Impregnation with PE Wax.
Cable B, 13 mil slabs, 1 hour step test.
(o) Control, (•) Impregnated
Experiment Numbers 76B and 76D, respectively.

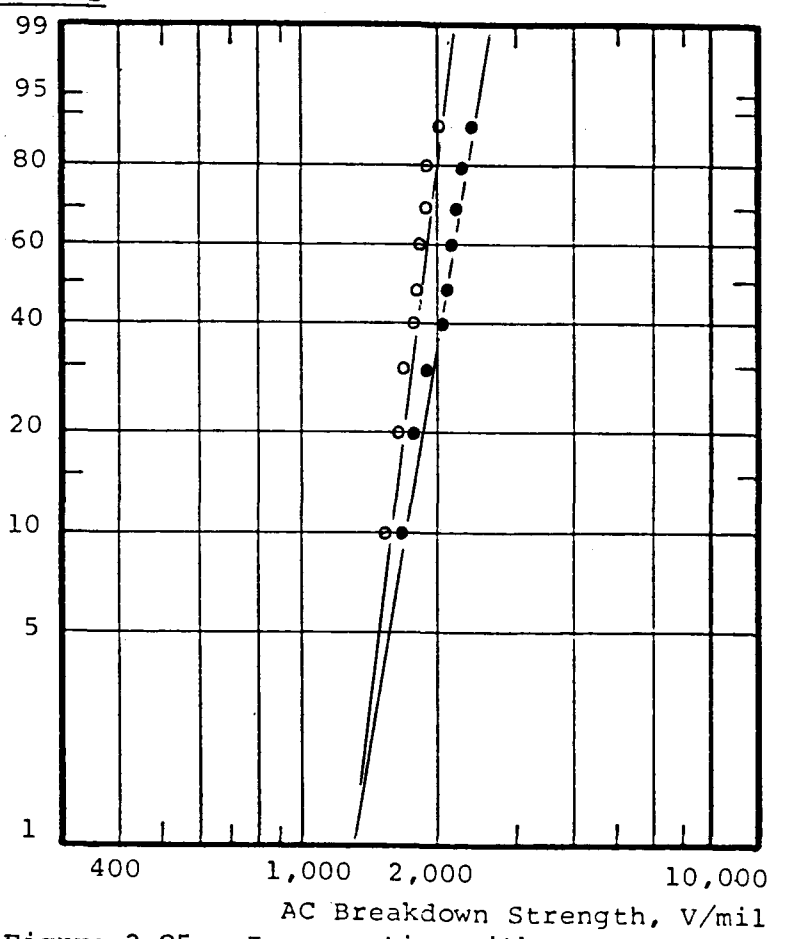

Figure 3-85. Impregnation with PE Wax.
Cable B, 13 mil slabs, 24 hour step test.
(o) Control, (•) Impregnated
Experiment Numbers 76A and 76C, respectively.

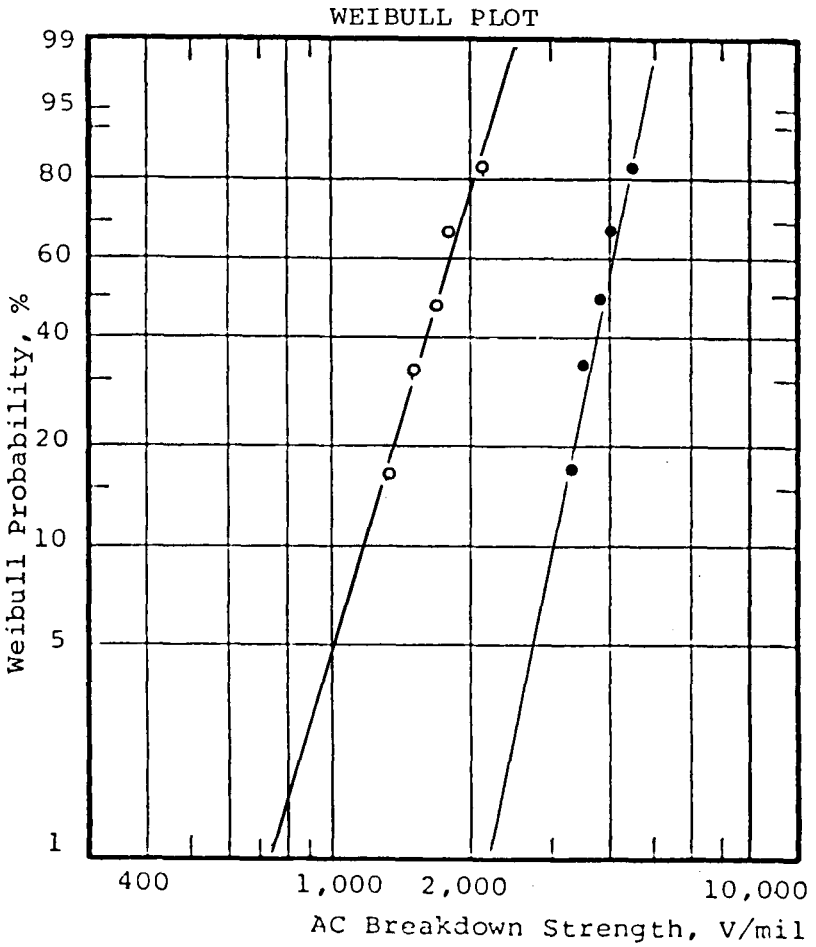

Figure 3-86. Impregnation with Naphthalene. Cable B, 13-mil slabs, 1 hour step test. (●) 1 hour step test. (o) 24 hour step test. Experiment Numbers 93A for 1 hour and 93B for 24 hour step test.

ear correlation. The V_{10}, V_{50} and V_{90} values from these Figures are presented in Table 3-12 along with the conditions of impregnation. The V T curves for the five impregnants are presented in Figures 3-87 to 3-91, and summarized in Figure 3-92.

It is evident from these results that:

- The AC BD values, accurate within 5 to 10% could be obtained if time and temperature history of the samples are maintained constant.

- The impregnants used in this test caused 10 to 50% improvement in dielectric strength over the controls of identical heat history.

In Figure 3-93 the results of the grid program are shown in a different way. The two broken diagonal lines represent slopes corresponding to 1:1 and to 1:1.5 ratios between the dielectric strength obtained in 24 hour and 1 hour step-up tests. A shift towards the right (1:1 ratio line) corresponds to an improvement in the slopes in the V. T. curves and a shift in the vertical direction corresponds to an improvement in average dielectric strength. As mentioned earlier, to appreciate true improvement, comparisons should be made with appropriate controls. It is clearly evident that the greatest change in the slope as well as in the height is by vinyl toluene. Dodecyl vinyl ether shows significant change in the slope but not in the height. PE wax shows the opposite, that is, increase in the height but not in the slope. This would thus indicate that vinyl toluene is the best candidate monomer.

3.3.5.4 Model Cables. Since vinyl toluene emerged as the best candidate monomer in the grid program with slabs, it was chosen for impregnation of model cables to confirm the earlier results and to obtain the optimum level of impregnation. The samples were tested in 10, 30 and 60 minute step-up tests. The Weibull plots for these tests are presented in Figures 3-94 to 3-96. The V_{10}, V_{50} and V_{90} values along with the conditions of treatment are reported in Table 3-13. Finally, in Figures 3-97 and 3-98, the V_{50} values are plotted against level of impregnation, both for the 10 minute and for the one hour step-up tests. In the same Figures the values of virgin control (corresponding to 100 normalized weight) and of the evacuated control (corresponding to 99) are given. Since all the samples were vacuum dried before impregnation, the breakdown strength of impregnated samples should be compared to that of the evacuated control. The spread between V_{10} and V_{90} values is indicated in each experiment with vertical lines. It would be apparent that the increase in dielectric strength versus per cent impregnation maintains more

Table 3-12

GRID PROGRAM SUMMARY

Expt. No. 116-	IMPREGNATION			POST TREATMENT		NORM. WEIGHT	NO. OF SLABS	AC BD TEST			
									V/mil		
	Impregnant	Hrs.	°C	Hrs	°C			Hrs.	V_{10}	V_{50}	V_{90}
70	--	-	-	67	25	100	10	1	1900	2300	2600
71	--	-	-	67	25	100	10	(24)	(1150)	(1460)	(1700)
19		-		67	25	100	10	((168))	((1170))	((1400))	((1550))
91B	Vinyl Toluene	3	25	64	25	102-6	10	1	2200	2900	3500
91A	"	3	25	64	25	102-6	10	(24)	(2000)	(2200)	(2400)
79D	--	-	50	67	50	99.9	5	1	1450	2250	2970
79C	--	-	50	67	50	99.9	5	(24)	(1260)	(1600)	(1900)
79B	Dodecyl	6	50	61	50	102.3	5	1	2100	2550	2800
79A	Vinyl Ether	6	50	61	50	102.3	5	(24)	(1750)	(2150)	(2400)
80A	--	-	50	67	50	99.8	10	1	1750	2275	2720
81B	--	-	50	67	50	99.8	10	(24)	(1450)	(1750)	(2050)
80C	Styrene Oxide	17	50	50	50	101.8	10	1	1800	2550	3200
80B	"	17	50	50	50	101.6	10	(24)	(1550)	(1875)	(2100)
76B	--	-	100	67	100	99.6	10	1	1670	2150	2560
76A	--	-	100	67	100	99.6	10	(24)	(1670)	(1890)	(2050)
76D	PE Wax	16	100	51	100	103	8 (1)	1	2900	3200	3450
76D	"	16	100	51	100	103	10	1	1850	2800	3800
76C	"	16	100	51	100	103	10	(24)	(1780)	(2200)	(2500)
93B	--	-	-	67	150	99.2	10	1	2080	2700	3200
93A	--	-	-	67	150	99.2	10	(24)	(1800)	(2100)	(2300)
92A	Naphthalene (2)					102.3	5	1	1920	2700	3400
92B	"					102.3	5	(24)	(1200)	(1700)	(2250)
95	PP Sheet	-		-	25	100	10	1	2250	2875	3450

(1) Two points eliminated.
(2) Vapor phase impregnation in several steps.

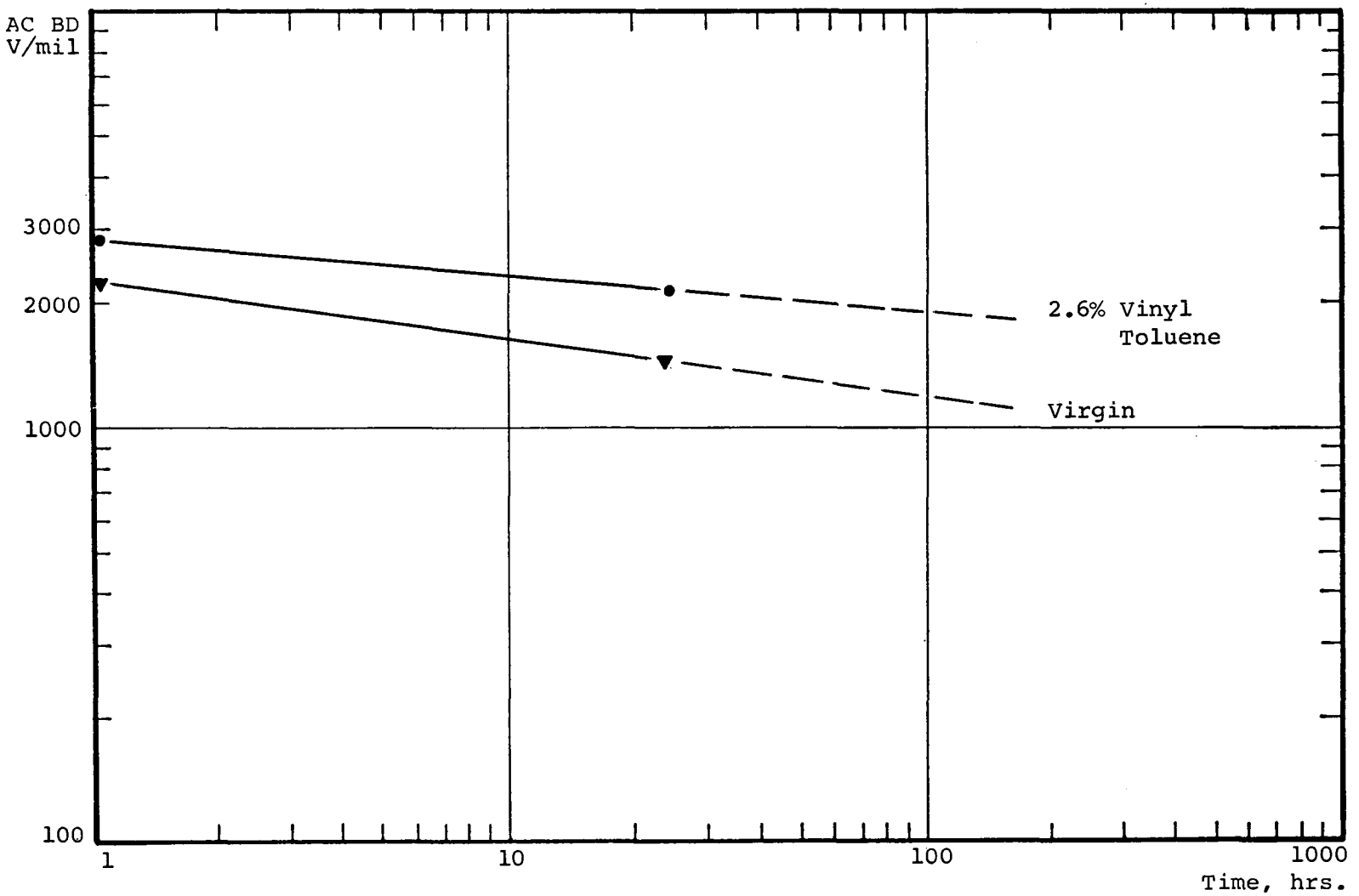

Figure 3-87. Effect of Vinyl Toluene on AC Breakdown Strength.

Sample: Cable B slabs, 13 mil.

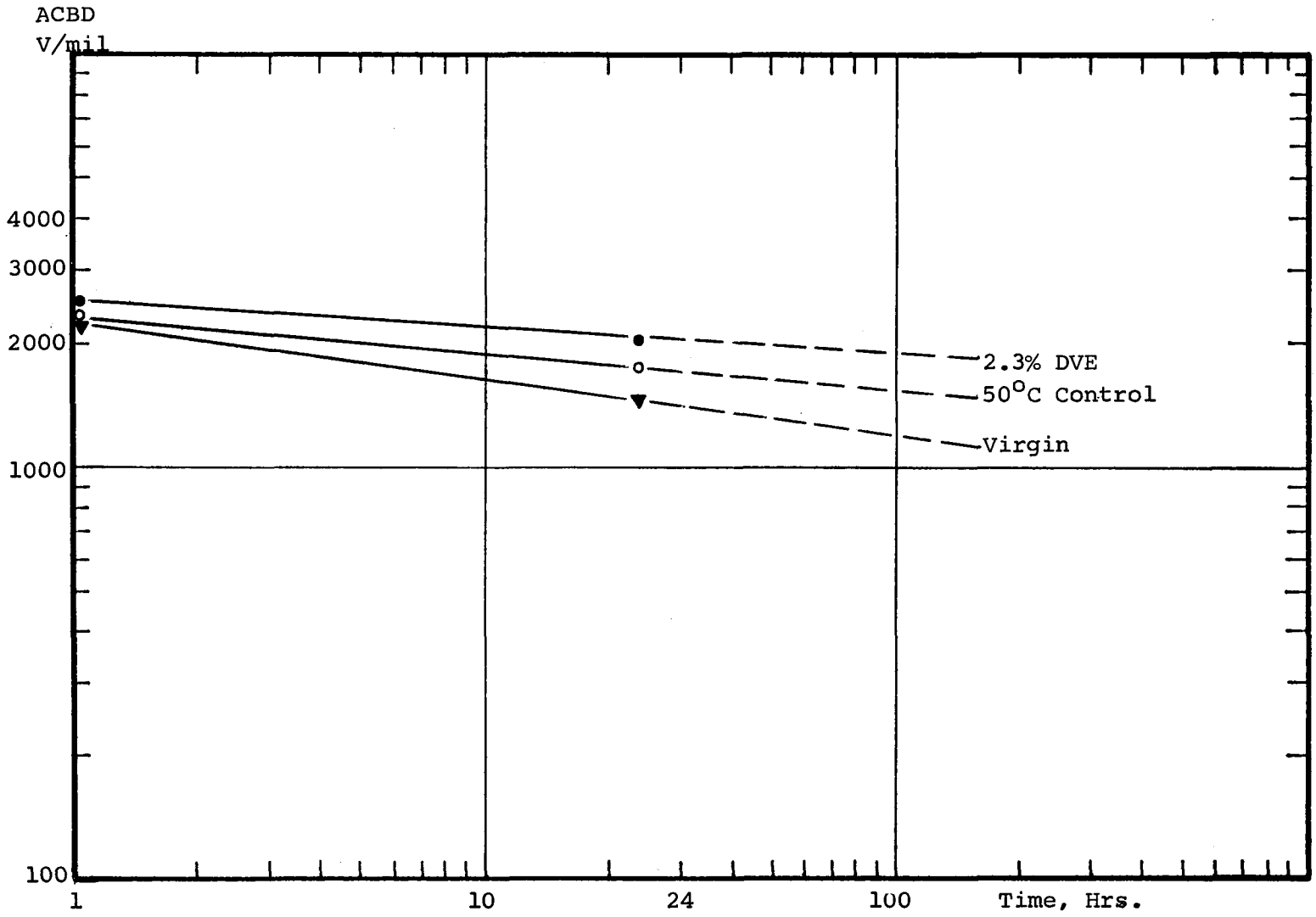

Figure 3-88. Effect of Dodecyl Vinyl Ether on AC Breakdown Strength.

Sample: Cable B slab, 13 mil, treated for 67 hours.

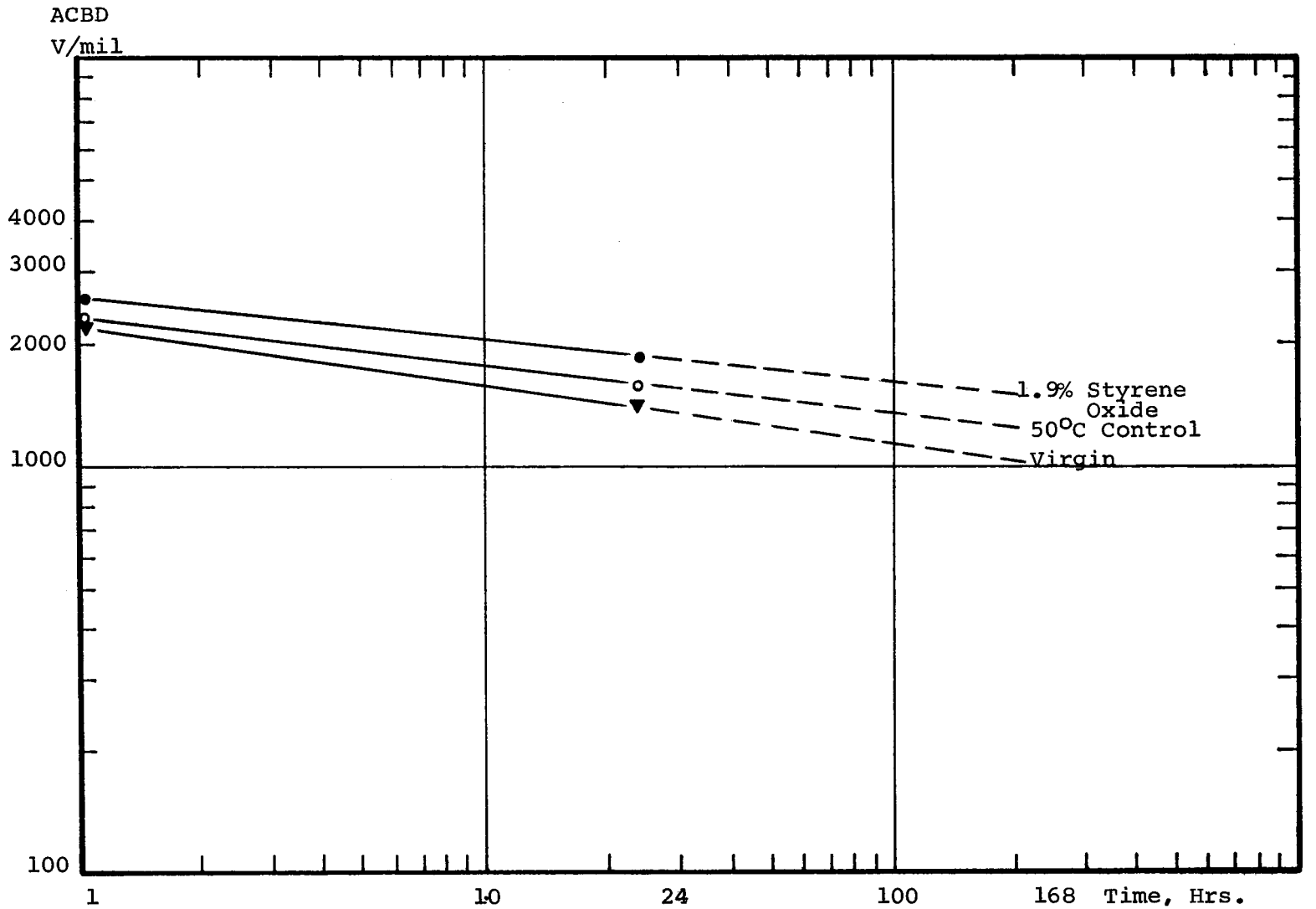

Figure 3-89. Effect of Styrene Oxide on AC Breakdown Strength.

Sample: Cable B slab, 13 mil, treated for 67 hours.

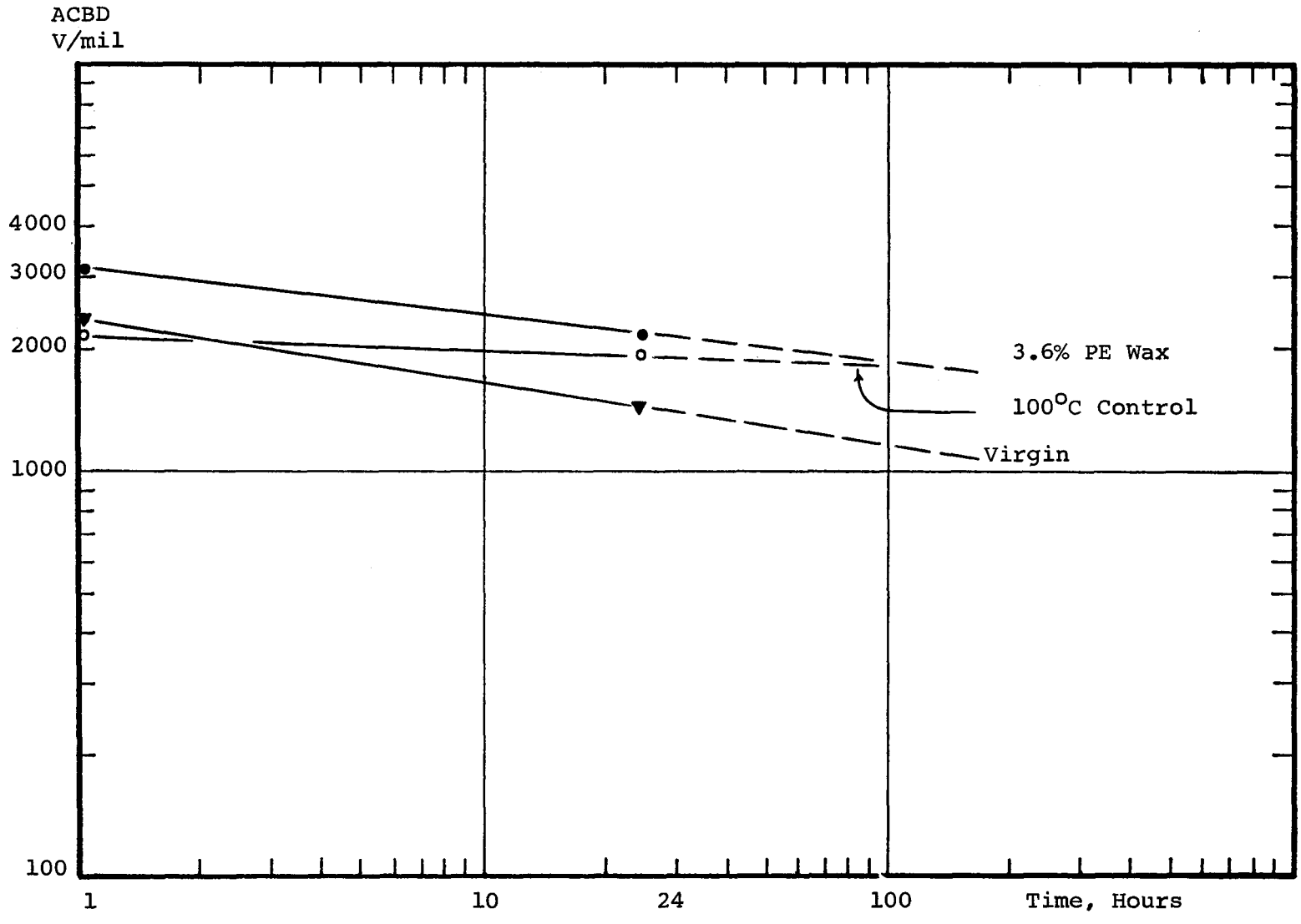

Figure 3-90. Effect of PE Wax on AC Breakdown Strength.

Sample: Cable B slab, 13 mil, treated for 67 hours.

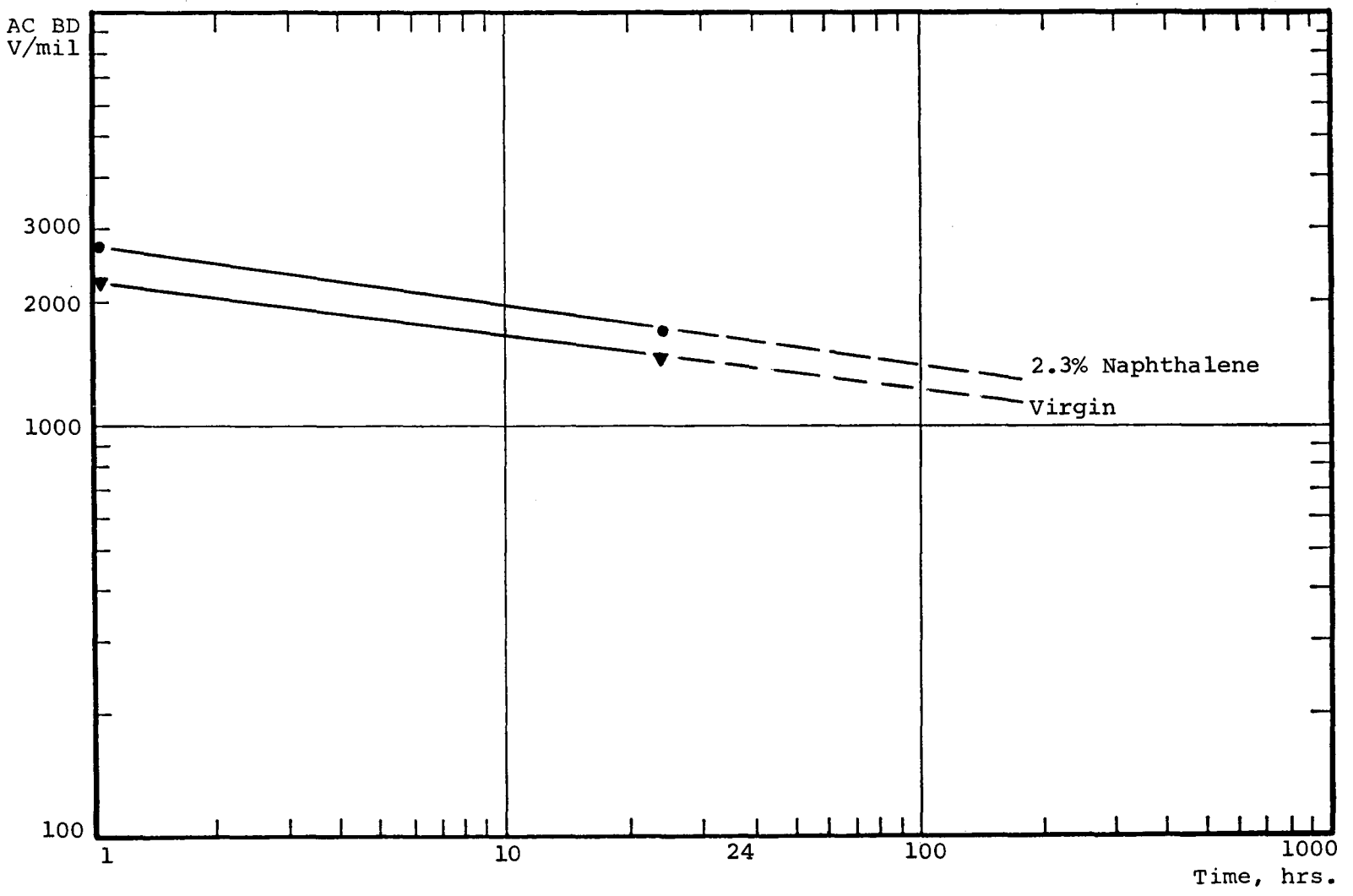

Figure 3-91. Effect of Naphthalene on AC Breakdown Strength.

Sample: Cable B slab, 13 mil, impregnated in gas phase.

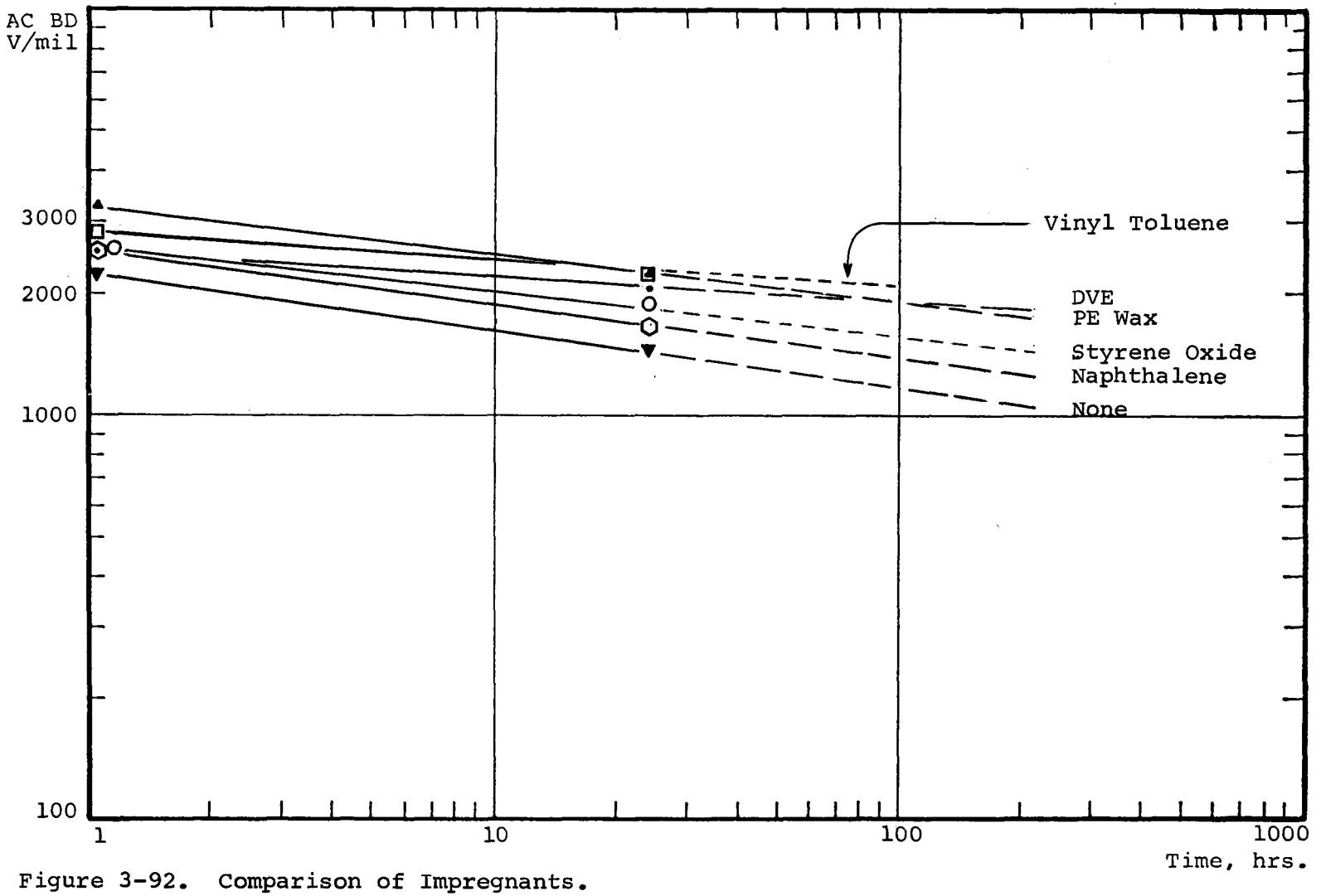

Figure 3-92. Comparison of Impregnants.

Sample: Cable B slab, 13 mil, treated for 67 hours.

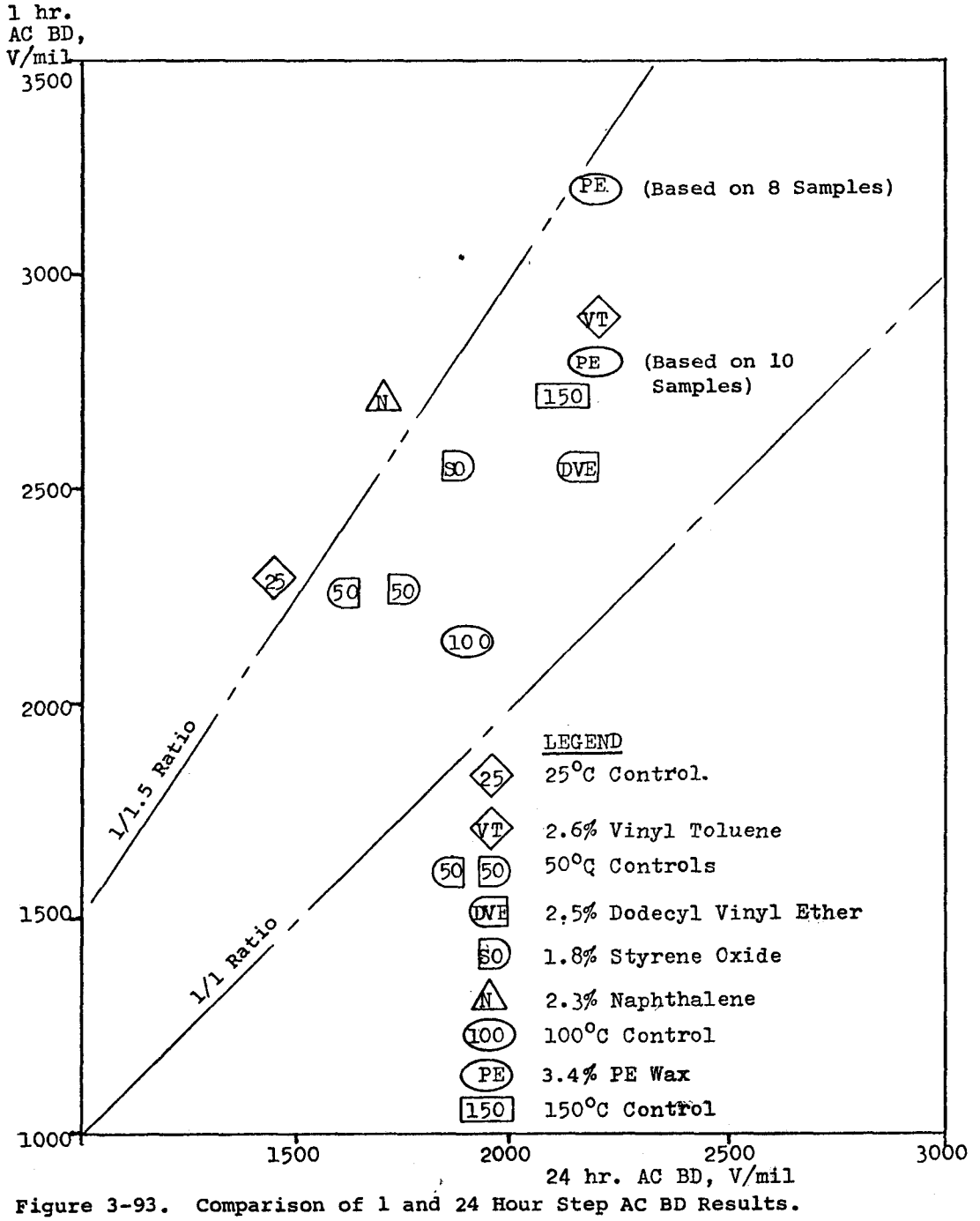

Figure 3-93. Comparison of 1 and 24 Hour Step AC BD Results.
Sample: Cable B slabs, 13 mil.

WEIBULL PLOTS

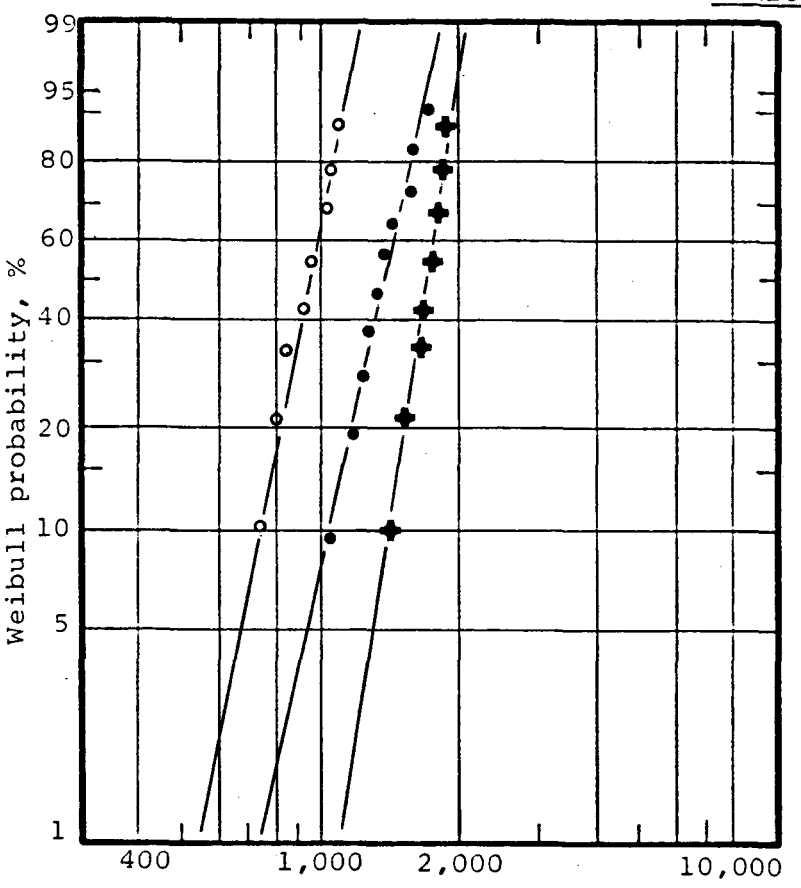

Figure 3-94. Impregnation with VT.
Model cable E, 1 hour step test.
(o) Vacuum dried control. Exp. No. 144.
(•) Impregnated with 3.7% VT. Exp. No. 162.
(✚) Impregnated with 4.7% VT. Exp. No. 146.

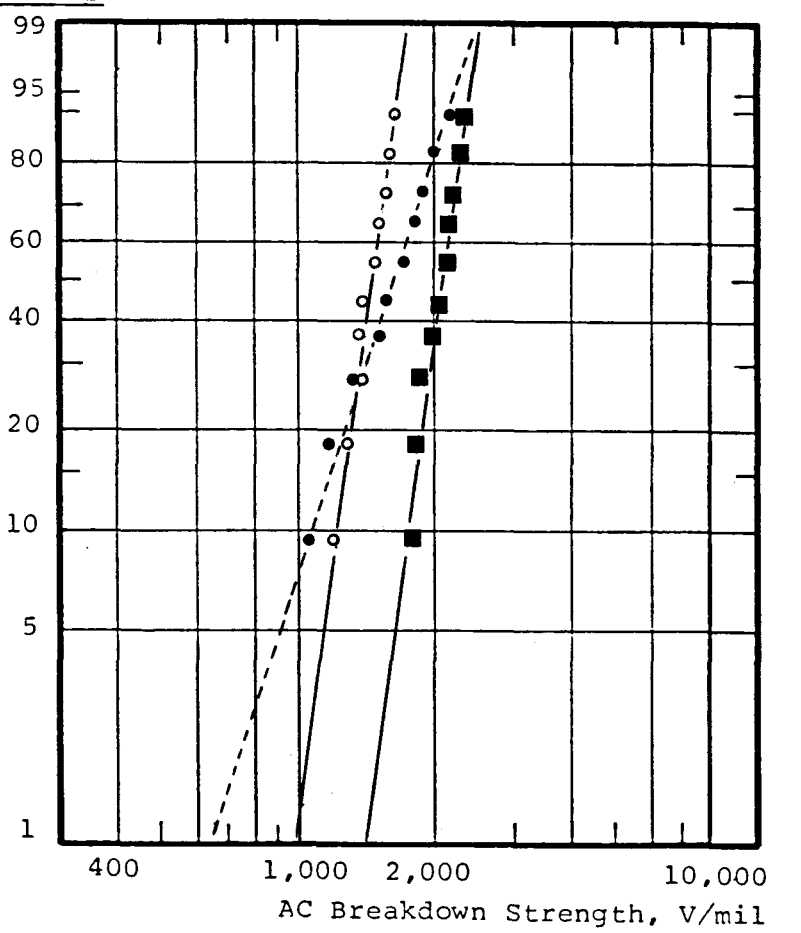

Figure 3-95. Impregnation with VT.
Model cable E, 10 minute step test.
(o) Control. Exp. No. 157.
(•) Impregnated with 1.9% VT. Exp. No. 155.
(■) Impregnated with 3.3% VT. Exp. No. 154.

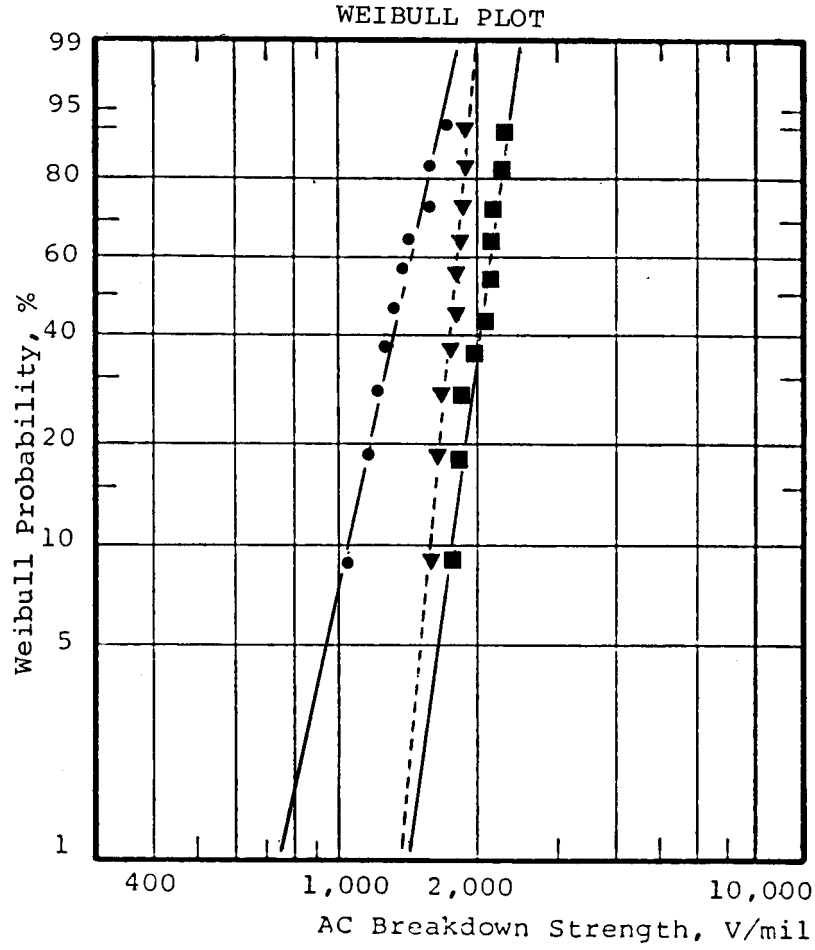

Figure 3-96. Impregnation with VT.
Effect of step time. Model cable E.
(●) 1 hour step time (@ 3.7% VT).
(▼) 30 minute step time (@ 3.2% VT).
(■) 10 minute step time (@ 3.3% VT).
Experiment Numbers 162, 152, and 154, respectively.

Table 3-13

EFFECT OF VINYL TOLUENE ON AC BREAKDOWN STRENGTH
Sample: Model Cable E

Exp. No.	Cable Treatment	Step Time, Min.	AC BD Strength, V/mil V_{10}	V_{50}	V_{90}	Relative V_{50}, % (1)	(2)
141	Control	60	830	1188	1494	100	
142	"	"	819	1218	1570		
144	Vac. dried	"	712	944	1131		100
162	3.7% VT	"	1057	1427	1727	131	151
146	4.7% VT	"	1435	1688	1871	155	179
164	5.4% VT	"	1036	1603	2117	147	170
163	5.5% VT	"	1119	1536	1880	141	163
157	Control	10	1296	1493	1635	100	
155	1.9% VT	"	1120	1660	2134	111	
153	2.7% VT	"	1329	1699	1987	113	
154	3.3% VT	"	1752	2097	2352	140	
156	3.7% VT	"	1239	1713	2106	115	
162	3.7% VT	60	1057	1427	1727		
152	3.2% VT	30	1655	1852	1991		
154	3.3% VT	10	1752	2097	2352		

(1) Virgin control = 100

(2) Vacuum dried control = 100

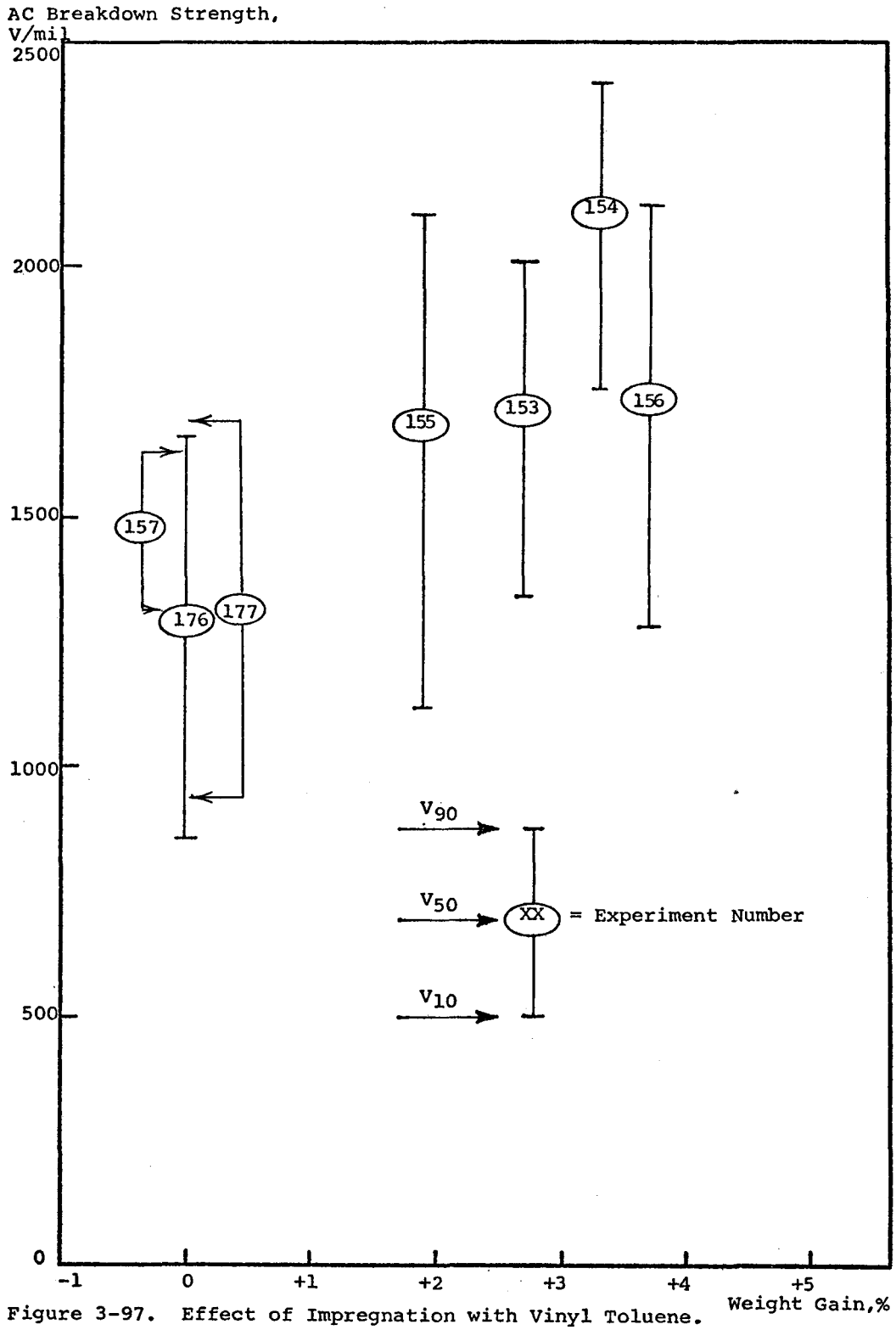

Figure 3-97. Effect of Impregnation with Vinyl Toluene.
Sample: Model Cable E. Ten minute step test.

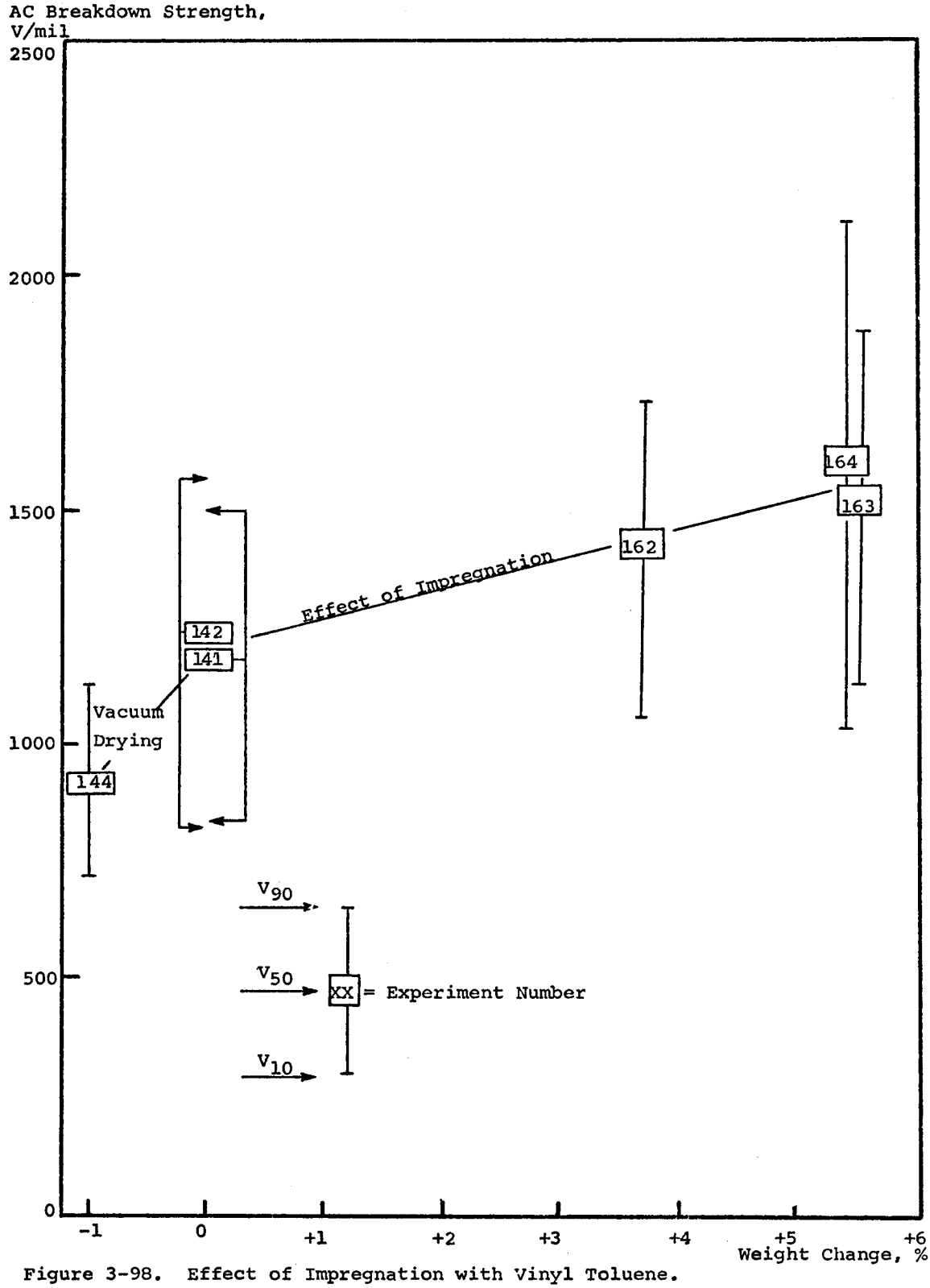

Figure 3-98. Effect of Impregnation with Vinyl Toluene.
Sample: Model cable E. One hour step test.

or less the same type of relationship as shown earlier for slabs. The highest improvement, 50 to 60%, appears at 4 to 5% impregnation level. With the limited number of experiments carried out so far, the possibility of achieving higher dielectric strength at higher levels of impregnation should not be excluded. However, high levels of impregnation may not be desirable.

The volt-time curve for vinyl toluene impregnated cables is presented in Figure 3-99 along with the control. The higher position of the line for the impregnated cables shows that its dielectric strength is higher. Its slope is comparable to the control. However, the low number of experiments does not justify the drawing of conclusions regarding expected life times.

The relative effect of vinyl toluene impregnation on slabs and model cables is compared in Table 3-14.

The AC breakdown strength of slabs, when impregnated with 2.6% vinyl toluene, increased from 2300 to 2900 V/mil showing a 26% increase. In model cables 2.7% impregnant effected an improvement from 1218 to 1705 V/mil amounting to 40 relative per cent.

3.3.6 Microscopy

3.3.6.1 Optical Microscopy. One slab from each set of 10 impregnated samples was examined by the optical microscope after performing the AC breakdown test. The micrographs of samples containing TEG-p-xylene-ethanol, acetophenone, lauryl methacrylate, vinyl toluene and polyethylene wax are presented in Figures 3-100 to 3-104. In addition to spherical voids there appears to be voids of irregular shape. They probably are the true structure of the voids depicting round holes with cracks propagating from them. Since these impregnants wet the surface of polyethylene more than the dye solution, they may enter into the cracks and absorb more dye. The results are summarized in Table 3-15.

The micrographs of p-xylene-ethanol triethylene glycol impregnated samples show bow tie structures aligned in the direction of stress. This is similar to the control. The acetophenone impregnated samples do not show such structures. Though the number of observations is insufficient for quantitative comparisons, some general trends are noticeable. The number of voids in the PE wax filled samples is significantly smaller compared to the control. The vinyl toluene impregnated samples also show less number of voids, but the decrease is not as significant as in the case of the PE wax. In the case of LMA and acetophenone impregnated samples, the decrease is even less. It may be pointed out that the samples during testing may be heated up

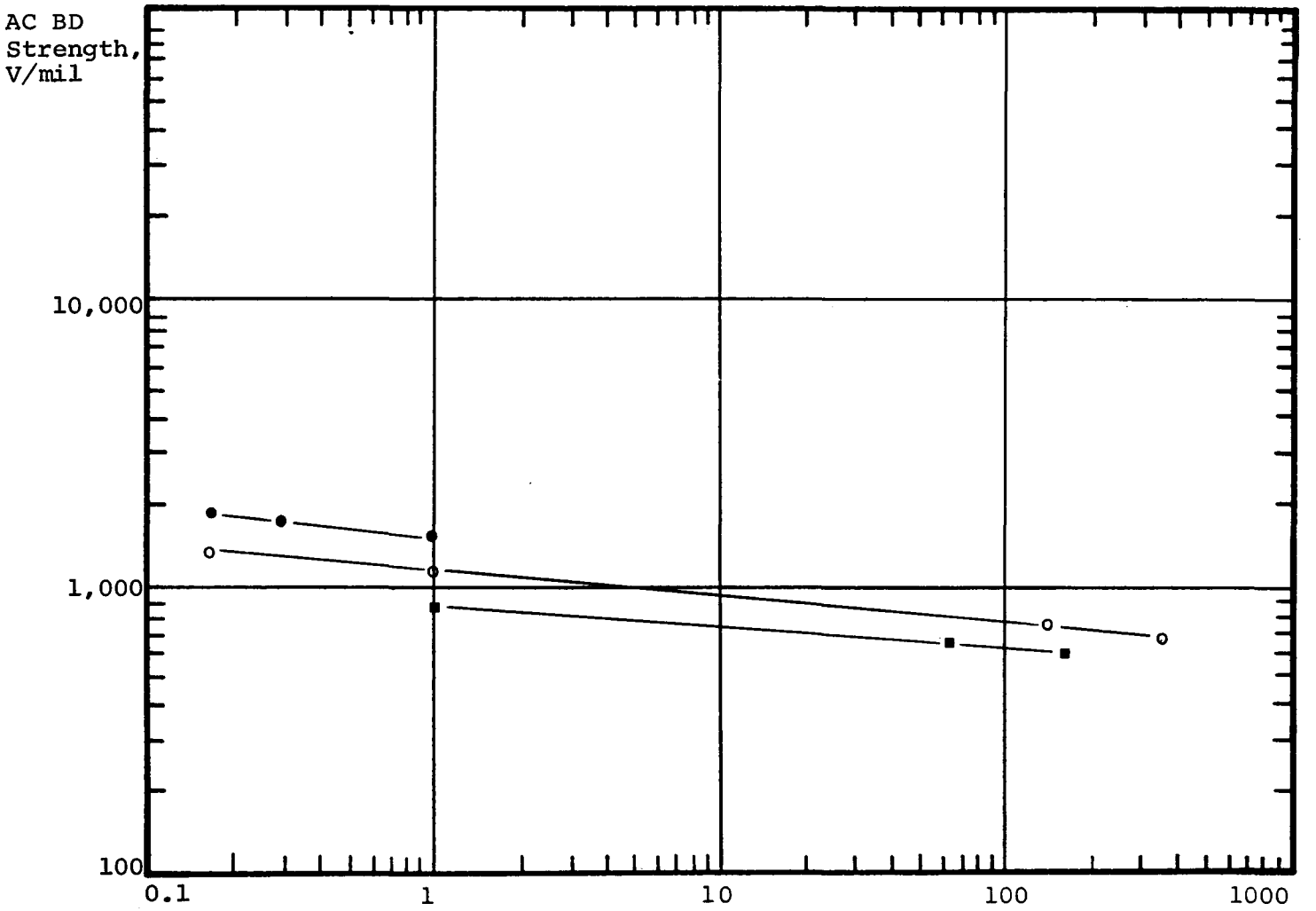

Figure 3-99. Stress-Time Correlation for Model Cables.
(●) Cable E, impregnated with 3.2 to 3.7% vinyl toluene.
(o) Cable E, control. (■) Cable H, control.

Table 3-14

COMPARISON OF SLABS AND MODEL CABLE

	Slab	Model Cable	Slab/ M.C.*	Slab	Model Cable	Slab/ M.C.*
Treatment	None			Impregnation With VT		
Sample Number	70	142		91B	153	
Thickness, mil	13	25	0.52	13	25	0.52
V_{50}, V/mil	2300	1218	1.89	2900	1699	1.70
V_{90}, V/mil	2600	1570	1.66	3500	1987	1.76
V_{10}, V/mil	1900	819	2.32	2200	1329	1.65
% Range	30	58	0.52	45	78	0.58
Effect of Treatment						
Change in Weight, %	0	0		+2.6	2.7	0.96
Change in V_{50}, V/mil	0	0		+600	487	1.23
Change in V_{50}, %	0	0		+26	40	0.65

* = Ratio Slab to Model Cable.

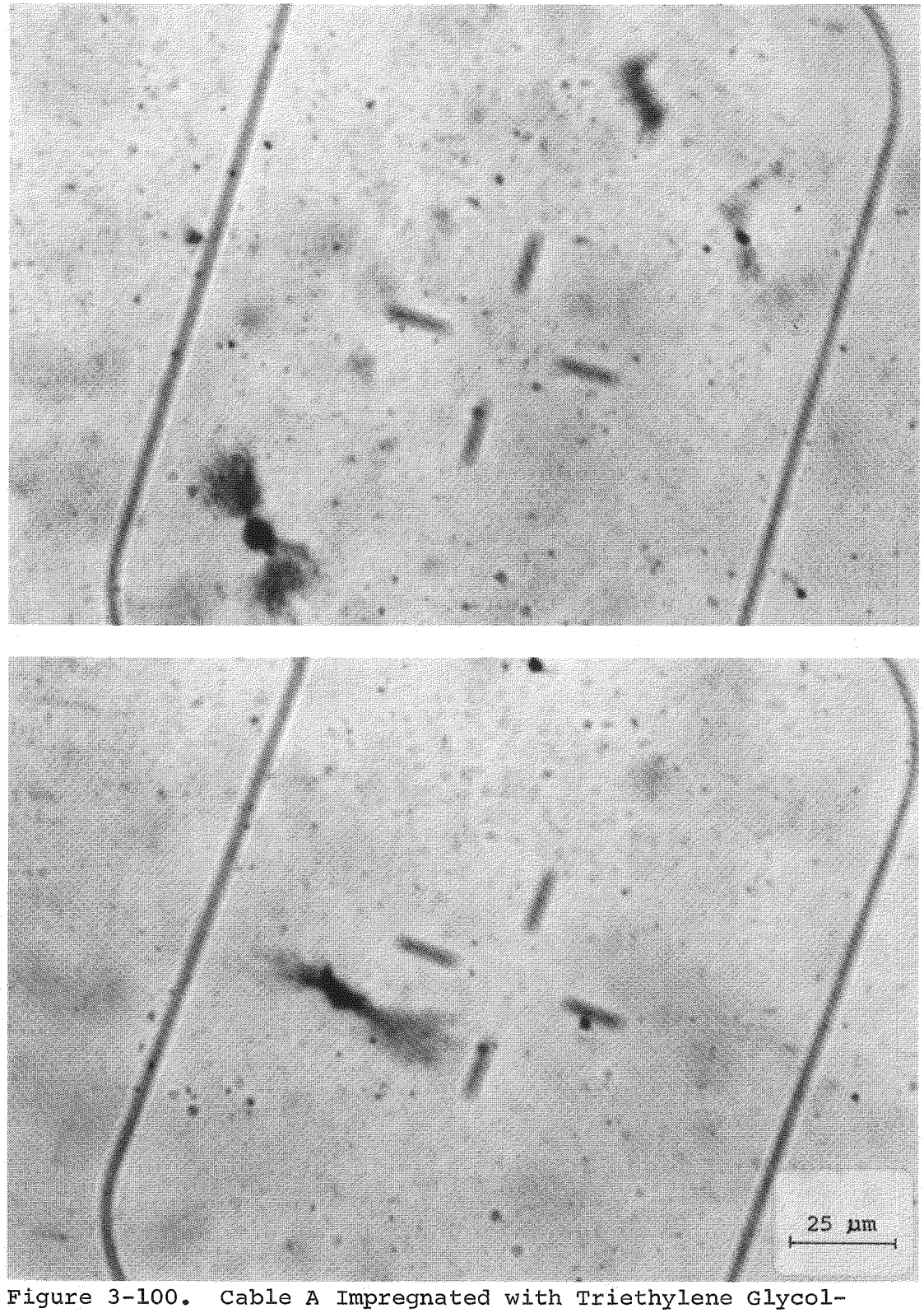

Figure 3-100. Cable A Impregnated with Triethylene Glycol-p-Xylene-Ethyl Alcohol Mixture.

OPTICAL MICROGRAPHS

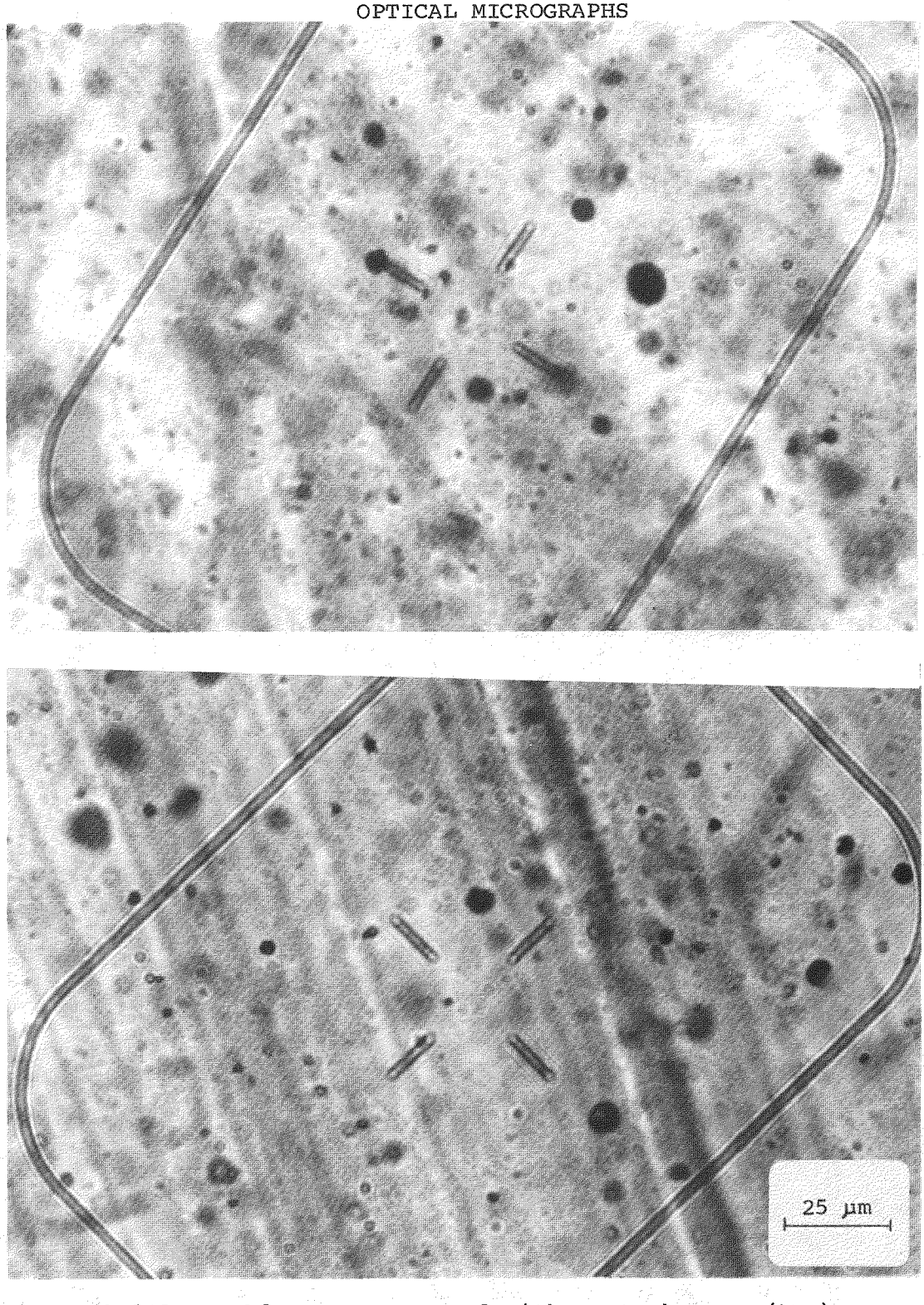

Figure 3-101. Cable A Impregnated with Acetophenone (top).

Figure 3-102. Cable A Impregnated with Lauryl Methacrylate (bottom).

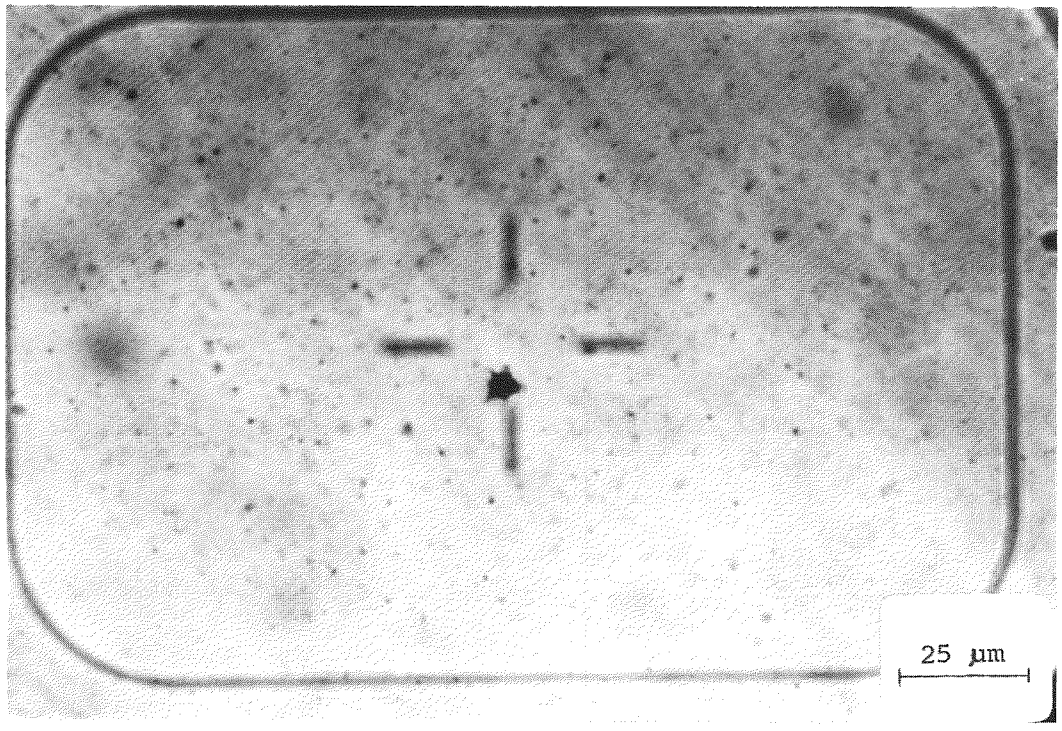

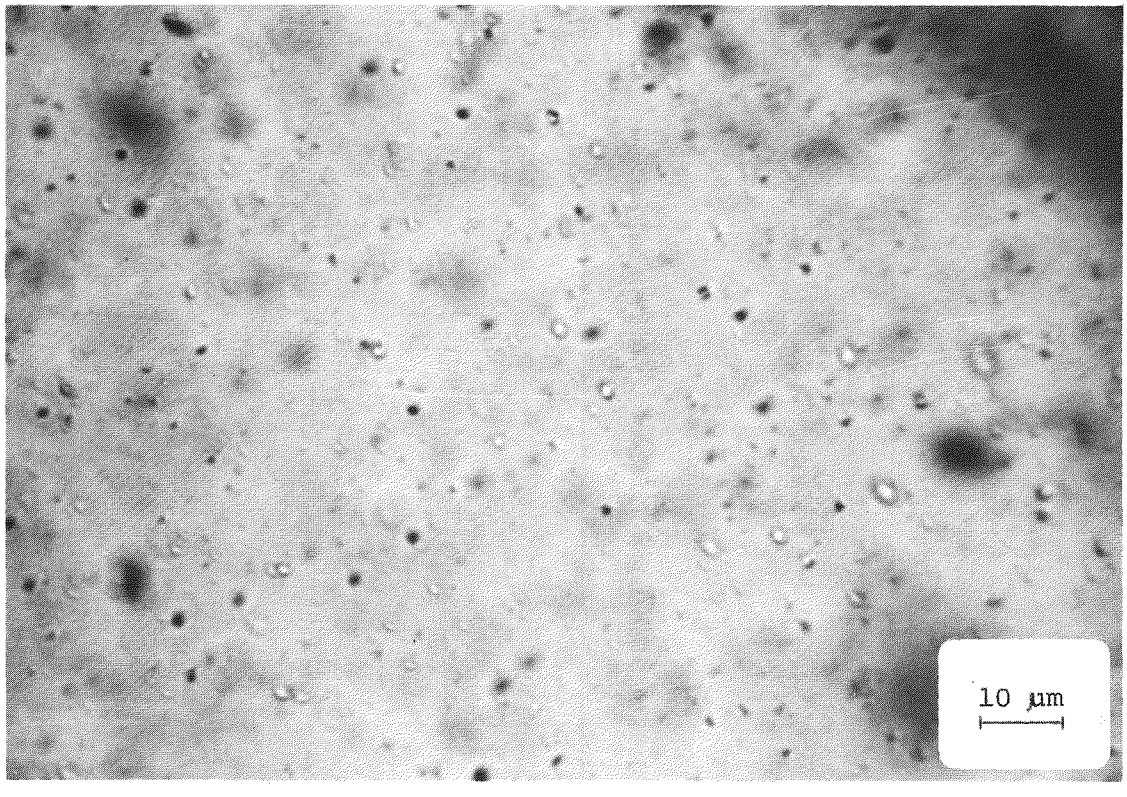

Figure 3-103. Cable A Impregnated with Vinyl Toluene (top).

Figure 3-104. Cable A Impregnated with PE Wax (bottom).

Table 3-15

SUMMARY OF OPTICAL MICROGRAPHS
Controls and Liquid Impregnated Slabs

Exp. No.	Cable	Treatment	AC BD Strength V/mil	Voids				Figure No.
				Number	Size, μm	Shape	Other Features	
2	A	Control	1980 *	Many	Max. 25	Spherical Ellipsoid	Bow tie trees	3-10
14	B	Control	2000 *	Many	Max. 20	Same		3-11
12	J	Control, dry cured	2000 *	Few	Max. 8	Spherical		3-12
142	E	Control, model cable, 25mil ins.	1218	Many	Max. 10	"		3-13
16	A	Vacuum dried	1530 *	Same as Control		A		3-37
69	B	" "	1620 *	" " "		B		3-38
50	J	" "	1900 *	" " "		J	Halo around some voids.	3-37
15	B	Control, 1 hr. step AC BD test.	2300	" " "		B		3-39
19	B	" , 168 hr. step AC BD test.	1400	Similar to Control		B	Bow tie trees	3-40
76	B	Heat treated, 67 hrs. @ 100°C.	2150	Fewer & smaller than Control			"Collapsed" voids?	3-41
93	B	" " " " " 150°C.	2700	Fewer & smaller than 100°C treated.				3-41
5	A	Impregnated with TEG-pX-EtOH	2300 *	Similar to Control		A	Bow tie trees	3-100
24	A	" " Acetophenone	2700 *	" " "		"		3-101
25	A	" " LMA	2260 *	" " "		"		3-102
51	B	" " Vinyl toluene.	>2600 *	" " "		B	Some star shaped voids	3-103
42	A	" " PE wax	2200 *	" " "		A	Dark voids with halo Light voids (filled with PE)?	3-104

* = V_{50} data at 18 mil thickness, all others at 13 mil.

due to electrical stress and the impregnants like acetophenone, vinyl toluene and LMA, which are somewhat volatile at higher temperatures, may have diffused out in the process. Further leaching of the liquid monomer is possible during the 24 hour dyeing process at 80°C. Although solubility of these aromatic monomers is small in water, the high temperature and the long time may have eliminated most of these impregnants.

3.3.6.2 Scanning Electron Microscopy. Scanning electron microscopy has been done with samples impregnated with selected liquids and polyethylene wax. The samples are cold fractured in each case. The micrographs are presented in Figures 3-105 to 3-109 and summarized in Table 3-16. Comparable micrographs for controls were presented earlier in Figures 3-16 to 3-20, 3-42 and 3-43.

As mentioned earlier, the characteristic features of the morphology are the spherulite-like structures separated by boundaries. In the center of these structures are holes or voids with dark shade. Impregnation with vinyl toluene and styrene which are relatively good solvents of polyethylene does not eliminate the appearance of the voids, possibly because they volatilize in the process of testing. However, they make the boundaries less defined. If the boundary represents amorphous portion, this indicates interaction of the aromatic solvents with amorphous polyethylene. If the boundaries are merging sections of fractured parts, then this would probably indicate slow yield under tearing stress instead of sharp yield. The voids in polyethylene wax and napthalene impregnated samples appear to be filled up (no dark shade in the center). There is no change in the boundary region. In the case of napthalene, however, dark shades develop when the samples are held longer under electron beam. It is suggested that napthalene present in the filled voids may sublime under heat and cause the voids to reappear.

3.4 POLYMERIZATION

3.4.1 Polymerization of LMA

3.4.1.1 Preliminary Experiments with Wafers. Wafers from cable A weighing 0.2 to 0.3 grams were impregnated with a monomer catalyst solution containing 1% of the latter. Three different catalysts having 10 hour half-life temperatures from 70 to 135°C were used. Polymerization was carried out according to the procedure in Section 4. The results presented below show that Benzoyl peroxide (BPO)with a 10 hour half-life temperature of 73°C and 1 hour half-life temperature of 91°C gives maximum weight gain.

5 μm

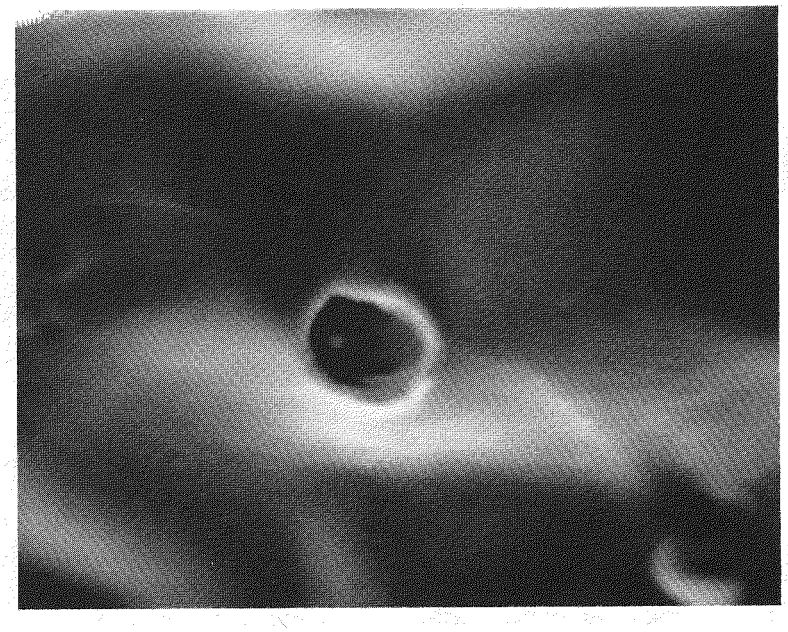

5 μm

Figure 3-105. Impregnation with LMA Cable A.

SCANNING ELECTRON MICROGRAPHS

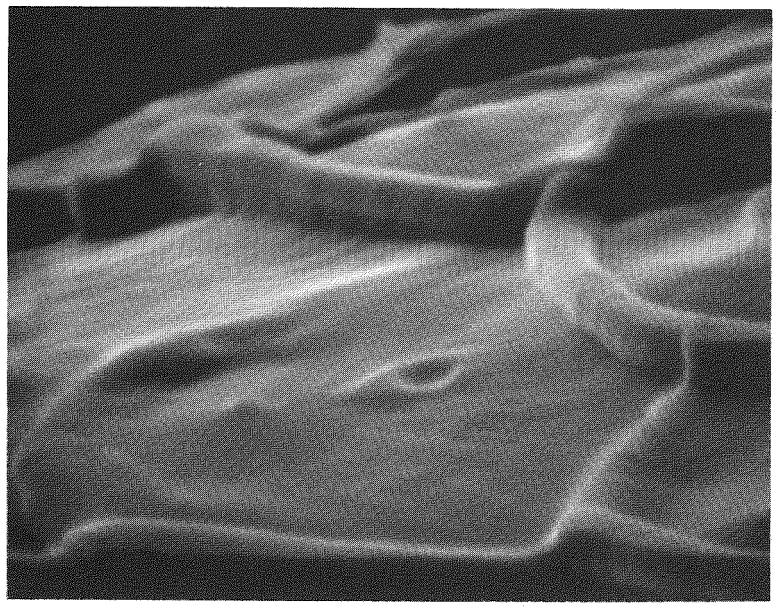

5 um

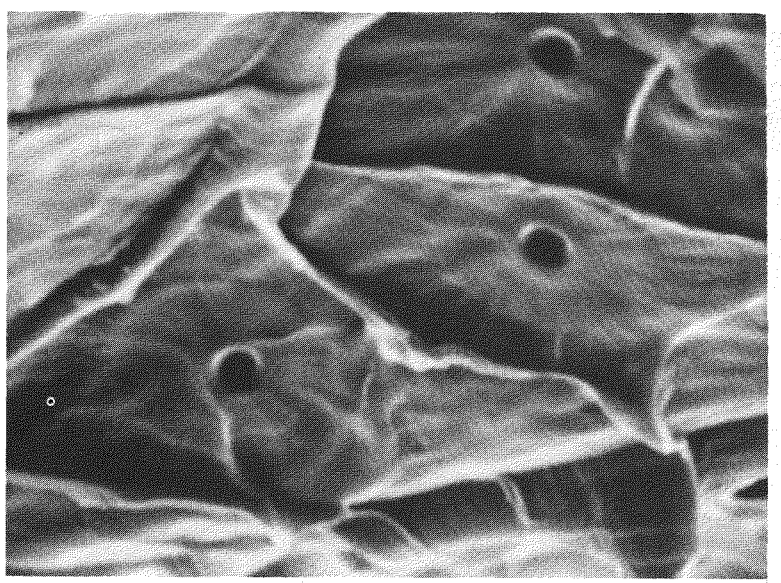

10 um

Figure 3-106. Impregnation with Vinyl Toluene.

SCANNING ELECTRON MICROGRAPHS

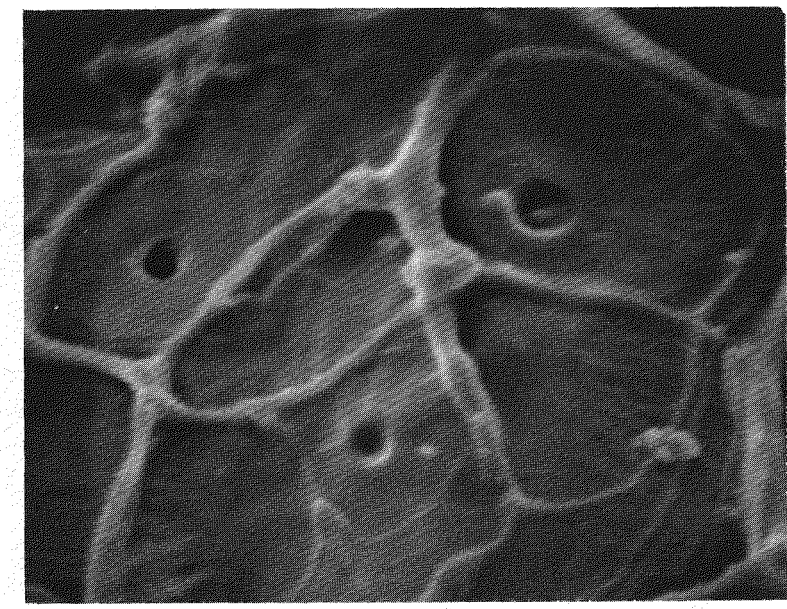

5 µm

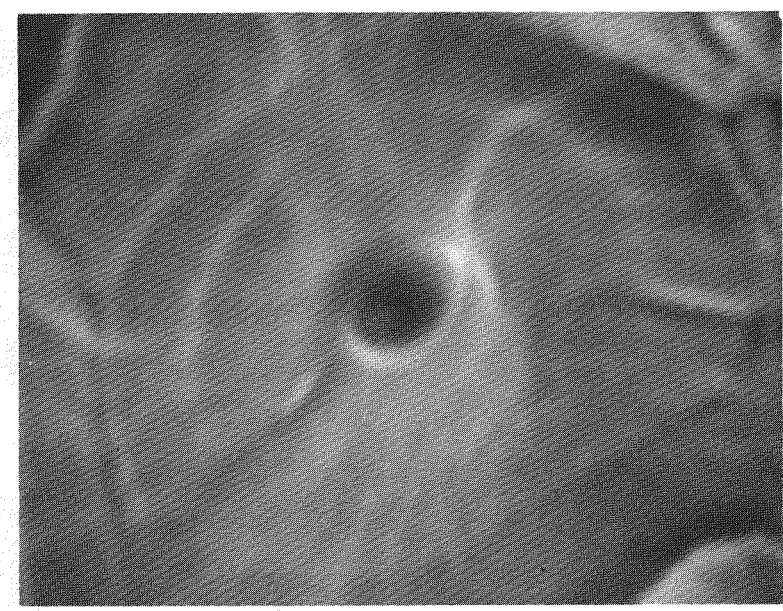

5 µm

Figure 3-107. Impregnation with Mineral Oil.

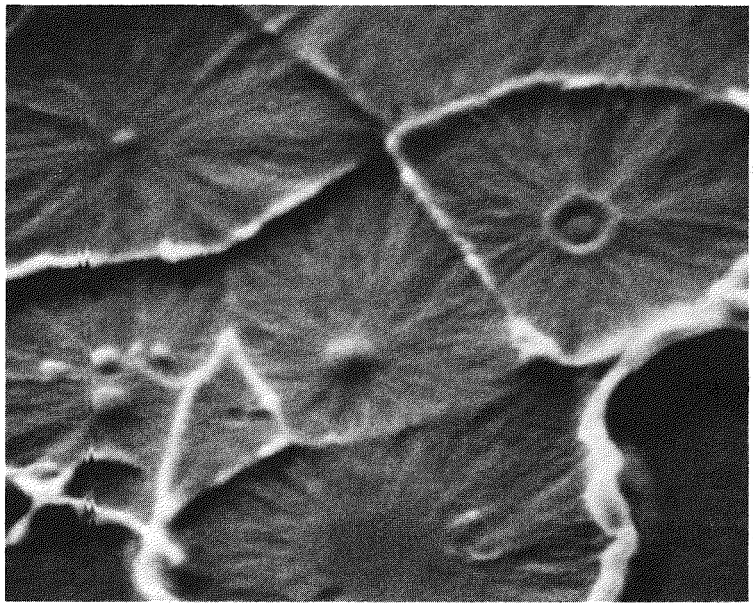

5 µm

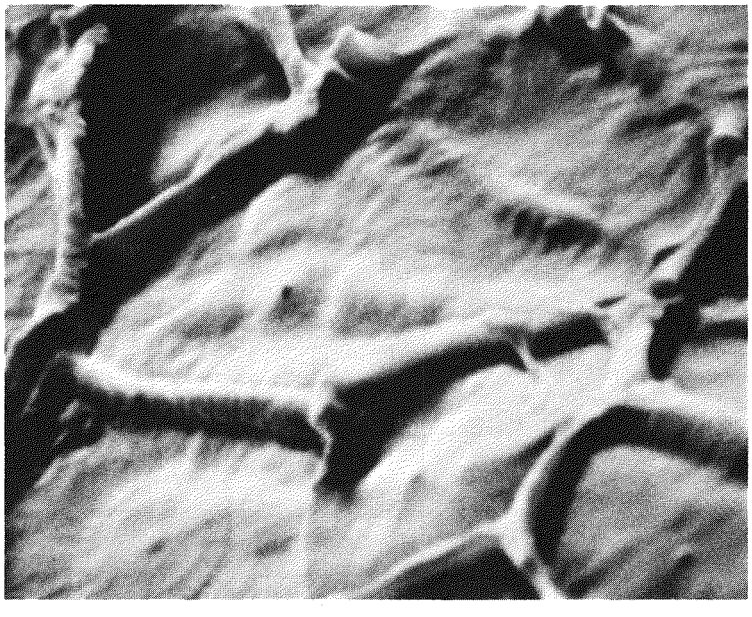

5 µm

Figure 3-108. Impregnation with PE Wax.

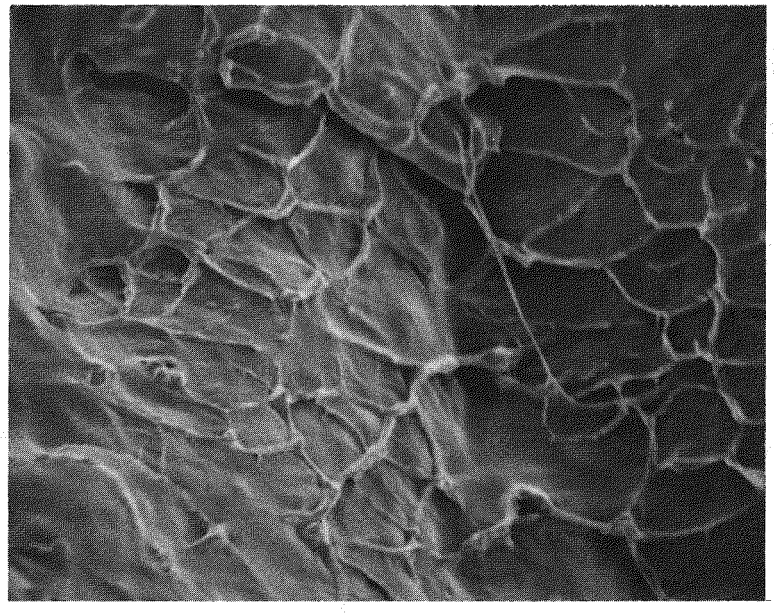

25 μm

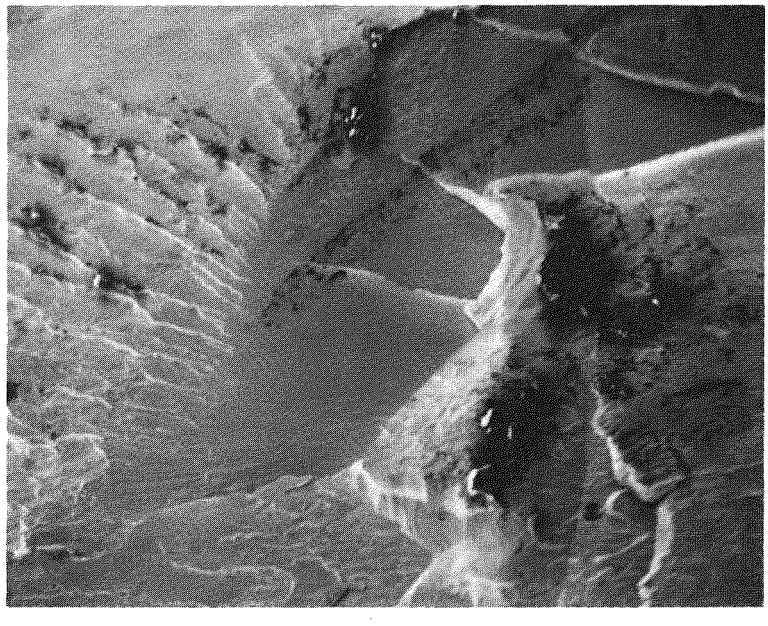

100 μm

Figure 3-109. Impregnation with Naphthalene. Note "charging" due to evaporation (bottom).

Table 3-16

SUMMARY OF SCANNING ELECTRON MICROGRAPHS

Exp. No.	Cable	Treatment	AC BD Strength V/mil	Voids (um)	Spherulite-Like Structures	Characteristic Features	Figure No.
2	A	Control	1980 *	(4) Drop Shape	No (Blade Cut Specimen)	Cracks	3-14
12	J	"	2000 *	(10) Irregular	No (" " ")		3-15
2	A	"	1980 *	(5) Round	Yes (Cold Fractured Spec.)	Fibrous dividers	3-16
14	B	"	2000 *	(2-6) Round	Yes	" "	3-17,-18
142	E	" , Model cable, 25mil, ins.	1218	(2) Round	Yes (Cold Fractured Spec.)	Similar to Cable A or B	3-19
190	G	" , " " , 20 " "	840	(1) Round	Yes " " "	" " " " " "	3-20
--	A	" , "Ditch" surface	--	--	No	Grooves perpendicular to machine direction, 2-5um	3-21,-22
2	A	" , Breakdown channel	1980 *	(25) Irregular	Some in Figure 3-25.	Voids and cracks caused by breakdown.	3-23,-25
16	A	" , Vacuum dried	1530 *	(5) Round	Yes	Similar to Cable A, Control	3-42
69	B	" , " "	1620 *	(6) Round	Yes	" " " B, "	3-43
76	B	Heat treated, 67 hours @ 100°C	2150	No	Yes	Fine structure decreases	3-44,-45
93	B	" " , " " @ 150°C	2700	No	Yes	Different fracture surface, no fine details	3-46,-47
25	A	Impregnated with LMA	2260 *	(2-5) Round	Yes	Partial plasticizing effect.	3-105
51	B	" " Vinyl toluene	>2600	(3) Round	Yes ("Swollen" Dividers)	Plasticizing effect	3-106
25A	A	" " Mineral oil	2330 *	(3-5) Round	Yes		3-107
42	A	" " PE wax	2200 *	No	Yes	Filled voids	3-108
92	B	" " Naphthalene	2700	No	Yes	Charging due to evaporation	3-109
9	A	" " LMA + BPO	1830 *	(10) Filled	No (Blade Cut Specimen)	PLMA filler shrank under electron beam	3-126
36	A	then polymerized in situ	2160 *	No	Yes (Cold Fractured Spec.)	Voids may be filled	3-127
57	B	Impregnated with Vinyl toluene + BPO then polymerized in situ	2750	No	Yes	Voids may be filled. Strong plasticizing effect decreased fine structure.	3-128 3-129

* = V_{50} data at 18 mil thickness, all others at 13 mil.

SELECTION OF CATALYSTS
(Catalyst Concn. 1 PHM*, Polymerization Time-3Hrs. at 70°C)

Monomer	Weight Gain (%) Benzoyl Peroxide	Chlorobenzoyl Peroxide	Dicumyl Peroxide
Isobutyl MA**	1.20	0.05	0.10
Ethyl Hexyl MA**	1.66	0.05	0.03

* PHM = parts per hundred parts of monomer

** MA = methacrylate

In a set of similar experiments three monomers, namely isobutyl, ethyl hexyl and lauryl methacrylate were compared at two levels of catalyst, 0.5 and 1%.

COMPARISON OF MONOMERS
(Catalyst-Benzoyl Peroxide, Polymerization Time-2 Hrs. at 70°C)

Monomer	% Weight Gain for Two Catalyst Concentrations 0.5 PHM	1 PHM
Isobutyl MA	0.40	0.6
Ethyl Hexyl MA	0.45	0.6
Lauryl MA	0.60	1.2

The maximum weight gain was obtained with lauryl methacrylate using 1% benzoyl peroxide. There is some increase in the weight gain as the aliphatic chain length increases from isobutyl (4 carbon atoms) to ethyl hexyl (8C) to lauryl (12C). It may be observed that the rate of polymerization, R_p, is given by the equation:

$$R_p = \frac{K_p}{K_t^{\frac{1}{2}}} \cdot K_i^{\frac{1}{2}} \left[M\right] \left[I\right]^{\frac{1}{2}} \qquad (3\text{-}4)$$

where: R_p = the rate of polymerization
K_p, K_t, K_i = rate constants for propagation, termination and initiation steps respectively.
$[M], [I]$ = concentrations of monomer and initiator respectively.

Hence, the rate increases when the catalyst concentration, [I] increases. Further, for the same catalyst and the same concentration, the rate depends on the $K_p/K_t^{\frac{1}{2}}$ ratio. The length of the alkyl chains in the methacrylates does not change the reactivity of the radicals as seen from their Alfrey Price reactivity ratio, (34) r_1 (0.58 and 0.57 for IBMA and LMA respectively), but increases the reactivity of the monomer, r_2 (0.56 and 0.63 respectively). Further, whereas propagation takes place by addition of small molecules to the growing chain end, the termination process requires bringing together two large sections of chain radicals. This makes the termination process diffusion controlled. The longer the aliphatic chain is, the smaller the K_t value and the greater the value of the $K_p/K_t^{\frac{1}{2}}$ ratio, which leads to a greater resistivity for LMA (35).

Subsequently, the effect of temperature and catalyst concentration was studied using benzoyl peroxide as the catalyst.

RATE OF POLYMERIZATION AT DIFFERENT TEMPERATURES
(Catalyst: BPO, 0.5 PHM-Time 2 Hrs.)

	% Weight Gain at:		
Monomer	70°C	90°C	110°C
Isobutyl MA	0.40	0.1	0.1
Ethyl Hexyl MA	0.45	0.1	0.1
Lauryl MA	0.60	0.3	0.3

It became evident that maximum weight gain is obtained at 70°C with lauryl methacrylate. The lower polymerization yield at higher temperature was attributed to the loss of monomer due to evaporation.

The effect of BPO concentration on LMA polymerization was investigated over a wider range:

EFFECT OF CATALYST CONCENTRATION
(Monomer-LMA, Catalyst-BPO, Temp. 70°C, Time 3 Hrs.)

Catalyst Concentration (PHM)	Weight Gain (%)
0.5	0.5
1.0	1.2
3.0	2.1
5.0	2.25
7.5	1.7
10.0	1.4

It appears that maximum yield was obtained at a catalyst concentration of 3 to 5%. The lower yield at higher catalyst concentration may be attributed to the induced decomposition of the peroxide where the decomposition does not yield new free radicals but saturated molecules (36).

Higher concentration of catalyst may induce premature polymerization leading to a shorter shelf life of the impregnating solution. Qualitative experiments had shown that addition of small amounts of hydroquinone (HQ) inhibits polymerization. However, the level of inhibitor has to be adjusted so that it delays the polymerization at impregnation temperature but does not lower the yield when polymerization is carried out at higher temperature. To study the effect of the inhibitor, its concentration has to be precisely known. The monomer usually is shipped with some inhibitor to prevent autopolymerization. The actual concentration depends on the age of the monomer and is difficult to analyze. Therefore, the inhibitor was removed from the monomer by washing it three times with a 5% solution of sodium hydroxide followed by three washings with distilled water and drying over anhydrous sodium sulfate. The dry monomer was vacuum distilled and measured amounts of inhibitor and catalyst were added to make up the monomer: catalyst: inhibitor solution. Impregnation, polymerization and drying were carried out as before. The results are presented in Table 3-17. It appears that the presence of 0 to 500 ppm inhibitor has no significant effect on the yield.

Table 3-17

EFFECT OF INHIBITOR PRESENCE ON THE DEGREE OF POLYMERIZATION

MONOMER: LAURYL METHACRYLATE
CATALYST: Bz_2O_2, INHIBITOR:HQ

SAMPLE - WAFERS, POLYMERIZATION - 16 HRS. AT 70°C

Expt. No.	Catalyst PHM	Inhibitor PPM	Degree of Impregnation %	Degree of Polymeriz.%
1	1	00	8.6	3.0
2	1	50	9.0	3.27
3	1	100	9.0	3.0
4	1	500	9.3	2.5
5	2	00	10.4	5.4
6	2	50	9.0	3.5
7	2	100	9.7	3.4
8	2	500	8.8	3.3

3.4.1.2 Experiments with Slabs. The preliminary work on wafers was followed by similar work on slabs cut from cable A. The results presented below confirmed the higher yield with higher catalyst concentration.

LEVEL OF POLYMERIZATION AS A FUNCTION OF CATALYST CONCENTRATION

Samples: XLPE Slabs
Monomer: LMA
Impregnation: 16 Hours at 25°C
Polymerization: 16 Hrs. at 70°C
Drying: 120 Hrs. at 90°C
All Data is an Average of Four Samples

Catalyst Concentration PHM	Inhibitor ppm	Original Dry Wt. (Gms.)	Level of Impregnation %	Level of Polymerization % of LMA
A. 0.50	100	1.79	4.85	21.7
B. 1.0	100	1.74	4.94	52.0
C. 2.5	200	1.56	5.21	91.6

Based on these initial findings, lauryl methacrylate and benzoyl peroxide were chosen as the primary candidates for monomer and catalyst. Full scale experiments were carried out with sets of 5 or 10 ditched test slabs. They were impregnated with the monomer catalyst solutions, surface washed and subjected to polymerization for 16 hours at 70°C followed by drying for 120 to 168 hours at the same temperature. All weight changes were normalized assuming initial weight as 100 and the level of polymerization was calculated as percentage weight gain due to impregnation. The results are presented in Table 3-18. Though it appears that the highest yield is obtained at the highest catalyst concentration, it was found impractical due to the tendency of the solution to autopolymerize. Hence, subsequent experiments were carried out at 1 PHM catalyst level. The range of yield, 42 to 72% corresponds to the level of impregnation.

It followed from this work that in order to obtain a higher level

Table 3-18

EFFECT OF CATALYST CONCENTRATION

Sample: Cable A slabs, 400 mil.
Impregnation: LMA, 16 to 560 hrs. at 25°C.
Polymerization: 3 to 24 hrs. at 70°C.

Expt. #	Catalyst Concn.%	NORMALIZED WEIGHT AFTER			% LMA polymerized
		drying	impregnation	polymeriz.	
2	3.5	99.00	100.65	100.6	97
3	1.0	99.3	100.0	99.6	42
9	1.0	98.8	99.9	99.6	73
13	1.0	98.6	99.7	99.4	73
4	1.0	98.5	99.7	99.4	75
21	1.0	98.5	99.89	99.5	72
22	1.0	98.5	100.30	99.6	61
20B	1.0	100.0	102.65	101.5	57
23	1.6	98.55	100.12	99.97	90
29A	1.5	98.50	100.6	99.3	38

of in situ polymerization, the level of impregnation has to be higher. This in turn required a higher temperature for impregnation. The results of a polymerization study are presented below. The impregnation of slabs was carried out at 25 and 40°C. It is obvious that a higher temperature of impregnation leads to higher levels of impregnation and polymerization. The higher amount of inhibitor used to prevent autopolymerization at 40°C had no significant effect on the yield.

EFFECT OF CATALYST CONCENTRATION AND TEMPERATURE OF IMPREGNATION ON THE LEVEL OF POLYMERIZATION (Time of Impregnation - 3 Days)

Catalyst Concentration %	HQ Concentration ppm	Temperature of Impregnation	Level of Impregnation	Level of Polymerization %
1.0	100	25°C	3.1	60.9
1.0	100	40°C	5.5	84.0
2.5	250	40°C	5.5	98.0
2.5	500	40°C	5.55	97.0

A systematic study was carried out on factors effecting polymerization. Full slabs were used for this purpose. All of them were impregnated for the same length of time. The catalyst concentration and the time and temperature of polymerization were varied. Higher temperature (90°C) was used for drying. The results are presented in Table 3-19. The highest yield appears to be at 70°C for a time of polymerization of 16 hours. Increased time or temperature does not seem to have much effect. An increase in BPO level from 1 to 2 PHM does not result in higher yield when the inhibitor is increased proportionally. In order to obtain some insight into this behavior, the weights of polymerized samples were plotted against the time of post polymerization drying in Figure 3-110. It appears that partial degradation occurs on continuous drying at 90°C under vac-

Table 3-19

STUDIES ON FACTORS AFFECTING POLYMERIZATION

(Time, Temperature & Catalyst Concentration)

Monomer: Lauryl Methacrylate
Catalyst: Benzoyl Peroxide, parts per hundred parts of monomer (PHM)
Inhibitor: Hydroquinone, PHM
Impregnation: Room Temperature
Sample: 4 x 0.5 x 8 cm XLPE slabs, Cable A
Prepolymerization Drying: Oven & Chamber drying at 90 and 70°C to constant weight.
Post polymerization Drying: Oven Drying at 90°C to constant weight.

CATALYST CONCENTRATION	INHIBITOR CONCENTRATION	POLYMERIZATION Temp. °C	POLYMERIZATION Time, Hrs.	WT. GAIN IMPREG.%	FRACTION OF MONOM. POLYMERIZED, %	NUMBER OF SLABS
1 PHM	100 PPM	70°C	16	1.77	76.0	2
			24	1.74	75.6	2
			46	1.68	74.0	2
		85°C	16	1.78	70.9	5
			24	1.79	72.6	5
			46	1.75	74.9	5
			144	1.79	72.0	5
		100°C	16	1.79	70.5	5
			24	1.76	68.9	5
			46	1.77	68.2	5
2 PHM	200 PPM	85°C	4	1.77	62.0	5
			8	1.78	72.0	5
			16	1.81	70.4	5
			24	1.80	69.8	5

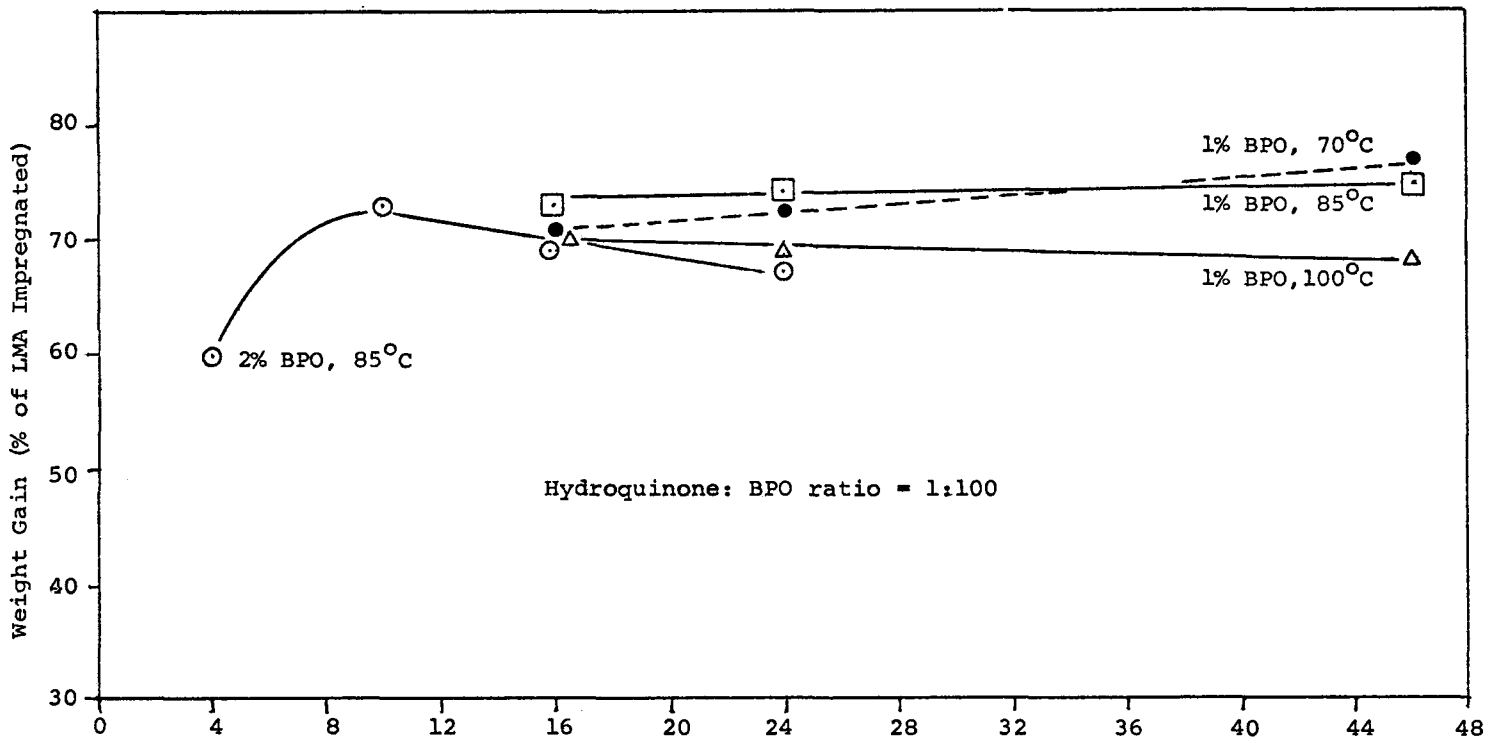

Figure 3-110. Effect of Post Polymerization Drying Time and Temperature on Weight Gain. Time, Hrs.

Sample : Cable A slabs, 400 mil.

uum.

Achieving 100% polymerization of the impregnated monomer would eliminate the tedious process of drying. Since higher temperatures and longer time did not achieve the 100% level, it was thought that use of peroxides other than benzoyl peroxide might have some beneficial effect. Hence, a number of peroxides, peroxy esters and acids were assessed. The results have been presented in Table 3-20. Full size slabs were impregnated at 40°C for 148 hours. All the catalysts chosen had 10 hour half-life temperature between 73 and 102°C and polymerization was carried out for 16 hours at 70°C. The benzoyl peroxide monomer solution polymerized in the impregnation chamber. The other solutions remained stable, possibly due to their higher half-life temperature. However, the polymerization yield in each case was low compared to previous BPO experiments. Therefore, benzoyl peroxide is probably the best catalyst for polymerization of lauryl methacrylate at 70 to 100°C. The less than 100% yield could be due to a slower rate of migration of the peroxide compared to the monomer, resulting in a peroxide concentration in the matrix insufficient to assure complete polymerization.

3.4.1.3 Radiation Induced Polymerization. In order to circumvent the problem of slow catalyst migration, polymerization with γ ray radiation was attempted. In one set of experiments 15 small slabs were impregnated with LMA for 23 hours at room temperature. The monomer was freed from the hydroquinone inhibitor for this purpose. The samples were subjected to radiation from a cobalt 60 source. The dose rate was 0.11 Mrad/hour and the exposure varied from 3 to 48 hours. The samples were maintained in an atmosphere of the monomer, as in catalyst initiated polymerization. The samples were vacuum dried to constant weight at 70°C. The results are presented below.

RADIATION INDUCED POLYMERIZATION OF LAURYL METHACRYLATE IN XLPE MATRIX

Sample: Small slabs cut from 138 kV cable, average weight 12 gms.
Impregnation: Inhibitor - free lauryl methacrylate - time 230 hours - temperature 25°C.
Radiation Dose Rate: γ radiation, 0.11 Mrad/hour.
Post Polymerization Drying: 70°C at 50μ vacuum.

Table 3-20

POLYMERIZATION OF LMA WITH DIFFERENT CATALYSTS

MONOMER - LMA 100 PARTS
SAMPLE: CABLE A SLABS
CATALYST 2%
IMPREGNATION 148 Hrs. at 40°C
POLYMERIZATION 16 Hrs. at 70°C

NO.	CATALYST	10 - HR. HALF LIFE (°C)	IMPREG. LEVEL (% MATRIX)	POLYMERIZ. LEVEL (% MONO. IMPD)	SOLUTION STABILITY
			Avg.	Avg.	
1	Benzoyl Peroxide	73	1.91 1.90 1.89 1.88 — 1.89	- - - -	Premature Polymn. after 4 days @ 40C
2	2,5 Dimethyl 2,5 DI (Benxopenoxy) Hexane	100	3.20 3.19 3.20 3.22 — 3.20	31.9 32.0 30.7 31.3 — 31.5	Stable
3	t Butylperoxy Maleic Acid	87	3.23 3.19 3.19 3.20 — 3.20	34.3 34.4 34.4 34.0 — 33.4	Stable
4	Di t. butyl diperoxy Phthalate	105	3.16 3.10 3.11 3.13 — 3.13	33.6 34.9 35.1 32.5 — 34.0	Stable
5	t-Butyl Peroxy Acetate	102	3.23 3.17 3.22 3.20 — 3.20	39.6 38.9 34.5 35.3 — 36.6	Stable

Slab No.	Original Weight	Normalized Wt. After Impregnation	Exposure Time Hrs.	Normalized Wt. After Polymerization	Polymerization Yield %
1	100	103.3	3	103.2	99.0
2	100	103.1	6	103.1	100.0
3	100	103.1	24	103.1	100.0
4	100	103.1	48	103.1	100.0

This demonstrates that almost 100% polymerization occurs in three hours. Subsequently, 10 full slabs were impregnated with LMA, to a level of 2.65%. They were subjected to polymerization for 3 hours at the same dose rate, followed by vacuum drying. The residual weight gain was 2.62%, which amounts to a net polymerization of 98.9%. This confirmed that efficient migration of the catalyst into the solid matrix is very important to obtain complete polymerization.

3.4.1.4 Bulk Polymerization of Lauryl Methacrylate. In order to see how fast the monomer alone polymerizes in bulk, 10 gms. of the purified monomer containing 1% catalyst, benzoyl peroxide was polymerized. The solution was degassed three times under vacuum in sealed tubes and heated in a water bath to 70°C. The polymerization was carried out for different intervals of time. Subsequently, the test tubes were broken, the raw polymer dissolved in methyl ethyl ketone, reprecipitated with methanol and dried to constant weight at 70°C under vacuum. The results presented below are indicative of the rate of bulk polymerization.

BULK POLYMERIZATION OF LAURYL METHACRYLATE
(Catalyst Concentration-1 PHM, Temperature-70°C)

Test Tube No.	Time of Polymerization (Hours)	Percent Conversion
1	1.0	53.3
2	1.5	57.0
3	2.0	66.8
4	3.0	77.6
5	4.0	80.2

3.4.2 Polymerization of Vinyl Toluene

3.4.2.1 Slab Experiments. The impregnation program (Section 3.3) showed that slabs impregnated with vinyl toluene have a much higher dielectric strength than slabs treated with lauryl methacrylate. Hence, the focus was changed from polymerization of lauryl methacrylate to vinyl toluene. The effect of catalyst concentration on polymerization is presented below.

POLYMERIZATION OF VINYL TOLUENE

Monomer: Vinyl Toluene (Grade 12T - 100)
Impregnation: 70 Hrs. at 25°C
Polymerization: 16 Hrs. at 70°C
Post Polymerization Drying: 150 Hrs. at 70°C
Catalyst: Parts per Hundred Parts of Monomer (PHM)

Catalyst	Catalyst Concentration PHM	Impregnation %	Polymerization %
Benzoyl Peroxide	1	10.7	25.2
	2	11.0	80.4
	3	10.6	96.7
2.5 Dimethyl (di benzoyl) Peroxy Hexane	2	10.6	35.8

Benzoyl peroxide and 2.5 dimethyl (di benzoyl) peroxy hexane (with a 10 hour half life temperature of 100°C) were used as catalysts. It is apparent that benzoyl peroxide is still the better catalyst and 2 to 3 PHM catalyst concentration is probably the optimum for achieving a high degree of polymerization.

3.4.2.2 Experiments with Model Cables. The initial experiments with model cable E resulted in low polymerization yield. Three potential causes were considered:

1. Low rate of catalyst migration.

2. Inhibiting effect of conductor shield possibly due to its high carbon black content.

3. Rapid volatilization of unreacted monomer from the thin insulation during the polymerization process.

The comparison of Experiment No's. 174 and 169 in Table 3-21 shows that cable H (containing no conductor shield) yielded 33% polyvinyl toluene, while cable E only 0.2% when impregnated and polymerized under identical conditions. This clearly indicates the carbon black has an inhibiting effect.

The inhibiting effect of carbon black on polymerization was observed in simultaneous experiments aimed at assessing volume resistivity of impregnated shields and is described in Section 5.2. The inhibition is attributed to functional groups on the carbon black surface such as quinone, hydroquinone, benzoquinone, etc. These groups combine rapidly with free radicals generated by the catalyst decomposition and interfere with the initiation step leading to a low yield of polymer. The scheme below (37) represents the various steps in the inhibition process.

The overall effect of these reactions is the conversion of active chain radicals into inactive species or into short chain oligomers. The latter ones may be volatile enough to be driven off in vacuum drying.

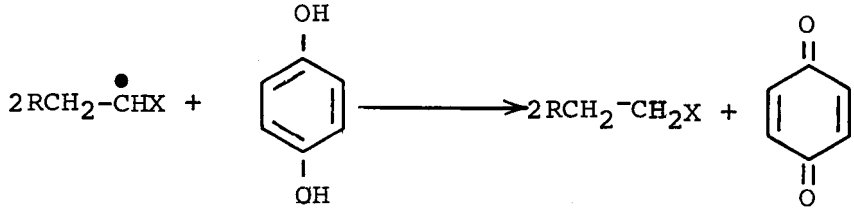

CHAIN RADICAL + HYDROQUINONE OLIGOMER + QUINONE

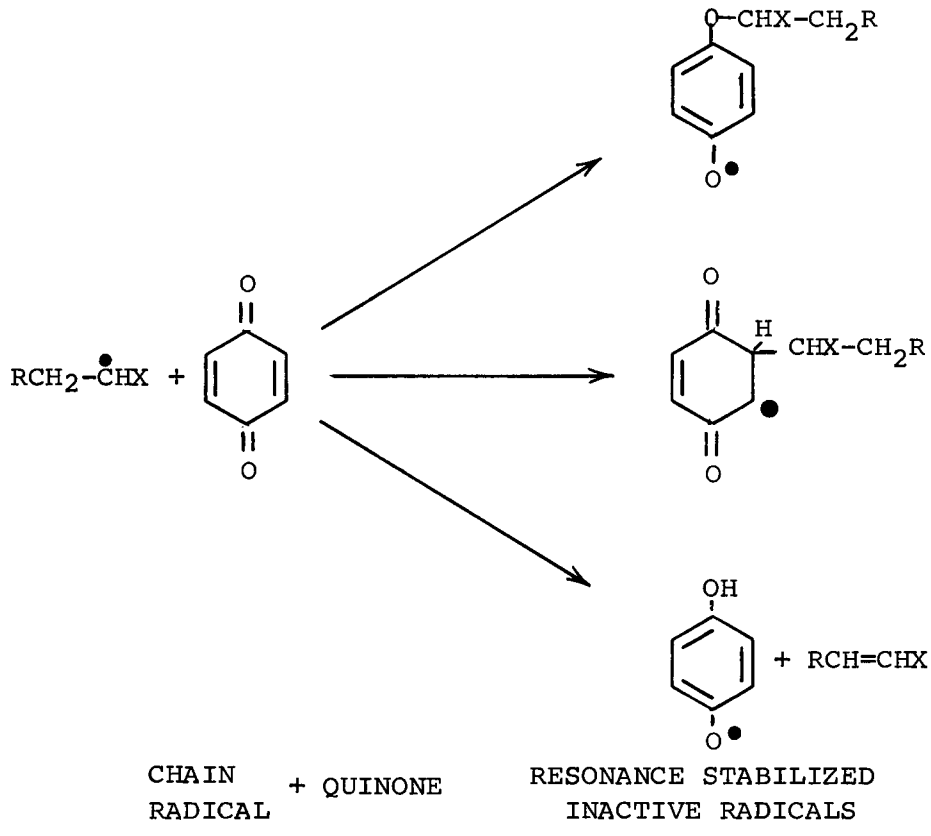

Gradually increasing insulation thickness resulted in increasing polymer yield in Experiment Nos. 169, 131 and 64 respectively. Since both the insulation thickness and the insulation carbon black ratio increased in this series, either the decrease in inhibition due to carbon black or less monomer volatilization through the thicker insulation could be responsible for the increase in the polymer yield. In Experiment No. 57 the semiconducting layers were removed. The polymerization yield was 59%. In experiment No. 64 the semiconducting layer was present. Note that both the time of impregnation and the weight gain in Experiment No. 64 are greater than those in experiment No. 57. In spite of that the polymer yield was only 57% demonstrating the inhibiting effect of carbon black. In experiment No. 131, 15 kV cables were used with an 8.6 volume % semiconducting layer. Their polymerization yield is approximately 32%=(54+10.2)/2 compared to about 0.1% polymerization yield in the model cable with 37.5 volume % semiconducting layer. This shows the important role of the semiconducting layer in controlling the polymerization yield of the cables. The limitations of the process involving direct impregna-

Table 3-21

IN SITU POLYMERIZATION OF VINYL TOLUENE

Expt. No.	Cable Type and History	Impregnation with MEK/BPO Solution				Impregnation with VT/BPO Solution				Polymerization				
		BPO %	Temp. °C	Time Hrs.	Weight Gain %	BPO %	Temp. °C	Time Hrs.	Weight Gain %	Temp. °C	Time Hrs.	Weight Gain %	Yield %	ACBD Strength V/mil
142	E, Control	-	-	-	-	-	-	-	-	-	-	-	-	1218
173	E, Vac. Dried	-	-	-	-	-	-	-	-	-	-	-	-	1054
186	E, Vac. Dried, Impregnated and Polymerized	-	-	-	-	3	30	2	4.2	70	18	0	0	-
169	E, Vac. Dried, Impregnated and Polymerized	-	-	-	-	3	30	20	19.0	70	20	0.36	0.2	1192
186	H, Vac. Dried, Impregnated and Polymerized	-	-	-	-	3	30	2	8.0	70	18	0.4	5.0	-
174	H, Vac. Dried, Impregnated and Polymerized	-	-	-	-	3	30	20	15.9	70	20	5.3	33	-
131	15 kV	-	-	-	-	3	25	72	4.3	70	20	0.53	10.2	-
131	" "	-	-	-	-	3	25	92	5.8	70	20	1.49	54.0	-
57	A, 4" length of cable (1)	-	-	-	-	1.5	25	310	4.9	70	17	2.7	59	2750
64	B, " " " " (2)	-	-	-	-	2.0	25	670	16.0	70	48	9.1	57	-
104	C, Control	-	-	-	-	-	-	-	-	-	-	-	-	1084
195	C, Heat Treated	-	40	69	-	-	50	2	-	60	20	-	-	1165
193	C, Impregnated	10	40	69	7.8	5	50	2	5.5	60	20	1.3	25	1402

(1) Conductor and shields removed. (2) With conductor and shields.

tion with a monomer-catalyst solution necessitated the development of a more efficient method. A two step process was devised, in which the catalyst is introduced first into the matrix, followed by impregnation with the monomer. Methyl ethyl ketone (MEK) was used as a solvent for the catalyst. Being a good solvent, it allowed the use of high catalyst levels. Since it is not polymerizable, it presented no danger of spontaneous polymerization. Its high volatility facilitated its removal in the final drying step. Experiment No's. 104, 193 and 195 in Table 3-21 demonstrate the process. A model cable was impregnated with MEK containing 10% BPO in 69 hrs. at 40°C temperature resulting in 7.8% weight gain. Based on data presented in Figure 3-66, the BPO content of insulation is estimated as 5% of this 7.8% weight gain, or 0.4% of the insulation. In the second step vinyl toluene containing 5% BPO was used as impregnant at 50°C for 2 hours, and 5.5% weight gain obtained. The polymerization step yielded 1.3% in situ polymer or 25% of the available monomer. This compares favorably to Experiment No. 186 where 4.2% impregnated monomer yielded no measurable polymer after one-step process polymerization.

Based on the favorable experience with model cables, the two-step process is recommended for impregnation and in situ polymerization of full size cables, and served as a basis in the economic evaluation in Section 6.

3.4.3 AC Breakdown Strength

3.4.3.1 Slab Experiments. A number of experiments were carried out in which sets of 10 slabs were impregnated with a solution of lauryl methacrylate and benzoyl peroxide followed by in situ polymerization for 16 to 20 hours at 70°C. The residual monomer was then taken out by vacuum drying and breakdown strength was measured for each set following the procedure outlined in Section 4. The results are presented in Table 3-22 along with the conditions of drying, impregnation and polymerization. The Weibull plots are given in Figures 3-111 to 3-114. They are quite linear showing that polymerization or subsequent drying does not invalidate the Weibull distribution.

The breakdown strength of each set has been plotted against the normalized weight gain in Figure 3-74. Data points representing the vacuum dried control and liquid LMA impregnated slabs, where no polymerization was carried out, are included for comparison. It is evident from the above results that:

- Impregnation and polymerization with lauryl methacrylate of vacuum dried slabs, improves their AC breakdown strength by up to 40% and brings it up a little above the original value of 2000 V/mil. Vacuum drying by it-

Table 3-22

SUMMARY OF THE RESULTS ON MONOMER IMPREGNATION AND *IN SITU* POLYMERIZATION

(All Weights are based on Original = 100)

Test No.	Drying Hrs.,	°C,	µm	Impregnation Hrs.,	PSI	°C	Polymeriz. Hrs.,	°C	Post Polymeriz. Drying (1500 Å) Hrs.	°C	Impreg. Materials LMA	BPO,%	HQ,PPM	Weight After: Drying	Imp.	Polym.	Drying	Breakdn. Voltage V/mil
2	60	70	50	16	0		3	70	48	70	100	3.5	0	99.00	100.7	100.65	100.6	1730
3	60	70	50	21	0		3	70	24	70	100	1	0	99.30	100.0	100.08	99.6	1874
1	72	70	25	61	0		Auto	Polym.	24	70	100	1	0	98.70	102.0	-	102.0	1810
9	72	70	1500)															
	72	23	25 (	72	0		16	70	57	70	100	1	100	98.80	99.9	99.9	99.6	1830
	08	70	25)															
13	72	70	1500)	66	0		21	70	125	70	100	1	100	98.60	99.7	99.60	99.4	1750
	48	70	25)	24	30 (N_2)													
4	72	70	1500)	48	0		20	70	30	90	100	1	100	98.5	99.70	99.50	99.4	1800
	48	70	20)	48	50													
21	168	70	20	168	50		16	70	120	90	100	1	100	-	99.89	-	99.5	1600
22	168	80	5	168	50		16	80	120	90	100	1	100	-	100.34	100.25	99.6	1500
20B	96	100	1500	560	0		24	70	120	90	100	1	100	-	101.05	101.15	100	2049
23	168	70	20	154	25		48	70	120	90	100	1.6	100	98.55	100.12	-	99.97	720
20A	96	100	1500	560	0		24	70	120	90	100 (1)	1	100	-	101.70	101.90	100.40	1656
29A	168	80	20	432	25.50		96	85	216	90	100	1.5	200	-	100.60	100.49	99.29	1730
36	240	70	30	96	-	25°	24	70	192	70	100	2.5	250	99.23	102.06	-	101.29	2160
				60	-	40°												
39	240	70	30	72	-	25											102.76	1720
				6		40			90	70	100	2.5	250	98.9	104.7			
44B	{254	50	{200	{96	-	{25	15	70	168	70	100	2.5	500	99.15	101.95		101.53	{1480 (2)
44A	{ 96		{ 30	{72	-	{40												{2300
43	576	70	400	480	-	25	5	25			100	(3)	0	99.4	102.56		102	1500
	312	70	30															
57	0	0	0	310	-	25	17	70	144	70	V.T.	1.5	500		107.54	106.00	102.74	2750

(1) 70% LMA, 10% Styrene, 20% HEGMA

(2) 24-Hour Step Test

(3) Polymerized by irradiation, Sample: Cable A, 18 mil slabs.

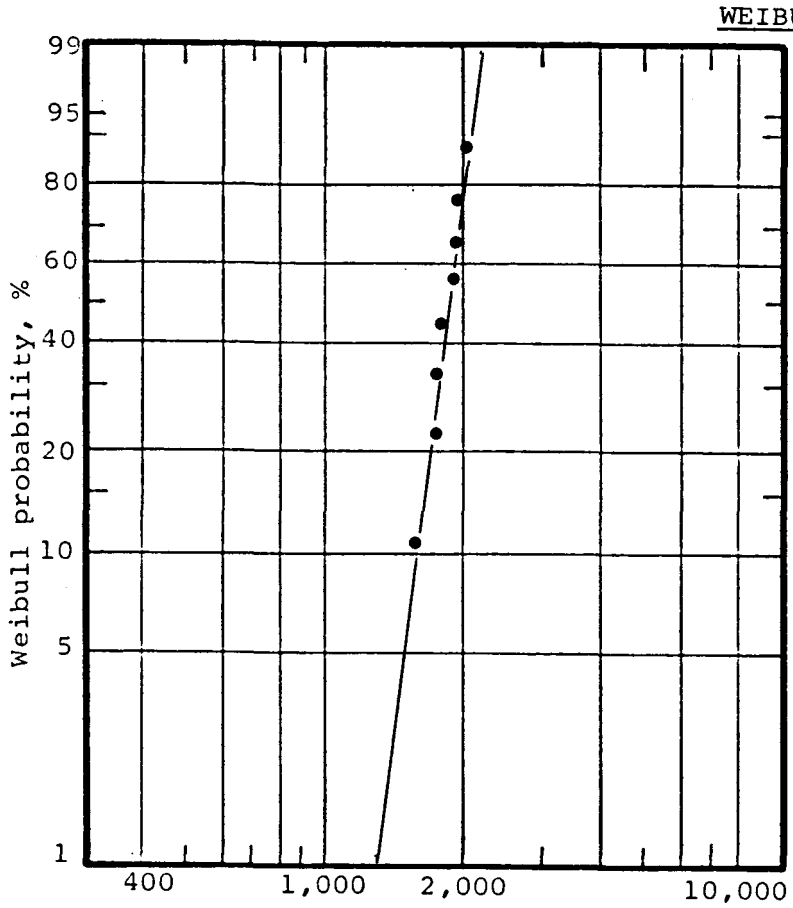

Figure 3-111. Effect of Polymerized LMA. Cable A, 18 mil slabs. Experiment #9.

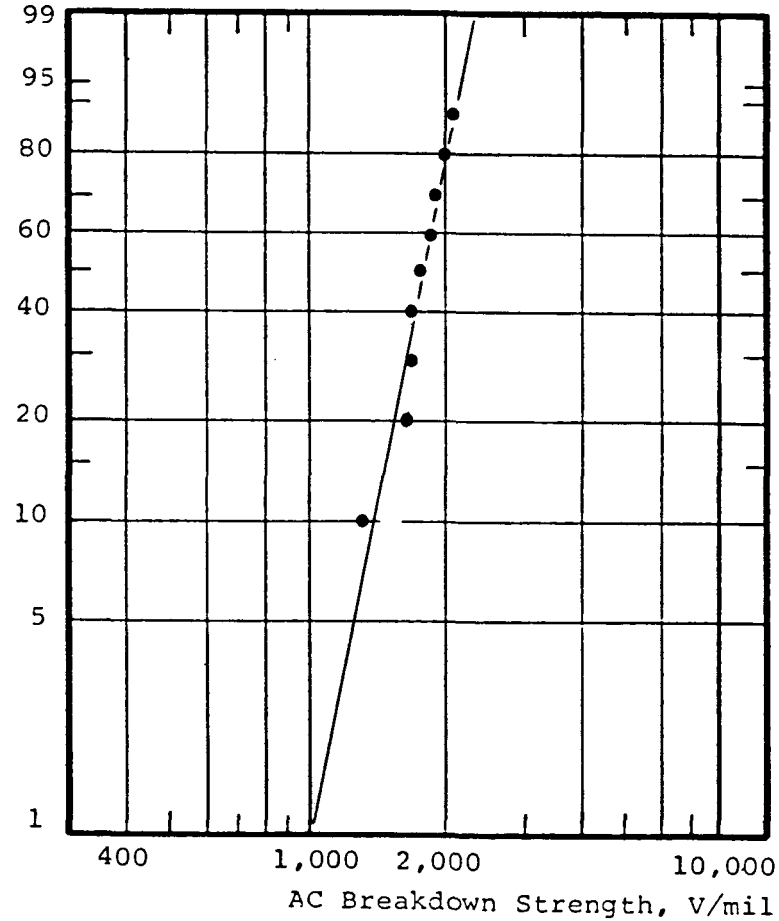

Figure 3-112. Effect of Polymerized LMA. Cable A, 18 mil slabs, Experiment #13.

WEIBULL PLOTS

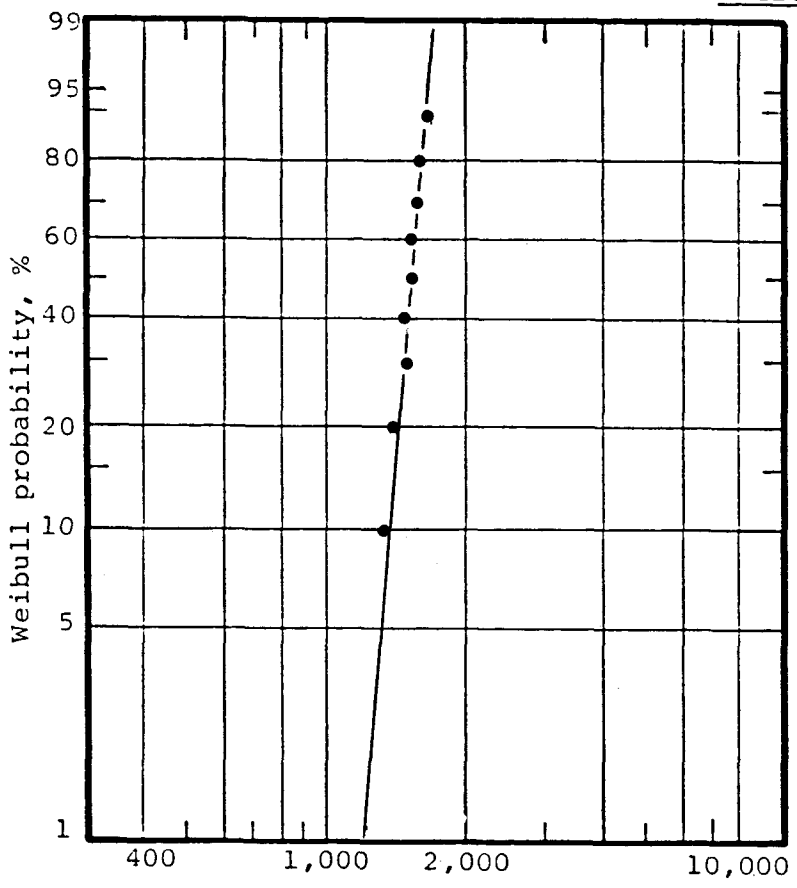

Figure 3-113. Effect of Polymerized LMA. Cable A, 18 mil slabs. Experiment #22.

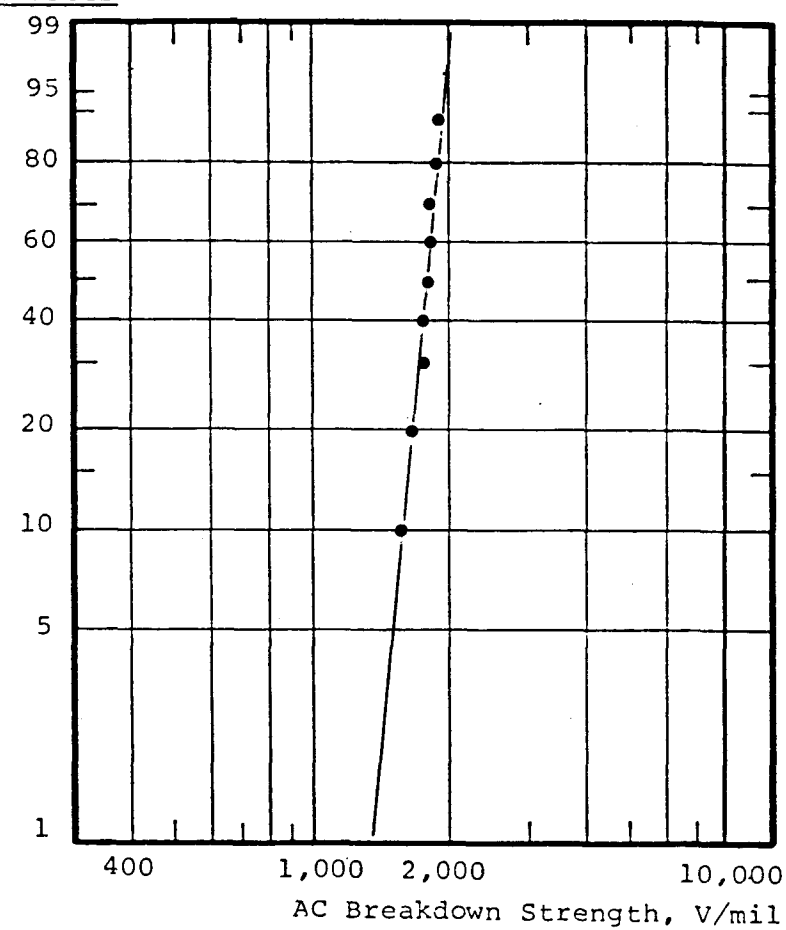

Figure 3-114. Effect of Polymerized LMA. Cable A, 18 mil slabs. Experiment #29.

self lowers the value by about 30%.

- The dielectric strength depends on the level of impregnation, reaches maximum at 2 to 3% impregnation and then levels off. It is suggested that at this point all the voids are filled up or their size sufficiently decreased to cause no electrical failure.

- For the same level of weight gain, the AC breakdown strength of polymerized samples are comparable to those of the monomer impregnated samples. This shows that the improvement may be independent of the physical state of the impregnant.

Since all the slabs in each set were identified separately, they were analyzed in respect to their weight loss on vacuum drying, weight gain on impregnation and polymerization and their individual breakdown values.

In Figure 3-115, an attempt was made to correlate the weight change with AC breakdown strength data for each specimen of a selected experiment, Experiment No.13. The horizontal axis measures the weight change, and the vertical one the V/mil values. Of the three diagrams, the middle one represents the actual test on polymerized and dried apecimens. The numbers in the circles are the serial numbers of the slabs and serve for identification only. Apparently the highest and lowest AC test values coincide at approximately identical weight changes. Similarly, the highest and lowest weight change data correspond to similar AC test data, dramatically demonstrating the lack of correlation.

The diagram at the left correlates the AC test data with weight loss in the first drying test for the same slabs investigated before. This correlation is theoretical only, since the specimens were not actually used in the AC test after drying, but were impregnated and grafted. The diagram on the right represents the imaginary correlation between AC test values and weight change after impregnation for the same specimens. Both of these imaginary steps fail to establish correlations between the variables. The similarity of the pattern in each of the three cases is striking, indicating that the real differences between individual specimens occur in the first drying step and both impregnation and polymerization show minimal variation compared to the weight loss in the first drying.

Experiment No. 43 gives the results on slabs in which lauryl methacrylate was polymerized by γ ray radiation. The breakdown strength shows no improvement over vacuum dried samples despite the high level of impregnation. Though a single experiment is insufficient to

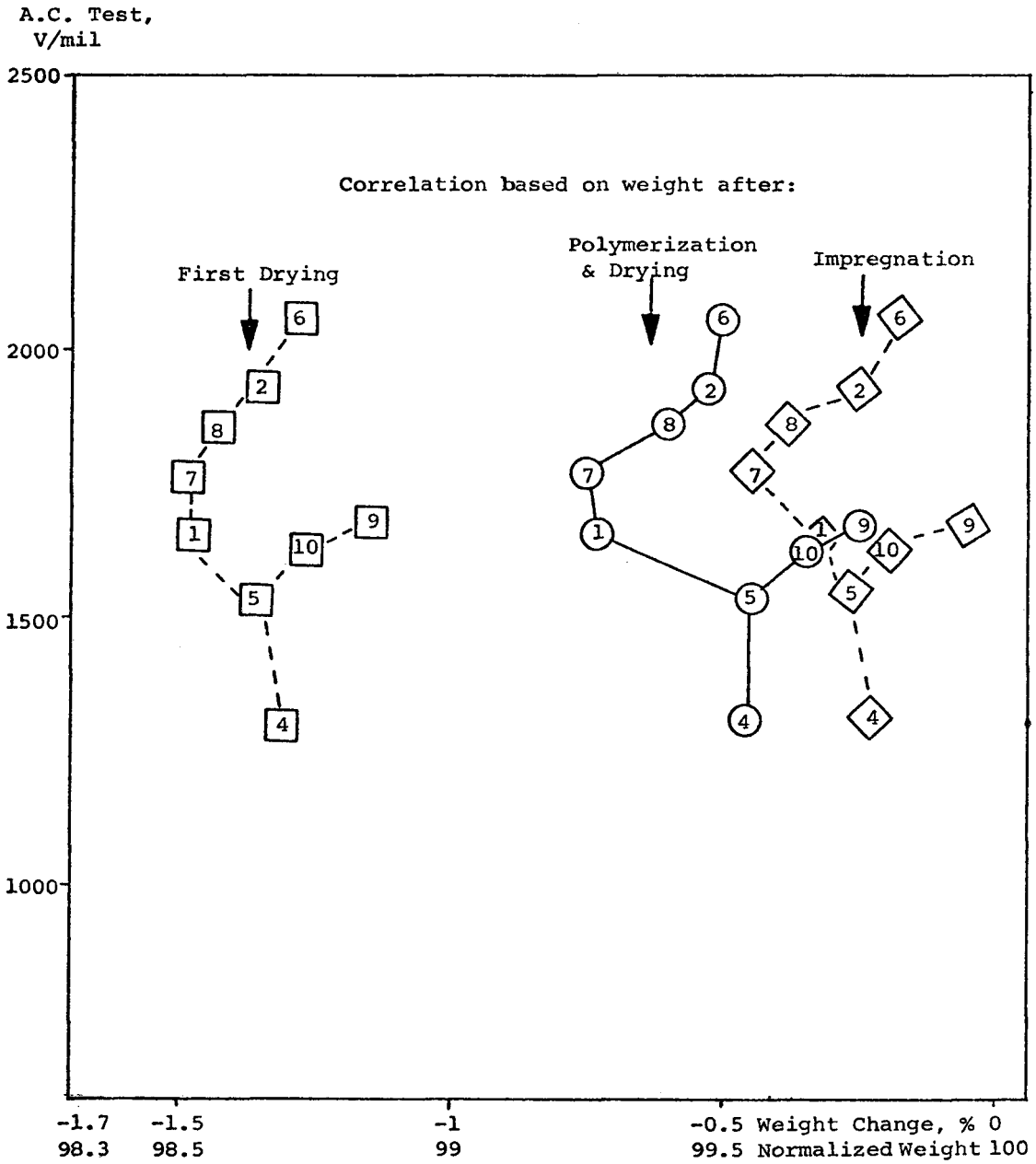

Figure 3-115. Slab Weight: AC Breakdown Strength Correlation.

Sample: Cable A slabs, 18 mil. Experiment No. 13.

gain insight into a complex process, some thoughts were generated in search of an explanation.

It is suggested that polyethylene is highly susceptible to decomposition by radiation. The following gives a scheme of reactions that might be occurring during this process:

$$\underset{\text{Polyethylene, PE}}{\sim CH_2 - CH_2 - CH_2 - CH_2\sim} \longrightarrow \underset{\text{PE Radical, PE}^\bullet}{\sim CH_2 - \overset{\bullet}{C}H - CH_2 - CH_2\sim} + \underset{\text{+ Hydrogen}}{\tfrac{1}{2} H_2}$$

$$\underset{\text{PE}}{\sim CH_2 - CH_2 - CH_2 - CH_2\sim} \longrightarrow \underset{\text{Vinyl Radical + Hydrogen}}{2 \sim CH = \overset{\bullet}{C}H} + H_2$$

$$\underset{\text{PE}^\bullet}{\sim CH_2 - \overset{\bullet}{C}H - CH_2 - CH_2\sim} \longrightarrow \underset{\text{Unsaturated PE + Hydrogen}}{\sim CH_2 - CH = CH - CH_2\sim} + \tfrac{1}{2} H_2$$

Thus, hydrogen is a major product in this reaction which escapes during polymerization and subsequent drying. Hence, it is possible that a number of microvoids are created in this process, although some or all of the original ones are filled up.

In a controlled set of experiments, 20 slabs from cable A were vacuum dried, impregnated with LMA and polymerized. Sets of ten slabs were broken down at 1 hour and in 24 hour step up times. The Weibull plots are given in Figure 3-116 and compared to the vacuum dried control, which is presented in Figure 3-30, and to the untreated control in Figures 3-1 and 3-2.

In the 1 hour test, the breakdown strength at 2300 V/mil is 50% higher than that for the vacuum dried sample, 1530 V/mil and 16% higher than the virgin control at 1980 V/mil. The improvement in the 24 hour step-up results, 1480 versus 1325 and 1260 V/mil amounts to 12 and 17% compared to the vacuum dried control, and virgin control respectively. The effect of electrical aging was examined by plotting the AC breakdown strength against step time in Figure 3-117 along with that for the controls. It is evident that impregnation and polymerization of lauryl methacrylate is beneficial both for the breakdown strength and for the stress-time relationship when compared to the virgin control. The effect on the breakdown strength is even larger in comparison with the vacuum dried control and this finding is confirmed in the same Figure.

In Experiment No. 20A, a mixture of lauryl methacrylate (70%), styrene (10%) and ethylene glycol dimethacrylate (20%) was used for impregnation and polymerization. The dielectric strength, approximately 1650 V/mil is comparable to that of the lauryl methacrylate impregnated samples.

In Experiment No. 57, a 6 inch long piece of cable A was used. The semiconducting shields were removed. The samples were used for im-

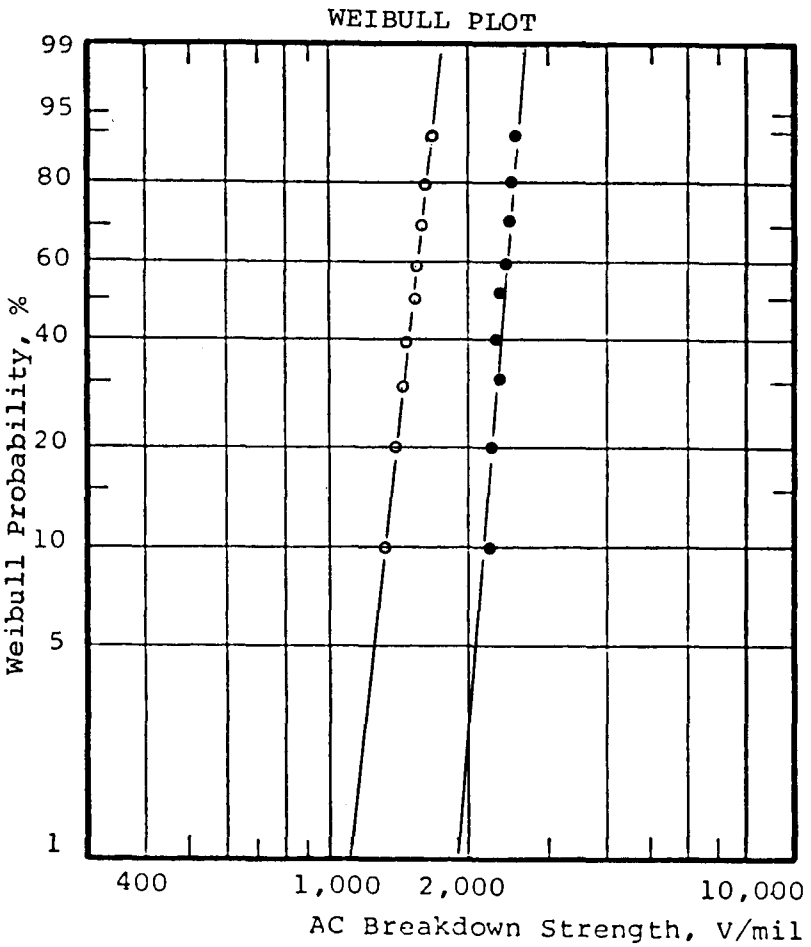

Figure 3-116. Effect of Polymerized LMA. Cable A, 18 mil slabs. Experiment No. 44. (o) 24 hour step test. (•) 1 hour step test.

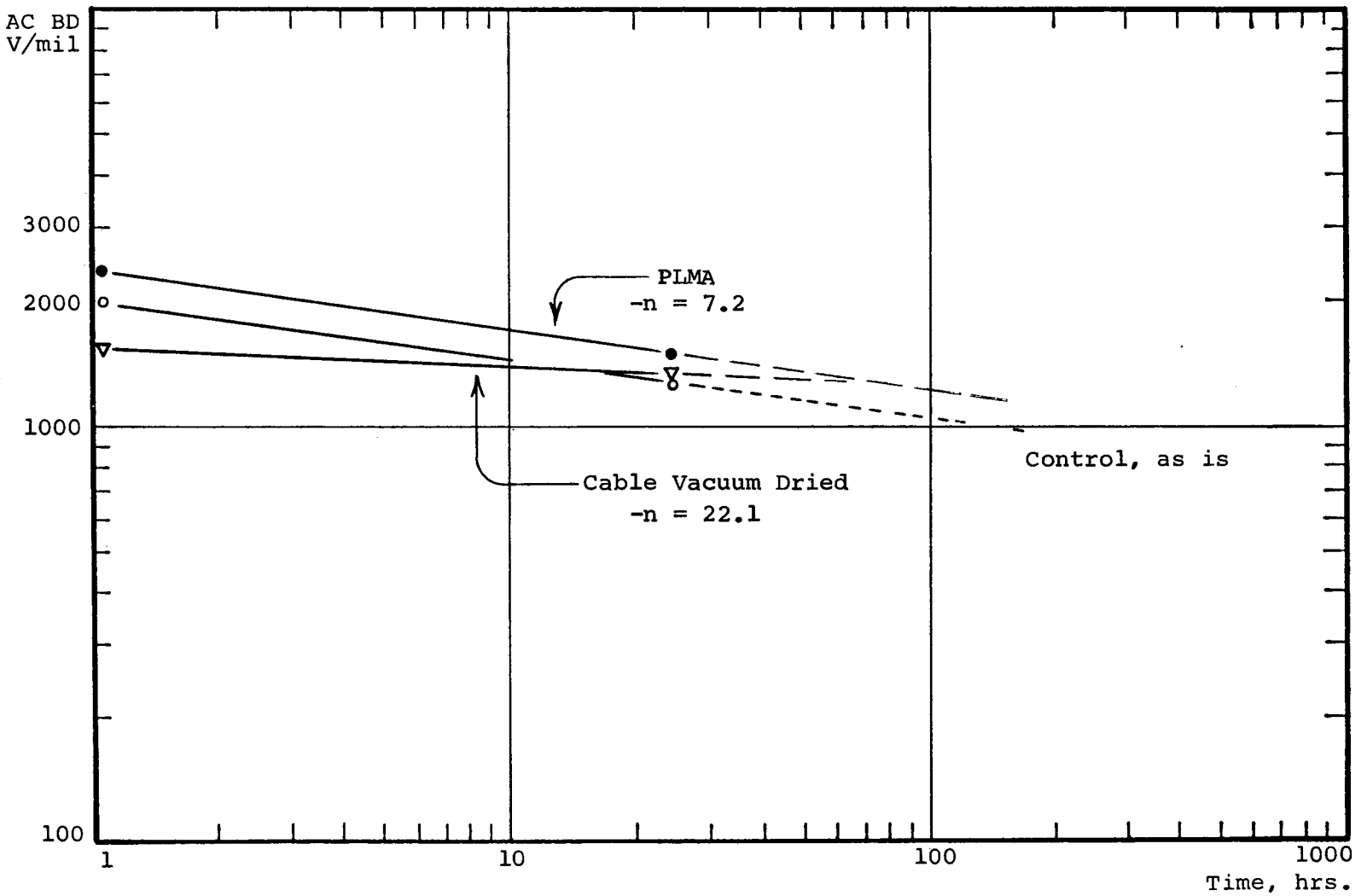

Figure 3-117. Effect of Polymerized LMA on AC Breakdown Strength.

Sample: Cable A slab, 18 mil.

pregnation and polymerization with vinyl toluene. After the removal of excess monomer by vacuum drying, four slabs were cut, ditched and used for breakdown tests. The V_{50} value, 2750 V/mil is about 80% higher than the vacuum dried control and 38% higher than the virgin control (Figure 3-118). This preliminary experiment demonstrates the importance of the chemical nature of the impregnant and the practicality of impregnating and polymerizing in a full size cable.

3.4.3.2 Experiments with Model Cables. Although the degree of polymerization in several of the vinyl toluene impregnated model cables was small, they were tested for their AC breakdown strength at one hour step-up times. The results are presented in Table 3-23. It is obvious that polymerized vinyl toluene increases the dielectric strength quite significantly.

Table 3-23

EFFECT OF POLYVINYL TOLUENE ON AC BREAKDOWN STRENGTH

Exp. No.	Cable Type and History	Normal Weight	AC BD Strength, V_{50} V/mil	Rel. %	Rel. %
173	E, Vacuum Dried	99.7	1054	100	
142	E, Control	100	1218	116	100
169	E, Impregnated and Polymerized	100.4	1192	113	98
104	C, Control	100	1084	100	
171	C, Heat Treated	99.4	1165	107	100
193	C, Impregnated and Polymerized	101.3	1402	129	120
16	A, Vacuum Dried (Slab)	98.9	1530	100	
2	A, Control	100	1980	129	100
57	A, Impregnated and Polymerized	102.7	2750	180	139

In Experiment No. 169 a weight increase of 0.66% resulted in 13% increase in the AC breakdown strength compared to the vacuum dried control (No. 173) and matched the performance of the untreated control, Experiment No. 142. In other words, the polymerized impregnant com-

WEIBULL PLOTS

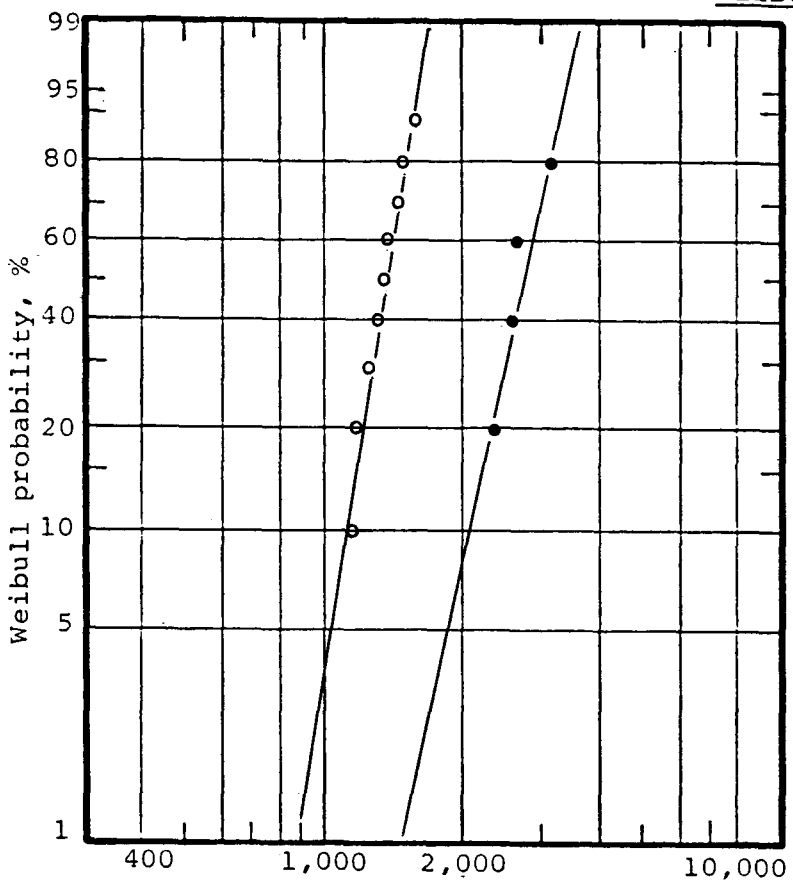

Figure 3-118. Effect of Polymerized VT.
Cable A, 18 mil slabs, 1 hour step test.
(o) Control, vacuum dried. Experiment No. 16.
(•) Contains 2.7% PVT. Experiment No. 57.

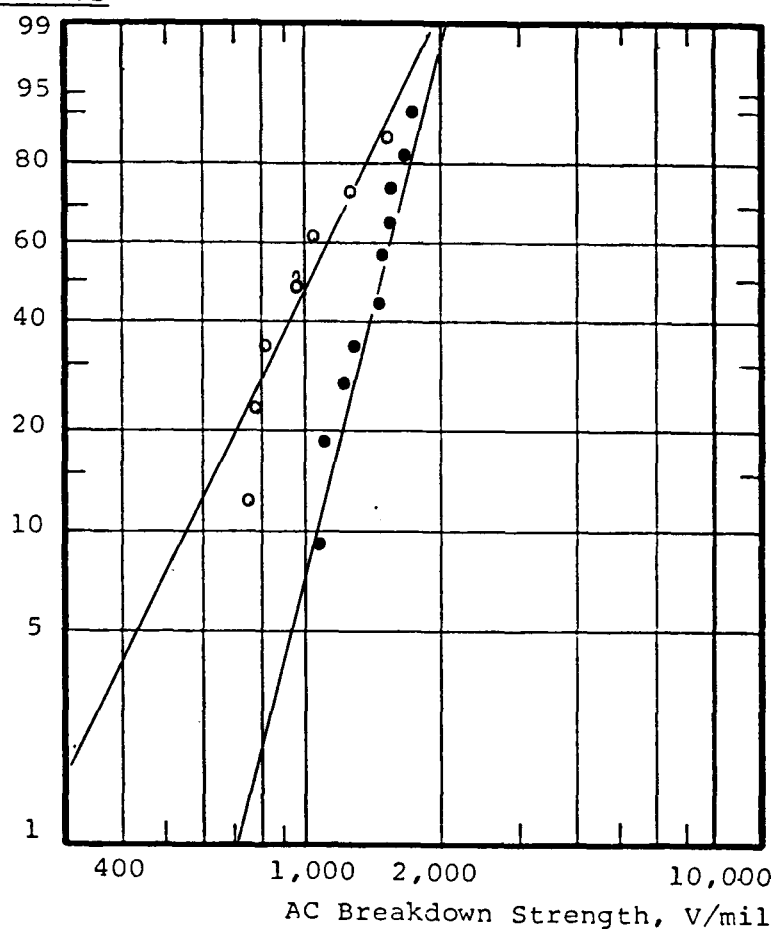

Figure 3-119. Effect of Polymerized VT.
Model Cable C, 1 hour step test.
(o) Control. Experiment No. 104.
(•) Contains 1. % PVT. Experiment No. 171.

pensated for the loss in breakdown strength attributed to the elimination of acetophenone. At 1.9% weight increase (Experiment No. 193) the breakdown strength rose 29% over the untreated control (No. 104) or 20% over the control subjected to identical heat treatment, Experiment No. 171.

The impregnation of a section of a full size 138 kV cable with vinyl toluene followed by in situ polymerization is described on page 3-144. This sample, Experiment No. 57, at 2.7% weight gain was tested in slab form and gave 39% higher V_{50} value than the untreated control, Experiment No. 2. The data suggests a gradual increase in the AC breakdown strength with increasing impregnant concentration. In Figure 3-120 the increase in AC breakdown strength is plotted against impregnant concentration for model cables. The data implies linear correlation up to 5.5% impregnant level, which is valid for monomer impregnated model cables, for those with polymerized vinyl toluene and for the full size cable. These values show that on an equal concentration basis vinyl toluene and its polymer are more efficient than lauryl methacrylate or its polymer. The difference is attributed to the voltage stabilizing effect of the aromatic structure (38).

3.4.4 Microscopy

3.4.4.1 Optical Microscopy. Optical micrographs of slabs containing polymerized lauryl methacrylate are presented in Figures 3-121 to 3-124 and the observations summarized in Table 3-24. Compared to the controls, Figures 3-10, 3-11, 3-37 and 3-38, a gradual decrease in the relative number and size of voids is observed with an increasing impregnation level. This is attributed to partial filling of the voids with the in situ formed polymer. No attempt was made to quantitatively determine the change in void volume, and the micrographs show that the voids were not completely eliminated at the impregnation levels achieved.

It may further be noted that whereas the voids in the virgin and vacuum dried samples are spherical or ellipsoid, several voids in the polymerized lauryl methacrylate containing samples are irregular. It is suggested that polymerization in the void may be associated with a certain amount of shrinkage. Thus, methyl methacrylate shows 21% shrinkage when polymerized in bulk. Although lauryl methacrylate probably shrinks less, it could be enough for the polymer to detach itself from the walls and collect at the center. It was demonstrated experimentally that polylauryl methacrylate takes up dye in the same way as the walls of the void. Hence, the irregularly shaped spots may be blobs of polylauryl methacrylate. Alternatively, the polylauryl methacrylate may be grafted to the wall of the void and as it shrinks, it may leave small irregular voids in the center.

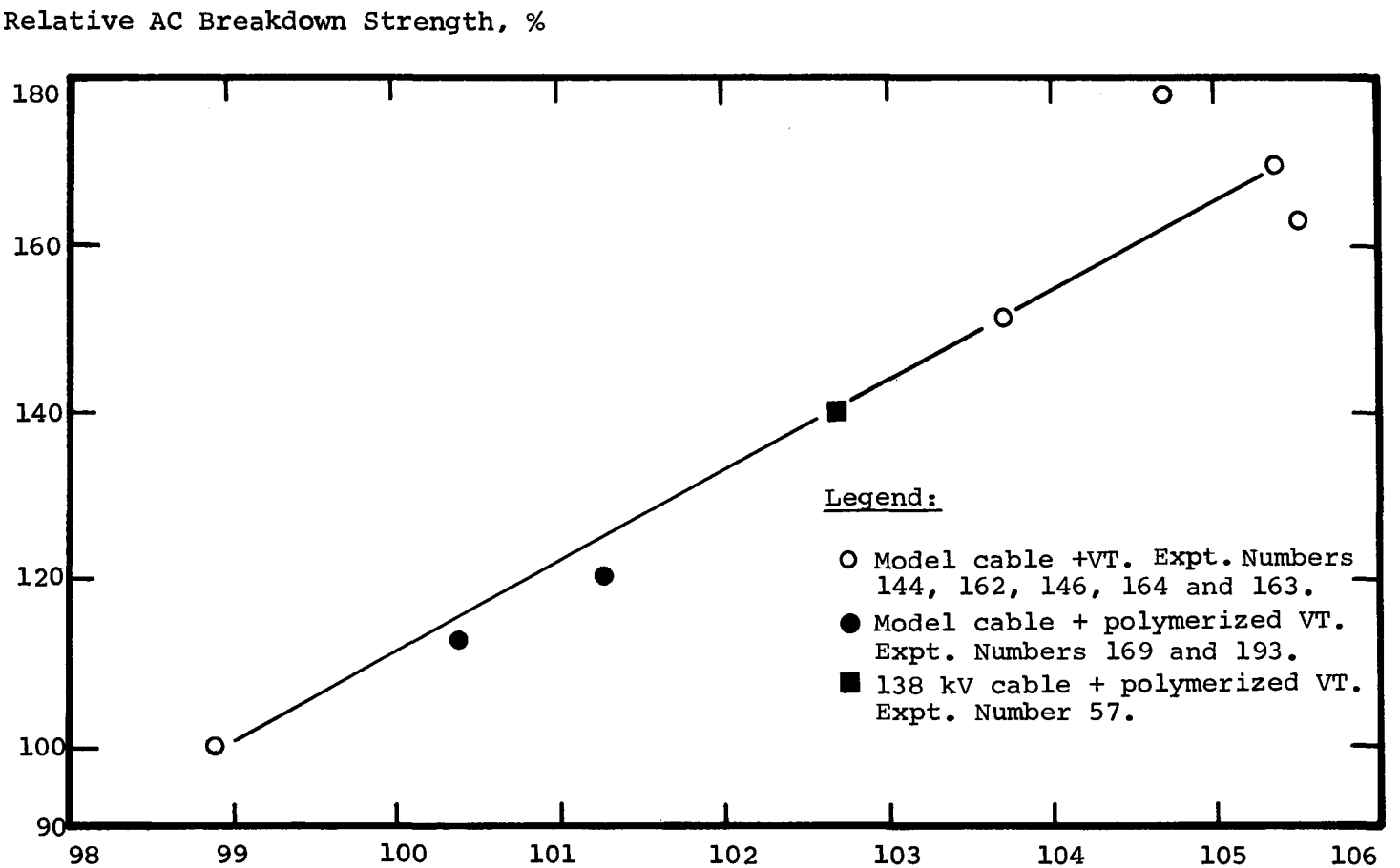

Figure 3-120. Effect of Vinyl Toluene and Polymerized Vinyl Toluene.

Samples: Cable E (O,●) and Cable A slab (■). One hour step test.

Section 4

EXPERIMENTAL DETAILS

4.1 MATERIALS

4.1.1 Test Samples

Crosslinked polyethylene (XLPE) specimens were used for impregnation and polymerization studies and for electrical property measurements. Three major configurations were considered:

1. Wafers and slabs cut from actual 138 kV cables.
2. Molded slabs.
3. Model cables.

The advantages and disadvantages of each configuration are summarized in Table 4-1. Since configurations 2 and 3 were unlikely to match the size and distribution of voids in 138 kV cables, configuration 1. was used in the majority of experiments.

The wafers and slabs were machined from 138 kV cables manufactured by Phelps Dodge Cable and Wire Co. using HFDB 4201 crosslinkable polyethylene compound supplied by Union Carbide Corporation. Cable "A" made in 1975 had 1750 KCMIL stranded aluminum conductor, 25 mil of semiconducting strand shield and 800 mil insulation. A second cable (Cable "B") particularly used in the screening experiments with liquids, had 1000 KCMIL stranded aluminum conductor, 25 mil semiconducting strand shield and 750 mil insulation. The wafers were lathe cut at about 20 mil thickness.

Full size slab specimens, approximately 2.75 x 1.5 x 0.4 inch in size were machine cut and "ditched" carefully for dielectric strength measurement. Half and quarter size slabs from the same insulation were used for measuring rates of impregnation and polymerization. The shape and geometry of the slabs are presented in Figure 4-1, and the scanning electron micrographs of the machined surfaces in Figures 3-21 and 3-22.

Model cables were constructed with 14 AWG solid copper conductor, 15 mil strand shield (HFDA 0580 from Union Carbide Corporation) and 25 mil insulation (HFDE 4201 also from Union Carbide Corporation).

Table 4-1

COMPARISON OF SPECIMEN CONFIGURATIONS FOR AC BD TEST

Sample Form	Advantage	Disadvantage
(A) Slab/Machine - cut out from 138 kV full-size cable - make cavity at center of slab by machine	1. These specimens have micro-structure identical to the actual cable insulation. 2. It should be possible to eliminate all external effects, such as edge effect, for the breakdown test. 3. The grafting and testing equipment are smaller.	1. It is relatively difficult to make a cavity with a good smooth surface. 2. It is not possible to make larger specimens. 3. It is not suitable for the study of additives.
(B) Molded Specimen - make a molded sample, similar to (A) - cut the bottom part of specimen to get the good surface on bottom and appropriate insulation wall thickness.	1. The size of specimen can be varied. 2. It should be possible to eliminate all external effects, such as edge effect, for the breakdown test. 3. The grafting and testing equipment are smaller. 4. It is suitable to study additives.	1. It may not have the same micro-strncture as actual cable insulation.
(C) Model Cable	1. It is easy to do the various kinds of electrical tests. 2. It is easy to make the sample. 3. The test procedure is simple. 4. It is suitable to study additives.	1. It may not have same micro-structure as actual cable insulation. 2. There may be edge effects during the breakdown tests.

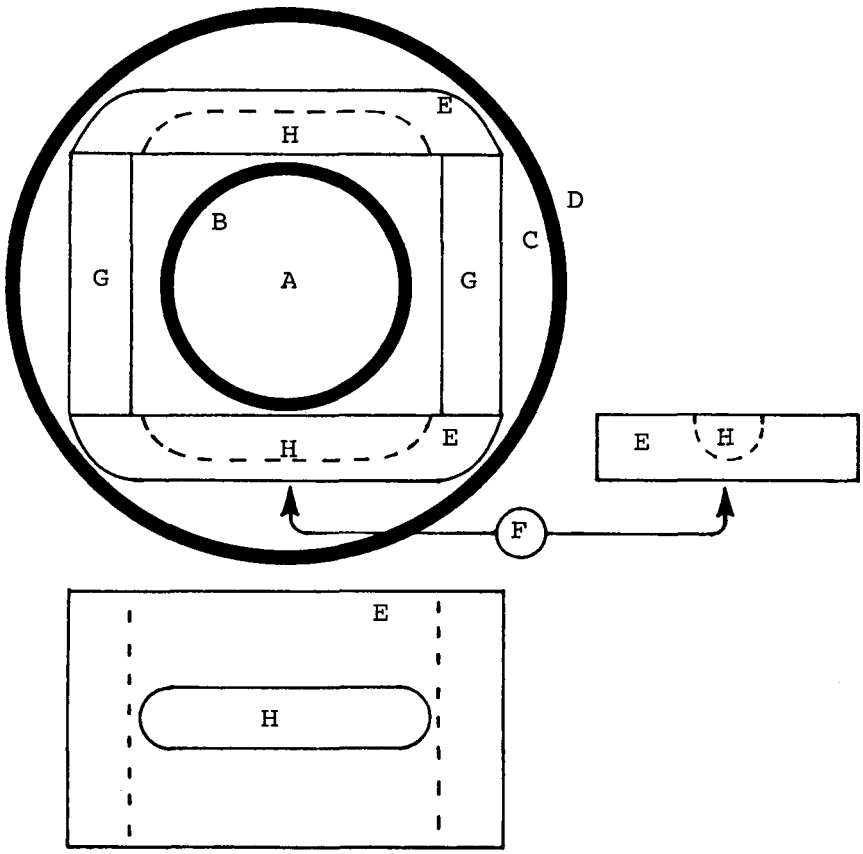

Legend:

A. Conductor
B. Conductor shield
C. Insulation
D. Insulation shield
E. Full size slabs
F. Minimum thickness at "ditch" bottom, 13 or 18 mil
G. Half size slabs
H. "Ditch"

Figure 4-1. Schematic View of 138 kV Cable and Slabs.

Those designated as Cables "C, D, E or F" were made by Cyprus Wire and Cable Company, Rome, N. Y., and Cable "G" by Phelps Dodge Cable and Wire Company, Yonkers, N. Y. They were treated as follows:

Cable C: Steam cured in a continuous process in a steam tube adjacent to the crosshead.

Cable D: Cooled to room temperature after extrusion-uncured.

Cable E: Same as Cable D, but then steam cured in a continuous process.

Cable F: Same as Cable D but then steam cured in a flash vulcanizer.

Cable G: Extruded at PDC&W Co., cooled, then steam cured in a flash vulcanizer.

Some of the impregnation experiments were carried out with model cables containing no conductor shield (Cable H). They were made by Phelps Dodge Cable and Wire Company in 1975 with 14 AWG tinned copper conductor, 30 mil HFDB 4201 insulation and crosslinked in a continuous process.

Cable J is a 110 kV cable manufactured by a cable company employing a steam free curing process and water cooling.

4.1.2 Impregnants

A number of organic liquids, mostly monomers were used for impregnation. Table 4-2 lists these liquids, their chemical structure, source and purity.

4.1.3 Catalysts

A number of peroxide and azo catalysts have been used to initiate polymerization of the monomers. They are listed in Table 4-3 along with their chemical structure, properties and sources. Most of the peroxides and azonitriles were supplied by Lucidol, except Vazo (azobisisobutyronitrile) which was provided by DuPont. All catalysts were used as received without any attempt to purify them. They were stored in a refrigerator to minimize deterioration.

4.1.4 Miscellaneous Materials

A number of solvents such as acetone, methylethyl ketone, benzene,

Table 4-2

IMPREGNANTS

Impregnants	Chemical Structure	Source	Purity Grade % Assay
Triethylene glycol	$(CH_2O\text{-}CH_2\text{-}CH_2OH)_2$	Kem Chemical	R
p-Xylene	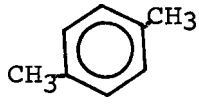	Mallinckrodt	AR
Ethyl alcohol	$CH_3\text{-}CH_2OH$	"	AR
Paraffin Oil	$CH_3\text{-}(CH_2)_n\text{-}CH_3$	"	Medical Grade
Polyethylene Wax (AC Polyethylene 1706)	$CH_3\text{-}(CH_2)_m\text{-}CH_3$	Allied Chem.	
Anisole	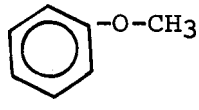	Pfalz & Bauer	R
Octanone	$CH_3\text{-}(CH_2)_5\text{-}CO\text{-}CH_3$	"	R
Cumyl alcohol	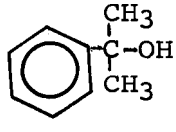	"	AR
Benzophenone	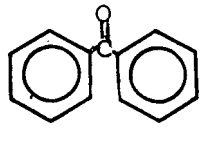	Eastman	R

(Continued)

Table 4-2 (Continued)

IMPREGNANTS

Impregnants	Chemical Structure	Source	Purity Grade % Assay	Inhibitor ppm
Ethyl benzene	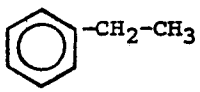	MC&B	R	-
Naphthalene	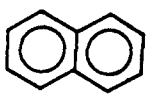	Commercial, Purified by Sublimation		-
Toluene	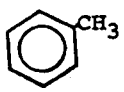	Mallinckrodt	AR	-
Acetophenone	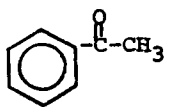	"	AR	-
Monomers				
Lauryl methacrylate	$CH_2=C(CH_3)-CO-OC_{12}H_{25}$	Rohm & Haas	97.5	100 ppm
N-butyl methacrylate	$CH_2=C(CH_3)-CO-O-C_4H_9$	"	98.5	10 ppm
Isobutyl methacrylate	$CH_2=C(CH_3)-CO-OCH_2-CH(CH_3)_2$	"	97.5	10 ppm
Ethyl hexyl methacrylate	$CH_2=C(CH_3)-COOC_8H_{17}$	DuPont	-	-
Styrene	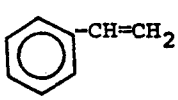	Dow Chemical	-	50 ppm

(Continued)

Table 4-2 (Continued)

IMPREGNANTS

Impregnants	Chemical Structure	Source	Purity Grade % Assay	Inhibitors ppm
Monomers				
Vinyl toluene	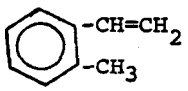	Dow Chemical	-	12 ppm
Vinyl pyrollidone	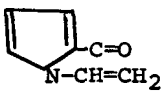	G. A. F.	-	-
Vinyl acetate	$CH_2=CH-O-COCH_3$	Pfalz & Bauer	-	-
2 Phenyl ethyl acrylate	$CH_2=CH-CO-O-CH_2-CH_2-C_6H_5$	Haven Chem.	-	-
Vinyl ethyl ketone	$CH_2=CH-CO-C_2H_5$	"	-	-
Dodecyl vinyl ether	$CH_2=CH-O-C_{12}H_{25}$	G. A. F.	-	-
Diallyl phthalate	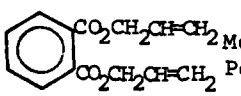	Monomer Polymer Lab	-	-
Vinyl Silane	$CH_2=CH-O-Si-(O-CH_3)_3$	Dow Corning	-	-
Styrene. Oxide	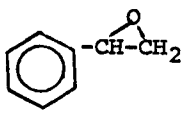	Pfalz & Bauer	-	-
Divinyl benzene	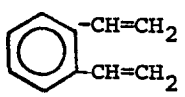	Dow Chemical	-	-

Table 4-3

POLYMERIZATION CATALYSTS

Peroxide		Composition	M. P. °C	Half Life Temp. °C 10 Hr.	1 Hr.
Benzoyl peroxide	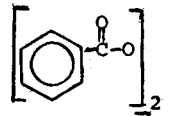	98%	32	73	91
Lauryl peroxide	$[CH_3-(CH_2)_{10}-CO]_2$	98%	130	62	80
Dicumyl peroxide	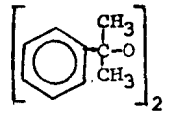	99%	86-100	123	143
Cumene hydroperoxide	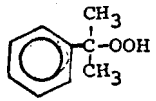	78%	--	158	190
Acetyl peroxide	$CH_3CO.O-O.COCH_3$	23-25	17	69	87
2.4 Dichlorobenzoyl peroxide	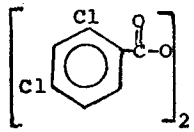	50	-30	54	73
2.5 Dimethyl 2,5 Bis (t Butyl peroxy) hexane	$(CH_3)_3-C.O_2-C(CH_3)_2-(CH_2)_2-C(CH_3)_2-O_2.C.(CH_3)_3$	66-70	101	154	186
Decanoyl peroxide	$CH_3(CH_2)_8-CO.O_2-CO(CH_2)_8CH_3$	98.5	104	61	80
Azo Compounds					
Azobis isobutyronitrile	$NC(CH_3)_2C.N=N.C(CH_3)_2CN$				
2t-Butyl azo cyanobutane	$(CH_3)_3CN=NC.CH_3C_2H_5CN$	-25°C	82	104	--
2t-Butyl azo cyanopropane	$(CH_3)_3C-N=NC.(CH_3)_2CN$	17°C	79	97	--

toluene, xylene, chloroform, methanol, isopropanol, n-hexane, petroleum ether, etc. were used in the course of the experiments. They were all reagent grade chemicals and were obtained from commercial sources such as Kem Chemicals, Pfalz and Bauer and V. W. Scientific Co.

Hydroquinone from Baker Chemical Co. was used as polymerization inhibitor.

Inorganic chemicals such as sodium chloride, sodium hydroxide, potassium iodide, lead oxide as well as methylene blue were obtained from Scientific Glass Apparatus Co.

Insulating oils used in the breakdown tests are listed below:

Oil	Grade	Source
Insulating Oil	Sun #6	Sun Oil Co.
Insulating Oil	Sun XX	Sun Oil Co.
Synthetic Oil	P. D. #9	Elk Refineries
Silicone Fluid	S. F. #200 (100 cps)	Dow Corning

Conducting silver paint (Choband 4900) was procured from Chomenics Co. of Woodburn, Massachusetts.

4.2 EQUIPMENT

4.2.1 Reaction Chambers

Glass and metal reaction chambers were used to treat the slabs and model cables in a series of operations such as:

- vacuum drying
- impregnation with liquids
- polymerization
- post polymerization drying

They ranged from 500 to 3000 ml in volume, were equipped with one large opening for specimen insertion, with a number of ports for vacuum pump, vacuum gauge, thermometer, liquid inlet and outlet, vent and pressure control attachments. Constant temperature was maintained either by using a heating tape controlled by a thermocouple and relay or by immersing the chamber in a controlled temperature

water bath.

The glass chambers were standard laboratory resin kettles such as Fisher Scientific Co. #11-847. Metal chambers were custom-made in our own machine shop from aluminum or stainless steel pipes of 5 to 8" diameter. One chamber was constructed from a cylindrical sight glass with stainless steel lid and bottom. A typical impregnation-polymerization set-up is presented in Figure 4-2.

4.2.2 Auxiliary Equipment

Standard laboratory equipment for material handling and sample treatment included:

- Vacuum ovens (Blue M)
- Air circulating ovens (Blue M)
- Vacuum pump, Duoseal (R.1400, Welch Scientific Co. Model R-1400)
- Diffusion pump (oil) Duoseal, Welch Scientific Co.
- Rotary evaporator, Fisher Scientific Co., Model No. 9-548-150
- Shaker (Blue M)
- Analytical balance (Sartorius Selecta)
- Constant temperature water baths (Blue M)
- Accumulator

4.2.3 Microscopic Equipment

Scanning Electron Microscope, Model Number MRS-22-2140.

Coater for gold coating SEM speciments, FILM-VAC, Inc., Model #EMS-76.

Optical microscope, Nikon AFM.

4.2.4 A. C. Breakdown Test

The plexiglass test cell developed for A. C. Breakdown Test on slabs is presented in Figure 4-3. A circular aluminum electrode (d=2½") was fastened to the bottom through an O ring to prevent any leakage of the insulating oil. The top electrode was machined from aluminum rod (d=3/4") with well-polished surface and rounded ends to provide a uniform field and held in place through a groove in the plexiglass top. The ditched portion as well as the bottom portion below the ditch of each sample were painted with a conductive silver paint. A small amount of clean mercury in the ditch improved contact be-

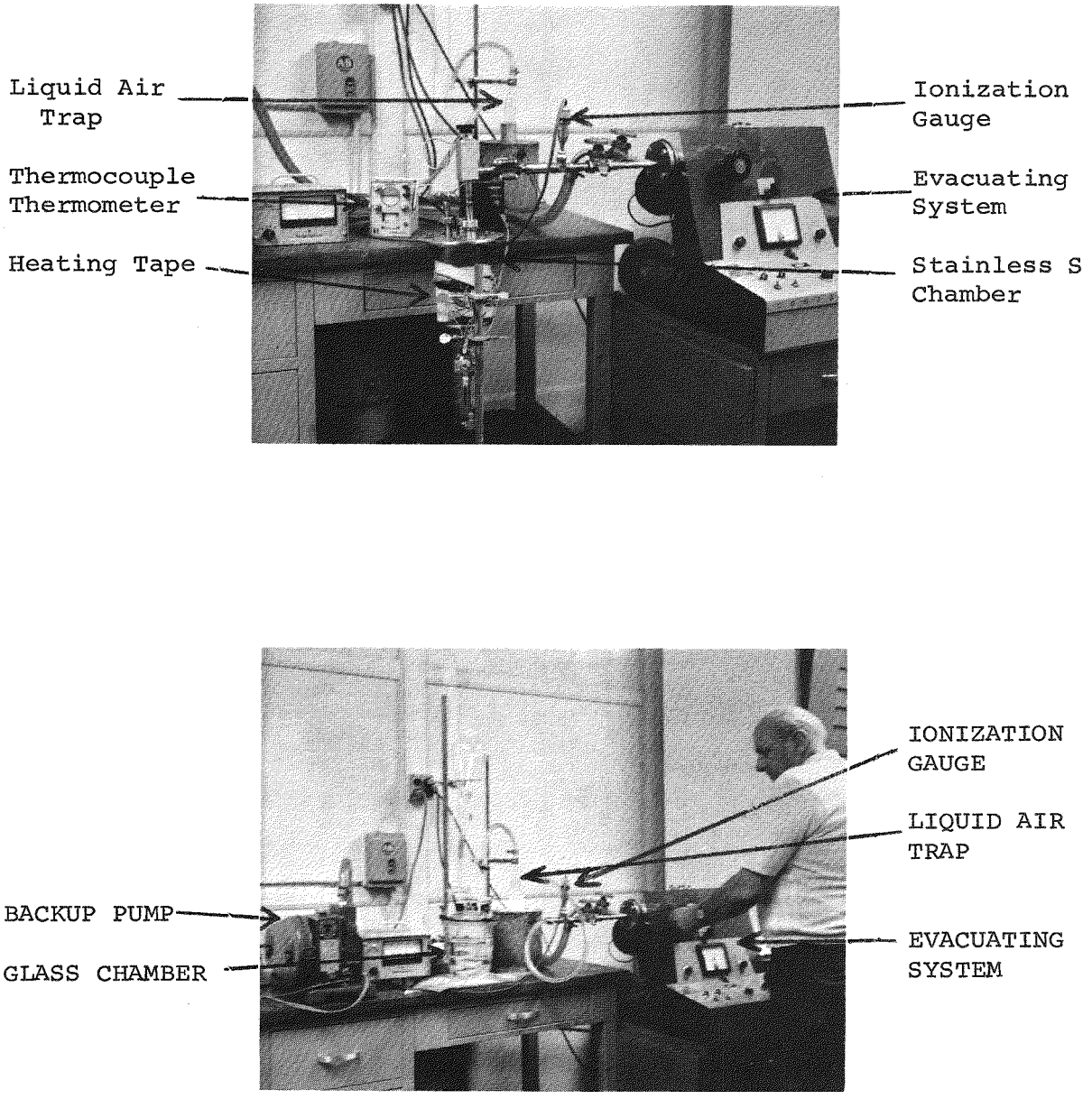

Figure 4-2. Setup for Vacuum Drying, Impregnation and Polymerization. Stainless steel chamber (top) and glass chamber (bottom).

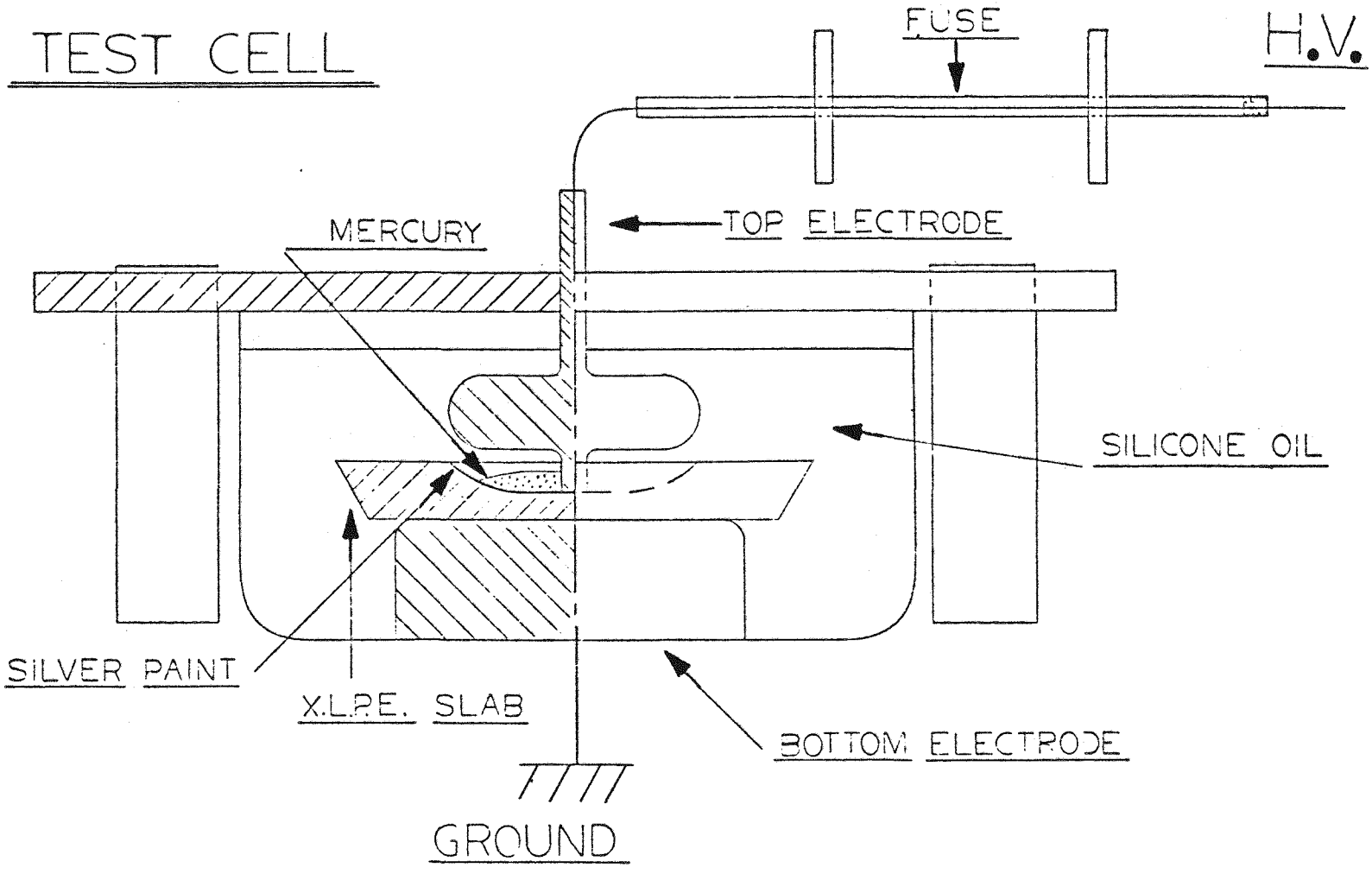

Figure 4-3. AC BD Test Cell for Slabs.

tween the silver painted insulation and the top electrode. The cell was filled with silicone oil (Dow Corning Silicone Fluid 200) to avoid flash-overs. Ten such cells were connected in parallel and to a variable high voltage source through appropriate fuses. All the electrical tests were done in a high voltage cage provided with automatic interlocks.

The model cables were tested in a glass tank, 12 x 15 x 24" in Figure 4-4. Ten samples, each approximately 3 feet in length were connected to ten clips, held by a plexiglas bar. The free ends of the samples were held in grooves made in another plexiglass strip, held parallel to the first one. These two plexiglass bars were placed approximately six inches apart over the glass tank. The latter was filled with three and a half inches of tap water and seven inches of mineral oil (Sun #6). The ground was connected to a flat copper plate at the bottom of the tank. The wires were approximately 1" above the bottom of the tank and at least 1" distance was kept between them. The stress was applied through a resistor to minimize transients.

4.3 PROCEDURES

4.3.1 Vacuum Drying

The slabs and model cables were surface cleaned with acetone and dried in an air circulating oven for 10 minutes at 70°C to evaporate residual acetone. They were individually weighed and subjected to drying in a vacuum oven or reaction chamber to constant weight. To assess the rate of removal of the volatiles, selected slabs were dried in a vacuum oven at 1500 μm pressure at 70 and 90°C for various periods, and analyzed in duplicate. Simultaneously the change in the weight of the control samples was being monitored. The analysis was carried out by taking samples from the surface as well as from the middle of the test slabs to see the role of thickness on drying. The volatiles are the decomposition products of dicumyl peroxide, namely acetophenone, cumylalcohol, and α methyl styrene, and water from the steam curing process. The analysis was done by gas chromatography using a Perkin Elmer Gas Chromatograph and an ionization detector. The results have shown that complete removal of volatiles is achieved by drying under vacuum (1500 μm) for 10 days at 70°C or for 7 days at 90°C. In the reaction chambers, higher vacuum level was achieved, and the removal of volatiles was monitored by vacuum drop tests (Figures 4-5 and 4-6). For this purpose the chamber was closed from the pumping system and the pressure rise monitored every minute for half an hour and plotted against time. The slope of the pressure versus time curve, with slabs, gives a measure of the exudation of the volatiles when compared to the "emp-

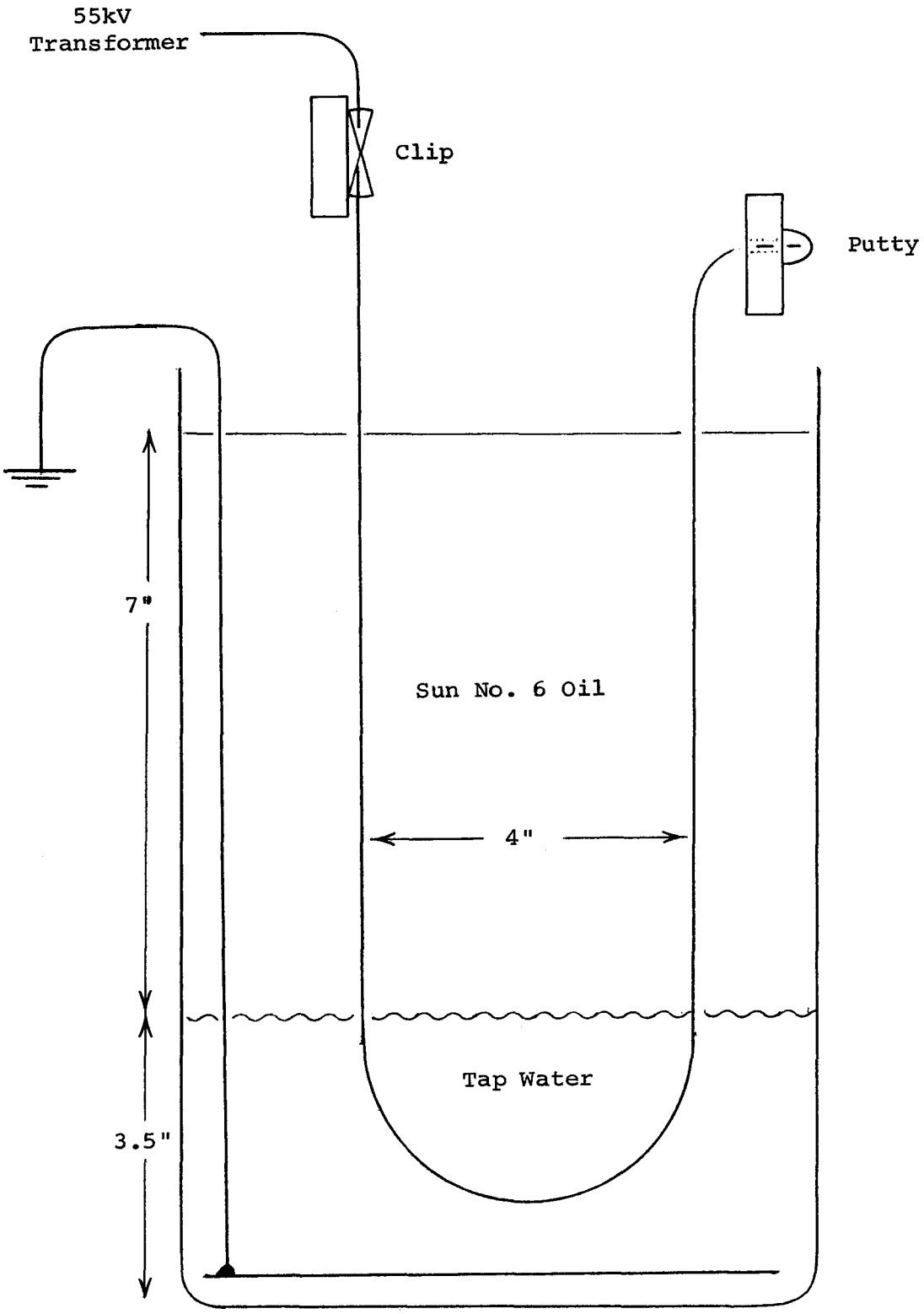

Figure 4-4. AC BD Test Setup for Model Cables.

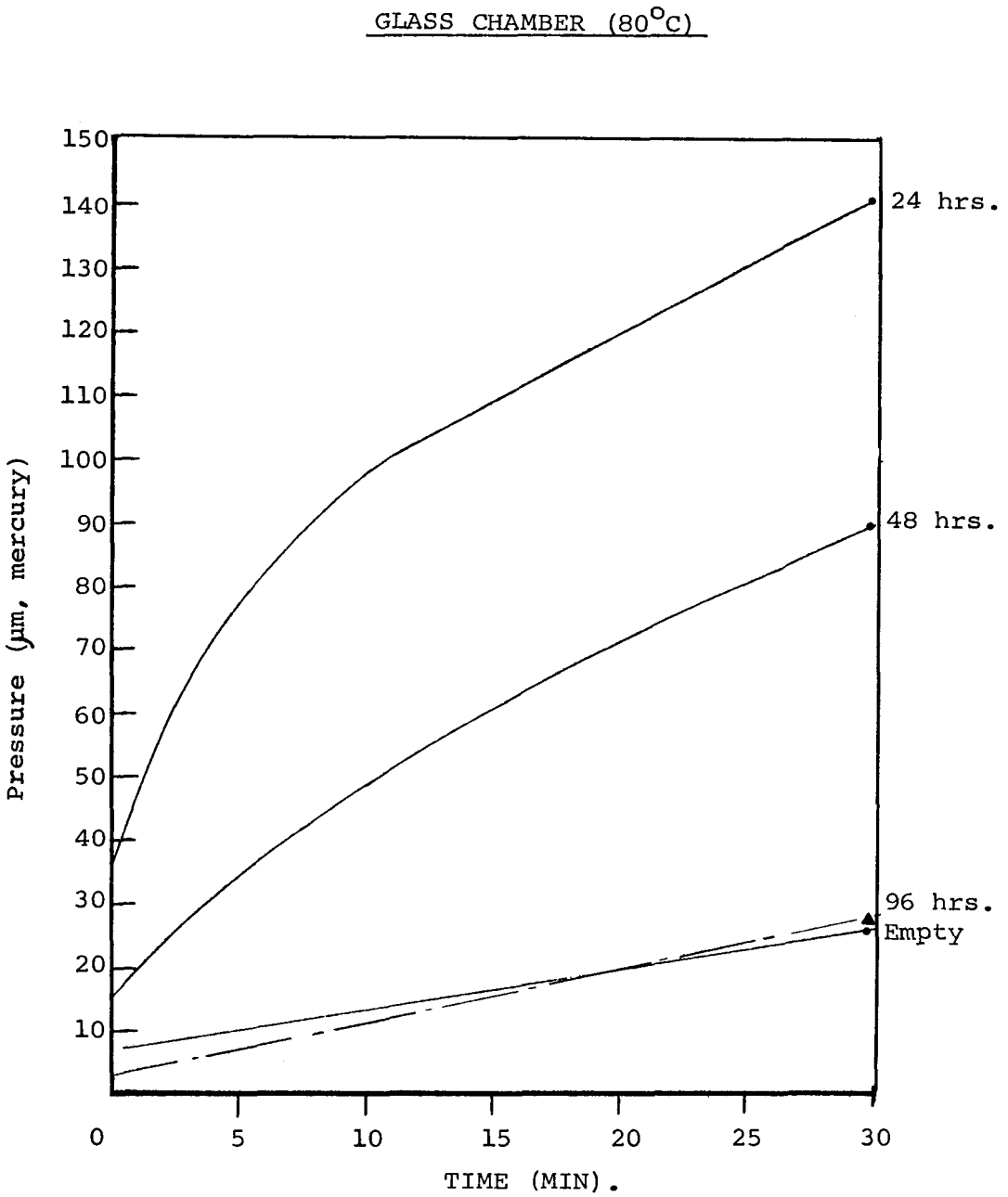

Figure 4-5. Vacuum Drop Test (Rate of Pressure Buildup).

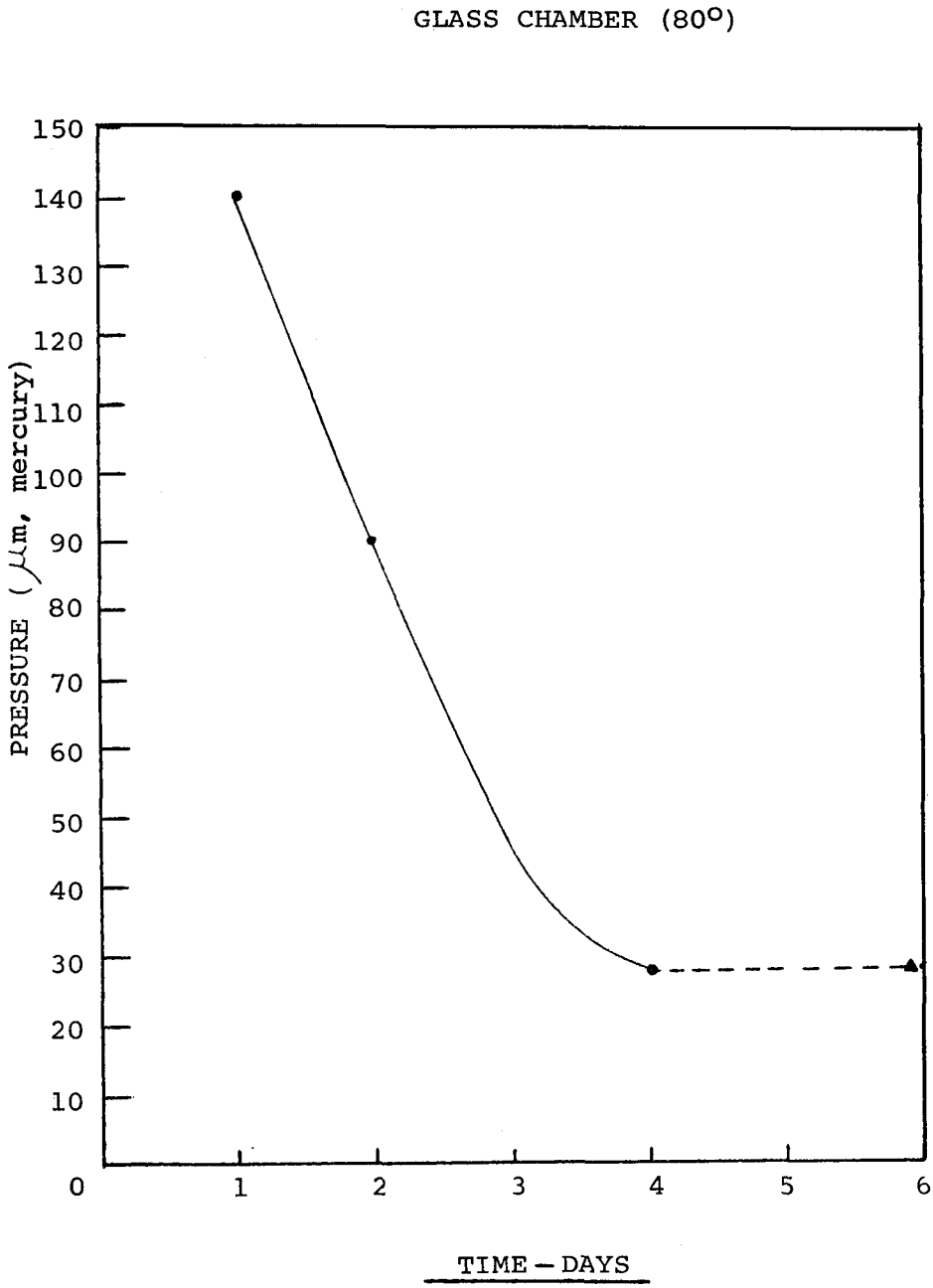

Figure 4-6. Vacuum Drop Test. Rate of Drying.

ty" curve in Figure 4-5. The final pressures after 30' taken daily are plotted against days of evacuation in Figure 4-6. The results indicated at 80°C in the glass chamber virtually complete removal of volatiles is achieved in 4 days.

4.3.2 Impregnation

The slabs and the mini-cables were impregnated either with polymerizable or with non-polymerizable liquids. In a number of experiments the impregnation with polymerizable liquids was followed by polymerization. Hence, the impregnant had to be mixed with a certain amount of polymerization catalyst. Since the catalysts decompose at a low rate even at room temperature, a small amount of hydroquinone was used to prevent premature polymerization. The shelf life of the impregnating solution was determined in test tube experiments before actual samples were impregnated. For this, monomer/catalyst solutions at different concentrations (50 to 500 ppm) were put in test tubes equipped with stopcocks. Oxygen was removed by flushing with nitrogen and the tubes were kept in constant temperature baths. Viscosity increase was monitored visually at regular intervals. The results showed that by careful adjustment of catalyst and inhibitor concentration, the autopolymerization of monomer solutions can be prevented for more than two weeks. The rate of impregnation with various monomers was determined by impregnating wafers and small slabs in closed test tubes and monitoring the weight gain as a function of time. For this, the samples were carefully wiped with Kleenex tissue paper before weighing.

In four experiments involving polymerization, the samples were impregnated while they were held under vacuum in the reaction chambers. The impregnant was degassed by evacuation and by bubbling pure nitrogen through the solution. After the vacuum source was cut off, the liquid was let in through the bottom stopcocks until the chamber was completely filled. Additional pressure, up to 100 psig, was applied in some experiments by stainless steel bellows or by a nitrogen gas operated accumulator. The time of impregnation was selected on the basis of the rate of permeation and the thickness of the sample.

The rate of impregnation with pure catalysts was studied on 16" lengths of model cables without semiconducting strand shield (Cable H). Test tubes fitted with stopcocks were used. The cable was bent into a U shape and the open ends were kept ½" above the level of the impregnant. They were taken out after appropriate time intervals, surface cleaned and weighed. Both the weight loss of the impregnant and the weight gain of insulation were monitored.

4.3.3 Polymerization

In some of the experiments the polymerization followed the impregnation without weighing the impregnated samples. In these experiments the liquid impregnant was drained from the chamber using nitrogen to flush out the liquid. Since even trace amounts of oxygen act as inhibitors in free radical polymerization, ingress of air had to be prevented. The residual impregnant was removed from the surface by brief evacuation to 500 μm followed by flushing with nitrogen and repeating this evacuation-flushing sequence five times. The in situ polymerization of the impregnant was triggered by heating the chamber to the appropriate temperature (e. g. 70 or 80°C in the case of benzoyl peroxide catalyst). High level of polymerization was achieved by holding the chamber at the selected temperature for 16 to 20 hours.

In experiments involving weighing of the samples, the impregnant was drained from the chamber. The samples were wiped with acetone wet tissue paper to remove the impregnant film from the surface. Brief drying at room temperature in air circulating oven removed the residual acetone. The samples were weighed and put back in the chamber, evacuated and flushed with nitrogen five times to remove oxygen. They were then heated to the proper temperature for polymerization.

In both procedures care was taken to prevent loss of impregnant during the polymerization process. A small quantity of the pure impregnant (containing inhibitor, but no catalyst) was placed in an open vessel inside the chamber. This assured the saturation of the nitrogen inside the chamber with monomer vapors and hindered the evaporation of impregnant from the sample.

4.3.4 Removal of Residual Monomer

To ascertain the level of filling with solid polymer, the residual monomer was removed after the completion of polymerization. The process of monomer removal was monitored by weighing the samples at regular intervals of drying at 90°C and at 1500 μm vacuum, and was continued until the weights were almost the same for two consecutive readings.

4.3.5 AC Breakdown Strength Measurement

Sets of ten slabs were tested at a time for AC breakdown strength in cells shown in Figure 4-3. At the beginning 15 kV stress was applied, then raised by 4 kV increments at the prescheduled step times either 10 minutes, 1 hour or twenty four hours. In a few experiments a one week step time was also used. The failure times and the voltage at breakdown were recorded and plotted on Weibull plots. Some breakdown tests on model cables (Figure 3-7) were carried out

at constant stress. In this case the voltage was maintained at 16, 18 or 20 kV and the time of failure was recorded.

4.3.6 Microscopic Examination

Both optical and scanning electron microscopy were carried out, with treated and non-treated samples to study the morphology and the size, number and distribution of voids.

For optical microscopy, the slab samples were first cut into thin slices and stained in a slurry containing 300 gms. of lead oxide, 300 gms. of distilled water and 9 gms. of methylene blue for 24 hours at 80°C (39). This was done in a resin kettle fitted with a condenser to maintain uniform concentration . The dyed pieces were then taken out, dried and cut with a razor blade into about 20 mil slices. The dyed specimens were observed with an optical microscope at magnifications ranging from 50 to 600x.

Scanning electron microscopy was performed on razor-cut slices as well as on slices fractured in liquid air. The slices, about 20 mil thick, were immersed in liquid air over night and fractured with pliers. The fracture surface was coated with sputtered gold under vacuum. The gold coated samples were examined by scanning electron-scope at magnification levels of 500 to 7000x.

Section 5

SUPPLEMENTARY INVESTIGATION

In addition to the main objective of the project, the elimination of voids through impregnation of the solid dielectric insulated cable, three ancilliary areas were investigated:

- Comparison of steam cured and dry cured insulations.
- Assessment of the effect of impregnation on semiconductive shields.
- Study of gas phase impregnation.

5.1 COMPARISON OF CURING PROCESSES

It seems logical that the cable with the fewest and smallest microvoids would be the easiest to heal with impregnation and subsequent polymerization or grafting. Several non-steam cure processes were developed in recent years by a variety of companies which substantially reduce the number and size of voids and claim to improve the dielectric properties of the cable. It seemed appropriate to compare these cables with the steam cured cable. For this reason samples of various dry cured cables were collected and partially characterized. The objectives of the work in this area are summarized as:

1. Characterize samples by optical microscopy and SEM.
2. Physico-chemical characterization (DSC, TGA, OIT, IR, GC).
3. Conduct economic analysis of processes.

Results on items 1 and 2 are presented in this Section, those on item 3 in Section 6.

5.1.1 Characterization of Samples by Optical Microscopy and by SEM

The optical microscopic study was carried out on spiral wafers obtained from several cable samples cured by various curing processes. These processes are referred to as SCP for the steam cured process and DP1 to DP4 for the dry cured processes. Table 5-1 shows the detailed results of this study. Figures 5-1 through 5-9 indicate the size, population and shape of voids in each cure process. The results are as follows:

- The size and population of voids were reduced remarkably by using dry cure processes, such as hot gas, long-die, and radiant cure, compared to conventional steam cure processes.

- No significant difference was observed in the size and population of voids among the dry cure processes. One significant difference in the void shape was observed in the case of DP4 process. XLPE insulation samples from DP4 exhibited many star shape voids compared with the almost spherical voids generally found in samples from the other dry cure and steam cure processes.

Limited work was done with Scanning Electron Microscopy and the results are summarized in Table 5-2. Selected micrographs on blade cut specimens (as opposed to cold fractured ones reported in Section 3) are reproduced in Figure 3-14 for the steam cure process, SCP, and in Figures 5-10 to 5-18 for the four dry cure processes, DP1 to DP4.

The comparison of the SEM data with those obtained by optical microscopy shows that the two techniques are complementary, rather than overlapping. Void frequency and distribution is more conveniently studied by optical microscopy, since it covers larger areas and more depth throughout the thickness of the specimen. The high magnification and better perspective of the scanning electromicrogram provides details of void and contamination shape and of morphological characteristics not obtainable by other techniques. As an example, the gel-like structures in the dry processed insulations of Figure 5-14 were not detected by the optical microscope.

5.1.2 Physico-Chemical Characterization

Thermo-analytical characterization of the insulations consisted of Thermogravimetrical Analysis (TGA), Differential Scanning Calorimetry (DSC) and the determination of Oxidative Induction Time (OIT). In each case a specimen was taken from the conductor side and from

Table 5-1

COMPARISON OF VOID DISTRIBUTION BY OPTICAL MICROSCOPY

CURE	STEAM	DP1	DP2	DP3	DP4
SIZE (μ)	Max. 25 Many 10-15	Max. 7 a few 2-4	Max. 8 a few 2-4	Max. 10 a few 4-5	A. Max. 10 B. Max. 8 A & B a few 2-4
RELATIVE NUMBER	Many, all sizes	A few	A few Slightly more of $< 1\mu$	a few, mostly $< 2\mu$	A few, Sample B mostly $< 2\ \mu$
SHAPE	Spherical	Spherical Some * shape near conductor	Spherical Some	Some spherical Many *	Some spherical Many *
DISTRIBUTION Inside Middle Outside	 Rel. few Many Many	Uniform	Uniform	Uniform	Rel. few, } A > B More }
MICROGRAPH presented in Figure #	3-10 5-1 5-2	5-3 5-4	3-12	5-5 5-6	5-7 5-8 5-9

OPTICAL MICROGRAPHS

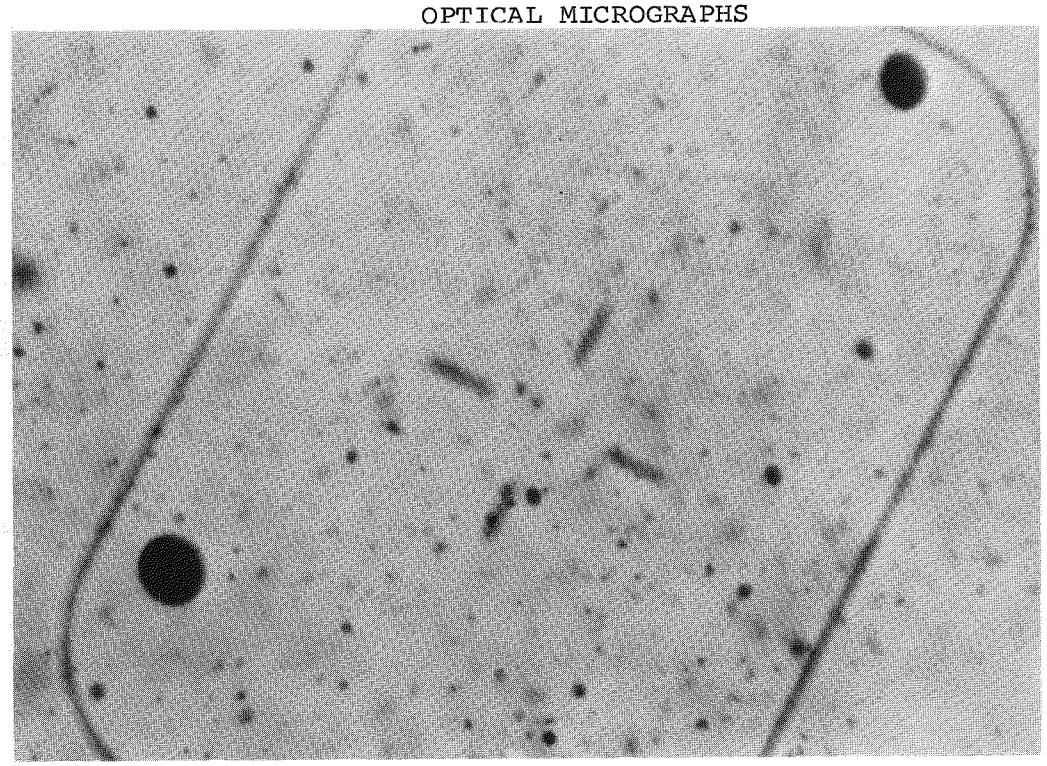

SCP 3/4 WALL FROM CONDUCTOR

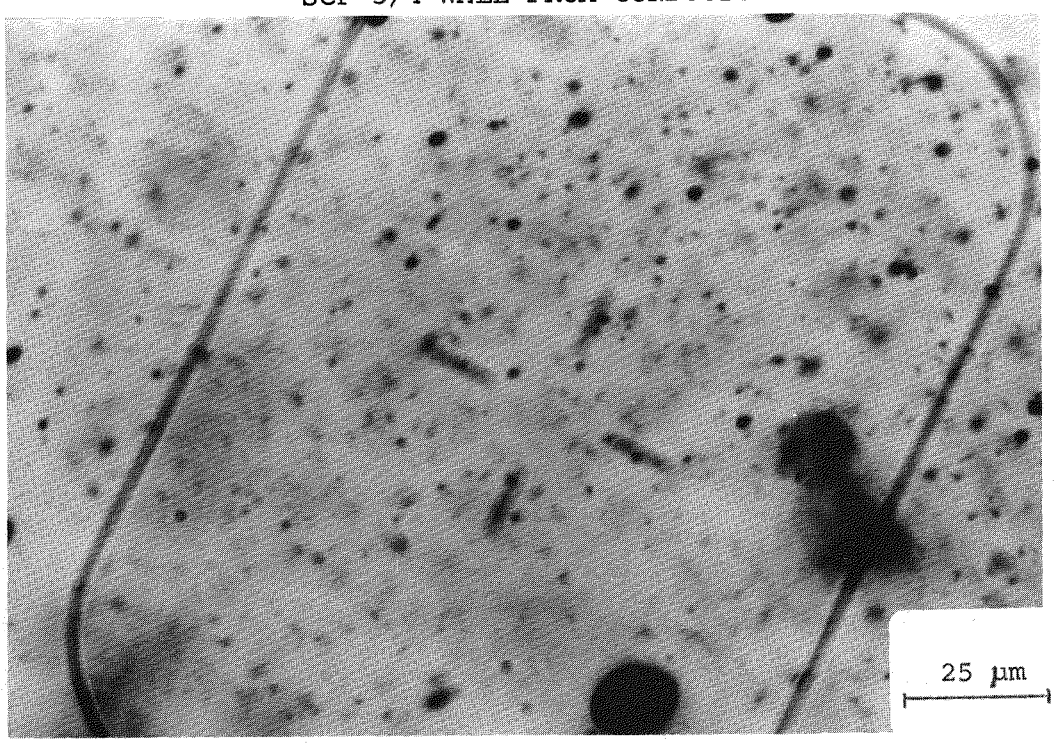

SCP AT INSULATION SURFACE

Figures 5-1 and 5-2. Voids in Steam Cured XLPE.

OPTICAL MICROGRAPHS

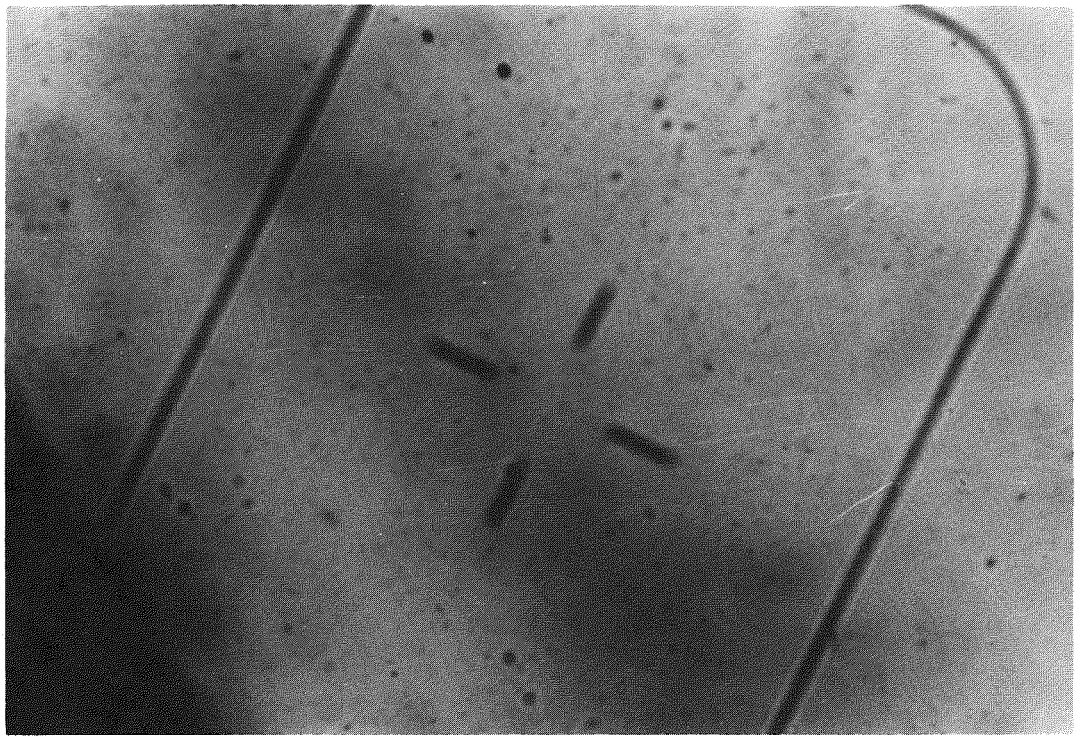

DP1 AT CONDUCTOR

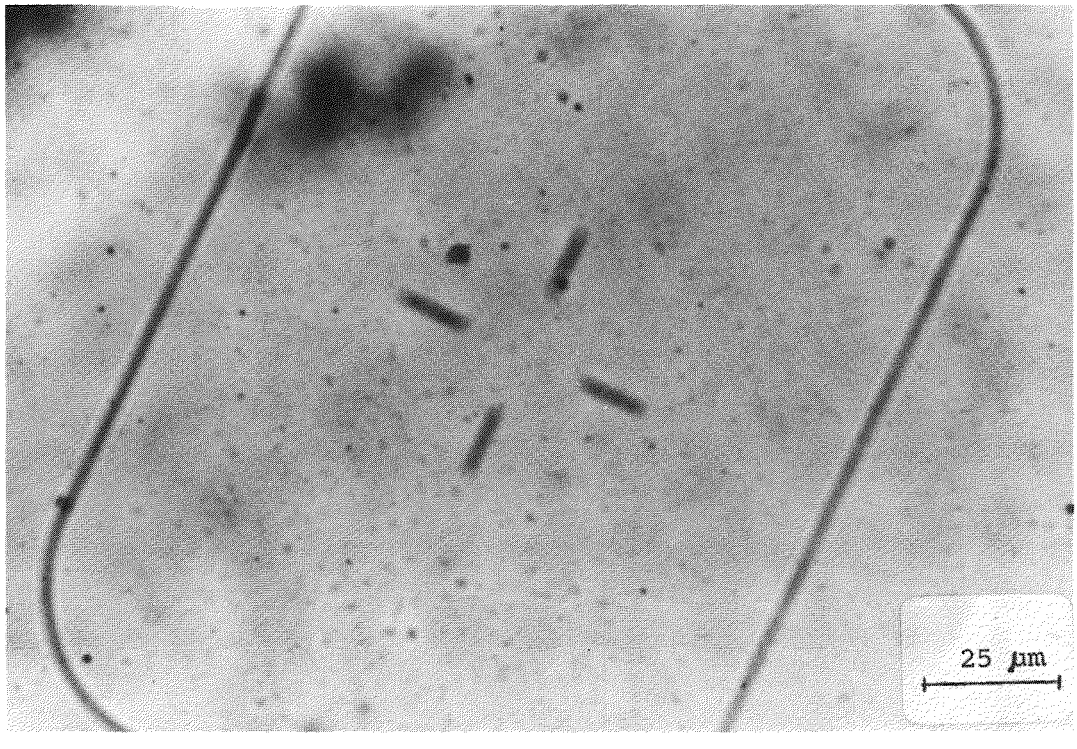

DP1 MIDDLE OF WALL

Figures 5-3 and 5-4. Voids in Dry Cured XLPE.

OPTICAL MICROGRAPHS

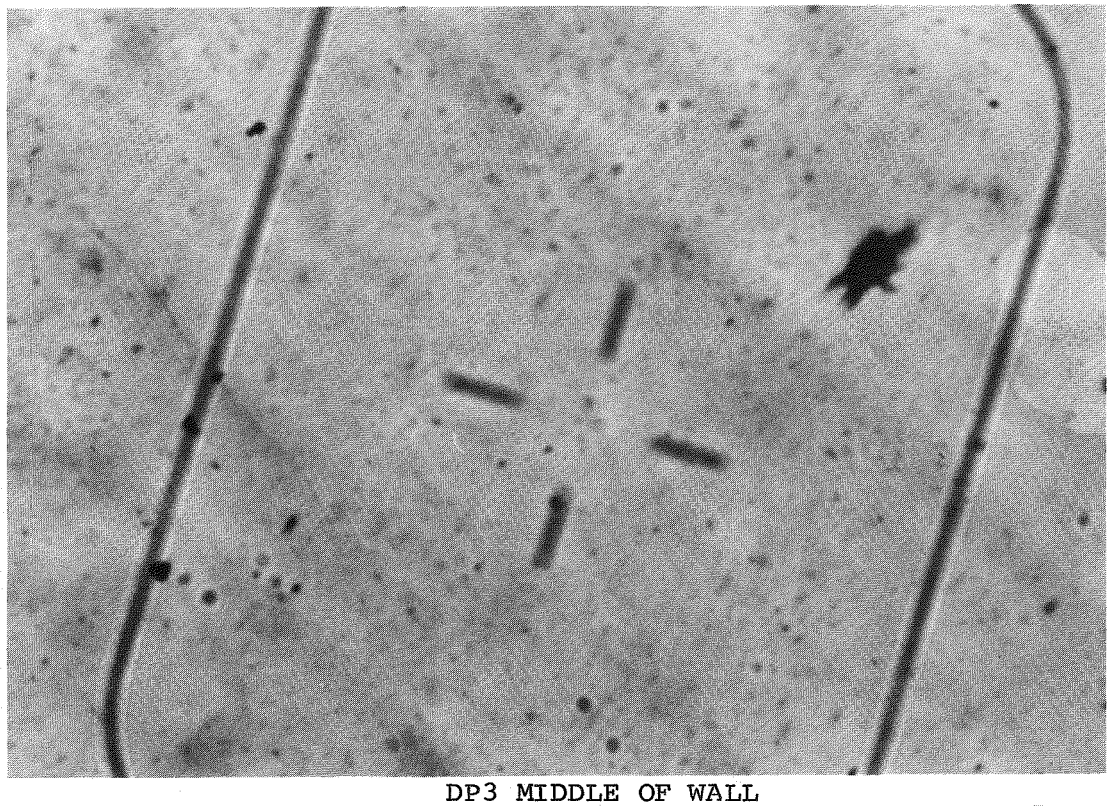

DP3 MIDDLE OF WALL

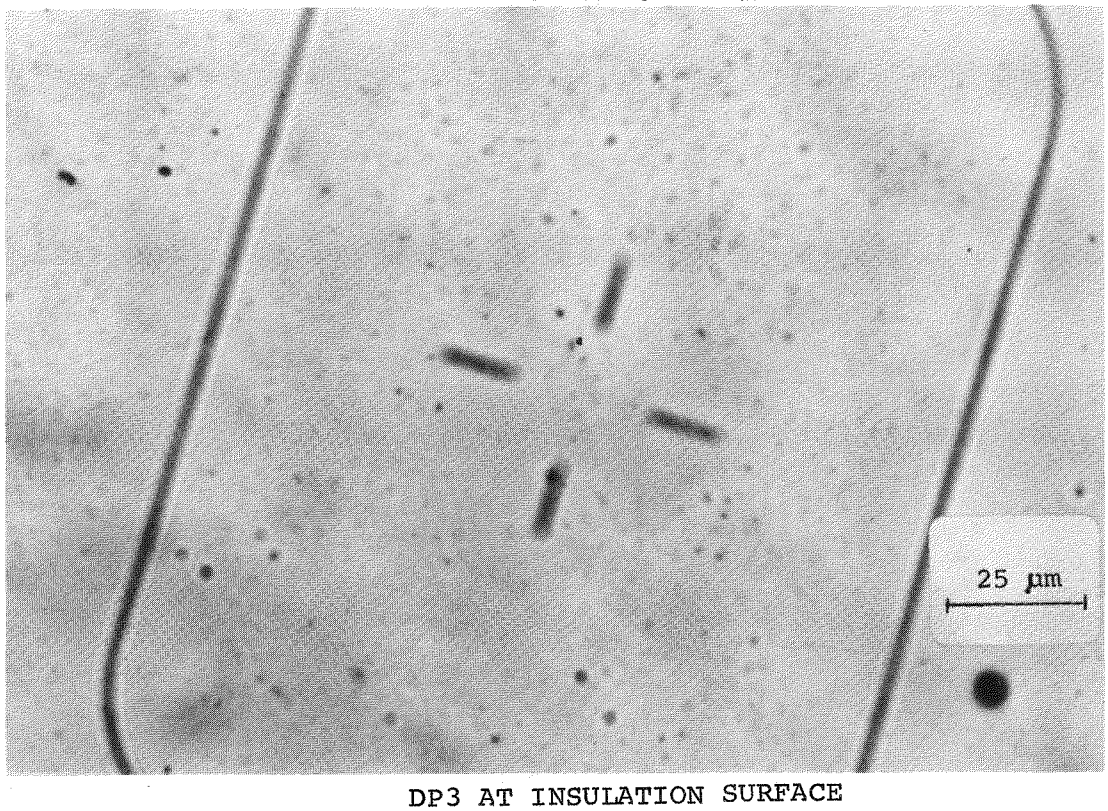

DP3 AT INSULATION SURFACE

Figures 5-5 and 5-6. Voids in Dry Cured XLPE.

OPTICAL MICROGRAPHS

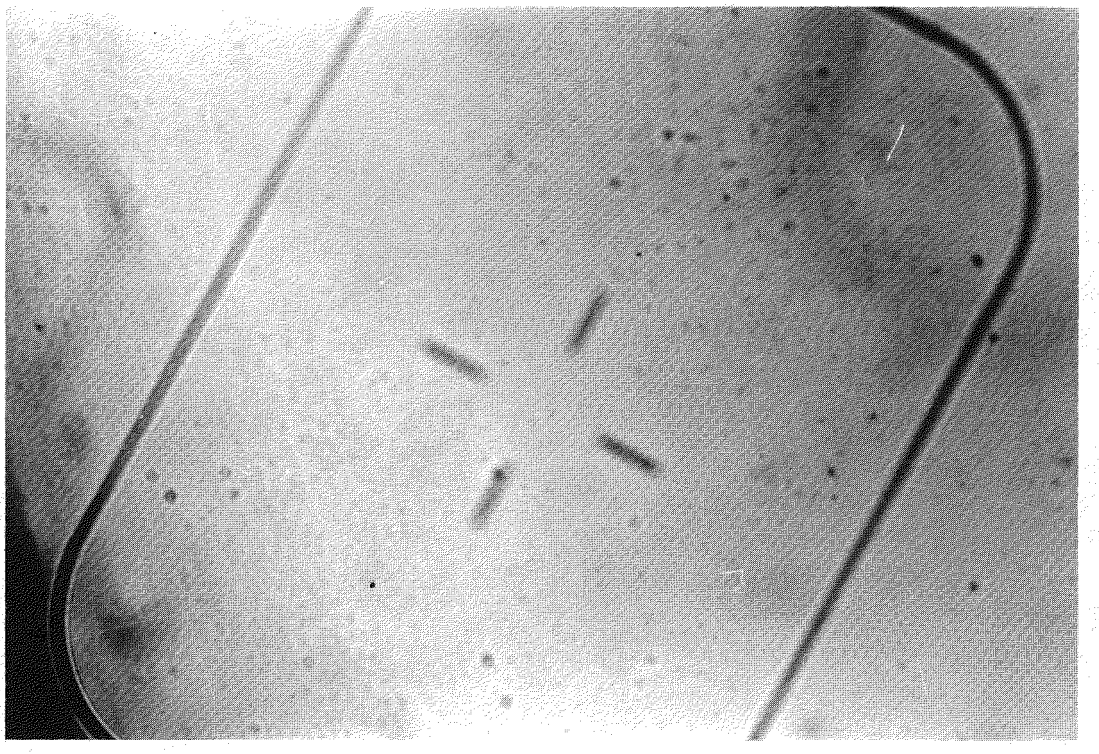

DP4 AT CONDUCTOR

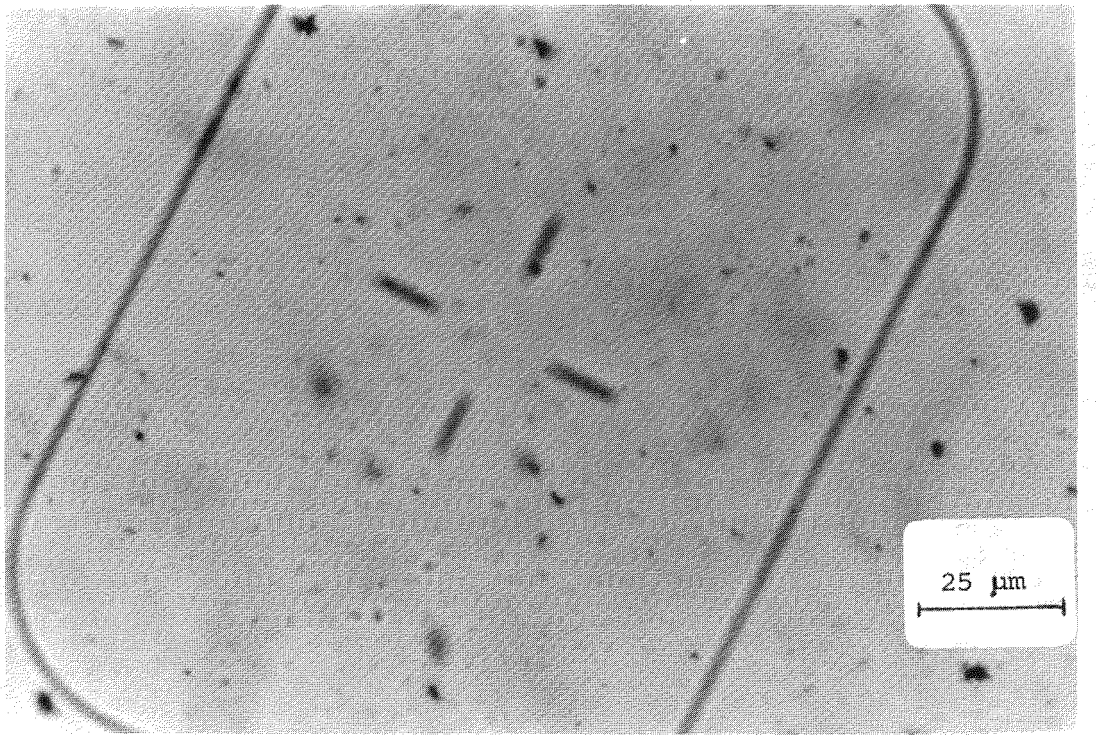

DP4 NEAR THE CONDUCTOR

Figures 5-7 and 5-8. Voids in Dry Cured XLPE.

OPTICAL MICROGRAPHS

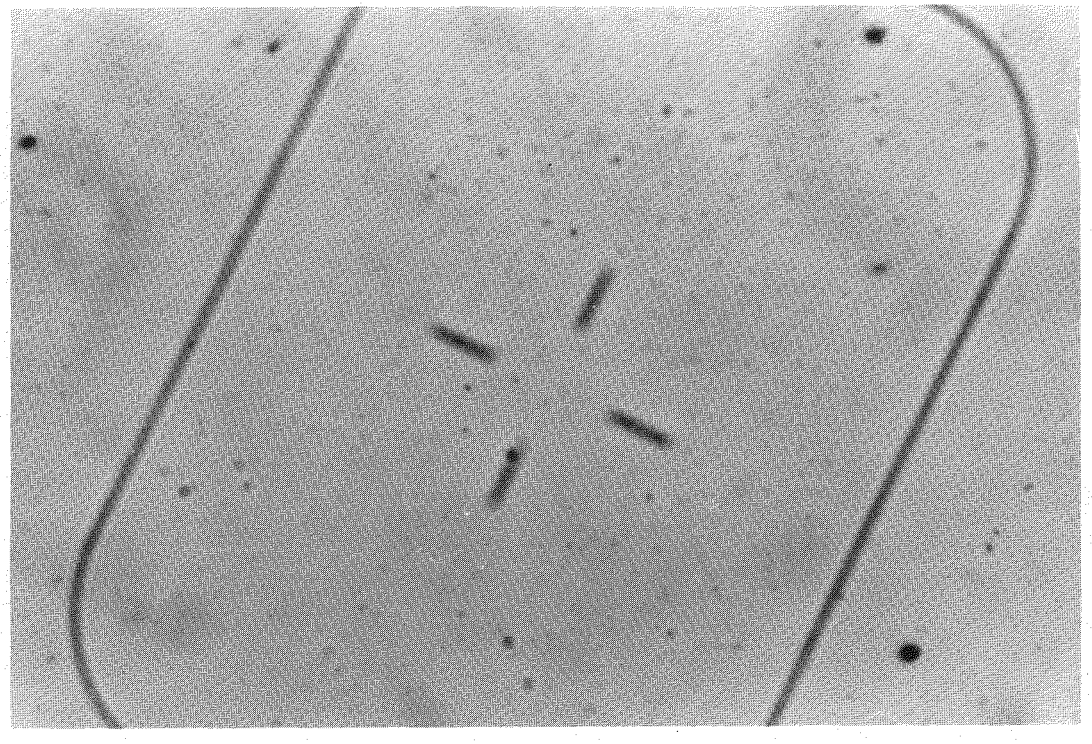

DP4 MIDDLE OF WALL

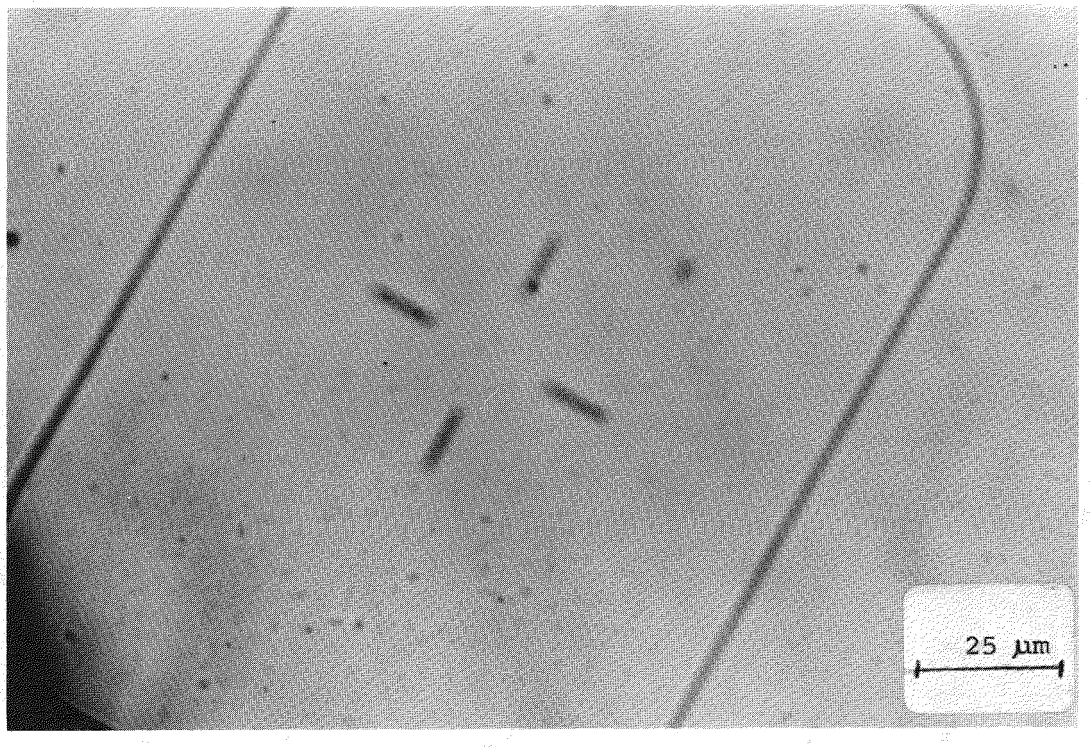

DP4 AT INSULATION SURFACE

Figure 5-9. Voids in Cry Cured XLPE.

Table 5-2

COMPARISON BY SCANNING ELECTRON MICROSCOPY

CURE	STEAM	DP1	DP2	DP3	DP4
VOIDS					
SIZE (μ)	1 - 6		1 - 7	2 - 10 (on S.C. surface)	
SHAPE	ROUND		LONG	LONG	
REL. NUMBER	HIGH		HIGH	V. LOW	
GEL LIKE PARTICLES					
SIZE (μ)		.5 - 20	.1 - 2	2 - 6	<0.5
SHAPE		VARIES	ROUND	IRREGULAR	ROUND
REL. NUMBER		LOW	V. LOW		HIGH
CONTAMINATION				10 μ	
FIGURES	3-14	5-10 5-11	3-15 5-12 5-13	5-14 5-15 5-16	5-17 5-18

SCANNING ELECTRON MICROGRAPHS

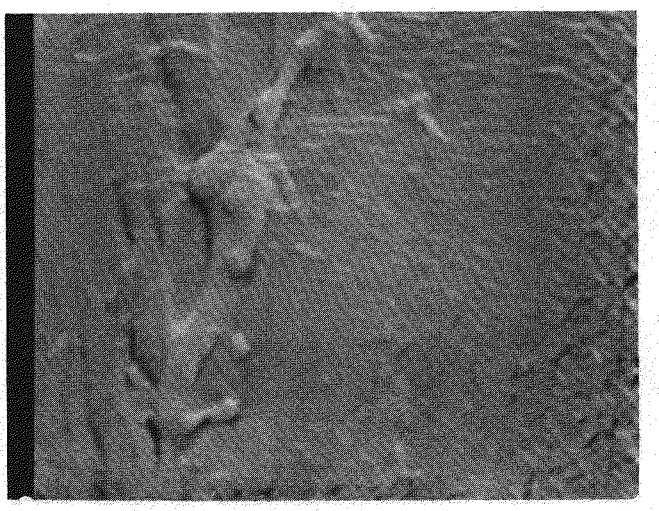

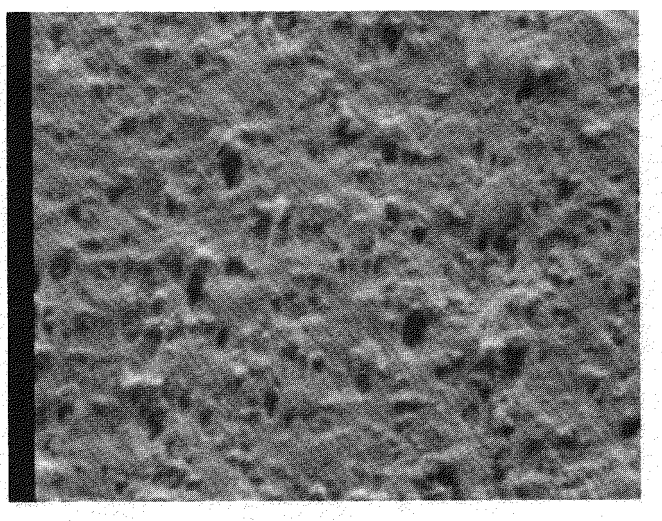

Figures 5-10 and -11. Dry Cured Insulation with Gel Particle (top) and Insulation Shield. Process: DP1.

10 μm

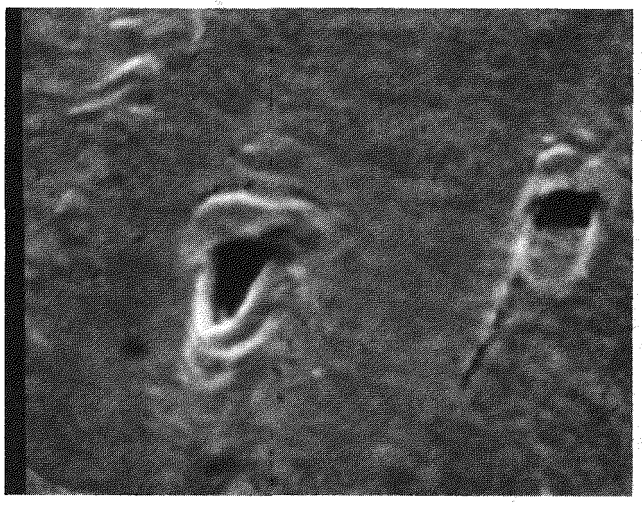

1 μm

Figures 5-12 and -13. Voids in Dry Cured XLPE.
Process: DP2.

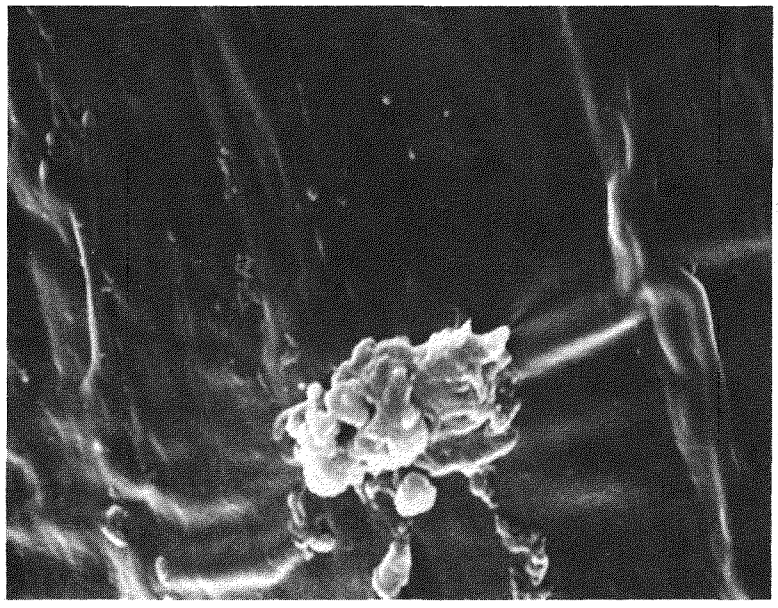

1 μm

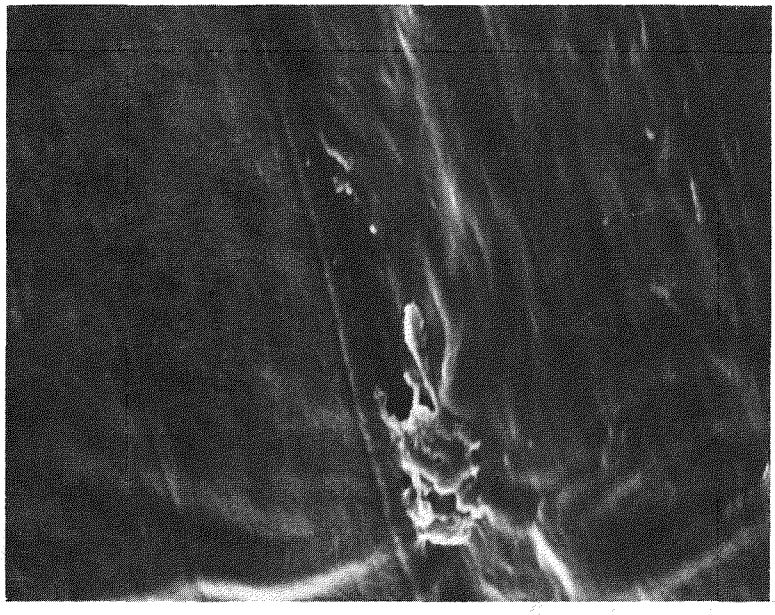

1 μm

Figure 5-14. Gel in Dry Cured Insulation. Process: DP3.

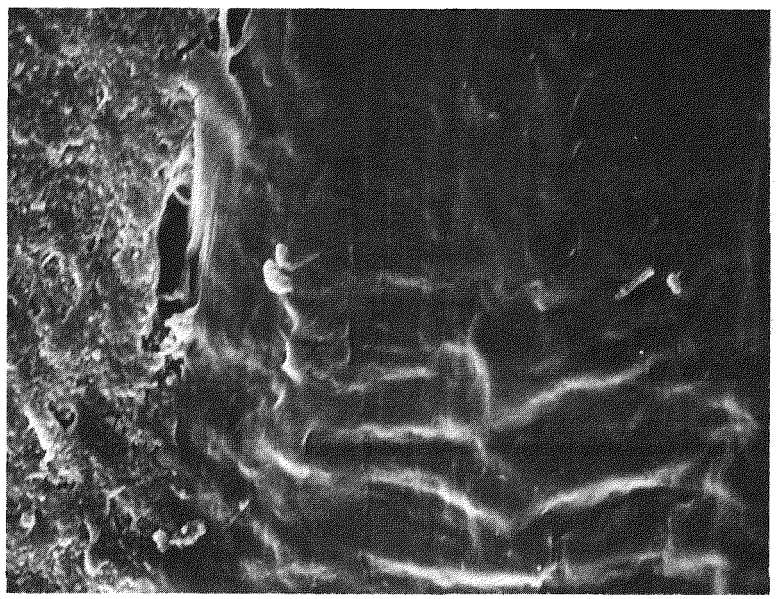

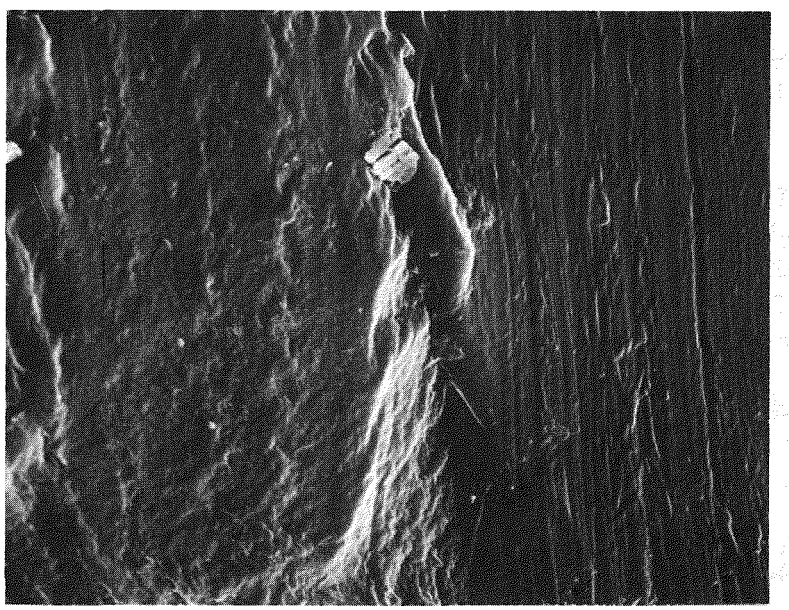

Figure 5-15. Voids at Conductor Shield-Insulation Interphase. Process: DP3.

SCANNING ELECTRON MICROGRAPHS

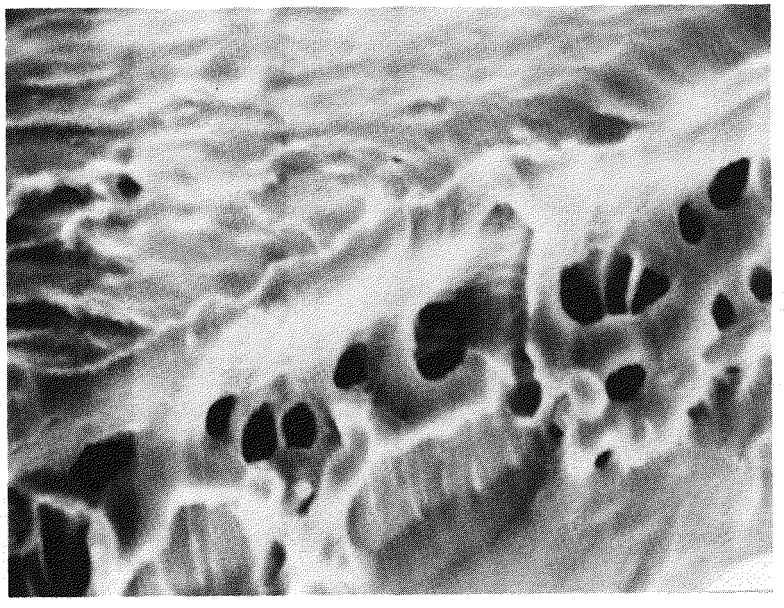

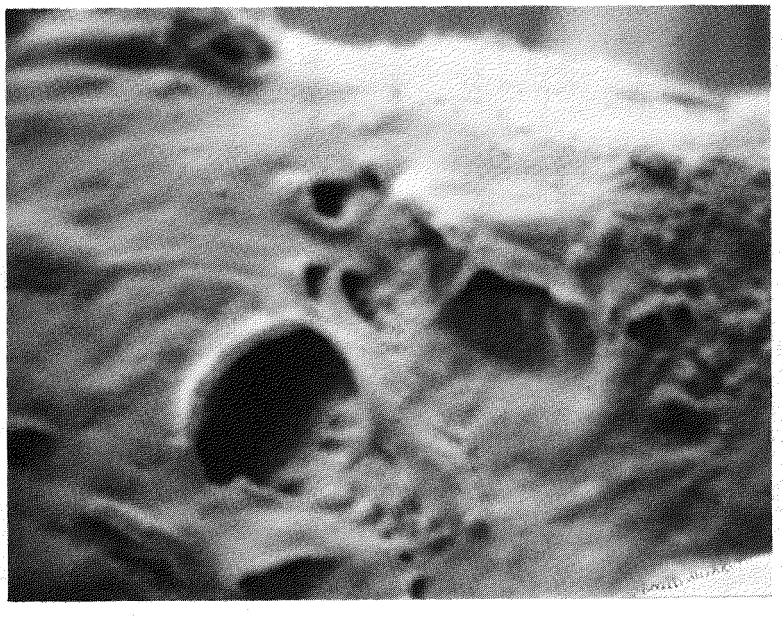

Figure 5-16. Voids in Dry Cured Insulation.
Process: DP3. Cold fractured specimen.

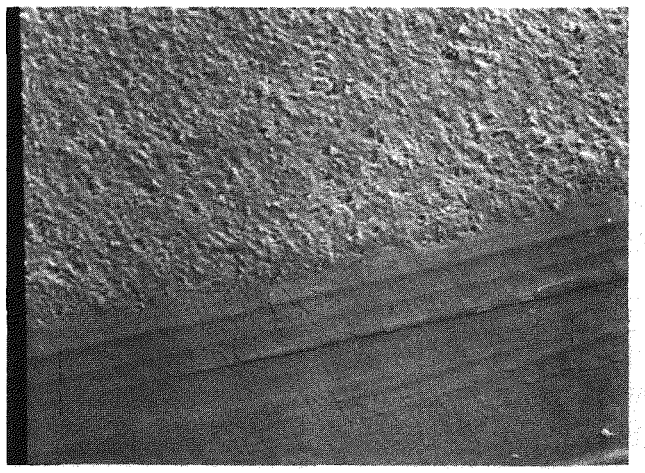

10 μm

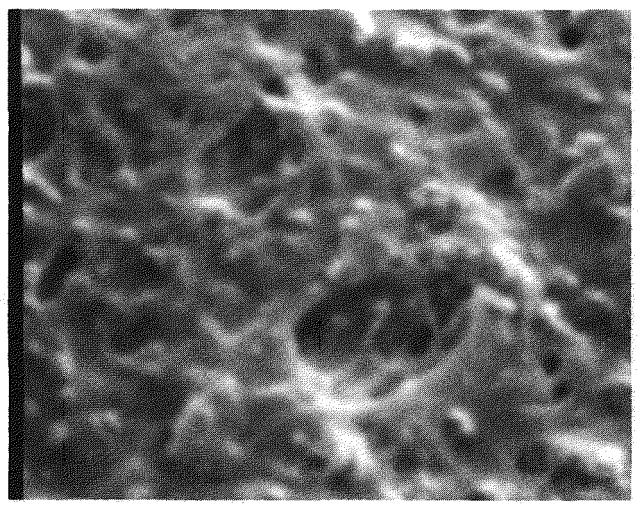

1 μm

Figures 5-17 and -18. Conductor Shield-Insulation Interphase in Dry Cured Cable (top) and Void Details in Insulation Shield (bottom). Process: DP4.

the outside of the insulation to assess potential differentiation in the radial direction. The results are presented in Table 5-3.

The TGA test consists of measuring the weight loss of the specimen in nitrogen atmosphere as a function of temperature. The temperature was raised at 10°C per minute and the weight remaining was automatically recorded. Figure 5-19 presents a typical TGA curve, showing the position of nine significant points. The volatilization onset (#1) and the temperatures representing 1 to 5 and 10% weight loss are directly obtained from the plot (numbers 2 to 7). The calculated volatilization temperature (#8) is the intercept of the linear extensions of the curves representing the initial slow weight loss and the steep, catastrophic type decomposition. The complete volatilization point is the similar linear intercept of the steep decomposition curve and of the practically horizontal line for the non-volatizable residue.

The tabulated data in Table 5-3 reveals no significant differences between steam and dry cured insulations, or between inside or outside locations. The differences in the volatilization onset temperatures are not significant in view of the limited readability of the curve in this region. The same comment applies to the variation in the residue levels.

The DSC measurements were carried out in nitrogen atmosphere, in aluminum pans at 10°C per minute temperature increase. Tracings of the curves from 60 to 120°C are presented in Figures 5-20 and 5-21. Arrows indicate the significant points, i. e. the onset and completion of the first and second endotherms. The first endotherm at 75 to 95°C is associated with a solid state transition, the second one at 90 to 110°C with the melting of the thermoplastic component. The area under the peaks is a measure of heat absorbed in these two endothermic processes.

Visual comparison shows no significant difference between steam and dry cured processes in the melting range of the insulation (Figures 5-20 and 5-21). Data tabulated in Table 5-3 confirms the lack of major differences in these insulations. The decomposition temperatures listed in Table 5-3 were obtained by continuing the DSC test to 400°C, and are not shown in Figures 5-20 and 5-21.

The DSC control curve for non-crosslinked polyethylene is distinctly different in the sharpness of the melting peak.

The OIT data was obtained in the DSC apparatus at 200°C in oxygen atmosphere. It is the induction time in minutes lapsed between the initiation of the test and the onset of endothermic oxidation. The range, 4 to 22 minutes is the same normally found in new cables.

Table 6-5

THERMOANALYTICAL CHARACTERIZATION

CURE	STEAM		DP1		DP2		DP 3		DP4	
Location	Inside	Outs.	Inside	Outs.	Inside	Outs.	Inside	Outs.	Inside	Outs.
Thermogravimetrical Analysis in Nitrogen										
Volatilization Onset, °C					130	185	135	155	320	290
1% loss at °C					360	351	225	245	380	395
2			421	420	422	419	421	410	424	425
3			435	435	441	442	441	448	445	453
4			447	443	452	456	450	460	451	455
5			458	451	456	463	454	469	456	458
10			475	468	471	479	475	490	471	471
Calc. Vol. Temp., °C			485	493	478	491	478	499	481	480
Vol. Complete, °C			519	516	516	526	518	533	520	517
Residue, %					0.25	0.25	0.3	0.2	0	0.3
Differential Scanning Calorimetry (DSC), °C										
1st Endotherm: Onset	84	84	80	81	-	-	92	98	71	71
complete	86	89	86	87	-	-	95	100	79	78
type (1)	+	++	+	++	-	-	+	+	++	++
2nd Endotherm: Onset	90	96	92	96	89	105	98	102	86	91
complete	102	103	106	105	104	102	106	108	103	102
Decompositon Temp.:	375	396	358	395	400	400	397	342	393	407
OIT, Minutes	21.0	21.0	9	12	8.9	3.8	6.6	14.2	21.1	21.2

(1) SYMBOLS: + Weak
++ Strong
- None

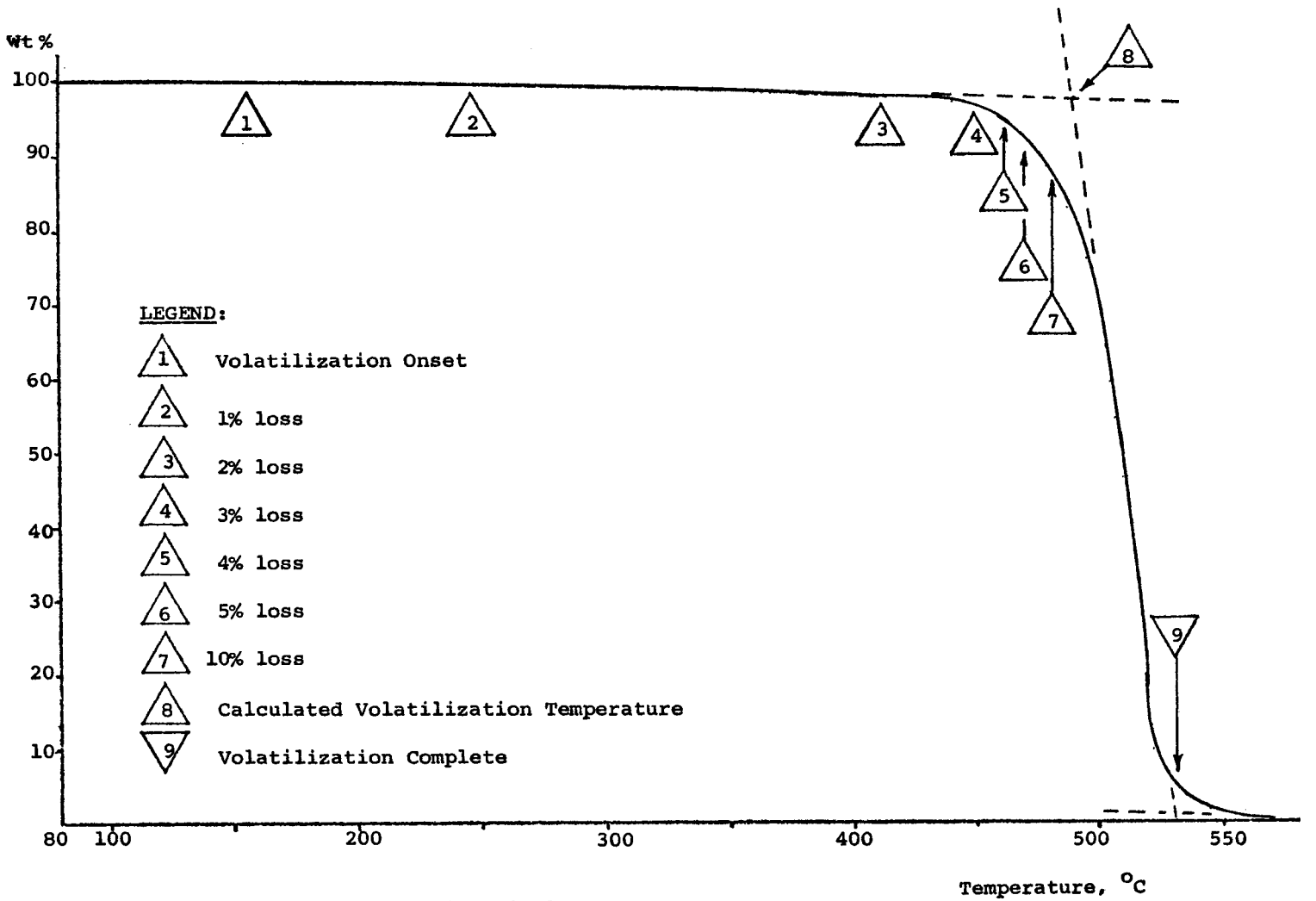

Figure 5-19. Typical Thermogravimetrical Curve.

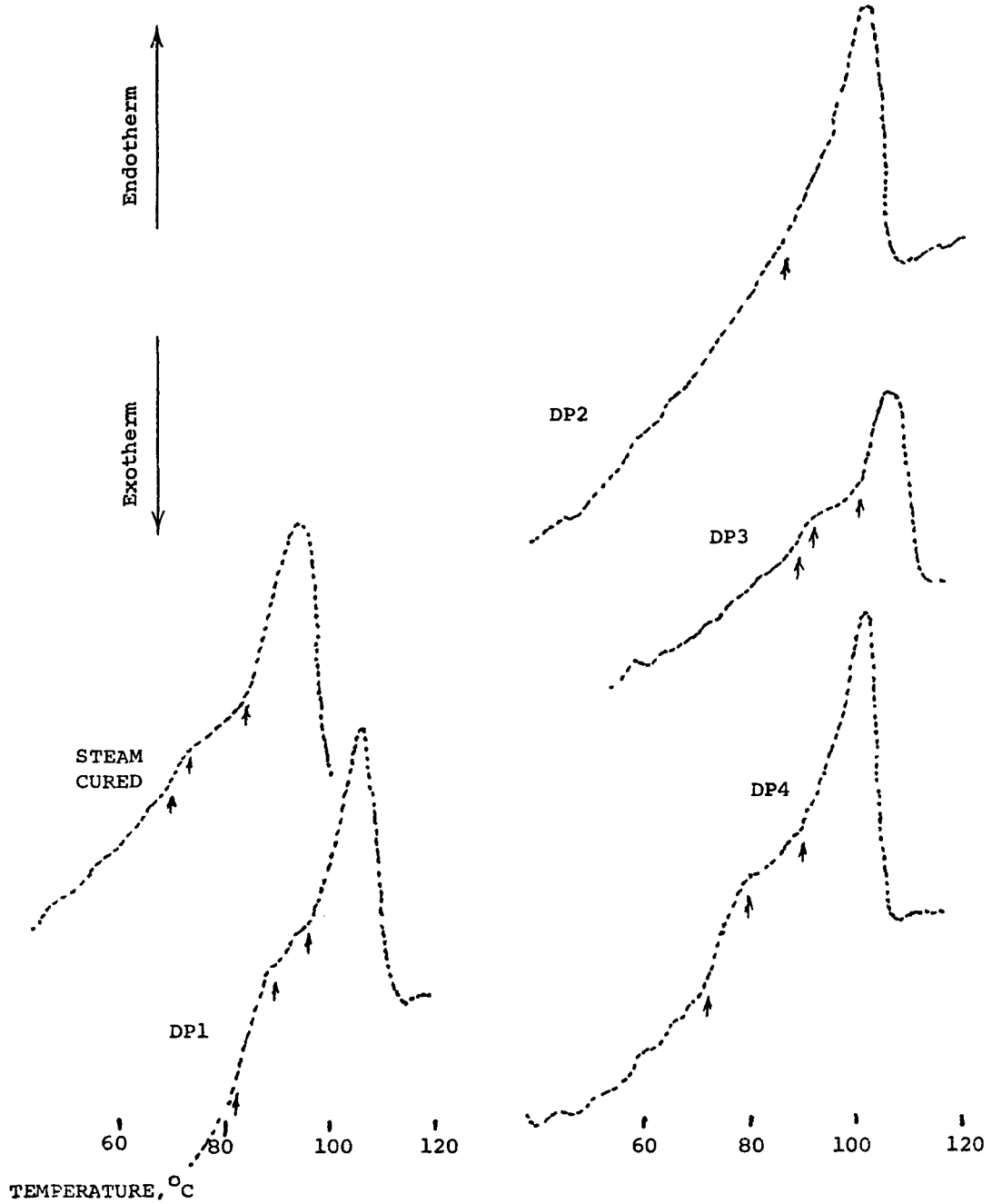

Figure 5-20. Melting Characteristics by DSC (Near Insulation Shield).

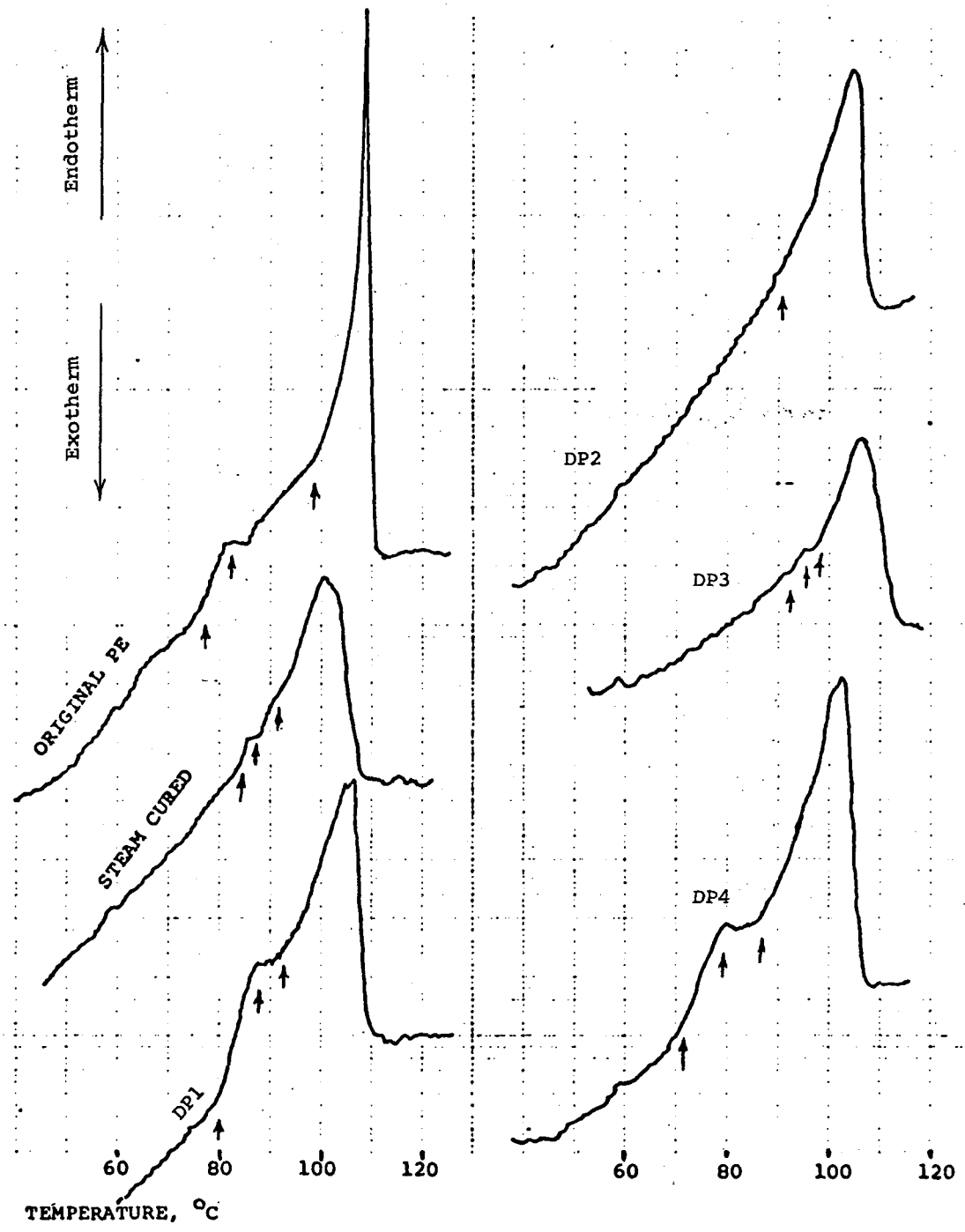

Figure 5-21. Melting Characteristics by DSC (Near Conductor).

5.1.3 Chemical Analysis

The chemical analysis of the insulation included the analysis of the volatiles by gas chromatography and compared the infrared spectra. Both techniques confirm the similarity of the insulations produced by either steam curing or by any of the four dry processes. Gas chromatographic technique was used to determine the following 3 volatile components: cumyl alcohol, acetophenone, αmethyl styrene.

The results are presented in Table 5-4 and in Figure 5-22. The total volatile content varies from 0.06 to 0.7% of the insulation. This variability is probably due to the differences in the samples' history rather than to processing characteristics. The presence of the same 3 volatiles proves that the same peroxide was used in each of the five processes. The similarity of the relative ratios of the components shows that no major difference exists in the reaction mechanism of peroxide decomposition whether steam (or water) are present or not. The similarity of volatile composition between inside and outside samples could imply similar heat history throughout the wall thickness. The predominance of cumyl alcohol and the low concentration of α methyl styrene in the volatiles are in line with the published literature.

The infrared analysis (Table 5-5) also confirms the similarity of these cables, and the lack of differentiation in the radial direction of the insulation. It shows the overwhelming presence of $-CH_2$ groups characteristic of XLPE, and the absence of any other monomer or bridging agent. The minor differences could be caused by differences in the stabilizer system and not by oxidative degradation of the insulation.

5.2 IMPREGNATION AND IN SITU POLYMERIZATION WITH SEMICONDUCTING SHIELDS

The conductor shield and insulation shield of power cables are made of semiconducting compounds which, in addition to the base resin (polyethylene, ethylene-vinyl acetate copolymer or ethylene-ethyl acrylate copolymer) contain 35 to 40 parts carbon black per hundred parts of resin (phr). The type of carbon black as well as its concentration is chosen not to exceed volume resistivity of 50,000 and 100,000 ohm-centimeter for insulation and conductor shield respectively at 90°C (40).

The question was raised whether in the process of impregnating the insulation with a monomer and polymerizing it in situ, the volume resistivity would increase beyond specification limits. Assuming that the monomer is absorbed in the semiconducting layer and polymerized there, it may cause separation of the carbon particles by an insulating polymer and hence loss of conductance. On the other hand,

Table 5-4

ANALYSIS OF INSULATION

Volatile components by Gas Chromatography, %

CURE / Location	SCP		DP1		DP2		DP3		DP4	
	Inside	Outs.	Inside	Outs.	Inside	Outs.	Inside	Outs.	Inside	Outs.
Methyl Styrene	.002	.002	.002	.002	.007	.040	.006	.028	.003	.002
Acetophenone	.057	.053	.014	.016	.076	.073	.261	.204	.115	.056
Cumyl Alcohol	.223	.257	.044	.037	.374	.153	.466	.283	.330	.156
TOTAL	.282	.312	.060	.055	.457	.266	.733	.515	.448	.214
RELATIVE RATIOS (Acetophenone =1)										
Methyl Styrene	.035	.038	.143	.125	.092	.545	.023	.137	.026	.036
Acetophenone	1	1	1	1	1	1	1	1	1	1
Cumyl Alcohol	3.9	4.85	3.14	2.31	4.92	2.10	1.79	1.39	2.87	2.79

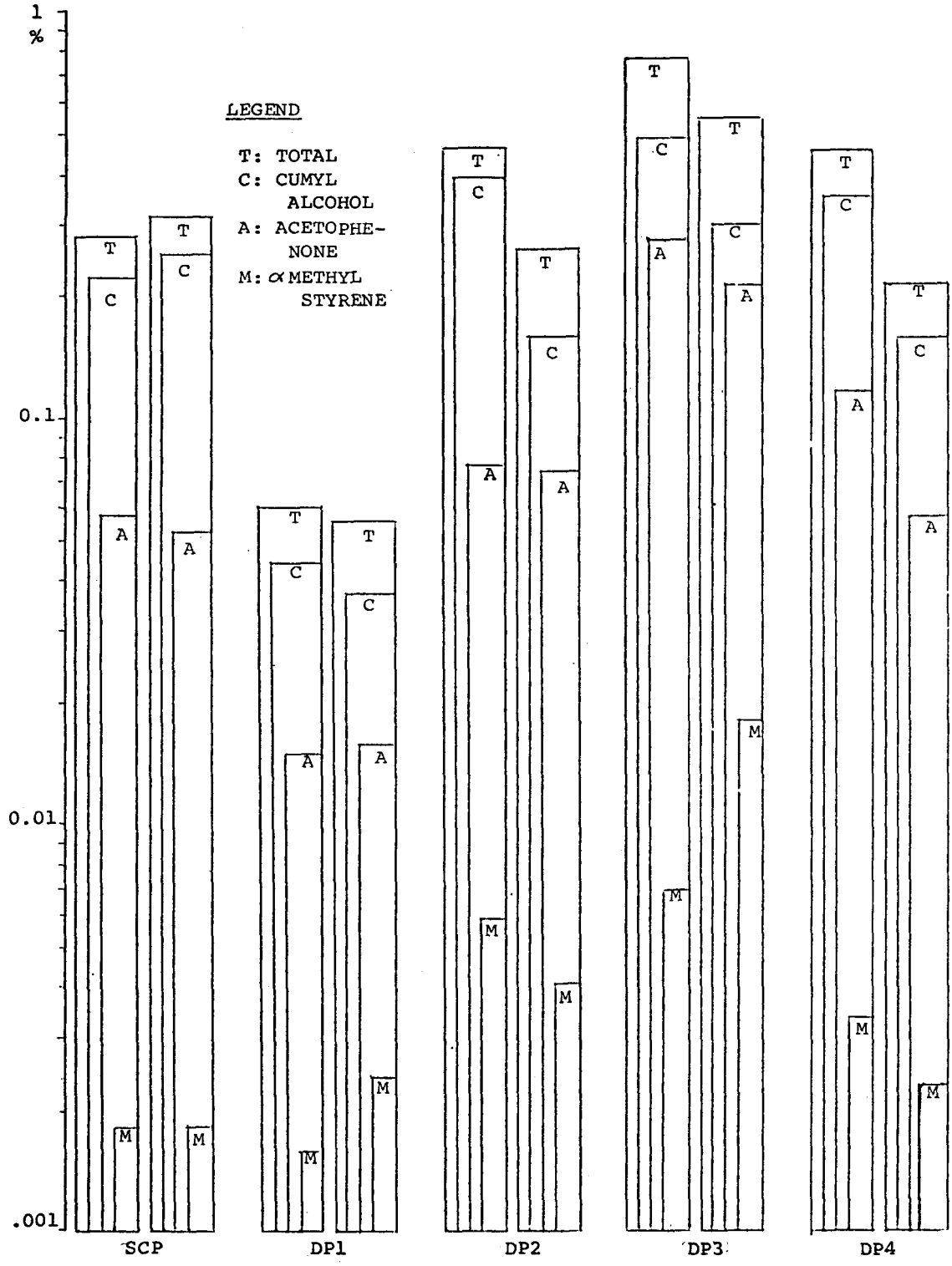

Figure 5-22. Volatiles by Gas Chromatography.

Table 5-5

COMPARISON OF IR SPECTRA

CURE Location	STEAM Middle	DP1 Middle	DP2 Inside	DP2 Outs.	DP3 Inside	DP3 Outs.	DP4 Inside	DP4 Outs.
3.4μ Saturated CH	S	S	S	S	S	S	S	S
4.35μ CO_2 Assym.	S	S	-	-	-	T	-	T
4.9μ Aromatics	S	S	W	T	T	W	T	W
5.25μ Aromatics, Subst.	S	S	-	T	-	T	-	T
5.80μ C = O	-	S	W	S	-	T	-	T
5.95μ C = C	W	T	S	-	S	W	-	T
6.8μ $-CH_2-$ $-CH_3$ Assym.	-	-	-	-	-	-	-	-
7.20μ $-HC(CH_3)_2$	-	-	-	-	-	-	-	-
7.25μ $-CH_3$	-	-	-	-	-	-	-	-
9.5μ -OH	-	-	-	-	-	-	-	-
10.1μ -C = C-	-	-	W	-	-	-	-	-
10.4μ -C = C-	-	-	W	-	-	-	-	-

SYMBOLS: - None W Weak
T Trace or shoulder S Strong

if the level of impregnation is moderate or the polymerization yield is low, the conductance may not be affected seriously. A series of experiments was carried out on impregnation with polyethylene wax and on in situ polymerization of vinyl toluene monomer on semiconducting profiles to study their effect on conductivity with and without aging.

5.2.1 Experimental

Two different profiles were used:

- Rods of 0.5 inch diameter, extruded from Union Carbide semiconducting compound No. 0580 and cured in a flash vulcanizer.
- 15 kV cable with insulation shield, 6 inches in length.

The samples were impregnated with solutions of BPO in vinyl toluene monomer. They were surface cleaned, weighed and placed in a polymerization kettle in an atmosphere saturated with the monomer. The polymerization was carried out at 70°C for 16 to 20 hours. This was followed by vacuum drying to remove the residual monomer. In another series of experiments the rods were impregnated with a low molecular weight polyethylene wax (Allied Chemicals compound No. 1702).

The resistivity of the rods and the shields of the 15 kV cable was measured per IPCEA Procedure #S-66-524, part 6, paragraph 12. A conducting silver paint was sprayed around the specimens at two points, two inches apart and connected to the conductance bridge. Sets of six samples along with controls were used in each experiment. After the initial reading, the specimens were aged in an air circulating oven at 90°C to 130°C and the readings were taken after 7, 14, 28, 42, 56 and 70 day intervals.

5.2.2 Results and Discussion

The rate of impregnation of vinyl toluene monomer and polyethylene wax into semiconducting rods is presented in Figure 5-23. In the same Figure the rate of impregnation of the above materials into crosslinked polyethylene insulation are presented for comparison. The curves are reminiscent of the impregnation curves for liquid impregnants into the insulation (Section 3.3). It is evident that the impregnants migrate much faster into the semiconducting specimens, than into the insulation, although the resin in both cases is crosslinked polyethylene. This large difference is attributed to the porous nature of the semiconducting specimen. An electron

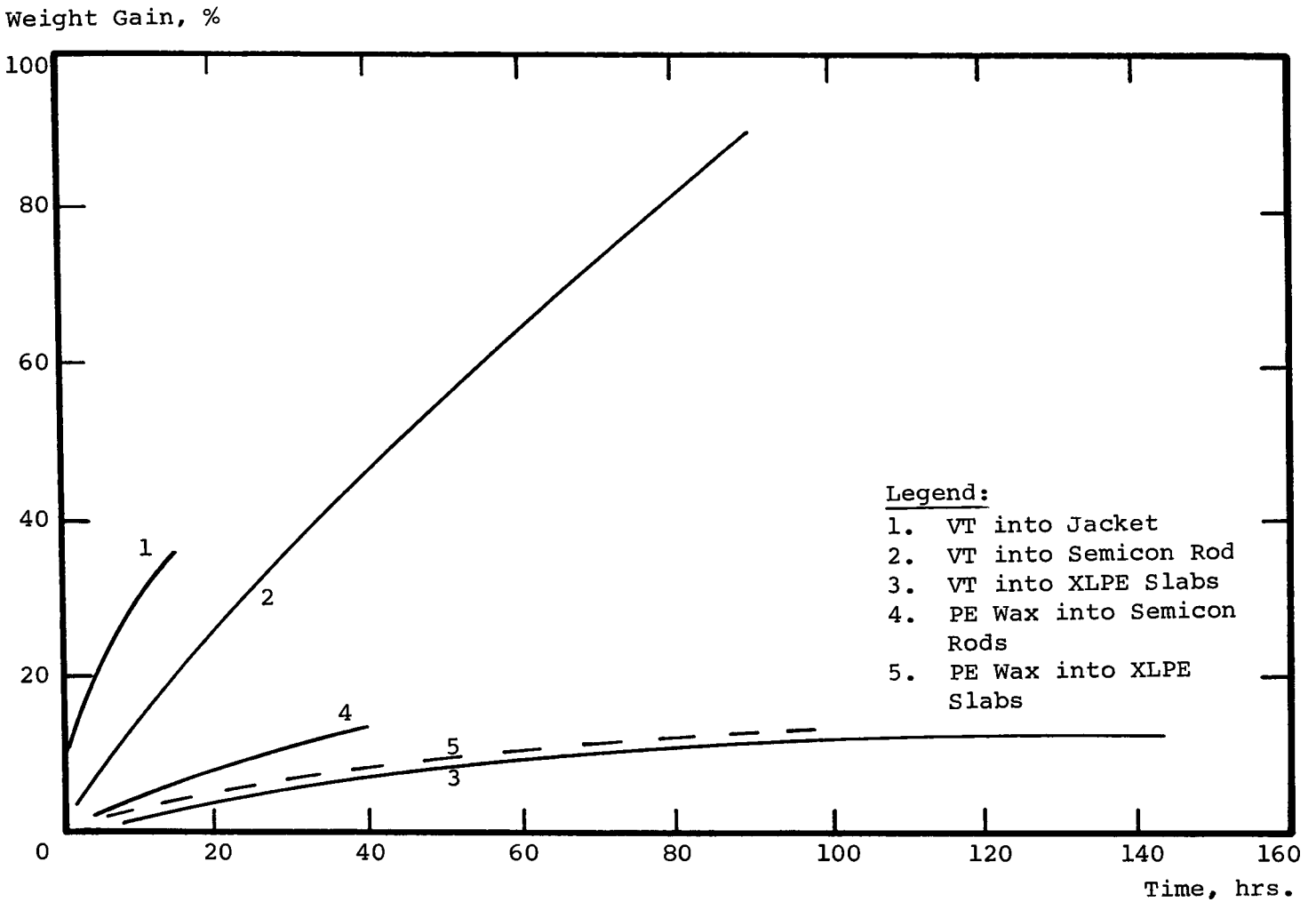

Figure 5-23. Rate of Impregnation into Semicon Specimens and XLPE Slabs. Nos. 1, 2 and 3 at room temperature. Nos. 4 and 5 at 100°C.

micrograph presented in Figure 5-15 provides evidence to this effect. Further, the rate of impregnation is somewhat greater for the outer shield compared to rods. This may be due to their smaller thickness or greater surface to volume ratio.

In Table 5-6 the yield of vinyl toluene polymerization is presented along with the data on impregnation. It is evident that although the impregnation levels are very high, the polymerization yield is extremely low. This could be either due to slower diffusion of peroxide catalyst into the semiconducting matrix or due to some scavenging process, by which the free radicals are consumed and are not allowed to initiate polymerization. Since the semiconducting specimens are porous, there is no reason to believe that the diffusion of peroxide into the matrix will be slower than that into the solid insulation. On the other hand, it is well known that the carbon black particles contain a substantial amount of quinone and hydroquinone type groups on their surface(41). As mentioned in Section 3.4, these groups react with primary chain radicals and produce radicals which are resonance stabilized. Hence, the polymerization process is inhibited, resulting in very poor yields.

The volume resistivity of the impregnated samples has been plotted against weight gain in Figure 5-24 on a semi-log scale. The weight gain shows linear correlation with volume resistivity and is maximum for the polyvinyl toluene semicon rod system. Thus, for 1% weight gain the volume resistivity for polyvinyl toluene impregnated samples changes from 22 ohm-cm to 730 ohm-cm whereas that for the polyethylene wax impregnated sample changes from 22 to 50 ohm-cm. It is suggested that the low viscosity of vinyl toluene at the temperature of impregnation ($25^{o}C$) may help it to get in between the carbon particles and separate them. The high viscosity polyethylene wax does not allow it to penetrate between the carbon particles, although the temperature ($100^{o}C$) is high enough to soften the crosslinked polyethylene matrix.

The effect of aging on the volume resistivity of impregnated samples is presented in Figures 5-25 to 5-27. The high volume resistivity of the impregnated shield drops to below 4000 ohm-cm after the first 24 hours of aging and decreases gradually during the seventy day period of testing (Figure 5-25). The vinyl toluene impregnated rods also show similar behavior at $120^{o}C$ (Figure 5-25). The polyethylene wax impregnated rods at $90^{o}C$ show an initial increase in the resistivity, followed by a sharp drop. Figure 5-27 shows that up to 3.8% impregnant content, the resistivity remains well within the specifications. Impregnation with 8% PE wax raised the resistivity beyond 100,000 ohm-cm and required 70 days to drop below 50,000 ohm-cm. Obviously, the limiting concentration for this impregnant is between 3.8 and 8%. The preliminary experiments indicate strongly that neither of the two impregnants change the volume resistivity of the semiconducting shields at practical concentrations beyond the specified range.

Table 5-6

IMPREGNATION AND POLYMERIZATION OF

VINYL TOLUENE IN SEMICON RODS

VT - 100 gms.
Bz_2O_2 - 2.5"
Impregnation Temp. 25°C

POLYM. TEMP. 70°C
TIME 20 HRS.
ROD DIAMETER 3/8"

No.	Time of Impregnation Hrs.	NORMALIZED WEIGHT AFTER Impregnation	Polym.	% VT Polymerized
1	16	121.4	100.6	
2	16	123.3	101.4	
3	16	124.2	100.8	
Average		123	100.9	2.8
4	40	149.0	101.8	
5	40	141.8	101.0	
6	40	148.4	102.3	
Average		145.7	101.7	3.7
7	70	165.3	102.5	
8	70	165.1	102.4	
9	70	160.8	100.5	
Average		165.1	102.5	3.8
10 (1)	70	110.8	108.7	80.4

(1) Control: XLPE Slab, 3/8" Thick.

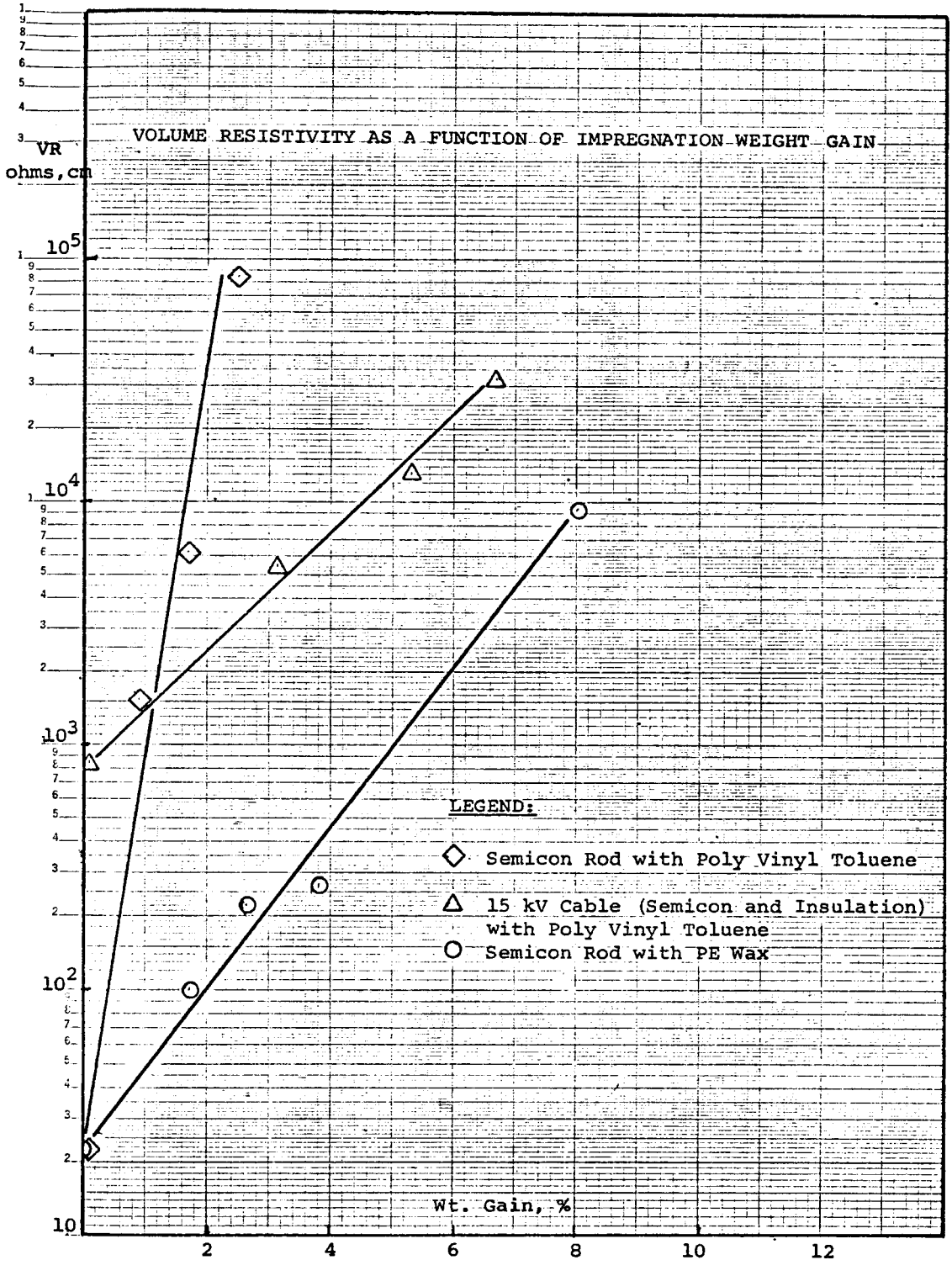

Figure 5-24. Volume Resistivity of Impregnated Semiconducting Rods.

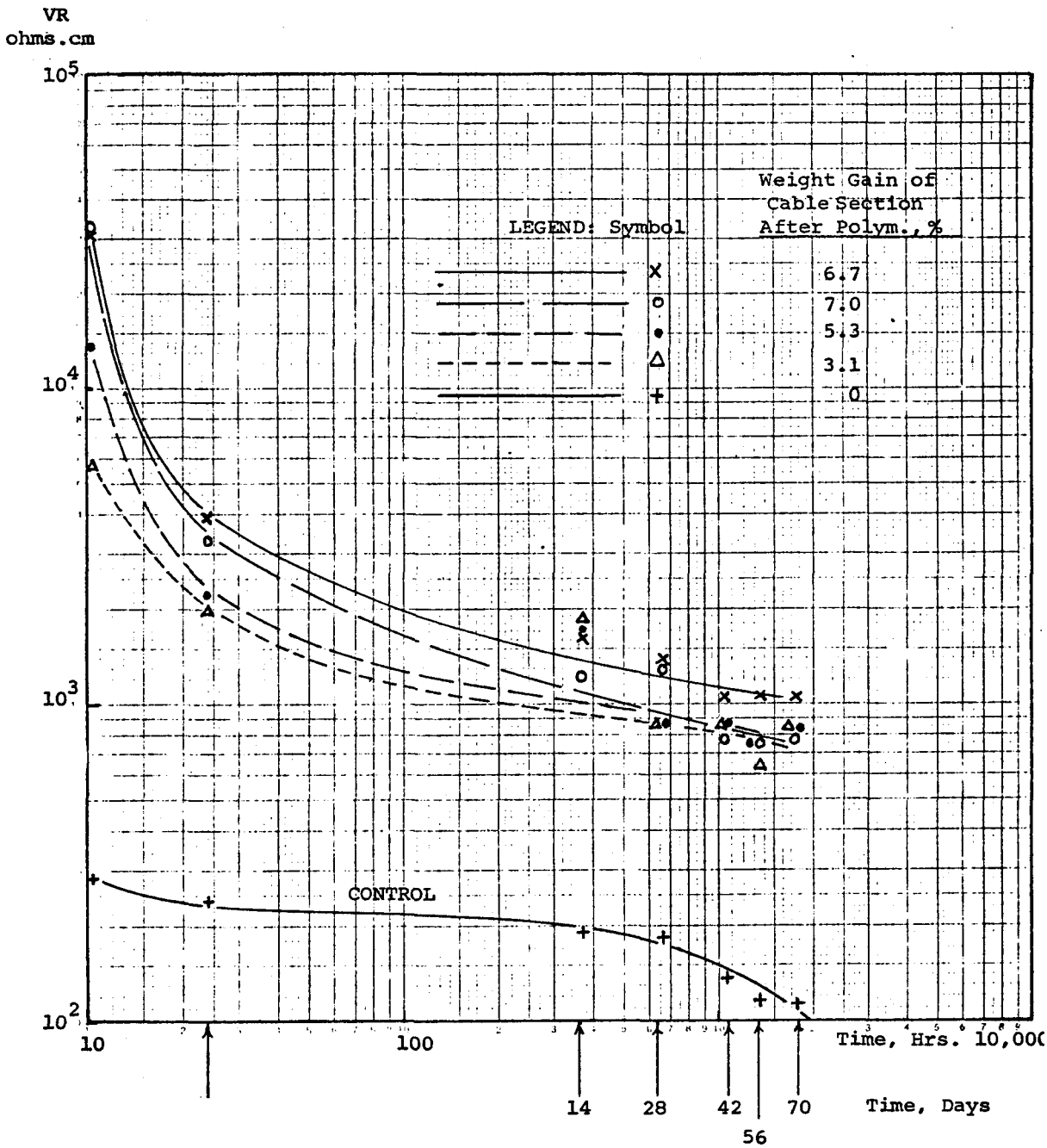

Figure 5-25. Effect of Aging on Volume Resistivity.
Specimen: Insulation shield of 15 kV cable.
Impregnant: Vinyl toluene polymerized in situ.
Temperature: 120°C

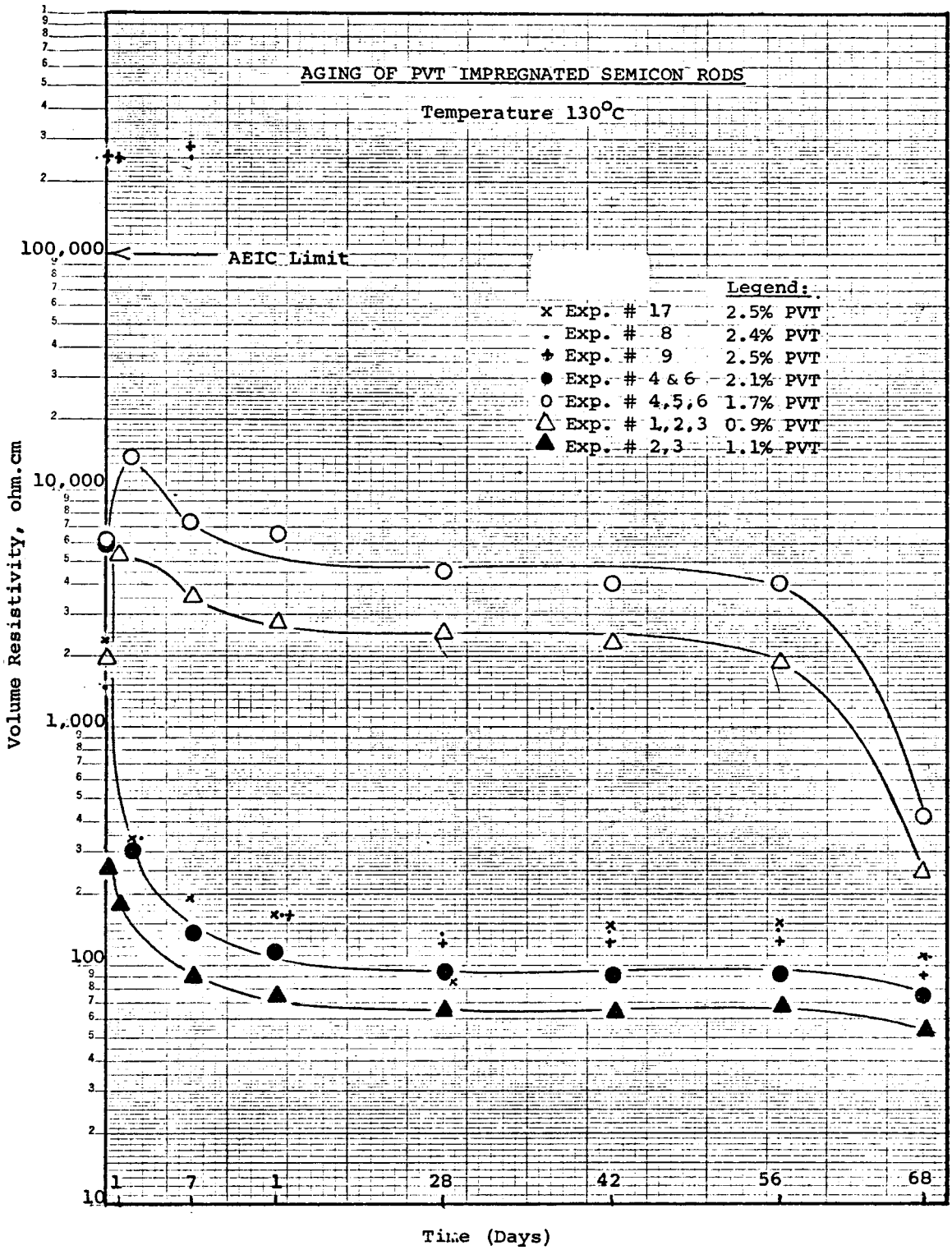

Figure 5-26. Effect of Aging on Volume Resistivity.
Specimen: Semicon rods
Impregnant: Vinyl toluene polymerized in situ.
Temperature: 130°C

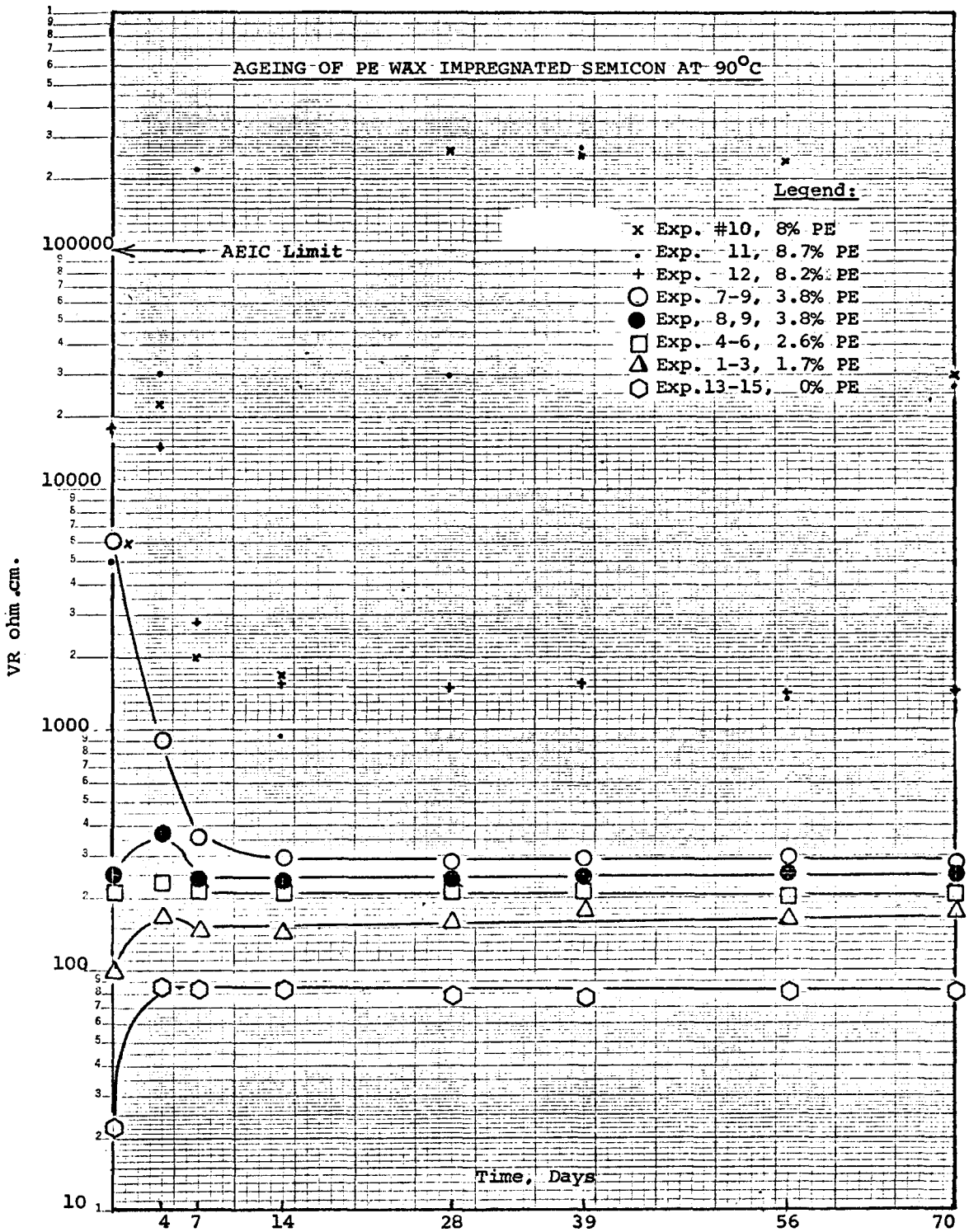

Figure 5-27. Effect of Aging on Volume Resistivity.
Specimen: Semiconducting rods
Impregnant: Polyethylene wax
Temperature: 90°C

5.3 IMPREGNATION WITH A CARBONIZABLE GAS

As mentioned in Section 2, electrical failure probably takes place due to ionization of gas caused by corona discharge in the voids and at the interfacial gaps in the insulation. It was suggested that if the cable is impregnated with an appropriate gas, which decomposes under high electrical stress to give nascent carbon and if the latter coats the walls of the void, then the inside of the void will be an equipotential surface and corona inception can be permanently suppressed(42). Consequently, the cable will have long service life. Some preliminary experiments were carried out with the objective of verifying this hypothesis. The experimental procedure and the results will be discussed in this Section.

A number of gaseous materials were considered with respect to their carbon content and susceptibility to decomposition. Two classes of gases, namely the hydrocarbons and the fluorocarbons met part of these criteria, and the following were recommended, based on their carbon content, susceptibility to thermal decomposition and commercial availability.

Gas	Structure	Carbon Content %	Remarks
Ethylene	$CH_2 = CH_2$	85.7	
Acetylene	$CH \equiv CH$	92.3	Might explode
Methylacetylene	$CH_3-C \equiv CH$	90.0	
1,2, Dimethyl Acetylene	$CH_3-C \equiv C-CH_3$	88.9	
Tetrafluoroethylene	$CF_2 = CF_2$	24.0	

A 15 kV cable, manufactured by Phelps Dodge Cable and Wire Company, was used in this study. The center portion of insulation in the test specimens was necked down to 25 mils to allow breakdown at relatively low stress. A "Christmas tree" test chamber built specifically for gas impregnation studies and described earlier (10) was used for this purpose.

The cable samples were baked in an air oven at 80°C for two weeks. Then they were installed in the test chamber and evacuated to eliminate the volatiles. Ethylene gas was introduced at 45 psig pressure and a week was allowed for impregnation. The AC breakdown

tests were carried out at 1, 6 and 24 hour step-up times to establish the stress time correlation.

The Weibull plots are presented in Figures 5-28 to 5-30. The data points for the 1 hour and 24 hour step-up test show close to linear correlation, while those for the 6 hour test suggest two intercepting lines. It is believed that during the 6 hour test, some change was taking place under electrical stress and the cable was not in an equilibrium state. It was speculated that the process might be leading to carbon deposition, since the dielectric strength increased substantially. The V_{50} values estimated from these plots are plotted in the volt time curve in Figure 5-30 along with that for air as control. The six hour V_{50} value appears to be marginally higher than those for 1 and 24 hour step-up times. Linear correlation based on the 1 and 6 hour V_{50} values would result in a positive slope suggesting an increase in dielectric strength with time. Even the most pessimistic line based on the 6 and 24 hour V_{50} values yields a lower slope than the control as reflected in the "-n" values, 27 for ethylene and 24.7 for air.

These preliminary results suggest that impregnation of the cable with a gas that decomposes to give carbon and subjecting the cable to electrical stress, could improve the service life of the cable.

WEIBULL PLOTS

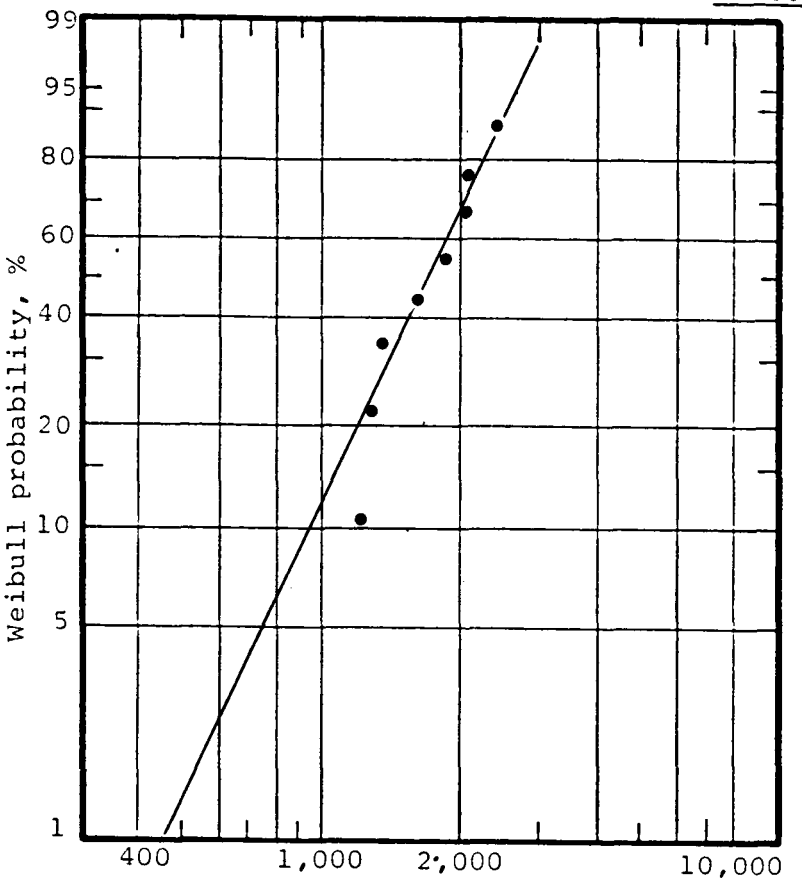

Figure 5-28. Impregnation with Ethylene. Sample: 15 kV cable necked down to 30 mil. One hour step-up test.

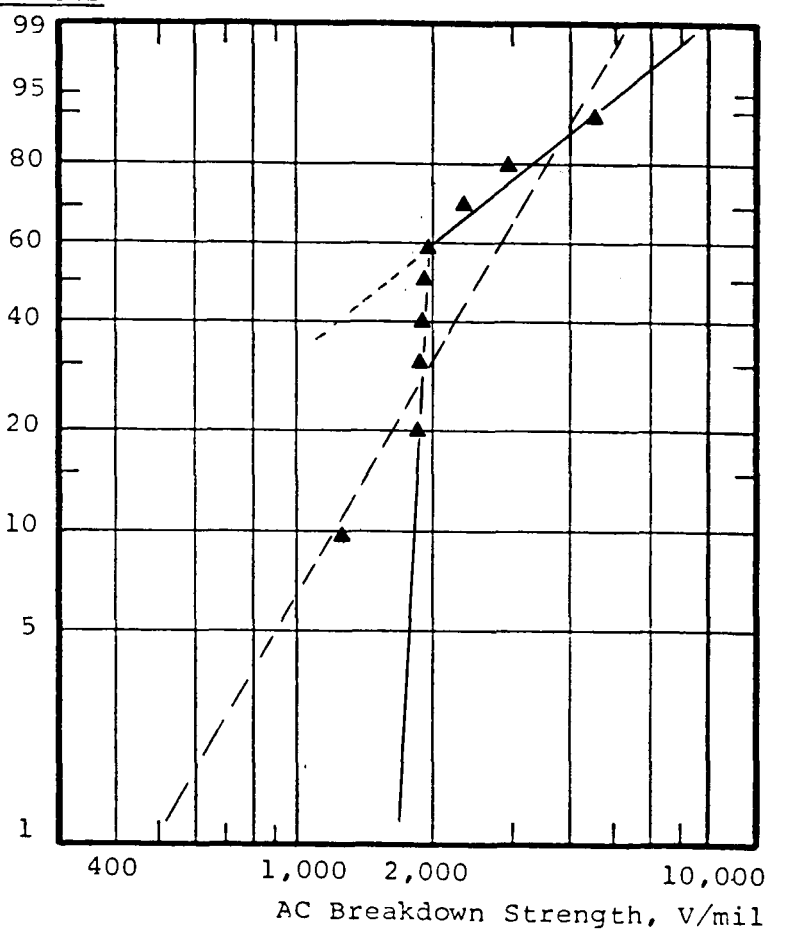

Figure 5-29. Impregnation with Ethylene. Six hour step-up test.

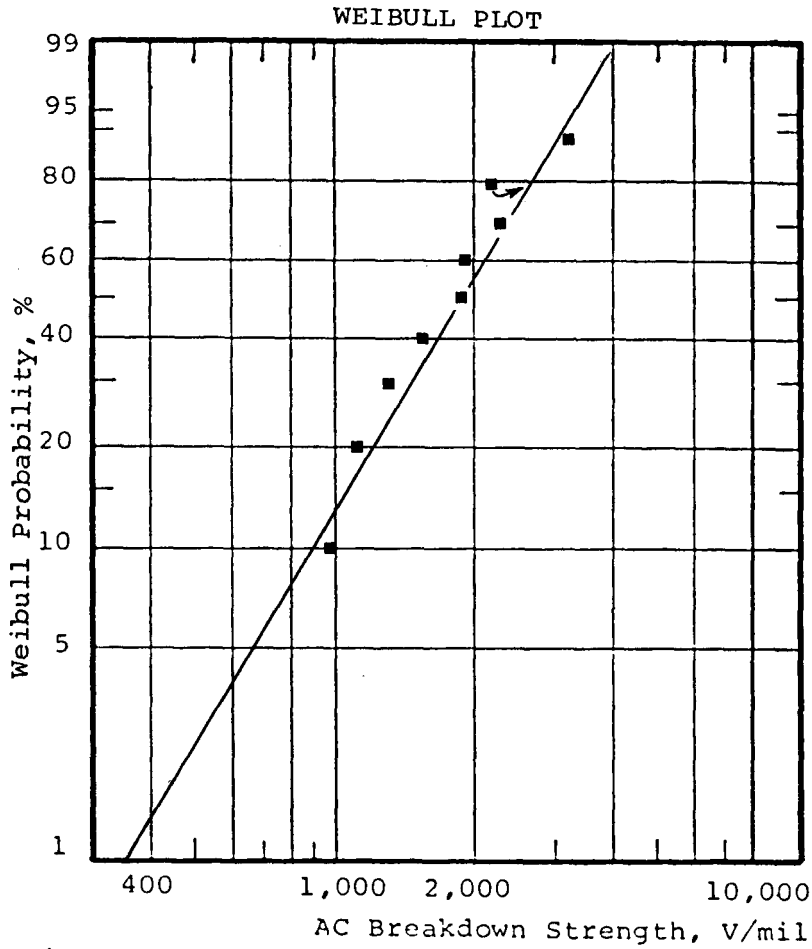

Figure 5-30. Impregnation with Ethylene. Twenty-four hour step-up test.

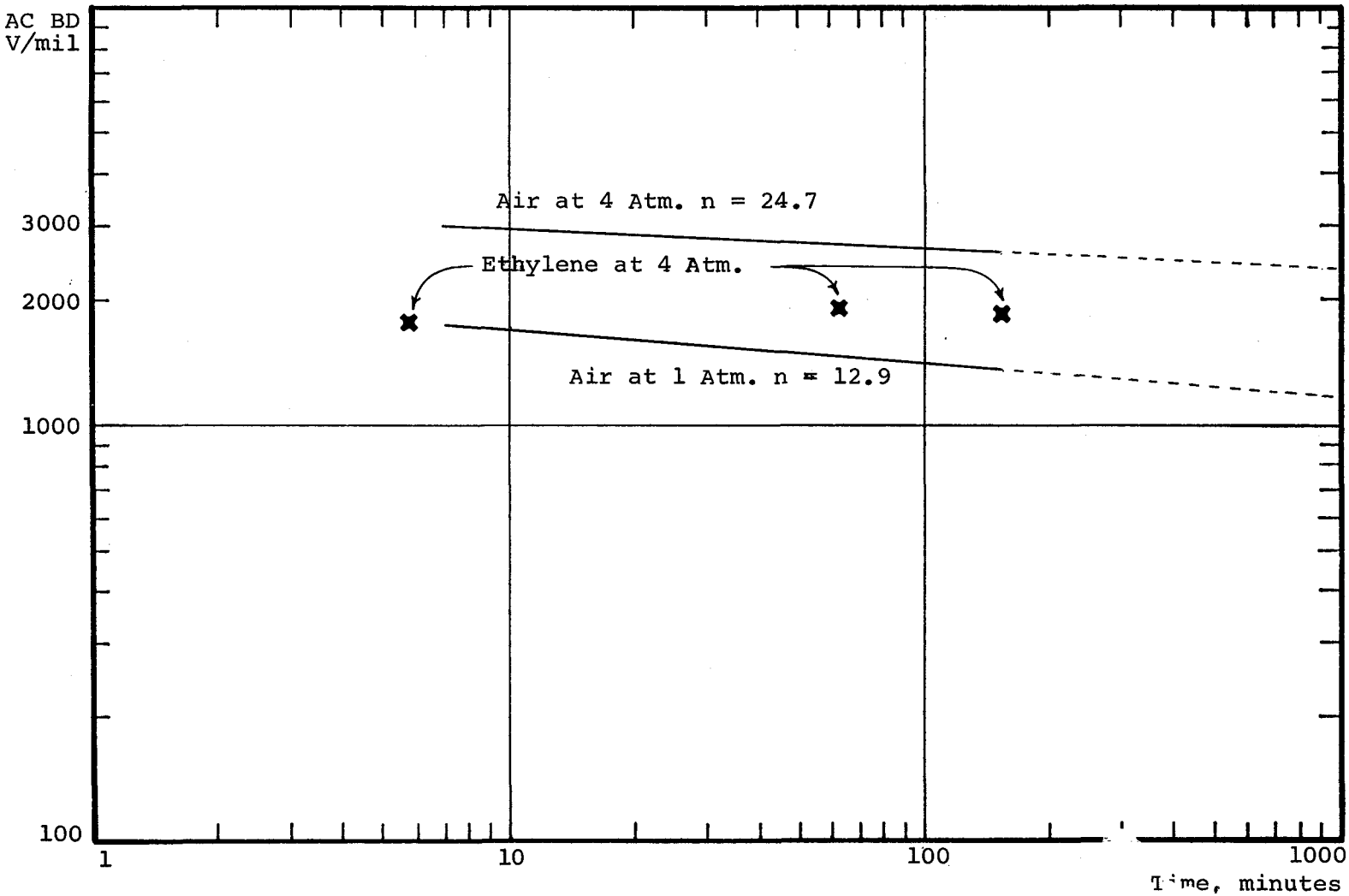

Figure 5-31. Impregnation with Ethylene Gas.
(15 kV cable necked down to 30 mil.)

Section 6

ECONOMIC ANALYSIS

As a sub-task of this 138 kV XLPE cable development project, it was considered pertinent to perform an economic study, providing a comparison of several different relevant cable constructions. It was performed in two parts:

1. Preliminary study comparing the actual cost of a variety of solid dielectric cable constructions representing present industrial practice, with the estimated cost of their "impregnated" counterparts. In addition, a typical oil-filled cable provided additional perspective.

2. Comprehensive economic analysis of the cost of impregnation and in situ polymerization of solid dielectric cable, and its comparison to cables made by advanced technology still in the development stage (e. g. dry cured or tree resistant insulation).

In both cases actual costing procedures were used. Raw material and manufacturing costs were based on actual figures, and items not in standard industrial practice were estimated. The results are presented in relative cost figures in comparison to standard products to protect the proprietary nature of cost information.

6.1 PRELIMINARY STUDY

Major emphasis was focused upon the significance of different metallic shield-jacket assemblies influencing cable cost, particularly in view of the increased importance now being placed on hermetically-sealed sheaths as a positive means for preventing electrochemical treeing and assuring maximum service life.

The several different series of cable constructions are detailed in Tables 6-1, 6-2 and 6-3, involving three cable groups with I-Wire Shield, II-Lead Sheath, III-CLX (welded and corrugated copper sheath) respectively.

In addition, the study involved 500, 1000, 2000 KCMIL copper conductors and their aluminum equivalents, 750, 1500, 3000 KCMIL. Finally,

Table 6-1

CABLE CONSTRUCTION

GROUP No. 1 - WIRE SHIELD - PE JACKET

GENERAL DESCRIPTION: 1/C Class B compact round bare copper (CRC) or Class B compressed concentric stranded bare copper (CCC) or H19 Class B compact round aluminum alloy 1350 conductor (CRA) or H19 Class B compressed concentric stranded aluminum alloy 1350 conductor (CCA) as noted below, extruded semi-conducting thermosetting conductor shield, natural THERMOLENE insulation, 0.050" (0.040" min. spot) extruded semi-conducting thermosetting auxiliary insulation shield, 0.010" printed semi-conducting butyl-nylon tape half lapped, bare copper wire shield composed of number of wires of wire size noted below applied 9 X lay, 0.010" double faced rubber filled fabric tape binder half lapped, black HMW polyethylene (HABIRLENE) jacket, 138 kV 100% insulation level.

DETAILED CONSTRUCTIONS

	CONDUCTORS		THICKNESSES			WIRE SHIELD		
ITEM	SIZE	TYPE	CDR SHLD-1	INSUL-2	JKT -3	No. of WIRES	WIRE SIZE	APPROX O.D.
1	500 kcmil	CRC	0.020"	0.800"	0.140"	25	#14 AWG	3.05"
2	1000 kcmil	CRC	0.020"	0.800"	0.140"	31	#12 AWG	3.42"
3	2000 kcmil	CCC	0.035"	0.800"	0.140"	31	#9 AWG	4.06"
4	750 kcmil	CRA	0.020"	0.800"	0.140"	23	#14 AWG	3.23"
5	1500 kcmil	CCA	0.035"	0.800"	0.140"	28	#12 AWG	3.77"
6	3000 kcmil	CCA	0.035"	0.800"	0.140"	28	#9 AWG	4.43"
7	500 kcmil	CRC	0.020"	0.500"	0.110"	25	#14 AWG	2.37"
8	1000 kcmil	CRC	0.020"	0.500"	0.110"	31	#12 AWG	2.74"
9	2000 kcmil	CCC	0.035"	0.500"	0.140"	31	#9 AWG	3.44"
10	750 kcmil	CRA	0.020"	0.500"	0.110"	23	#14 AWG	2.55"
11	1500 kcmil	CCA	0.035"	0.500"	0.140"	28	#12 AWG	3.15"
12	3000 kcmil	CCA	0.035"	0.500"	0.140"	28	#9 AWG	3.81"

1. Minimum spot thickness 0.012" for 0.020" min. avg. thickness and 0.025" for 0.035" min. avg. thickness.

2. Minimum spot thickness 90% of min. avg. thickness specified.

3. Minimum spot thickness 80% of min. avg. thickness specified.

Table 6-2

CABLE CONSTRUCTION

GROUP II - LEAD SHEATH - PE JACKET

GENERAL DESCRITPION: 1/C Class B compact round bare copper (CRC) or Class B compressed concentric stranded bare copper (CCC) or H19 Class B compact round aluminum alloy 1350 conductor (CRA) or H19 Class B compressed concentric stranded aluminum alloy 1350 conductor (CCA) as noted below, extruded semi-conducting thermosetting conductor shield, natural THERMOLENE insulation, 0.050" (0.040" min. spot) extruded semi-conducting thermosetting auxiliary insulation shield, lead sheath, black HMW polyethylene (HABIRLENE) jacket, 138kV 100% insulation level.

DETAILED CONSTRUCTION

	CONDUCTORS		THICKNESSES				APPROX.
ITEM	SIZE	TYPE	CDR SHIELD-1	INSULATION-2	LEAD	JACKET-3	O.D.
1	500kcmil	CRC	0.020"	0.800"	0.110"	0.095"	2.97"
2	1000kcmil	CRC	0.020"	0.800"	0.110"	0.110"	3.34"
3	2000kcmil	CCC	0.035"	0.800"	0.125"	0.110"	3.94"
4	750kcmil	CRA	0.020"	0.800"	0.110"	0.095"	3.15"
5	1500kcmil	CCA	0.035"	0.800"	0.125"	0.110"	3.72"
6	3000kcmil	CCA	0.035"	0.800"	0.125"	0.110"	4.30"
7	500kcmil	CRC	0.020"	0.500"	0.095"	0.080"	2.29"
8	1000kcmil	CRC	0.020"	0.500"	0.110"	0.095"	2.69"
9	2000kcmil	CCC	0.035"	0.500"	0.110"	0.095"	3.26"
10	750kcmil	CRA	0.020"	0.500"	0.110"	0.095"	2.53"
11	1500kcmil	CCA	0.035"	0.500"	0.110"	0.095"	3.04"
12	3000kcmil	CCA	0.035"	0.500"	0.125"	0.110"	3.68"

1. Minimum spot thickness 0.012" for 0.020" min. avg. thickness and 0.025" for 0.035" min. avg. thickness.

2. Minimum spot thickness 90% of min. avg. thickness specified.

3. Minimum spot thickness 80% of min. avg. thickness specified.

Table 6-3

CABLE CONSTRUCTION

GROUP III - CLX SHEATH - PE JACKET

GENERAL DESCRIPTION: 1/C Class "B" compact round bare copper (CRC) or Class "B" compressed concentric stranded copper (CCC) or H19 Class "B" compact round aluminum alloy 1350 conductor (CRA) or H19 Class "B" compressed concentric stranded aluminum alloy 1350 conductor (CCA) as noted below, extruded semi-conducting thermosetting conductor shield, natural THERMOLENE insulation, 0.050" (0.040" min. spot) extruded semi-conducting thermosetting auxiliary insulation shield, seam welded and corrugated copper sheath of thickness noted below, black HMW polyethylene (HABIRLENE) Jacket, 138kV 100% insulation level.

DETAILED CONSTRUCTION

	CONDUCTORS		THICKNESSES				
ITEM	SIZE	TYPE	CDR SHIELD-1	INSULATION-2	COPPER SHEATH-4	JACKET-3	APPROX. O.D.
1	500kcmil	CRC	0.020"	0.800"	0.025"	0.140"	3.12"
2	1000kcmil	CRC	0.020"	0.800"	0.025"	0.140"	3.45"
3	2000kcmil	CCC	0.035"	0.800"	0.025"	0.140"	4.02"
4	750kcmil	CRA	0.020"	0.800"	0.025"	0.140"	3.29"
5	1500kcmil	CCA	0.035"	0.800"	0.025"	0.140"	3.80"
6	3000kcmil	CCA	0.035"	0.800"	0.025"	0.140"	4.39"
7	500kcmil	CRC	0.020"	0.500"	0.025"	0.110"	2.44"
8	1000kcmil	CRC	0.020"	0.500"	0.025"	0.110"	2.77"
9	2000kcmil	CCC	0.035"	0.500"	0.025"	0.140"	3.40"
10	750kcmil	CRA	0.020"	0.500"	0.025"	0.110"	2.61"
11	1500kcmil	CCA	0.035"	0.500"	0.025"	0.140"	3.18"
12	3000kcmil	CCA	0.035"	0.500"	0.025"	0.140"	3.77"

1. Minimum spot thickness 0.012" for 0.020" min. avg. thickness and 0.025" for 0.035" min. avg. thickness.

2. Minimum spot thickness 90% of min. avg. thickness specified.

3. Minimum spot thickness 80% of min. avg. thickness specified.

4. Adder for CLX sheath is 0.270" and is based on 0.110" depth of corrugation plus 2 x tape thickness.

groups of cables having standard .800" insulation wall, and also .500" reduced-wall were analyzed. Additional construction details are summarized in these same Tables.

The ampacities and MVA ratings for the different cable constructions and sizes have been calculated as presented in Table 6-4. Typical installation parameters were assumed, including:

- Ambient Earth - 20°C
- Maximum Condition Temperature - 90°C
- Thermal Earth Rho - 90°C-Cm/watt
- Load Factor - 100%
- Single Point Bonding
- Direct Buried - Flat Lay - 36" Depth - 7.5" Centers

A review of the data presented in Table 6-4 indicates that the type of shield construction causes only a very small change in ampacity (MVA), variation ranging from 1-3%. However, it is to be noted that the lead sheath designs are almost twice the weight of the wire-shield constructions.

Relative cable costs have been developed for the several different constructions, previously described, and the results are plotted in Figures 6-1, 6-2 and 6-3. The results have been expressed as Cost per MVA, taking the 500 kcmil copper conductor, .800" wall, wire-shield construction as a reference base at 100%.

There are several aspects of this study which should be noted in passing. The influence of conductor size on ampacity is not linear, but is a square-root function, resulting in an increasing copper or aluminum cost per ampere (Cost per MVA) with increasing conductor size:

Influence of Conductor Size on Ampacity

Conductor Size (kcmil)	Relative Cost*	AMPS	Cost/AMP
1000	1	$\frac{1}{\sqrt{2}}$	$\frac{1}{\sqrt{2}}$
2000	2		
4000	4	2	2

* For conductor material only

In addition, the actual cable ampacity curves exhibit some exponen-

Table 6-4

CONSTRUCTION DETAILS OF 138 kV CABLES

CABLE PARAMETERS					AMPACITIES SHIELDS			MVA SHIELDS		
Item	Cond.	Cond. Size	Wall	Jacket	Wire	Lead	CLX	Wire	Lead	CLX
1	Cu	500	.800"	Poly	609	613	608	145	146	145
2	Cu	1000	.800"	"	881	882	875	210	210	209
3	Cu	2000	.800"	"	1251	1196	1186	290	285	283
4	A	750	.800"	"	596	600	596	142	143	142
5	A	1500	.800"	"	869	866	860	207	206	205
6	A	3000	.800"	"	1198	1172	1162	286	280	277
7	C	500	.500"	"	629	635	630	150	151	150
8	C	1000	.500"	"	908	912	907	216	217	216
9	C	2000	.500"	"	1246	1246	1228	297	296	293
10	A	750	.500"	"	615	620	616	146	148	147
11	A	1500	.500"	"	891	896	887	212	214	212
12	A	3000	.500"	"	1227	1213	1203	293	289	287

Installation Parameters:
1. Ambient Earth - 20°C
2. Max. Cond. Temp. - 90°C
3. Thermal Earth rho - 90°C/watt-cm
4. Load Factor - 100%
5. Single Point Bonding

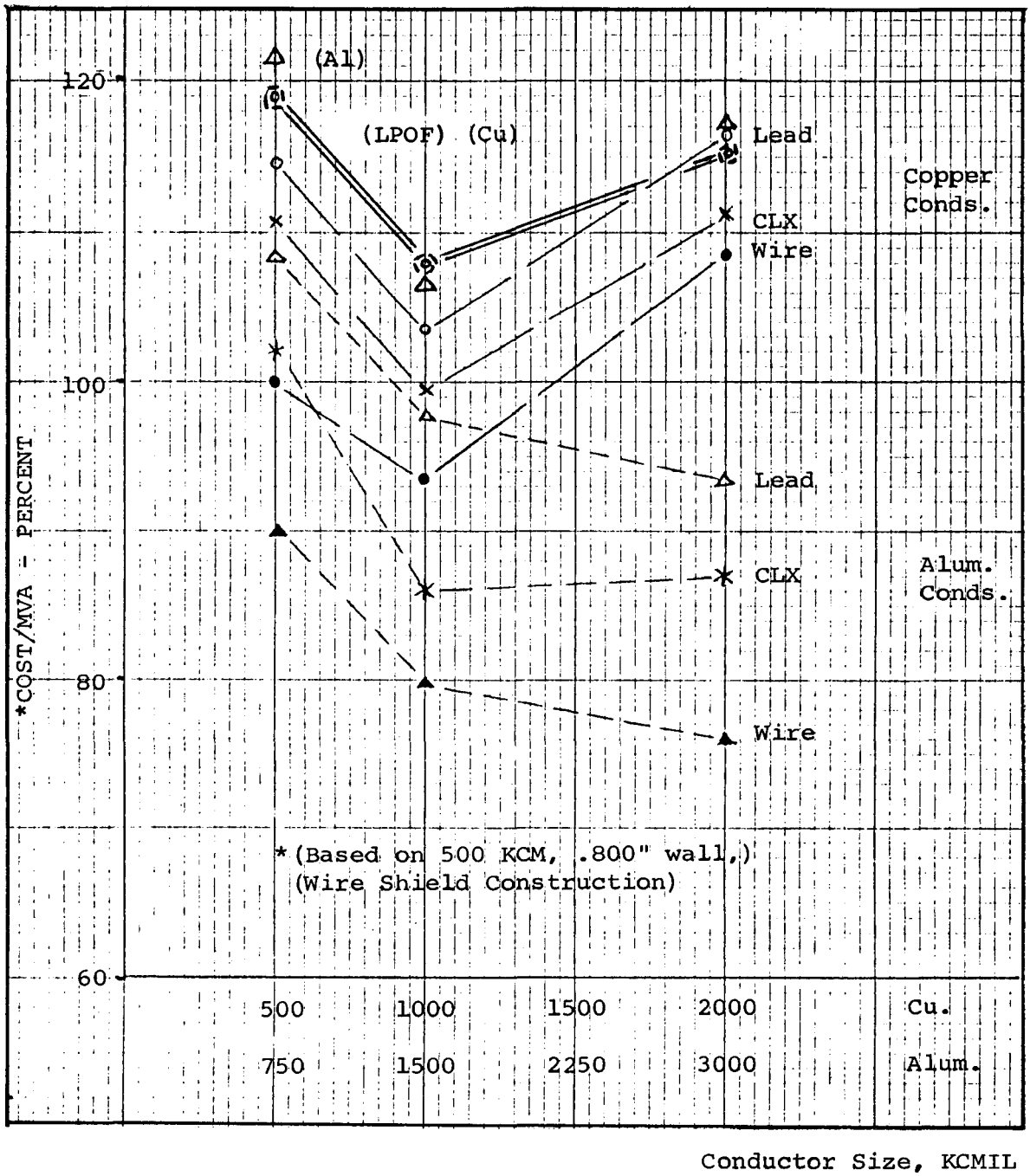

Figure 6-1. Estimated Cost of 138 kV Cables at 800 mil Insulation Thickness. Comparison of Constructions.
Normalized Cost/MVA, based on 500 KCM, 800 mil wall design.

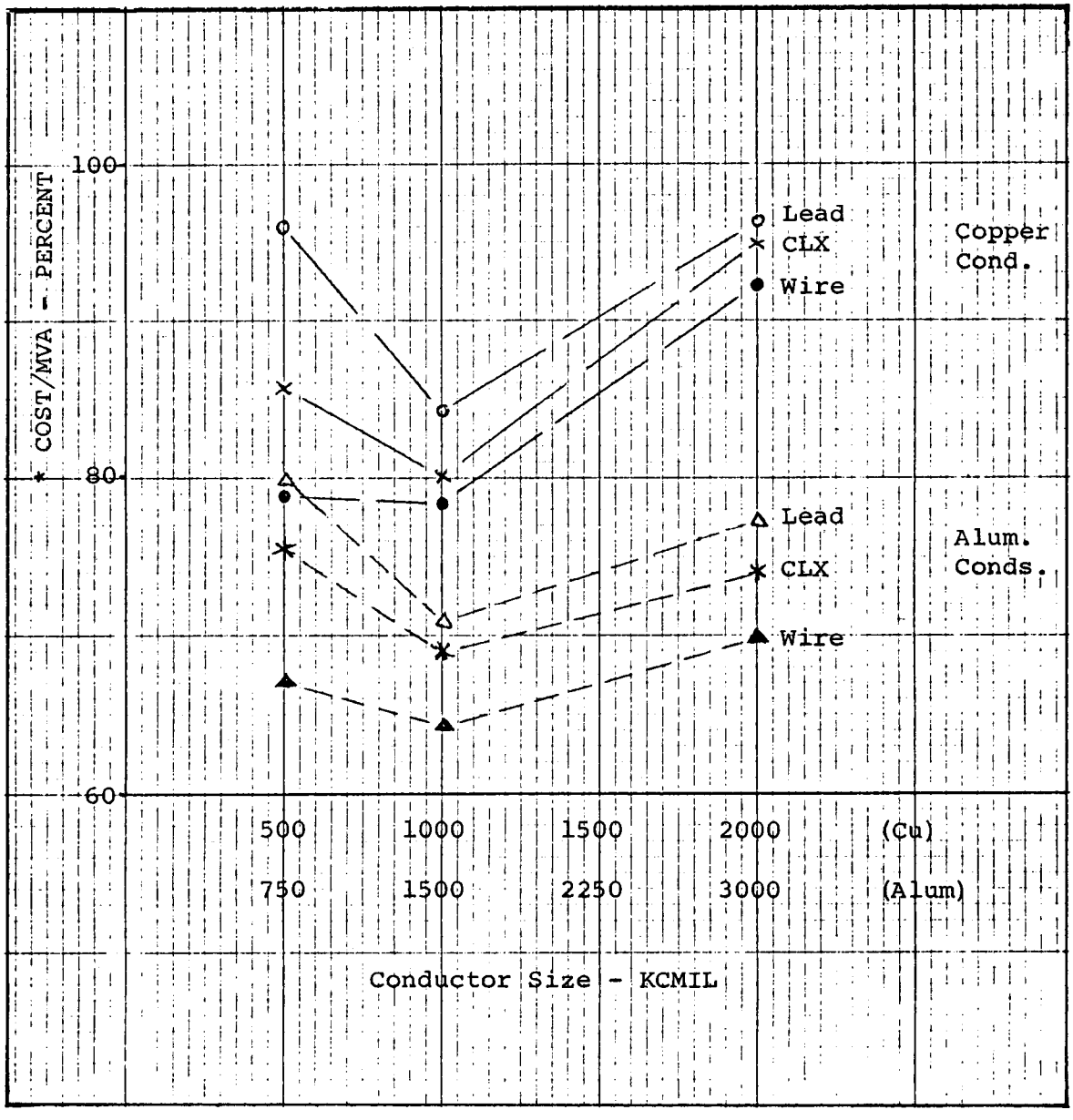

Figure 6-2. Estimated Normalized Cost of 138 kV Cables at 500 mil Insulation Thickness. Comparison of Constructions. Normalized Cost/MVA, based on 500 KCM, 800 mil wall design.

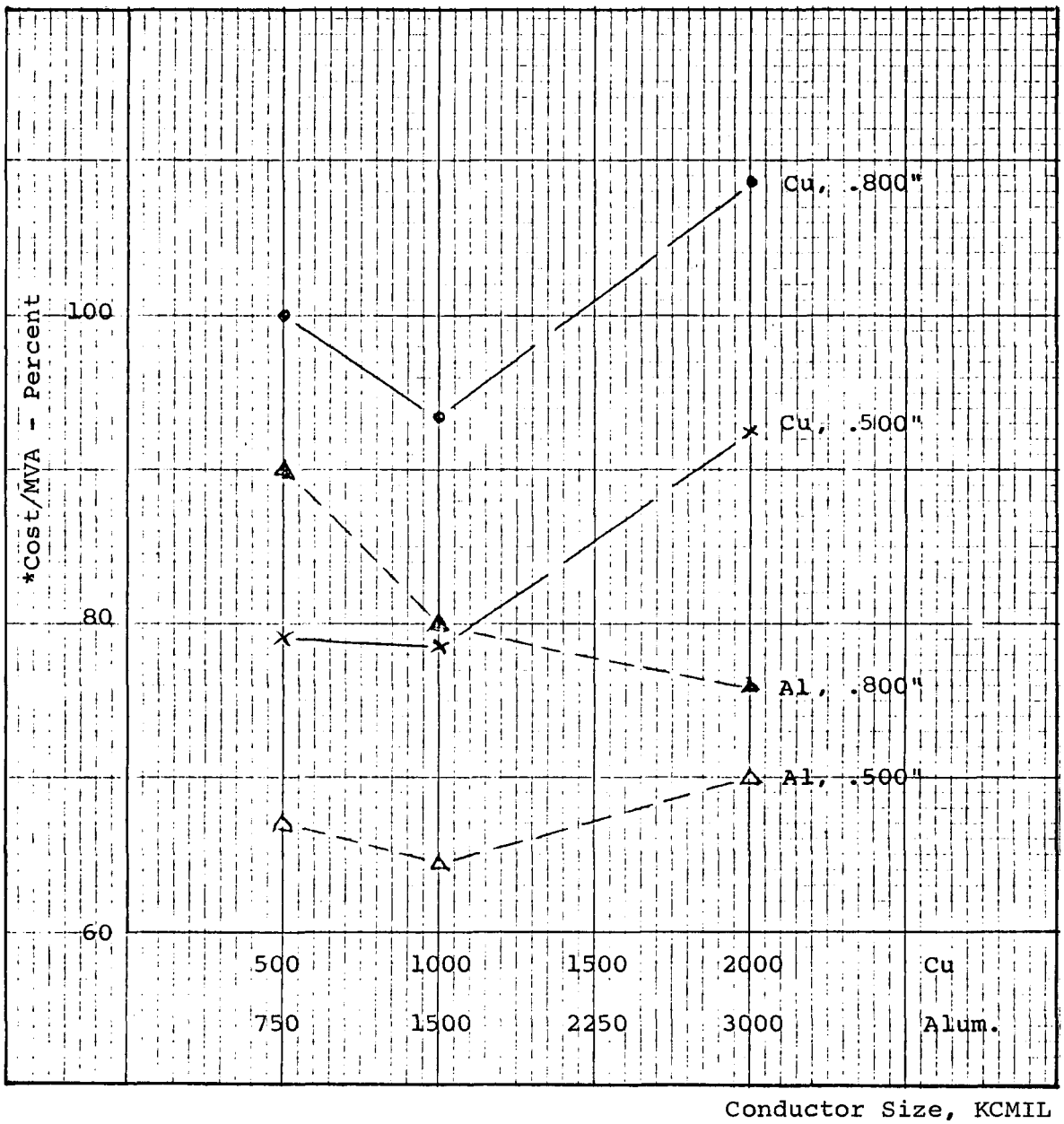

Figure 6-3. Estimated Normalized Cost of 138 kV Cables at 800 and 500 mil Insulation Thicknesses. Wire Shield Construction.
Cost/MVA based on 500 KCM, 800 mil wall design.
Normalized Cost/MVA based on 500 KCM, 800 mil wall design.

tial tendency, tending to saturate at higher size conductors. On the other hand, cable costs appear essentially linear with conductor size.

The Cost/MVA Curves for the different (.800") cable constructions reveal moderate differences between designs, with the lead sheath running about 10% higher (on average) than wire shield for copper conductors, and about 18% higher for aluminum conductors. In the case of the .500" wall cable designs, these corresponding increments reduce to about 6% and 10% for copper and aluminum, respectively. CLX sheath designs appear to run about midway between lead and wire shields, in general.

In contrast with copper conductors, aluminum constructions appear to run about 25% less (on average) for .800" walls, and 15% less for .500" walls, reflecting to some extent the significant cost advantage of the aluminum conductor component.

It is pertinent to recall that the wire-shield designs here considered provide only 20% of the conductivity of the conductor. Obviously, wire-shield designs providing higher conductivities would closely approach the costs of CLX designs.

The group of wire-shield cable constructions are shown separately on Figure 6-4, in order to compare the cost of similar "impregnated" cables (with .500" wall).

Standard impregnating-tank processing was assumed, using appropriate impregnant-liquid costs at $1.50/lb. Impregnation would appear to impose an additional 5 to 10 percent cost factor, based on this simplistic estimate.

Comparative LPOF cable construction costs were also introduced on Figure 6-1, as a matter of interest. It is clear that for 2000 KCM copper conductor, the Cost/MVA is virtually identical with the .800" wall XLPE design, and running slightly higher for small sizes. Accordingly, LPOF designs show a definite cost penalty (about 20%) where compared to the .500" wall cables. LPOF aluminum conductor designs show similar relationships.

6.2 COMPREHENSIVE ANALYSIS OF ADVANCED CABLES

6.2.1 Basis of Analysis

The cost of manufacturing selected cables of advanced design was computed based on present costing methods for 138 kV rated cables on input from material and equipment suppliers regarding their pre-

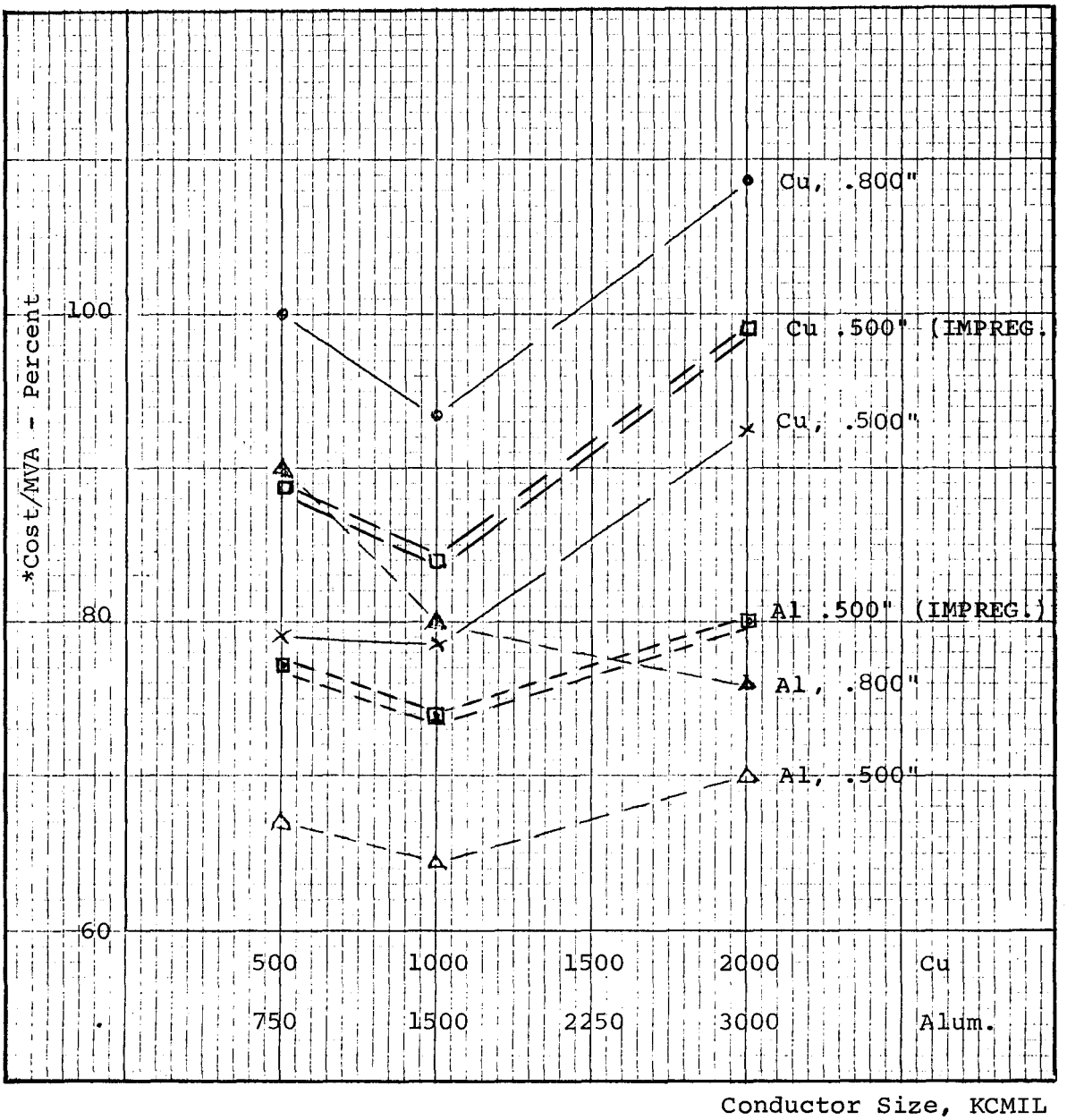

Figure 6-4. Estimated Normalized Cost of 138 kV 500 KCM Cables. Comparison of Standard and Impregnated Cables. Wire Shield Construction.
Normalized Cost/MVA based on 500 KCM, 800 mil wall design.

sent and projected prices, and on estimates. Attempts were made to keep the estimates as realistic as possible, based on best technical judgment at the time of writing, and, if in doubt, to lean to the conservative side. The following cable constructions were considered:

- Standard construction with wire shield and extruded polyethylene jacket representing present state of art manufacturing methods and described in detail in Table 6-1.

- Lead sheath with PE jacket, identical to that described in detail in Section 6.1, preliminary estimate, presented in Table 6.2.

- Impregnated with PVT - This construction is an example of the present project. It involves a standard cable impregnated with vinyl toluene and benzoyl peroxide and the in situ polymerization of the impregnant to yield 2% (on insulation weight) of polyvinyl toluene (PVT).

- Voltage stabilized, comparable to the standard cable but using commercial insulation compound with voltage stabilizing additive system instead of standard cross-linkable polyethylene.

- Dry cured and lead jacketed, similar to the construction in Table 6-2 but using commercially offered dry curing technology instead of steam curing.

The following items were considered in the analysis:

- Conductor type and size - Copper conductor of 500, 1000 and 2000 kcmil and aluminum of 750, 1500 and 3000 kcmil same as in the preliminary analysis and presented in Table 6-4.

- Insulation thickness - The computations cover standard 800 mil and 500 mil thicknesses for each construction.

- Life time of standard cable was the basis of comparisons. When advanced designs were assumed to result in doubling the lifetime, the cost of a second standard cable was also added on the basis of "present worth" of a second cable to be manufactured at the end of standard life time. Interest rates of 7, 8 and 9% were used in calculating present worth.

- Cost of lead - Both the actual price of lead, 48.0¢/lb. and 25¢/lb. were used in this analysis. The preliminary estimate was based on 24.6¢/lb. price.

- Impregnation and polymerization time - Three cycle times 12, 16 and 24 days were considered for the combined impregnation, polymerization and drying cycle for the impregnated cable. Costs of energy, labor and overhead were computed on the basis of full utilization of the impregnating tank and related equipment. An alternative, the cost to manufacture a single reel, was also computed and shown under the designation, "dedicated operator."

- Voltage stabilized insulation compound was priced at 120% of the price of standard crosslinkable polyethylene compound.

- Dry cure processing cost included depreciation of cost of converting existing steam cure line to dry cure.

6.2.2 Comparison of Designs

The basic characteristics of insulations, the expected performance of cable types considered and their relative costs are compared in Table 6-5. The standard cable with 800 mil steam cured insulation (#I) is the basis of comparison both in electrical characteristics and in cost. A decrease in insulation thickness to 500 mil (#VI) lowers the initial AC breakdown strength and the impulse strength to 63% of those of the standard, and is expected to lower the lifetime due to faster penetration of the insulation with water trees. Voids, protrusions and contaminations should be comparable to the standard. Its relative cost averages at 83% of the standard, and it varies from 77 to 87% of the standard for the six items listed in Table 6-4.

Lead jacket by itself (Nos. II and VII) is expected to decrease water treeing due to prevention of water ingress during service. Since its steam cured insulation may contain up to 0.5% water, it is not considered a candidate either for prolonged life or for lower cost cable. It is listed for comparison to dry cured, lead jacketed cables (Nos. V and X in Table 6-5).

Impregnated cable (containing 2% PVT) at 800 mil insulation thickness (#III) is expected to show an elimination or at least a drastic reduction of both in the number and in the size of voids. Its AC breakdown strength is estimated as 150% of the standard, based on laboratory scale results. Its lifetime is expected to be superior

Table 6-5

Comparison of Improved Cables

No.	Insul.	Cable Type	Insulation Characteristics			Initial short term AC BD	Impulse	Water tree resistance Life in wet environment.	Slope of V/t curve	Relative Cost	
			Voids	protrusions	contaminants					average	range
I	.800" XLPE	Standard	many $\leq 25\mu$	$\leq 250\mu$	$\leq 250\mu$	100%	100%	Good	n = 9-12	100	100 - 100
II		Lead jacket	many $\leq 25\mu$	$\leq 250\mu$	$\leq 250\mu$	100%	100%	Better-as water ingress prevented	n = 9-12	140	123 - 156
III		Impregnated	Voids filled, may be "Voltage Stabilizing" effect.			150%	150% (PD liquid imp. test)	Better-void filling & Volt Stabilizing effect.	PD Liq. impregnated n $\geq$100 Higher than Std. on Polymerized slabs	119	113 - 124
IV		Voltage Stabilizer Included	Voltage stabilizing effect may retard defects from causing failure			100%	100% Designed to improve long term ageing.	Better - Volt. stabilizing effect.	?	108	105 - 109
V		Dry Cured + lead jacket	few $\leq 8\mu$	$\leq 250\mu$	$\leq 250\mu$	150%	110%	Excellent - Cable dry & water ingress prevented.	n = 9-12	147	128 - 165
VI	.500" XLPE	Standard	Same as I			63%	63%	Marginal - tree growth proportional to E^2	Same as I	83	77 - 87
VII		Lead jacket	Same as II			63%	63%	Good - Water ingress prevented.	Same as II	111	103 - 116
VIII		Impregnated	Same as III			94%	94%	Same as III	Same as III	94	89 - 98
IX		Volt Stab. included	Same as IV			63%	63%	Same as IV	Same as IV	87	81 - 90
X		Dry Cured + lead jacket	Same as V			63%	69%	Same as V	Same as V	115	109 - 121

to the standard due to a decrease in water treeing and to the voltage stabilizing effect of the impregnant. A drastic increase in the "n" coefficient in the life equation improves its slope in the V/t curves and hence contributes to prolonged lifetime. It is a candidate for a cable with twice the lifetime of the standard. The same cable at 500 mil insulation thickness (#VIII) is expected to match the performance of the standard cable (#I), and is a candidate for lower cost standard life cable.

Cables with voltage stabilized insulation (Nos. IV and IX at 800 and 500 mil insulations respectively) were not tested at the time of writing this report. There is no ground to assume that imperfections are smaller or fewer than those for the standard cables, however the effect of these imperfections may be lower due to the retarding effect of the voltage stabilizer system included. The same effect should improve water tree resistance and contribute to prolonged lifetime. The value of the "n" coefficient and hence the V/t performance is unknown. At 800 mil thickness (#IV) its lifetime should be longer than that of the standard (#I) but lifetime is unknown compared to the impregnated cable (#III). At 500 mil insulation thickness (#IX), it may match the lifetime of the standard at 800 mil (#I).

Dry cured cables with lead jacket (Nos. V and X) are expected to contain drastically less voids of smaller size compared to the steam cured standard (#I). Limited data to date indicates a potential 50% increase in short term AC breakdown strength over the standard (#I) possibly matching the impregnated cable (#III). However, its impulse strength at 10% over standard could be inferior to that of the impregnated cable. Because there is no water initially in the cable (dry cure) and no water can enter in service (lead sheath), water treeing should not occur. At 800 mil insulation thickness (#V), it is a candidate for doubled lifetime, and at 500 mil (#X) for standard lifetime at lower cost. Its cost depends heavily on the price of lead.

6.2.3 Details of Cost Comparison

The cost of impregnation and in situ polymerization of the impregnant is best illustrated with an example presented in Figure 6-5 for 500 kcm copper conductor cable. Detailed analysis has shown that the material cost of impregnant, catalyst and auxiliary materials is minimal compared to the material cost of standard cable. The major factors, labor and energy are proportional to the time of treatment. Figure 6-5 represents the relative cost (standard cable =100) as a function of residence time in the impregnation tank including impregnation, polymerization and driving off the unpolymerized monomer. Separate lines represent the 800 and 500 mil insula-

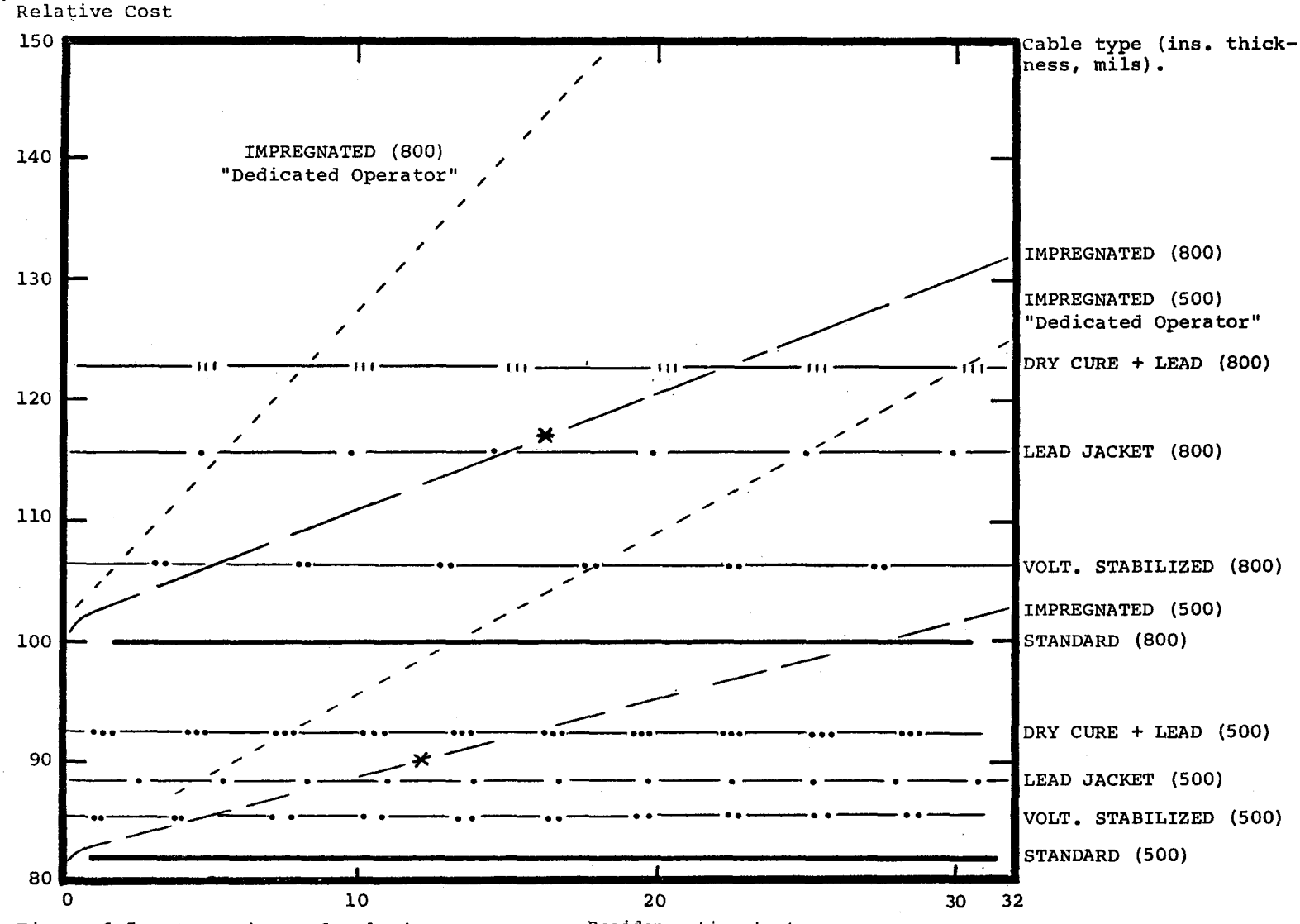

Figure 6-5. Comparison of Relative Cost.
Construction: 500 kcm, copper conductor.

tions. Both are based on complete filling of the tank, and thicker insulation allows less cable to be treated per tank resulting in higher unit cost. The two lines are linear except the initial steep increase due to low material cost.

The other cable types are represented by horizontal lines. The intersection of these horizontal lines with either of the two inclining ones determines the residence time equivalent in cost to the other cables. The residence time requirements are estimated as 16 days for 800 mil and 12 days for 500 mil insulation and represented by a * in Figure 6-5.

Similar comparisons for other conductor types, not included in this Report, differ only in the relative positions of the lines and in the slopes of the two inclining curves. They are summarized in a bar diagram in Figure 6-6. Relative costs are measured on the vertical scale. Relative cost of standard cable is set at 100 for each cable size (items 1 to 6 in Table 6-4), that for other cables is shown by individual bars. The bars for impregnated cables are shown with stepwise tops representing 12, 16 and 24 days residence time in the impregnating tank. The double lines for 500 mil thickness at 12 days and for 800 mil thickness at 16 days indicate the estimated residence times. The height of bars for cables with lead jackets is based on 37.5¢/lb. lead price, the 0 mark inside these bars shows the relative cost at 24.6¢/lb. lead price.

6.2.4 Cost of Comparable Performance

Two comparisons were made in assessing the economic feasibility of impregnated cables:

- Comparison of lower cost candidates for standard lifetime (comparison "Y" in Table 6-6).
- Comparison of candidates of extended lifetime (comparison "X" in Table 6-6).

The candidates for standard lifetime at lower cost are compared to the standard steam cured cable with 800 mil thick XLPE insulation (Relative Cost = 100). Both the impregnated cable containing 2% PVT and the voltage stabilized cable at 500 mil insulation are expected to meet this performance level at 93.6 and 87.3 relative costs respectively.

The dry cured cable with lead jacket is also expected to be comparable in performance but at 115 relative cost is more expensive. A decrease in lead price to 25¢/lb. would make it more promising at the relative cost of 95.

Table 6-6

SUMMARY OF RELATIVE COSTS

		Rel. Cost (1)	X (2)	Y (3)	(Alternates)
I.	Standard Cable, 0.800" XLPE	100		Y	
	Same, replaced after 20 years, (9% interest)	117.8			
	" 8 "	121.5	X		
	" 7 "	125.8			
VI.	Standard cable, 0.500" XLPE	83.4			
III.	Impregnated, 0.800" XLPE, 12 days impregnation	114.9			137 (4)
	" 16 "	119.1	X		149 (4)
	" 20 "	123.3			161 (4)
IX.	Impregnated, 0.500" XLPE, 12 days impregnation	93.6		Y	107.7 (4)
	" 16 "	96.6			115 (4)
	" 20 "	99.6			122.3 (4)
II.	Standard, + lead jacket, 0.800"	140.0			113 (5)
	" 0.500"	111.1			91 (5)
V.	Dry Cured + lead jacket, 0.800"	147	X		121 (5)
X.	" 0.500"	115		Y	95 (5)
IV.	Standard with Voltage Stabilized XLPE, 0.800"	107.5	X		
IX.	" 0.500"	87.3		Y	

(1) Average of six sizes, Items 1 to 6
(2) X Candidates for extended life
(3) Y Candidates for standard life at lower cost
(4) "Dedicated operator" in 3 shifts
(5) Lead price $0.246 instead of current $0.48/lb.

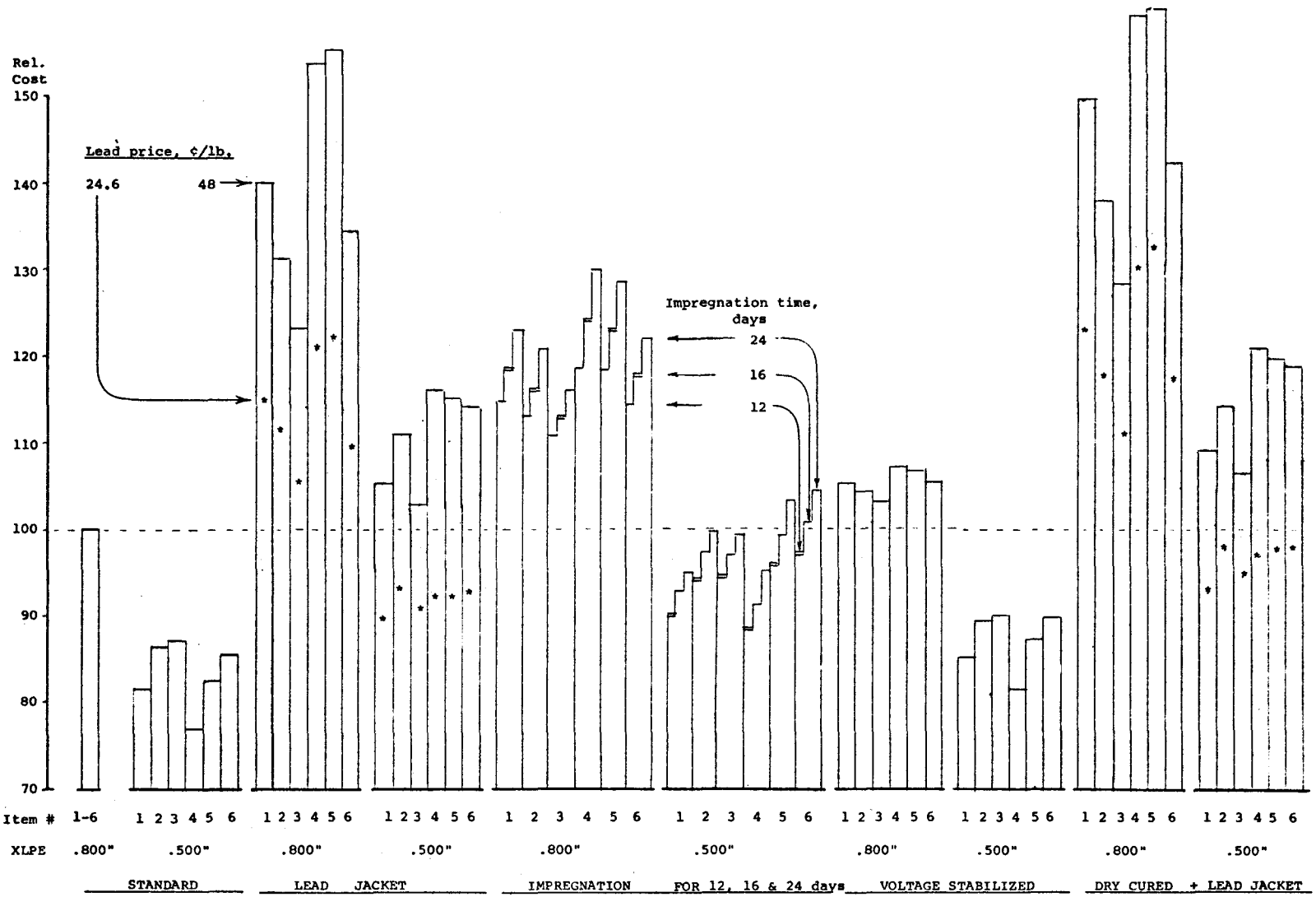

Figure 6-6. Comparison of Relative Costs.

The candidates for extended life are compared on the basis of 100% increase in the lifetime compared to the present standard. This would necessitate the replacement of the standard cable after failure. The present worth of the second cable is estimated as 21.5 relative cost assuming 8% interest rate and no inflation raising the relative cost of two consecutive cables to 121.5.

Impregnated cable at 800 mil insulation is expected to match this double lifetime performance at the comparable relative cost of 119.1. Should the voltage stabilized cable at comparable thickness be equivalent in performance, at 107.5 relative cost, it could be more economical. The dry cured cable with lead jacket is less economical at 147 relative cost.

Section 7

CONCLUSIONS

This report embodies the objectives, experimental details, results and discussion of a research program on the impregnation and in situ polymerization of monomers in crosslinked polyethylene insulation of high voltage cables. The objective was to permanently fill the voids by impregnation of the cable with a monomer and catalyst, followed by polymerization of the monomer in situ. Dielectric strength measurement and microscopic evaluation, both optical and scanning type, were used to monitor the improvement in the service life of the cable and the degree of void filling. More than three hundred experiments were carried out in the course of two and a half years. The broad conclusions from this work are:

1. The short term dielectric strength of high voltage cables with polyolefinic insulation can be substantially improved by impregnating the cable with monomer and polymerizing the latter in situ. This improvement is due to the filling of voids and interfacial gaps and apparently also due to the "voltage stabilizing" effect of certain monomers employed.

2. By careful monomer selection, this process could combine void filling with voltage stabilizing and tree resistant treatments and might bring better results because the impregnant is concentrated in a critical region (voids and interfacial gaps).

3. Cable made with this postmanufacturing process is about 20% more expensive than presently available processes for making quality cables, but the additional cost should be compensated by improved quality and longer service life.

4. The time required for impregnation and in situ polymerization of suitable monomers into XLPE insulation is well within practical limits.

5. The improvement brought about in the quality of the cable depends on the nature as well as on the amount of impregnant. Thus, whereas some impregnants like lauryl methacrylate act principally as a void filler, impreg-

nants like polyvinyl toluene act both as a void filler and voltage stabilizer.

6. The level of impregnant necessary for maximum improvement depends on the nature of the impregnant and not on whether it is liquid or solid state.

Specific conclusions based on detailed experimentation are reported below in the same order as they appear in the body of the report.

1. Steam cured crosslinked polyethylene (XLPE) cables are microporous. The void size and distribution are relatively independent of the thickness of insulation.

2. All crosslinked polyethylene cables contain volatiles, mainly the decomposition products of dicumyl peroxide (Dicup) such as acetophenone, cumyl alcohol, ∝ methyl styrene and water.

3. The concentration of the volatiles depends on the original amount of dicumyl peroxide present in the polyethylene compound and the thickness of the insulation, presence of the outer shield and the conditions of processing and storage. The thin model cables contain only 0.07% volatiles because (due to their thin walls) most of them are lost in a few days. Model cables cured continuously after extrusion contain higher amounts of volatiles, compared to the ones which are extruded and cured in separate operations.

4. Optical microscopy reveals numerous spherical voids of sizes from 10 to 25 μm. Scanning electromicrographs present spherulite-like structures with dark spots in the center which appear to be voids. These voids are sometimes irregular in shape and occasionally connected by microchannels.

5. AC breakdown strength of XLPE slabs is approximately 2000 V/mil compared to about 1200 V/mil for model cables. AC breakdown strength is higher for thinner dielectric, 2300 V/mil for samples ditched to 13 mil compared to 2000 V/mil for those ditched to 18 mil.

6. Removal of volatiles by high vacuum drying at 70 to 80°C decreases the AC breakdown strength by approximately 25% in slabs and 15 to 20% in model cables. This is probably because the volatiles such as acetophenone, cuminol and ∝ methyl styrene, present in the unevacuated samples, have voltage stabilizing properties and hence

their removal lowers dielectric strength.

7. High vacuum drying at temperatures sufficiently below the crystalline melting point of polyethylene does not alter the morphological characteristics, such as void size and distribution, spherulite-like structures and their boundary areas.

8. The rate of removal of volatiles is controlled by the vacuum level and temperature, the latter playing a more dominant role.

9. Heat treatment of the XLPE slabs from 138 kV cables increases their dielectric strength and the reciprocal slope of the volt-time curves. The voids in the center of the spherulite-like structures also appear to have been partially filled up. It is believed that the improvement in dielectric properties is due to partial filling of the voids and to the removal of residual stress built up in thick cables during extrusion, curing and cooling.

10. The rate of impregnation with monomers is not affected by the level of drying or the application of moderate pressure during impregnation. This shows that impregnation takes place mainly by permeation and not by capillary flow as one would expect in the presence of microchannels. The rate is however highly affected by temperature and the nature of the impregnant. Thus, for a 20^{o} rise in temperature, the rate of impregnation is increased by approximately 2 times. Further, the rate is highly influenced by the chemical nature of the impregnant. The time required for 3% impregnation (0.37" slabs) varies from 12 hours for vinyl toluene to 66 hours for 2 phenyl ethyl acrylate. Thus, the rate is higher for aromatic liquids followed by liquids having long alkyl chains. Polar liquids containing -OH, -COOH or -CO groups diffuse much slower, the slowest being water and silicone fluids. Diffusivity values do not vary over a wide range, although in a particular class it depends on the molecular size. Detailed analysis shows that the variations in the rate of impregnation are mainly due to the difference in solubility of the liquids in the polyethylene matrix.

11. The rate of impregnation of polymerization catalysts such as peroxides or azonitriles is 10 to 20 times smaller than that of the monomers.

12. Calculations based on Fickian diffusion showed that ca-

bles of 800 mil thick insulation could be impregnated up to the 2 to 3% level in a reasonable time ($\approx$104 hours) and experimental verification at room temperature confirmed this finding. At 35°C, the time required will be almost half as much.

13. The AC breakdown strength of the impregnated slabs and cables initially increases with the increase in the level of impregnation, comes to a maximum and then appears to taper off.

14. The concentration for maximum increase in dielectric strength depends on the impregnant. It is 0.5% for acetophenone, 2% for lauryl methacrylate and 1.5% for paraffin oil. The percent increase also depends on the chemical nature of the fluid. Thus, whereas vinyl toluene can bring about a 70% increase in the strength, lauryl methacrylate increases it by about 30%. This shows that void filling is important but even greater improvement can be brought about by impregnating the insulation with liquids which have voltage stabilizing properties due to their special chemical structure. These structures are mainly aromatic nuclei in conjugation with carbon carbon or carbon oxygen double bonds. The best candidate monomers were vinyl toluene, styrene, styrene oxide, 2 ethyl phenyl acrylate, dodecyl vinyl ether and vinyl pyrrolidone.

15. The degree of improvement brought about in the dielectric strength of the slabs by different impregnants was about the same as that for model cables. This led to the conclusion that the irregular surface of the ditched portion in the slab did not affect the results obtained.

16. Impregnation alone does not cause any permanent change in the morphology of the XLPE insulation, particularly when this is carried out at temperatures far below the softening point.

17. In situ polymerization of the impregnated monomer can be brought about by heating the impregnated insulation at a suitable temperature. The latter depends on the nature of the catalyst and the volatility of the monomer. Higher temperature increases the rate of decomposition of the catalyst but at the same time increases the rate of evaporation of the monomer.

18. Most monomers in the presence of catalysts will polymerize over a short period of time. However, the shelf-life of monomer catalyst solutions can be greatly im-

proved by adding 100 to 200 ppm of hydroquinone.

19. Among the various peroxides and azo compounds tried, the maximum yield was obtained with benzoyl peroxide.

20. The polymerization yield increases initially with catalyst concentration and with time and temperature of impregnation.

21. In the polymerization of lauryl methacrylate and vinyl toluene, 70 to 80% yield could be obtained using 2 parts of benzoyl peroxide as catalysts for 100 parts of monomer. The shelf-life of this solution can be increased to more than 27 days by adding 100 ppm of hydroquinone.

22. Whereas 100% polymerization of the impregnated monomer is very difficult to obtain with catalyst induced polymerization, it is easily obtained by γ ray induced initiation.

23. The failure to achieve a high rate and high level of polymerization by peroxide catalyzed reaction has been traced to the much lower rate of catalyst diffusion compared to that of the monomer. A two-step procedure in which the peroxide is impregnated in a methyl ethyl ketone solution followed by monomer impregnation and polymerization increases the yield.

24. The rate as well as the yield of polymerization was found to be too low in model cables. This was partly due to the thin walls of the insulation (25 mil) which facilitated the escape of the monomer during polymerization. The presence of carbon black in the strand shield, however, played the main role in preventing polymerization probably due to the inhibiting effect of quinone-type groups present on the surface of the black. Model cables with no strand shield and higher voltage cables (15 kV, 138 kV) at lower shield to insulation ratios, gave much higher yields under similar conditions for polymerization. Hence, the problem of not achieving higher yields was peculiar to the model cable with a high ratio of shield to insulation. A two-step process, involving impregnation of peroxide from MEK solution followed by impregnation with a monomer and in situ polymerization, showed the potential of overcoming this difficulty.

25. The AC breakdown strength of slabs and model cables subjected to impregnation and polymerization, is higher

than the controls. The degree of improvement for any level of impregnation with a polymer is almost the same as that of the monomer, showing that the physical state of the impregnant probably does not play a major role in determining the improvement. Thus for 1.1% impregnation, the polylauryl methacrylate brings about a 14% improvement compared to 13% by lauryl methacrylate. The corresponding figures for vinyl toluene polymer and monomer are 42 and 45% respectively. This is further supported by the fact that polyethylene wax and paraffin oil (its low molecular weight analogue) both bring about the same improvement in the dielectric strength at the same percent impregnation.

26. XLPE slabs impregnated with lauryl methacrylate and polymerized in situ by γ radiation, did not show any improvement in dielectric strength, probably due to chain scission and degradation of the main polyethylene chain.

27. Optical micrographs of polymerized slabs showed a smaller number of microvoids both for lauryl methacrylate and vinyl toluene. The highly irregular shape of the dyed portion in optical micrographs of polylauryl methacrylate (PLMA) treated slabs is possibly caused by poor wetting of the polyethylene and by PLMA gaps caused by shrinkage during polymerization.

28. Scanning electron micrographs of polylauryl methacrylate impregnated samples showed that the dark spots in the center of the spherulite-like structures had been filled without otherwise affecting the morphology. Polyvinyl toluene impregnated samples, on the other hand, not only exhibit void filling but appreciable obliteration of the boundary region. This has been ascribed to the dissolution of the amorphous region at the boundary during polymerization followed by reprecipitation on cooling, leading to a different morphology.

29. Impregnation and in situ polymerization of the semiconducting shields showed that polymerization of the impregnated monomer is strongly inhibited by the carbon black. Further, the increase in the volume resistivity and its behavior on aging, are within limits specified by IPCEA for crosslinked polyethylene cables.

30. Impregnation of the cable with a carbonizable gas and its subsequent aging on electrical stress shows improvement in the dielectric strength and the reciprocal slope of the VT curve.

31. XLPE cables cured by dry processes have smaller voids and they are also smaller in number.

Section 8

REFERENCES

(1.) H. C. Doepken Jr. Treeing, Insulation Material and Cable Life. Wire Technology, No. 9, October 1978, pp. 109-111.

(2.) D. Mangaraj, K. D. Kiss, E. Malawer and H. C. Doepken, Jr. Dielectric Strength of Crosslinked Polyethylene Insulation, Part II. Annual Report, Conference on Electrical Insulation and Dielectric Phenomena, October 1978, pp. 195-205.

(3.) J. Muccigrosso and P. J. Phillips. The Morphology of Crosslinked Polyethylene Insulation. IEEE Transactions on Electrical Insulation, El-13, No. 3, June 1978, pp. 172-178.

(4.) K. D. Kiss, B. S. Bernstein, et al. Aging of Polyolefin Electrical Insulation. Presented at the Macromolecular Symposium on Chemical and Physical Limits for Macromolecular Materials, Miami, 1978. To be published in Advances in Chemistry Series, 1979 by the American Chemical Society.

(5.) A. L. McKean. Breakdown Mechanism Studies in Crosslinked Polyethylene Cables. IEEE Transactions, Power Apparatus System, PAS-95, No. 1, 1976, pp. 253-260.

(6.) N. Srinivas, H. C. Doepken, Jr., et al. Electrochemical Treeing in Cables. Final Report, EPRI EL- 647, January 1978.

(7.) R. M. Eichhorn. Treeing in Solid Extruded Electrical Insulation. IEEE Transactions on Electrical Insulation EI-12, No. 1, February 1977, pp. 2-18.

(8.) T. P. Lactoe, J. R. Lawson and W. L. McVey. Investigation of Insulation Deterioration in 15 kV and 22 kV Polyethylene Cables Removed from Service. IEEE PES Summer Meeting, Los Angeles, 1978, Paper No. A78509-2.

(9.) G. Bahder, R. G. Lucac, et al. Development of Extruded Dielectric Underground Transmission Cables Rated 138 kV, 230 kV and 345 kV. Final Report, EPRI EL-428 and ERDA E(49-18)-1827, May 1977.

(10.) A. L. McKean, H. C. Doepken, Jr., et al. Investigation of the

Mechanism of Breakdown in XLPE Cables. Final Report, EPRI-TD 138 and ERDA-E(49-18)-1422, July 1976, p. 5.

(11.) H. Wagner and J. Wantusch. About the Significance of Decomposition Products in XLPE Cable Insulations. IEEE Transactions on Electrical Insulation E1-12, No. 6, November 1977, pp. 395-401.

(12.) J. Crank and G. S. Park. Diffusion in Polymers. London: Academic Press, 1968, p. 2.

(13.) W. Washburn. International Critical Tables of Numerical Data, Physics, Chemistry and Technology. Vol. III Vapor Pressure of Organic Liquids. New York: McGraw Hill Book Co., 1928, pp. 215-227.

(14.) D. E. Augood. Some Properties of XLPE Cable Materials. IEEE Summer Power Meeting, 1976, Paper No. A76-360-8.

(15.) W. Schwartz. Handbook of Chemistry and Physics. 40th Edition, Cleveland, Ohio Chemical Rubber Publishing Co., P. 2154.

(16.) J. Crank and S. Park. Diffusion in Polymers. London: Academic Press, 1968, p. 46.

(17.) Ibid, p. 5.

(18.) Ibid, p. 97.

(19.) J. H. Daane, H. E. Bair, et al. The Nature of Water in Submarine Cable Core and Its Relationship to Dielectric Loss. Proceedings of 25th Wire and Cable Symposium, November 1976, p. 296.

(20.) J. Brandrup and E. H. Immergut. Polymer Handbook. New York: John Wiley and Sons, 1965, p. V-23.

(21.) D. Mangaraj, G. Odian, et al. Effect of Diffusion on Rates and Molecular Weights on Graft Polymerization. Journal of Polymer Science, Polymer Chemistry Ed., Vol. 13, No. 3, 1975, pp. 623-644.

(22.) J. Crank and S. Park. Diffusion in Polymers. London: Academic Press, 1968, p. 16.

(23.) P. J. Flory. Principles of Polymer Chemistry. Ithaca, New York: Cornell University Press, 1953, p. 37.

(24.) Ibid, p. 75.

(25.) F. W. Bilmeyer. Textbook of Polymer Science. New York: Interscience, 1962, p. 279.

(26.) L. L. Alston Ed. High Voltage Technology. London: Oxford University Press, 1968, pp. 3-6.

(27.) A. L. McKean, H. C. Doepken, Jr., et al. Investigation of the Mechanism of Breakdown in XLPE Cables. Final Report ERPI-TD 138 and ERDA-E(49-18)-1422, July 1976, pp. 83-84.

(28.) Ibid, pp. 77-82.

(29.) H. Wagner. Pseudo Spherulite Structures in Crosslinked Low Density Polyethylene. IEEE Trans. Electrical Insulation EI-13, No. 2, April 1978, pp. 81-86.

(30.) T. Mizukami, K. Takahashi, et al. Insulation Properties of Crosslinked Polyethylene Cables Cured in Inert Gas. IEEE Transactions on Power Apparatus and System, Vol. 95, 1976, p. 467.

(31.) Product Bulletin. Diacyl Peroxides. Lucidol Penwalt, New York.

(32.) F. D. Schwartz. Handbook of Chemistry and Physics. 40th Ed. Chemical Rubber Publishing Co., Cleveland, 1958.

(33.) Electrical Properties of Acrylic Polymers and Monomers. Rohm and Hoas Co. Bulletin No. TMM-26 B/eh.
E. W. Washburn International Critical Tables. Dielectric Constant of Pure Organic Compounds. Vol. VI, London: McGraw Hill Book Co., 1929, pp. 81-108.

(34.) Longchain Alkyl Methacrylates. Rohm and Hoas Co. Bulletin No. CM-34, 1976, p. 3.

(35.) L. S. Luskin and R. J. Myers. Acrylic Ester Polymers. Encyclopedia of Polymer Science and Technology, New York: John Wiley and Sons, Inc., 1964, Vol. 1, pp. 246-328.

(36.) F. R. Mayo, R. A. Gregg and M. S. Matheson. Kinetics of Polymerization of Styrene. Journal of American Chemical Society, Vol. 73, 1951, p. 1691.

(37.) P. J. Flory. Inhibition and Retardation. Principles of Polymer Chemistry, Ithaca: Cornell University Press, 1953, p. 164.

(38.) A. C. Ashcraft, R. M. Eichhorn and R. G. Shaw. Laboratory Studies of Treeing in Solid Dielectrics and Voltage Stabilization of Polyethylene. IEEE International Symposium on Electrical Insulation, June 1976, Montreal, pp. 213-218.

(39.) M. Matsubara, S. Yamanouchi, et al. Annual Report of Conference on Electrical Insulation and Dielectric Phenomena, Washington, D. C., 1975, p. 270.

(40.) IPCEA-NEMA. Standard Publication. Crosslinked Polyethylene Insulated Wire and Cable for the Transmission and Distribution of Electrical Energy. IPCEA S-66-524 NEMA WC-7, Sept. 1977, Part 4, p. 2.

(41.) Carbon. Kirk and Othmer. Encyclopedia of Chemical Technology, 2nd Edition, New York: Interscience Publishers, Inc., 1960, Vol. 2, p. 827.

(42.) E. J. McMahon, D. E. Malony and J. R. Perkins. A Study on the Effects of Corona on Polyethylene. Paper 59-800, AIEE Summer and Pacific General Meeting and Air Transportation Conference, Seattle, Washington, June 21-26, 1959, pp. 654-662.